MULTI-PARAMETER FLOW CYTOMETRIC ANALYSIS OF IKAROS FAMILY EXPRESSION IN HUMAN T CELL DEVELOPMENT AND T-ALL

By

Julie Lynne Mitchell

Submitted to the graduate degree program in Microbiology, Immunology, and Molecular Genetics and the Graduate Faculty of the University of Kansas Medical Center in partial fulfillment of the requirements for the degree of Doctor of Philosophy.

Chairperson Thomas M. Yankee, Pharm.D., Ph.D.

Stephen H. Benedict, Ph.D.

Michael J. Parmely, Ph.D.

Kenneth R. Peterson, Ph.D.

Edward B. Stephens, Ph.D.

Date Defended: March 29, 2016

The Dissertation Committee for Julie Lynne Mitchell
certifies that this is the approved version of the following dissertation:

MULTI-PARAMETER FLOW CYTOMETRIC ANALYSIS OF IKAROS FAMILY EXPRESSION IN HUMAN T CELL DEVELOPMENT AND T-ALL

Chairperson: Thomas M. Yankee, Pharm.D., Ph.D.

Date approved: March 29 2016

Abstract

The Ikaros family transcription factors are critical regulators of T cell development and leukemogenesis. Loss of function of all five family members leads to an early block in murine lymphocyte development, whereas reduced function results in the development of T cell leukemias. Loss of a single family member has only minimal affects on T cell development, suggesting compensating functions of the family members, and emphasizing a need to study expression and function of the whole Ikaros family. We analyzed the expression of all five family members in human and murine thymocytes as they progressed from the $CD4^{-}CD8^{-}$ double negative (DN) to the $CD4^{+}CD8^{+}$ double positive (DP) developmental stages, and found differences in the expression of Helios and Eos mRNA between the two species. Further, whereas Ikaros and Aiolos mRNA levels increased in both species, protein levels only increased in murine thymocytes. These data suggest that regulation of Ikaros family expression during T cell development differed between the two species.

To further examine expression of Ikaros family members during human T cell development, we used multi-parameter flow cytometry to identify subpopulations of human thymocytes. We defined seven populations of $CD3^{-}$ $CD4^{+}CD8^{-}$ immature single positive (ISP) and $CD3^{-}$ DP cells to identify when TCRβ is expressed. We were able to delineate the pre-β-selection ISP1 and DP1 populations and the TCRβ expressing ISP2 and DP2 populations using expression of CD1a, CD28, and CD44. The ISP2 and DP2 populations had a higher percentage of proliferating cells, consistent with these being post-β-selection stages. Protein levels of Ikaros, Helios, and Aiolos all increased with β-selection, however this increase was transient for Ikaros and Helios levels.

We further identified 22 populations of thymocytes that express CD3 and showed that CD4 expression is down-regulated after positive selection to create a $CD8^+CD4^{-/lo}$ transitional single positive (TSP) developmental stage. Commitment to the CD8 T cell lineage occurs in TSP thymocytes and is marked by expression of CD27. Among $CD4^+$ cells, expression of CD27 can first be seen in MSP2 $CD4^+$ thymocytes, suggesting that commitment to the CD4 lineage occurs at this stage. Ikaros levels increased during the DP9 stage, and Helios and Aiolos expression increased in TSP thymocytes. The increase in Helios was transient, and Helios levels decreased as cells developed through the MSP $CD4^+$ and MSP $CD8^+$ stages. Aiolos levels increased in cells proceeding from the TSP to the MSP $CD8^+$ stage. Within MSP $CD4^+$ thymocytes, Aiolos levels increased transiently beginning in the MSP2 $CD4^+$ thymocytes suggesting that increases in Aiolos protein are associated with CD4/CD8 lineage commitment.

Pediatric T cell acute lymphoblastic leukemia (T-ALL) is a heterogeneous disease that develops as a result of clonal expansion of thymocyte populations that bypass regulatory selection steps. We analyzed expression of the Ikaros family members in the leukemic cells from pediatric T-ALL patients and compared them to normal thymic populations, finding that mRNA levels of at least one Ikaros family member were elevated in the cells from every T-ALL patient analyzed. By comparing the ratio of the Ikaros family mRNA levels, we were able to classify the T-ALL patients into groups that showed diverse expression of surface markers. The lack of correlation between Ikaros and Aiolos mRNA and protein levels within the T-ALL suggest that further studies are needed to determine the significance of both mRNA ratios and protein levels in T-ALL patients. Further, studies are required to identify the roles of the Ikaros family members during the key selection steps of normal thymic development in order to understand how altered expression may contribute to leukemogenesis.

Acknowledgements

My deepest gratitude goes to those who have helped make the completion of this dissertation possible. First and foremost my appreciation must be expressed for the mentoring I received from Dr. Yankee: for his encouragement, his constructive criticism, and his patience. As much as a graduate degree is measured by the production of data and the completion of a dissertation, it is not complete without a development of critical thinking skills to analyze the data and develop new hypotheses. For his nurturing of the latter in me, I am most thankful to Dr. Yankee. Particular thanks must also go to the members of my committee for their continued input towards the development of my research project and analysis of the results. To Drs. Benedict, Peterson, Parmely, and Stephens: thank you for your critical analysis, wisdom, and difficult questions that made me look at my data from a new perspective.

Many thanks must go to the members of the Yankee lab over the course of my career. In particular, I would like to thank Brooks Parker for teaching me the ropes when I joined the lab and for always being able to get experiments to work when I couldn't. My gratitude must also be expressed to Amara Seng for helping me get the most out of a thymus and supporting my coffee habit. To the members of the Flow Core, Dr. Rich Hastings, Alicia Zeiger, and Sonia Soto, who stayed late while spending hours sorting thymocyte populations with me, thank you. Additionally, I would like to thank Drs. Steve Benedict, Marci Chan, Mary Markiewicz, members of their labs, and members of the Immunology Group for allowing me to regularly present my data and asking pertinent, thought provoking questions.

These experiments would have been impossible without the thymi and T-ALL samples that were analyzed. My best wishes go to the children from which the samples came. Many thanks must also go to their parents for giving consent. Special thanks go to Diana Connelly for

working so hard to obtain thymus samples for me, as well as Dr. Robert H. Ardinger, Jr., Dr. James E. O'Brien, Jr., and Jennifer Marshall for their assistance. Thank you also to Dr. Keith August for his assistance in obtaining T-ALL samples.

Finally, I would not have completed this work without support from friends and family. My friends have kept me sane throughout this process: supporting my sports addiction, eating the results of my baking therapy, laughing with me, and encouraging me. To my family, thank you for putting up with me for all these years: the excessive singing, talking, and requests for proper manners. In the end, I blame you and the support you gave me growing up, encouraging me to like math, science, and puzzles, for the research pains of these past years. Of course, without those pains, this work wouldn't be complete. Thank you all for encouraging me on this journey.

Table of Contents

List of Figures

List of Tables

Abbreviations

Ai-Δn – Aiolos splice variant missing exon "n"

AIRE – autoimmune regulator

APL – altered peptide ligand

APC – antigen presenting cell

Btk – Bruton's tyrosine kinase

C - constant

Cat - cathepsin

CBP – $CD34^{+}lin^{-}$ cord blood progenitors

CDK9 – cyclin-dependent kinase 9

CK2 – casein kinase 2

CLIP – class II-associated Ii peptide

CT – cytoplasmic tail

cTEC – cortical thymic epithelial cell

D - diversity

DAPI – 4',6'-diamidino-2-phenylindole

DC – dendritic cell

DL – Delta-like

DN – double negative

DP – double positive

ECD – extracellular domain

ER – endoplasmic reticulum

ERK – extracellular signal-related kinase

ETP – early thymic progenitor

FTOC – fetal thymic organ culture

GMFI – geometric mean fluorescence intensity

GSI – γ-secretase inhibitor

H3K27me^3 – histone H3 lysine 27 trimethylation

Hel-Δn – Helios splice variant missing exon "n"

HSC – hematopoietic stem cell

ICN – intracellular Notch

icTCRβ – intracellular T cell receptor β

Ii – invariant chain

Ik$^{\Delta F1}$ – Ikaros isoform missing the first zinc finger

Ik$^{\Delta F4}$ – Ikaros isoform missing the fourth zinc finger

Ik-Δn – Ikaros splice variant missing exon "n"

Ik^{DN} – Ikaros dominant negative isoform

Ik$^{\Delta F1}$ – Ikaros isoform missing the first zinc finger

Ik$^{\Delta F4}$ – Ikaros isoform missing the fourth zinc finger

IL-7R – IL-7 receptor

IL-7Rα – IL-7 receptor α

ISP – immature single positive

ITAM - immunoreceptor tyrosine-based activation motif

J - joining

JNK - Jun amino-terminal kinase

MAPK – Ras-mitogen activated protein kinase

MHC – major histocompatability complex

MSP – mature single positive

mTEC – medullary thymic epithelial cell

NK – natural killer

NuRD – nucleosome remodeling and histone deacetylase

PC-HC – pericentromeric heterochromatin

PCR – polymerase chain reaction

PI3K – phosphatidylinositol 3-kinase

PKC – protein kinase C

PMA – phorbol myristate acetate

pMHC – peptide/MHC complex

PP1 – protein phosphatase 1

PRC2 – polycomb repressive complex 2

pTα – pre-T cell receptor α-chain

$pT\alpha^{b}$ – pre-T cell receptor α-chain variant missing the extracellular IgG domain

P-TEFb – positive-transcription elongation factor b

qRT-PCR – quantitative reverse transcription polymerase chain reaction

RAG – recombination-activating gene

SCID – severe combined immunodeficiency

SOCS1 – suppressor of cytokine signaling-1

SP – single positive

SWI/SNF – switching defective/sucrose non-fermenting

SYK – spleen tyrosine kinase

T-ALL – T cell acute lymphoblastic leukemia

TCR – T cell receptor

TdT – terminal deoxynucleotidyl transferase

T_{reg} – regulatory T cell

TSA – tissue specific antigen

TSP – transitional single positive

TSSP – thymus-specific serine protease

V - variable

Chapter 1. Introduction

T cells are a major contributor to the functional immune system. There are two classes of T cells, αβ T cells and γδ T cells, which are identified by the T cell receptor (TCR) chain heterodimer that they express. αβ T cells compose 95% of the T cell population in the blood and peripheral lymphoid organs and can be separated into two major subpopulations according to their expression of the CD4 or CD8 co-receptor. $CD4^+$ T cells are known as helper T cells and produce cytokines necessary for activation and differentiation of other immune cells. $CD8^+$ T cells are cytotoxic cells that function to kill cells that are infected with intracellular pathogens or are cancerous.

Before they can function in the periphery, T cells must go through a highly regulated process of development. In order to add diversity to the TCR repertoire, TCR loci undergo V(D)J recombination. V(D)J recombination is an error filled process, and developmental checkpoints ensure that thymocytes produce functional TCR chains before they egress from the thymus. For development of αβ T cells, there are at least six major selection points: T cell lineage commitment, αβ/γδ lineage commitment, β-selection, positive selection, negative selection, and CD4/CD8 lineage commitment.

A thorough understanding of human T cell development is important for determining the mechanisms by which immunologic diseases develop and identifying potential therapeutics. The selection steps that regulate thymic development are associated with bursts of proliferation and increased susceptibility to apoptosis. Defects in proliferation and apoptosis can lead to the development of leukemia. Further, improper survival or apoptosis during selection can lead to autoimmunity or immunodeficiency, respectively. The Ikaros family transcription factors are key regulators of survival, proliferation, and differentiation during T cell development. The

current work focuses on the Ikaros family of transcription factors, their expression during selection steps in human thymic development, and their role in the development of T cell acute lymphoblastic leukemia (T-ALL).

Ikaros Family of Transcription Factors

Structure

This family of five proteins, Ikaros, Helios, Aiolos, Eos, and Pegasus, shares a similar structure containing two highly homologous zinc finger domains: a N-terminal DNA binding domain and a C-terminal dimerization domain (Fig 1-1A). Dimerization is required for high affinity DNA binding, and the two zinc fingers in the C-terminal domain mediate both homodimerization and heterodimerization with any of the other family members (1-5). The N-terminal DNA binding domain contains four zinc fingers for all family members except Pegasus, which only has 3 (Fig. 1-1B). The high homology at this domain between Ikaros, Helios, Aiolos, and Eos, allows for binding of a similar DNA consensus sequence (GGGAA) (Fig 1-1D), whereas Pegasus binds with high affinity to the consensus sequence GXXTGTXG (3, 4, 6). The Ikaros family members are also able to undergo alternative splicing, which can result in the loss of one or more zinc fingers from the DNA binding domain. Further, though the Ikaros family is highly conserved in humans and mice (7), alternative splice sites are used in the processing of human Ikaros to produce isoforms containing a sixty base pairs intronic sequence following exon 2 or missing thirty base pairs at the 3' end of exon 6 (Fig. 1-1C) (8-11).

DNA Binding

The DNA binding zinc fingers are encoded in three exons: one in exon 3, two in exon 4,

Figure 1-1. Ikaros family protein structure. *A*) The protein structure of Ikaros, Helios, Aiolos, and Eos. The four zinc fingers of the DNA binding domain (F1-F4) and the two zinc fingers of the dimerization domain (F5-F6) are shown (dark boxes). *B*) The three exons and five zinc fingers of the Pegasus protein are shown. *C*) Alternative splicing of human Ikaros mRNA can result in the insertion of 60bp after exon 2 (black box) or 30bp deletion at the 3' end of exon 6 (white box). *D*) Alignment of the amino acids flanking the DNA binding zinc fingers of the Ikaros family members. The cysteine and histidine residues that coordinate the zinc ions are highlighted in grey.

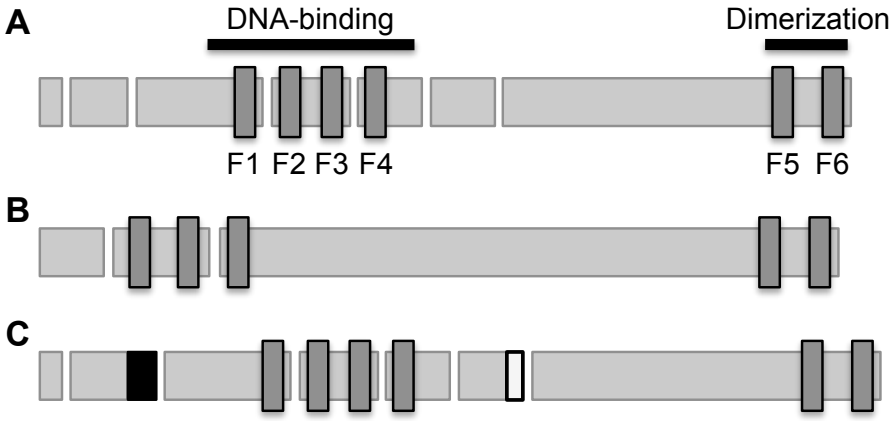

D

```
Ikaros     107 vggirlpngklkcdicgiicigpnvlmvhkrshtgerpfqcnqcgasftqkgnllrhiklhsge
Helios     102 eggirlpngklkcdvcgmvcigpnvlmvhkrshtgerpfhcnqcgasftqkgnllrhiklhsge
Aiolos     108 fdssrptsgkmncdvcglscisfnvlmvhkrshtgerpfqcnqcgasftqkgnllrhiklhtge
Eos        149 pggirlpngklkcdvcgmvcigpnvlmvhkrshtgerpfhcnqcgasftqkgnllrhiklhsge
Pegasus     73 -gfertfdgklkcrycnyaskgtarliehirihtgekphrchlcpfasayerhleahmrshtge

Ikaros     171 kpfkchlcnyacrrrdaltghlrthsv-----gkphkcgycgrsykqrssleehkerchnylesm
Helios     166 kpfkcpfcsyacrrrdaltghlrthsv-----gkphkcnycgrsykqrssleehkerchnylqnv
Aiolos     172 kpfkchlcnyacqrrdaltghlrthsv-----ekpykcefcgrsykqrssleehkercrtflqst
Eos        213 kpfkcpfcnyacrrrdaltghlrthsvssptvgkpykcnycgrsykqqstleehkerchnylqsl
Pegasus    137 kpykcelcsfrcsdrsnlshhrrrkhk-----mvpik--------gtrsslsskk----------
```

and one in exon 5. The second and third zinc fingers are required for binding to the consensus sequence, GGGAA (12, 13). The first and fourth zinc fingers impart more specific gene targeting, and their loss, through alternative splicing of exons 3 and 5, results in more promiscuous DNA binding and a more diffuse nuclear localization pattern (1, 6, 14). These different isoforms not only bind DNA sequences with varying affinity, but also are capable of differentially activating or repressing transcription (6, 14, 15). In particular, abnormalities in T cell development were more severe in mice expressing an Ikaros isoform missing the fourth zinc finger ($Ik^{\Delta F4}$) than one missing the first zinc finger ($Ik^{\Delta F1}$), with aggressive T cell lymphomas developing in the former (14). RNA-Seq analysis revealed that expression of $Ik^{\Delta F4}$ resulted in up-regulation of more genes than expression of $Ik^{\Delta F1}$, particularly those associated with cell adhesion, cell communication, and signal transduction. Loss or mutation of the second and third zinc fingers produces a dominant negative isoform that is unable to bind DNA, but can still heterodimerize with other family members and prevent their DNA binding (1, 12, 16).

Subcellular Localization

Subcellular localization can be affected through alternative splicing and loss of phosphorylation sites not associated with the zinc finger domains. Full length Ikaros isoforms with the exon 2 insertion have different DNA binding preferences and have a more diffuse nuclear localization than full length Ikaros without the insertion (17). Ikaros family isoforms normally show punctate nuclear staining at pericentromeric heterochromatin (PC-HC), however some isoforms have cytoplasmic localization and can recruit other isoforms to the cytoplasm (1, 6, 15). The isoforms located in the cytoplasm are missing multiple exons, and interestingly, while not all cytoplasmic isoforms are missing exon 6, the loss of exon 6 results in a change in

localization. Thus, both expression of different family members and different isoforms can affect DNA binding and function of the Ikaros family.

Ikaros function and DNA binding is also regulated by phosphorylation. Ikaros can be phosphorylated at multiple sites by casein kinase 2 (CK2), at conserved linker sequences between the DNA-binding zinc fingers by an as yet unidentified kinase, and at two sites each by spleen tyrosine kinase (SYK) and Bruton's tyrosine kinase (Btk) in B cells (18-24). Phosphorylation within the linker sequences is conserved among proteins with C2H2 zinc finger proteins similar to Ikaros, and mediates detachment from the DNA during the G_2/M phase of the cell cycle (18). Phosphorylation by SYK and Btk are required for nuclear localization of Ikaros and increased DNA binding affinity, whereas CK2 mediated phosphorylation at amino acids 13 or 294 prevents PC-HC localization of Ikaros and decreases binding affinity (19-21). Interestingly, activation of thymocytes with phorbol myristate acetate (PMA) and ionomycin resulted in dephosphorylation of Ikaros at amino acids 13 and 294, increased binding to the TdT regulatory element, and TdT transcriptional repression (20). CK2 dependent phosphorylation of a region in exon 7 of Ikaros is also necessary for progression through the cell cycle (22). Retroviral transduction of NIH 3T3 fibroblasts with Ikaros resulted in a cell cycle arrest in the late G_1 phase. The block in cell cycle progression was increased when CK2 phosphorylation sites were mutated to alanines, and abrogated in cells expressing an Ikaros DNA-binding mutant. Dephosphorylation of CK2-specific sites is mediated by PP1, resulting in increased DNA binding, PC-HC localization of both Ikaros and PP1, and increased protein stability (25). Together, these results point to the importance of posttranslational modifications to control Ikaros DNA binding and cellular localization. Though it has been shown that phosphorylation can similarly affect Aiolos localization and gene regulation (26), further studies are needed to

determine the mechanisms and affects of posttranslational modifications of Helios, Aiolos, Eos, and Pegasus.

Regulation of Gene Transcription

The Ikaros family is able to both activate and repress gene transcription. Ikaros, Aiolos, and Helios have all been shown to associate with the nucleosome remodeling and histone deacetylase (NuRD) complex (27-30). The NuRD complex has subunits capable of inducing ATP-dependent chromatin remodeling and histone deacetylation (31-33). The interaction of Ikaros with NuRD has been associated with gene repression, as seen in the ability of Ikaros family members to silence Notch target genes, as well as the *Il2* locus in anergy and tolerance (34-38). However, recent studies have identified both Ikaros and NuRD associated with transcriptionally active genes (27, 39, 40). A role for Ikaros in regulating transcription elongation was suggested by its association with cyclin-dependent kinase 9 (CDK9), the catalytic subunit of P-TEFb, as well as protein phosphatase 1 (PP1), a positive regulator of P-TEFb function and Ikaros DNA binding (25, 40, 41). Recently it was shown that a small percentage of Ikaros co-purified with subunits of P-TEFb, NuRD, and PP1, and this complex was required for transcription elongation at the *c-Kit* locus (40). This study suggested that higher levels of Ikaros were required for the recruitment of an elongation-competent NuRD/P-TEFb complex and PP1 to genes with stalled RNA polymerase II. Thus, increases in Ikaros expression in thymocyte subsets may serve to transition Ikaros from a transcriptional repressor to a transcriptional activator associated with the elongation-competent NuRD/P-TEFb complex.

Ikaros has also been associated with other chromatin remodeling complexes. Ikaros is able to interact with the polycomb repressive complex 2 (PRC2) and recruit it to repressed genes

to induce histone H3 lysine 27 trimethylation ($H3K27me^3$) (42). Ikaros-PRC2 interactions appear to be involved in regulating Notch target genes, as these genes are ectopically expressed in Ikaros deficient DP cells and show reduced $H3K27me^3$ marks (27, 43, 44). Ikaros also associates with the chromatin remodeling switching defective/sucrose non-fermenting (SWI/SNF) complex in T cells, and this interaction may be required for rearrangement of the *TCRA* locus (28, 45).

The Role of the Ikaros Family in T Cell Development

The Ikaros family of transcription factors is necessary for the development of T cells, B cells, and NK cells in mice (46). Homozygous expression of a dominant negative Ikaros isoform ($Ik^{DN/DN}$) resulted in a developmental block in the differentiation of common lymphoid progenitor cells in the bone marrow. The dominant negative isoform lacks the DNA binding domain zinc fingers of Ikaros but retains the ability to heterodimerize with the other family members, also altering their function (1). Thus, $Ik^{DN/DN}$ mice lack most, if not all, Ikaros family function. In contrast, $Ik^{DN/+}$ mice produce T cells, but rapidly develop T cell leukemias after loss of the single wild-type allele and clonal expansion within the thymus (47). Further, T cell leukemia/lymphoma also developed in $Hel^{DN/DN}$ mice, $Ik^{\Delta F4/\Delta F4}$ mice, and $Ik^{Plstc/+}$ mice, which have a single base mutation in the third zinc finger that inhibits DNA binding (14, 48, 49). The phenotypes of these mice suggest that the Ikaros family is necessary for differentiation to the T cell lineage and proper regulation of proliferation in developing thymocytes in order to prevent leukemogenesis.

While elimination of the function of the whole family causes profound defects, T cell development is only minimally affected in mice that are deficient in a single Ikaros family

member. Ikaros null mice ($Ik^{-/-}$) are able to develop T cells after birth, but lack fetal T cells (50). In contrast, neither $Hel^{-/-}$ nor $Ai^{-/-}$ mice show major defects in T cell development (51, 52). However, T cells in all of these models have increased proliferation in response to TCR signaling. The differences in severity between the null mice and dominant negative mice suggest a redundancy of function between the Ikaros family members, and that reduced functionality of multiple Ikaros family members is required for rapid development of T cell leukemias. Thus, it is important that studies examine the expression and function of the entire family of proteins in relation to one another.

Studying the whole Ikaros family is also important because each family member can affect transcription differently. For instance, in chicken B cells, expression of the Src homology 2-containing-inositol 5-phosphatase (SHIP) was up-regulated in Ikaros deficient cells but down-regulated in Helios deficient cells (53). Further, it has been shown that Aiolos is a more potent transcriptional activator than Ikaros, which is more potent than Helios (2, 5, 54). Even small changes in expression of one family member can have drastic affects on the cell. Transgenic mice developed B cell lymphomas after Helios was expressed in B cells at a level ten-fold lower than Ikaros (55). Further studies are needed to determine how heterodimerization of different family members affects gene targeting and function.

Regulation of Ikaros family expression and function is important for proper lymphopoeisis. Chromatin immuoprecipitation studies found that Ikaros can bind over 10,000 genomic sites associated with 6,746 genes (27, 43, 54). Potential Ikaros binding sites can be found in the promoters and enhancers of a number of genes critical for T cell development including those for Rag-1, Rag-2, TdT, pTα, TCRα, TCRβ, CD3γδ, CD3ε, Notch, IL-7R, IL-2R, IL-2, CD4, and CD8α (6, 44, 54, 56-67). Further, Ikaros family members can regulate

expression of proteins involved in survival, cell cycle progression, and the phosphatidylinositol 3-kinase (PI3K) signaling pathway, as well as other transcription factors including Ikaros, Aiolos, Eos, and Pegasus themselves (26, 44, 54, 59, 60, 68-76). Finally, the Ikaros family DNA binding consensus sequence is the same as that for the Notch co-factor RBP-Jκ, and Ikaros members can competitively bind and regulate Notch target genes (14, 43, 44, 60, 77). Notch signaling is required for proliferation and differentiation at multiple selection steps during thymic development, and the Ikaros family may be involved in regulation of Notch signaling at these steps.

The Role of the Ikaros Family in T Cell Acute Lymphoblastic Leukemia

T-ALL is a heterogeneous disease, with leukemic cells being derived from different stages throughout T cell development (78-80). T-ALL patients are grouped according to the expression of surface markers used to identify normal thymic populations (80) or expression of TCR chains by the leukemic cells (78). There is conflicting data regarding whether these surface markers can be used to predict patient outcomes. While one group determined that patients with leukemic cells expressing a pre-TCR had a better four-year disease free survival rate than those lacking intracellular TCRβ expression or expressing a mature TCR (79), another group found no difference between these groups (81). Likewise, CD34 expression has been associated with poor prognosis by one group, but not by another (82, 83). The different findings in these studies may be due to the heterogeneity of the T-ALL cells. For example, some $CD34^+$ T-ALL cells do not express a TCR, similar to normal DN cells, while other $CD34^+$ T-ALL cells do express a TCR, unlike any normal thymic population. Further studies attempting to associate protein expression

and prognosis thus will either need to include multiple surface markers, or focus on the underlying mechanisms within the cell that are regulating surface protein expression.

A role for the Ikaros family in the development of T-ALL was first suggested by the rapid development of leukemia in $Ik^{DN/+}$ mice with one hundred percent penetrance (47). A role for Ikaros family members in pediatric T-ALL has not been established. While some studies reported the expression of dominant negative isoforms of Ikaros in all cases of pediatric T-ALL studied (8-10), others were only able to find these isoforms in a few cases (84-92). Aberrant Helios isoforms and loss of Helios have been reported in cases of adult T-ALL (93-96), but are as yet to be reported in pediatric T-ALL. In contrast, aberrant expression of Ikaros family members has been reported in B cell and myeloid leukemias (87-92, 97-103). Further, Aiolos expression is up-regulated in cases of B cell chronic lymphocytic leukemia (104-106). These data suggest that aberrant Ikaros family member expression does occur in human hematopoietic malignancies, though it is not highly associated with T-ALL as expected from murine models.

The limited identification of altered Ikaros family expression in T-ALL brings to question differences in the function and expression of these proteins in murine and human thymocytes. The Ikaros literature focuses on the function of Ikaros itself in murine thymocytes. Further studies are needed that assess expression and function of all family members, particularly in human thymocytes. In order to identify roles for these proteins in human thymocyte development and leukemogenesis, a more thorough understanding of the processes of human thymocyte development and selection is necessary.

Human αβT Cell Development

Although there are similarities between murine and human T cell development, there are

also significant differences that discourage a complete reliance on murine models to make inferences about the mechanisms regulating human thymic development. In general, both murine and human thymocytes progress from a $CD4^{-}CD8^{-}$ (DN) stage to a $CD4^{+}CD8^{+}$ double positive (DP) stage before maturing to either a single positive (SP) $CD4^{+}$ or SP $CD8^{+}$ cell prior to thymic egress. However, the surface markers used to identify some subpopulations differ between the species. Whereas murine DN subpopulations are identified according to their expression of CD44 and CD25 (107), human DN subpopulations are identified by their expression of CD34, CD38, and CD1a (108, 109). Further, human DN thymocytes up-regulate CD4 first to become immature single positive (ISP) $CD4^{+}$ cells before entering the DP stage (110), but murine thymocytes transition through an ISP $CD8^{+}$ stage (111). The altered expression of surface markers between the species is indicative of more substantial differences in signaling and transcriptional regulation, and makes direct comparisons between murine and human thymocyte populations difficult.

Thymocytes in both species must rearrange their TCR loci and proceed through similar selections steps to complete development. However, there are differences in what stage of development the selections steps occur, how cells respond to thymic signals, and the genes that are expressed in response. For instance, strong Notch signals induce αβ T cell development in murine thymocytes, but γδ T cell development in human thymocytes (112-114). Further, TCRβ protein is expressed in DN murine thymocytes, but is not found until the ISP or DP stage of human T cell development (115-119). These differences have implications on the signals that thymocytes receive for survival, proliferation, and differentiation, and thus may be important for species-specific mechanisms of disease development.

While the literature describing T cell development in the murine thymus is vast, there is limited information on human thymocyte development. In depth studies of human development are necessary to identify the mechanistic differences between the species and gain a better understanding of human T cell related disease development. Within this chapter, we review the lineage commitment and selections steps for αβT cell development, focusing on what is known in human T cell development when possible.

T Cell Lineage Commitment

T cells are derived from hematopoietic stem cells (HSCs) in the bone marrow, but complete their development in the thymus. As cells differentiate toward the lymphoid lineage, they lose their self-renewal capabilities as well as their ability to differentiate along the megakaryocyte/erythroid and myeloid pathways. Early thymic progenitors (ETPs) do not express the co-receptors CD4 or CD8 and are thus referred to as DN thymocytes. The immature nature of these cells can be seen by their expression of CD34 and their lack of TCR components (120). DN cells in the human thymus are commonly separated into three populations based on their expression of CD38 and CD1a: $CD38^{-}CD1a^{-}$ DN1 cells, $CD38^{+}CD1a^{-}$ DN2 cells, and $CD38^{+}CD1a^{+}$ DN3 cells (109). Human DN thymocytes first up-regulate CD4 to enter the $CD4^{+}CD8^{-}$ ISP stage, then cells enter the DP stage with expression of CD8 (121). Prior to thymic egress, cells down-regulate either CD4 or CD8 to become mature single positive (MSP) cells that can function in the periphery.

ETPs maintain the ability to differentiate into T cells, natural killer (NK) cells, and dendritic cells (DCs) (122-126). As DN thymocytes develop, they become restricted to the T cell lineage. Whereas DN2 thymocytes have potential for DC and NK differentiation, DN3

thymocytes differentiate almost exclusively into T cells (127). Restricted potential to the T cell lineage is also associated with down-regulation of CD34 (122). Thus ETPs are tripotent for the T cell, NK cell, and DC fates, but differentiation is restricted to the T cell fate as CD34 expression is lost and CD1a expression is gained.

Commitment to the T cell lineage occurs when thymocytes begin to rearrange the TCR loci. The TCR chains are composed of a variable and a constant region. The variable region is generated through recombination of variable (V), diversity (D), and joining (J) segments within the TCR loci. The variable regions of TCRα and TCRγ are composed of only V and J segments, whereas TCRβ and TCRδ variable regions contain V, D, and J segments. There are multiple V, D, and J segments within in each locus, allowing for many potential V(D)J combinations.

Recombination is initiated by the introduction of double stranded breaks at the 5' end of the heptamer of the RSS sites by the recombination-activating genes (RAG-1 and RAG-2). This break leaves a hairpin end on the coding sequence for the gene segment. The RAG protein complex makes a single stranded break at a random site close to the hairpin, forming a single stranded tail that is made of the original coding sequence and its palindromic sequence, or P-nucleotides. Non-encoded N-nucleotides can then be added to the tail by terminal deoxynucleotidyltransferase (TdT). Nucleotides may also be deleted from the tail by exonuclease activity. Finally, the strands adjacent to the two segments are paired and joined by the nonhomologous end joining machinery. Diversity is thus introduced into the TCR heterodimer repertoire through the use of different combinations of V(D)J segments, the introduction of P- and N-nucleotides at the junction, deletion of nucleotides at the junction by exonuclease activity, as well as the random combination of TCRα/β or TCRγ/δ heterodimers.

Recombination events occur sequentially in the *TCRδ, TCRγ, TCRβ,* and *TCRα* gene loci (109, 115). DN1 cells are tripotent and have all TCR loci in the germline configuration, with the exception of <10% of cells that show Dδ2-Dδ3 recombination (109). The frequency of Dδ2-Dδ3 recombination increases with differentiation to the DN2 stage, and Dδ2-Jδ1 recombination events can be detected in these cells. Though complete Vδ1-Jδ1 and Vδ2-Jδ1 transcripts can be detected within DN3 cells, approximately 15% of DN3 cells still have the *TCRδ* locus in the germline configuration, consistent with the finding that a limited number of $CD1a^+$ DN cells have the ability to differentiate into NK cells (109, 115, 127). Germline configuration of the *TCRδ* locus was not detected in the ISP population (115). As conventional NK cells only express germline TCRδ transcripts (128, 129), these data suggest that T cell lineage commitment begins in the DN2 stage and is mostly complete within DN3 cells. Consistent with this timing of commitment, DN2 thymocytes express low levels of mRNA for the pre-T cell receptor α-chain (pTα), but mRNA levels increase significantly within DN3 cells (130).

Notch signaling has been identified as a key pathway in determining restriction to the T cell fate. There are four Notch receptors (Notch1-4) that can bind either the Delta-like (DL1, DL3,and DL4) or Searate-like (Jagged 1 and Jagged2) ligands to produce differential signals (131). Upon ligand binding, the Notch proteins undergo two proteolytic cleavage events, releasing the active intracellular Notch domain (ICN). The ICN moves to the nucleus where it regulates activation of a network of genes. T cell differentiation can be induced in human $CD34^+lin^-$ cord blood progenitors (CBPs) that are cultured on OP9-DL1 cells, a murine bone marrow derived stromal cell line expressing the DL1 ligand, but not untransduced OP9 cells (132, 133). Likewise, expression of the Notch1 ICN in CBPs inhibits differentiation of myeloid cells and B cells on MS-5 cells, a murine bone marrow derived stromal cell line, while

promoting differentiation of pre-T/NK cells (134). These ICN-transduced CBPs are also capable of ectopic differentiation of $CD3^+$ DP T cells in the bone marrow of sublethally irradiated NOD-SCID mice at the expense of monocyte and B cell differentiation. Conversely, inhibition of Notch cleavage via administration of a γ-secretase inhibitor (GSI) in an *in vitro* human-mouse fetal thymic organ culture (FTOC) system hinders T cell development while promoting differentiation of DCs, B, and NK cells (135).

Differences in expression of Notch ligands in the bone marrow and thymus may help to restrict T cell development to the thymus. ETPs enter the thymus at the cortical-medullary junction and traverse the cortical zone to the subcapsular region as they differentiate through the DN and ISP stages (136). DL4 and DL1 protein are expressed at low levels on cortical thymic epithelial cells (cTECs), and Jagged2 protein is abundantly expressed on both cTECs and medullary thymic epithelial cells (mTECs) (137). DL1, DL4, and Jagged2 are able to promote T cell development from CBPs and induce expression of Notch3 (132, 133, 137, 138). Notch3 is expressed on the earliest $CD34^+CD1a^-$ thymocytes but not CBPs (130, 131). Notch3 and Jagged2 provide the strongest Notch signaling, and their expression in the thymus may help to provide the strong Notch signal necessary for initial commitment to the T cell lineage (131, 135). Further, commitment to the T cell lineage may be restricted to the thymus by the expression of Jagged1 in the bone marrow instead of Jagged2 (138-142). Retroviral expression of Jagged1 on OP9 cells inhibits T cell differentiation of CBPs, and Jagged1 mRNA expression is limited to mTECs in the thymus (131, 137).

Notch activation alone is not sufficient for development of T cells, IL-7 signaling is required for T cell lineage differentiation in the thymus. Although retroviral expression of Notch1 ICN in thymic precursors can inhibit non-T lineages, cells are blocked at an early stage

of T cell development (134, 143). These cells up-regulate transcription of *RAG-1* and Notch target genes, but do not progress to the DN3 stage. Notch1 signaling also up-regulates and maintains IL-7 receptor α (IL-7Rα) expression on the cell surface (143, 144). IL-7 is required for survival of DN thymocytes when cultured with OP9 cells (144). Retroviral expression of the IL-7Rα on CBPs is not able to restrict differentiation to the T cell lineage, but promotes T cell differentiation past the DN2 stage (143). Consistent with a need for IL-7 signaling for differentiation, when CBPs from patients with severe combined immunodeficiency (SCID) caused by mutations in IL-7Rα were transferred into NOD-*Scid*-*Il2rg*$^{-/-}$ mice, T cell differentiation was blocked at an early CD1a^{-} stage prior to initiation of Dδ2-Dδ3 rearrangements (145).

Together these data suggest that strong Notch signaling upon thymic entry is needed to restrict cells to the T cell lineage and increase expression of Notch target genes, including IL-7Rα. Il-7R signaling is then necessary for further early T cell differentiation. IL-7 is also required for survival and proliferation of thymocytes prior to expression of a TCR, and survival and proliferation are increased with concurrent Notch signaling (144).

γδ/αβ Lineage Commitment

γδ T cells comprise an average of less than 5% of T cells in peripheral blood, lymphoid organs and epithelial layers, with the exception of increased presence in the splenic red pulp and intestinal epithelium (146-150). Though small, this population of cells is thought to play important rolls in the early defense against pathogens at mucosal membranes and cancer surveillance. The TCRδ and TCRγ chains are the first to complete rearrangement in the thymus (78, 109, 115). The human *TCRD* locus contains three Dδ segments (Dδ1-3), three Jδ segments

(Jδ1-3), and one constant region segment (Cδ) (109, 115). The location of the *TCRD* gene within the *TCRA* gene has made it difficult to distinguish Vα and Vδ gene segments, but six possible Vδ segments have been identified (Vδ1-6), with Vδ1 and Vδ2 preferentially used in human thymocytes and peripheral γδT cells, respectively. Complete Vδ1-Jδ1 and Vδ2-Jδ1 rearrangements can be seen in a small proportion of DN3 thymocytes and over 50% of ISP thymocytes. The human *TCRG* has eleven Vγ segments (Vγ1-11) and five Jγ (Jγ1.1-1.3, Jγ2.1, and Jγ2.3) segments associated with two constant regions (Cγ1-2). Vγ-Jγ1.1/2/1 rearrangements occur in the DN2 and DN3 stages of thymic development, whereas Vγ-Jγ1.3/2.3 rearrangements are not abundantly seen until the DN3 stage and peak in $CD3^-$ DP and $CD8^+$ MSP cells. Although these Vγ-Jγ1.3/2.3 rearrangements are preferentially used in the thymus in both $TCR\gamma\delta^+$ and $TCR\alpha\beta^+$ thymocytes, Vγ-Jγ1.2 rearrangements are rare in the thymus but preferentially seen in peripheral blood γδT cells.

These data suggest that TCR-dependent selection of γδT cells can occur as early as the DN3 stage, but human thymocytes retain γδT cell potential through the DP stage of development (116, 151). DN3, $CD4^+$ ISP, and early DP were all capable of differentiating into γδT cells in a human-mouse FTOC (116). The final CD4 and CD8 phenotype of the resultant γδT cells were not reported after FTOC. Freshly purified immature $CD1a^+$ $TCR\gamma\delta^+$ thymocytes express RAG-1 mRNA and have DN, CD4 SP, and DP phenotypes (151, 152). Mature $CD1a^-$ $TCR\gamma\delta^+$ thymocytes, however, have only a DN or CD8 SP phenotype, consistent with peripheral γδT cell phenotypes (148, 152).

Rearrangement of the *TCRB* gene for development of αβT cells occurs later in development. The *TCRB* locus contains two paired D and C segments (Dβ1/Cβ1 and Dβ2/Cβ2) separated by six or seven J segments, respectively (Jβ1.1-1.6 and Jβ2.1-2.7), and fifty-two

potential V segments (109). Dβ-Jβ rearrangements can first be seen in a large number of DN3 cells using mostly Jβ1 segments, and increase in ISP cells with a switch to Jβ2 usage (109, 115). A high frequency of in frame V(D)J rearrangements are first seen in ISP cells using Jβ2 rearrangements, and $CD3^-$ DP cells using Jβ1 rearrangements. When a TCRβ protein is expressed, it pairs with the pTα protein to form the pre-TCR. As pTα mRNA is expressed in $CD34^+$ cells prior to thymic entry (118), expression of the pre-TCR can occur upon expression of TCRβ after in frame *TCRB* rearrangements in the ISP and DP stages (115, 117, 119).

Both γδT cell selection and β-selection can occur during the ISP and DP stages of development (116, 117, 119, 151), thus some difference in signaling must help distinguish between TCRγδ and TCRαβ lineage. Three models have been proposed for αβ/γδ lineage commitment: the stochastic model, the instructive model, and the signal strength model. The stochastic model presumes that αβ/γδ lineage commitment occurs early in development prior to expression of any TCR chains, and only cells that produce functional TCR chains that match their predetermined lineage survive. This model was developed to explain the development of DP cells in $TCR\beta^{-/-}$ and TCRγδ transgenic mice (153, 154). As progression to the DP stage was considered to signify commitment to the αβ lineage in murine thymocytes and occurred in the absence of pre-TCR expression, these results were taken as support that lineage commitment occurred independent of TCR signaling.

The instructive model posits that it is the functional TCRγδ or pre-TCR produced by the cell that instructs the cells to enter the respective γδT or αβT cell lineages. Support for this model stems from the lack of in-frame γ and δ rearrangements in murine αβT cells, suggesting that cells that produced a functional TCRγδ are diverted from the αβ lineage (154-157). Recent studies using murine thymocytes suggest that the strength of signal received upon TCRγδ or pre-

TCR stimulation determines lineage fate, further developing the instructive model into the strength of signal model. γδ T cell development is promoted by stronger TCR signals while weaker signals promote αβ T cell development (158-160). Supplementation of a weak TCRγδ signal with a pre-TCR signal induces γδT cell development (160), whereas attenuation of TCRγδ signal promotes development to the DP stage (158).

Studies of γ, δ, and β rearrangement in mature human TCRγδ or TCRαβ expressing thymocytes, peripheral blood lymphocytes, and T-ALL cells support the instructive model. Nearly all TCRαβ$^+$ cells had completely rearranged the *TCRD or TCRG* locus, but these were rarely in frame, particularly at the *TCRD* locus (116, 161, 162). Production of in-frame rearrangement of both the *TCRD* and *TCRG* was estimated to occur in less than 7% of αβ thymocytes, and production of a functional TCRγδ would be further limited in these cells due to limited functional pairing of γ and δ chains (116). These data suggest that functional TCRγδ production precludes a cell from adopting the αβT cell lineage. In contrast, complete rearrangement at the *TCRB* locus was rare in TCRγδ$^+$ cells, averaging only 8.7% of γδ thymocytes as measured by *Joachims, et al.,* but partial rearrangement of *TCRB* was extensive (116, 161-163). This latter finding is not surprising given that completed γδ rearrangements are not seen until the DN3 stage, at which time Dβ-Jβ rearrangements have already begun. The low prevalence of complete *TCRB* rearrangements in γδ thymocytes supports data suggesting that γδT cell potential is highest in less mature cells but is retained through the DP stage when complete *TCRB* rearrangements are abundant (116, 151).

Studies into the signal strength model of human TCRγδ and pre-TCR are limited. One study measured the production of TCRαβ$^+$ and TCRγδ$^+$ thymocytes after transduction of CD34$^+$ or ISP thymocytes with a constitutively active form of the tyrosine kinase Lck, which is involved

in TCR signaling (115). Intermediate expression of Lck in $CD34^+$ thymocytes had no effect on the production of $TCR\gamma\delta^+$ thymocytes, but led to a large decrease in the production of $TCR\alpha\beta^+$ and a block at the ISP stage of development. Intermediate expression of Lck in ISP thymocytes had a similar negative effect on $TCR\alpha\beta^+$ thymocyte development, but increased $TCR\gamma\delta^+$ thymocyte production. High expression of Lck in either subset inhibited development of all TCR^+ thymocytes. These results suggest that signal strength may have different effects on lineage selection at different stages of development, and that TCRγδ strength may be lower in human thymocytes, as intermediate Lck levels did not induce negative selection in these cells.

Notch signaling is important for differential development of γδT and αβT cells. Whereas strong Notch signaling in early thymocytes is required for αβT cell development of murine thymocytes (112-114), strong signals are required for γδT cell development of human thymocytes (121, 130, 164). Inhibition of Notch signaling with a GSI increased the ability of DN2 or DN3 human thymocytes to develop into DP and express a TCRαβ, while decreasing the number of γδT cells produced upon culture with OP9-DL1 or OP9-DL4 cells (130). Likewise, ICN-transduction of $CD34^{hi}$ ETP increased the development of $TCR\gamma\delta^+$ cells and reduced the development of $TCR\alpha\beta^+$ in a human-mouse FTOC (164). More specifically, development of human $TCR\gamma\delta^+$ thymocytes is increased via Notch3 interactions with Jagged1 or Jagged2, but not DL4 (131), and culture of $CD34^{hi}$ ETP on OP9-DL1 cells in the presence of GSI decreases the expression of Notch3 mRNA in a dose dependent manner (130). These data suggest that the differential expression of Notch3 in human thymocytes but not in murine thymocytes may contribute to the different roles of Notch in the αβ/γδ lineage choice in the two species.

β-Selection

Cells differentiating along the αβ lineage must first successfully rearrange the *TCRB* locus. Following successful *TCRB* rearrangement, a functional TCRβ protein pairs with the invariant pTα chain, as well as CD3-δ, ε, γ, and ζ chains, to form the pre-TCR complex. The pTα has unique features that distinguish it from TCRα and contribute to the localization and signaling of the pre-TCR. The human pTα cytoplasmic tail (CT) is important for pre-TCR localization and function. At 114aa long, the human pTα CT is longer than both the TCRα CT (6-8aa) and murine pTα CT (30aa). Both the murine and human pTα CT contain a juxtamembrane cysteine residue that can be palmitated to direct surface localization of the pre-TCR to lipid rafts where it will be in close proximity to other signaling proteins (165, 166). The pTα CTs in both species also contain short proline-rich motifs, potential protein kinase C (PKC) substrate sites, and a CD2-like motif, all of which may participate in signal transduction through the pre-TCR (167, 168). The human pTα CT contains two unique motifs not found in the murine protein: an ER retention signal and a tyrosine-based internalization motif, both of which help to maintain low surface expression of pTα (168-170).

Unlike TCRα and TCRβ, which contain two extracellular IgG domains, pTα has only one extracellular IgG domain. The single IgG domain of pTα is able to interact with the constant IgG domain of TCRβ (Cβ) similar to the Cα domain of TCRα (171). The variable IgG domain of TCRβ (Vβ) has a hydrophobic patch that normally interacts with a similar hydrophobic region in the Vα domain of TCRα. Crystallographic studies of the human pTα/TCRβ complex revealed that pTα has a hydrophobic "top" that is able to interact with the hydrophobic region of Vβ from another pTα/TCRβ complex to form a dimer (171). This dual interaction of pTα with Cβ and Vβ suggests that pTα may play a chaperone role to ensure that both the Cβ and Vβ domains properly

fold. Expression of a pTα variant that is missing the extracellular IgG domain (pTα^{b}) or contains mutations of key hydrophobic amino acids in the IgG domain reduced surface expression of the pre-TCR and resulted in its retention in the endoplasmic reticulum (ER) in human T cell lines (171). This is in contrast to murine pre-TCR complexes composed of a pTα missing the extracellular domain, which successfully reach the cell surface and induce DP development (172, 173). The murine pTα would not be able to make the same contacts with Vβ due to the presence of an extra glycan in the region of interface, and lacks the ER retention signal in the CT to limit surface expression (168, 169, 174). These data suggest that the pTα extracellular domain plays a different role in murine and human thymus pre-TCR localization, and may serve a chaperone-like function that is necessary for surface expression in human thymocytes.

The pTα and CD3 chains are expressed prior to *TCRB* rearrangement (Mitchell, *et. al.*, unpublished data) (118, 175, 176), thus formation of the pre-TCR complex during development can occur after successful TCRβ expression. Production of a TCRβ protein that folds with pTα to form the pre-TCR may release the complex from the ER, allowing for localization to lipid rafts on the cell surface and signal transduction (165, 166, 171). Successful production of TCRβ and signaling through the pre-TCR is known as β-selection. Progress through β-selection is associated with cell proliferation, allelic exclusion of the *TCRB* locus, and opening of the *TCRA* locus for rearrangement (177-181).

The exact timing of β-selection in human thymocytes is not well understood. It has been suggested that β-selection could occur as early as the DN3 stage based on the identification of complete V(D)J rearrangement and one report of intracellular TCRβ (icTCRβ) expression in a minimal number of cells at that stage (109, 115, 116). Initial studies reported that β-selection occurred in the DP stage and was accompanied by expression of CD8β on the cell surface (119).

However, later studies reported that as many as 85% of early $CD4^{+}CD8\alpha^{+}CD8\beta^{-}$ DP cells expressed icTCRβ (115-117). Expression of icTCRβ was found in 5-40% of ISP cells in these studies (115-118), and was associated with expression of CD28 and CD71 (117).

Successful production of TCRβ and occurrence of β-selection may also be determined indirectly by measuring the resultant increase in proliferation. Early thymocytes maintain a low level of proliferation, with about 10% of cells in the S, G2, or M phase of the cell cycle (116, 118, 119). Expression of icTCRβ in ISP and DP thymocytes is associated with an increase in proliferation (118). Studies using $Rag^{-/-}$ mice, in which T cell development is blocked prior to β-selection, have shown that proliferation occurs as a result of pre-TCR signaling through similar pathways as TCRαβ activation. Both the PKC and Ras-mitogen activate protein kinase (MAPK) pathways are involved in mediating proliferation and differentiation downstream of pre-TCR signaling. Expression of TCRβ or activated forms of the signaling molecules Lck, PKC, Ras, or c-Raf-1 in $Rag^{-/-}$ murine DN thymocytes is able to induce proliferation, to restore thymic cellularity, and allow differentiation to the DP stage (182-185). Pre-TCR mediated proliferation is also dependent on Notch signaling, as human $CD28^{+}$ ISP cells did not undergo extensive cell division when cultured on OP9 stromal cells, but did when cultured on OP-DL1 cells (117).

Expression of TCRβ as part of the pre-TCR also results in allelic exclusion of the non-productive *TCRB* locus to ensure that only the productively rearranged TCRβ is expressed. Pre-TCR signaling leads to a decrease in Rag-1 and Rag-2 expression to prevent further rearrangement (117, 130). The exact mechanisms by which the non-productive *TCRB* locus is epigenetically modified to prevent expression are not well understood, but expression of a TCRβ transgene in murine thymocytes prevents rearrangement of the endogenous *TCRB* loci suggesting that pre-TCR signaling leads to allelic exclusion (186). Studies in murine thymocytes

suggest that the PKC pathway is involved in mediating allelic exclusion, as expression of activated forms of PKC or its upstream mediator Lck prevents TCRβ gene rearrangement (185, 187, 188). Expression of activated Ras or Raf does not inhibit TCRβ rearrangement at the DN stage, suggesting that the MAPK pathway is involved in proliferation and differentiation, but not initial allelic exclusion (183, 184). However, further studies found that Raf and the MAPK pathway activated transcription factor Ets1 are necessary for maintenance of allelic exclusion in the DP population when Rag proteins are re-expressed for *TCRA* rearrangement (189, 190).

After successful TCRβ production, the cell must be able to produce a functional TCRα protein to replace the pTα. Cellular activation leads to a decrease in full-length $pT\alpha^a$ mRNA expression (166), and mRNA levels of both $pT\alpha^a$ and $pT\alpha^b$, the variant lacking the extracellular IgG domain, decrease after β-selection in $icTCR\beta^+CD28^+$ ISP and blasting DP cells (117, 166). The ratio of $pT\alpha^b$:$pT\alpha^a$ mRNA increases as human thymocytes traverse β-selection, presumably retaining TCRβ protein in the ER and controlling the pre-TCR signal (166, 169, 191). Completion of β-selection also results in the opening of the *TCRA* locus in preparation for its rearrangement, as can be seen by the expression of TCR-Cα in $icTCR\beta^+CD28^+$ ISP and $CD3^-$ DP cells but not in $CD28^-$ ISP or DN cells (117, 130).

Positive and Negative Selection

Once thymocytes express both a TCRα and a TCRβ chain, selection steps must ensure that the resultant TCRαβ is capable of recognizing antigen presented by MHC molecules. Positive selection occurs when developing thymocytes recognize self-MHC and receive a signal for survival and further differentiation. Negative selection occurs when TCR engagement on developing thymocytes results in apoptosis as a means of self-tolerance. The affinity model has

been used to explain the difference between positive and negative selection: a low affinity interaction between the TCR and peptide/MHC complex (pMHC) leads to a weaker signal and positive selection, while a high affinity interaction leads to a stronger signal and negative selection.

This model has been supported in murine models in which presentation of low affinity or high affinity ligands are expressed in TCR transgenic animals. The HY TCR is a MHC-I restricted TCR that produces $CD8^+$ T cells in female mice, but results in negative selection of cells in males due to the presence of the high avidity Y chromosome-encoded antigen H-Y (192, 193). The ovalbumin peptide SIINFEKL induces negative selection in MHC-I restricted OT-I TCR transgenic mice, but single amino acid substitutions resulted in positive selection. These altered peptide ligands (APLs) had affinities for the OT-I TCR that were 3.5-8.8 times weaker than the original SIINFEKL peptide (194, 195). Further, the naturally occurring positively selecting ligands Catnb and Cappa1 have affinities that are 15.6 and 24.3 times lower than SIINFEKL when presented by the $H\text{-}2K^b$ MHC-I protein to OT-I TCRs (196). Though these affinities are low, they are still higher than non-selecting APLs (195). These studies, along with others, helped to establish TCR affinity thresholds necessary for positive selection and negative selection (197-201).

Cortex specific peptide production

Within the thymus, differences in pMHC affinities are achieved by distinct peptide processing and protein expression in cTECs and mTECs. Proteolytic pathways active in cTECs produce unique peptides for positive selection. Peptides that are presented by MHC-I molecules are derived from proteasomal degradation of proteins present in the cytosol. The peptides enter

the ER through the transporters associated with antigen processing (TAP) and are loaded into the MHC-I protein, completing its folding and allowing for its export to the cell surface. The 20S proteasome has three catalytic subunits β1, β2, and β5, which cleave after acidic, basic, and hydrophobic residues, respectively. An immunoproteasome contains altered catalytic subunits (β1i, β2i, and β5i) that can be induced by interferon-γ and are constitutively expressed in the spleen and thymus (202-205). Most MHC-I molecules preferentially bind peptides with a hydrophobic C-terminal amino acid, while some bind peptides with basic C-termini. The immunoproteasome preferentially produces peptides with hydrophobic and basic C-termini to bind MHC-I (206, 207). Both the housekeeping proteasome and immunoproteasome are present in mTECs. cTECs also express a third proteasome, the thymoproteasome, which contains a unique β5 sub-unit, β5t, along with β1i and β2i (208).

The thymoproteasome produces a unique set of peptides in cTECs for thymocyte positive selection. β5t is less efficient at cleaving peptides after hydrophobic amino acids than β5i, so the thymoproteasome preferentially produces peptides with hydrophilic C-termini, particularly cleaving after bases (208-210). Thymoproteasomes thus produce peptides which have similar affinities for OT-I TCR as positively selecting APLs when presented by MHC-I, while the TCR binding affinities of pMHC complexes made by immunoproteasomes are similar to the negative selecting SIINFEKL peptide (210). An alternate explanation for the low affinity interactions that result from thymoproteasome produced peptides is that the weaker peptide-MHC binding caused by the basic C terminal amino acid of the peptide results in partially or fully empty MHC-I molecules on the surface of cTECs. Empty MHC-I molecules have been reported to be expressed on the surface of cells, including cTECs, and weaker staining for MHC-I molecules on cTECs compared to mTECs may be a result of internalization of less stable, empty complexes

(211-214). The requirement of the thymoproteasome for positive selection of $CD8^+$ T cells has been shown in $5\beta t^{-/-}$ mice (208). These mice fail to produce $CD8^+$ T cells even though cTEC development is normal, MHC-I expression on cTECs is similar to wild type mice, and $CD4^+$ T cell selection is unaffected. Further replacement of 5βt with 5βi in cTECs was not able to restore normal positive selection, suggesting that the altered peptide production of the thymoproteasome is necessary for positive selection of a diverse $CD8^+$ T cell pool (215, 216).

Production of altered peptides for presentation by MHC-II complexes for positive selection of $CD4^+$ T cells is also predicted to occur in cTECs. MHC-II heterodimers formed in the ER are stabilized through interactions with the invariant chain (Ii), which targets MHC-II complexes to the endocytic pathway. Once in the endosome, Ii is cleaved by cathepsins, leaving only the class II-associated Ii peptide (CLIP) associated with the MHC-II. Exchange of CLIP for peptides processed in the endosome results in release of the pMHC complex for transport to the cell surface. Within professional antigen presenting cells (APCs), exogenous proteins are endocytosed and processed into peptides in the endosome. Neither cTECs nor mTECs are efficient at phagocytosis, but are able to present endogenous peptides that are presented in the endosome through increased macroautophagy in these cells, particularly cTECs (217).

cTECs uniquely express two proteases that affect peptide processing and presentation by MHC-II complexes. Human cTECs express cathepsin (Cat) V, while mTECs and APCs express Cat S and Cat L (218, 219). Mice do not encode for a Cat V protein, but murine Cat L shares higher homology with human Cat V than human Cat L (220), and is expressed exclusively in cTECs while murine Cat S is expressed in mTECs and APCs (221-223). Cat L knock out mice have impaired $CD4^+$ positive selection, even though MHC-II expression is normal and $CD8^+$ T cell production is not affected (221, 224). The role for Cat L in positive selection may

be two-fold. Cat L is involved in cleavage of Ii, and loss of Cat L in murine cTECs leads to an increase in the expression of CLIP-MHC complexes on the surface of the cells (221). The effects of altered Ii degradation are MHC-II haplotype dependent (224, 225), but defective $CD4^+$ T cell positive selection did not show the same haplotype dependence, indicating that Cat L plays a role in MHC-II peptide presentation that is independent of its function in Ii cleavage (224). Expression of Cat L in a fibroblast cell line altered a subset of peptides presented by MHC-II molecules, either through generation of new peptides or degradation of other peptides (226). Further, Cat L knock out mice show increased negative selection of $CD4^+$ SP cells, suggesting that a different repertoire of cells is positively selected in the presence or absence of Cat L (224).

The thymus-specific serine protease (TSSP) is only expressed in the endosomes of cTECs and thymic DCs, and also plays a role in $CD4^+$ T cell positive selection. Initial analysis of the role of TSSP in mice showed no significant changes in $CD4^+$ T cell selection, but further studies have shown that impairment of positive selection by loss of TSSP is peptide/TCR specific (227-230). As with Cat L knock out mice, when TSSP knock out mice show impaired selection, it is accompanied by increased negative selection, suggesting that TSSP may play a role in processing of specific peptides (229, 230). Further, the TSSP gene, *PRSS16*, is found in a diabetes susceptibility locus in humans, and loss of TSSP was found to be protective in NOD mice due to altered positive and negative selection of islet reactive T cells (229).

Presentation of tissue specific antigens in the medulla

Whereas protease expression in cTECs produces unique low affinity peptides for positive selection, the mTECs and thymic DCs are equipped to present self-peptides for negative selection of strongly self-reactive T cells, known as central tolerance. Single cell analysis of

murine mTECs has revealed that they can express almost 20,000 protein-coding genes, the most reported in any cell type (231). Gene expression is higher in mTECs than cTECs in both murine and human thymocytes, and includes expression of tissue-specific antigens (TSAs) (231-234). This promiscuous gene expression is caused, in part, by the expression of two proteins: autoimmune regulator (AIRE) and Fezf2. AIRE was first identified as the gene responsible for autoimmune polyglandular syndrome type 1 (APS-1), an autosomal recessive multi-organ autoimmune disease (235, 236). AIRE-deficient mice show decreased expression of TSAs in mTECs and also develop a multi-organ autoimmune disease, though the target organs are different (232, 237-239). Single cell transcriptome analysis of $AIRE^{+/+}$ and $AIRE^{-/-}$ murine mTECs identified almost 4000 tissue-specific genes that are up-regulated in the presence of AIRE, including 594 genes whose expression was fully dependent on AIRE expression (231).

AIRE induces expression of TSAs from chromosomal clusters normally associated with areas of repressed transcription, and different gene clusters are expressed in individual mTECs (231, 233). A DNA-binding domain has not been identified in the AIRE protein, but the first plant homeodomain finger (PHD1) is able to bind unmethylated histone H3 at lysine-4 (H3K4m0) (240, 241). Further, the SAND (Sp100, AIRE-1, NucP41/75, and DEAF-1) domain can bind the to a complex of activating transcription factor 7 interacting protein (ATF7ip) and methyl CpG binding protein 1 (MBD1), which target AIRE to transcriptionally repressed areas with methylated CpG islands (242). Together these features appear to target AIRE specifically to areas of repressed transcription, rather than specific genes, which would explain the broad expression profile of AIRE. AIRE also interacts with proteins involved in transcription, such as cyclic AMP response element-binding protein, positive transcription elongation factor b (P-

TEFb), and DNA-dependent protein kinase (DNA-PK), and pre-mRNA processing to affect expression of TSA transcripts (243-249).

AIRE is only expressed in a subset of mature $CD80^{hi}$ mTECs, but not all TSAs in $AIRE^{+}$ mTECs are AIRE-dependent, and some TSAs are expressed in $AIRE^{-}$ mTECs, suggesting the possibility of other proteins that regulate TSA expression in mTECs (231-233, 250-253). Only recently was it reported that Fezf2 also regulates TSA expression in thymocytes (251). Fezf2 is expressed in murine and human mTECs, with low expression levels in a subset of $CD80^{lo}$ mTECs and higher expression in all mature $CD80^{hi}$ mTECs. Nude mice engrafted with Fezf2-deficient thymi had splenomegaly and infiltration of inflammatory cells in multiple organs. Further, expression of some TSAs, including some known to be associated with autoimmune disease, was decreased in Fezf2-deficient mTECs in an AIRE-independent manner. While these findings help to explain some of the discrepancies in TSA expression in $AIRE^{-}$ mTECs and of AIRE-independent genes, microarray analysis of mTEC gene expression suggests that expression of only 60% of TSAs are AIRE- or Fezf2-dependent, and other unknown mechanisms of TSA regulation must exist.

mTECs are not the only source of peripheral antigens in the thymus. AIRE expression has recently been identified in murine thymic B cells, which can mediate negative selection of $CD4^{+}$ thymocytes (254). DCs are also able to pick up antigen in the periphery, migrate to the thymus, and present it to developing T cells (255, 256). Further it has been shown that antigen circulating in the blood can enter the thymus and be presented by $SIRP\alpha^{+}$ thymic DCs, which can be found near small vessels in the thymus (257-259). Thymic DCs are also able to present TSAs that have been produced by mTECs and transferred to the DCs, possibly via exosome release by the mTECs (260-263). The presentation of TSAs by DCs and B cells allows for professional

antigen presentation on MHC-II molecules, which may be necessary for proper $CD4^+$ T cell negative selection. Whereas $CD8^+$ T cells can be negatively selected by antigen presentation on either mTECs or DCS, CD4+ T cells appear to require thymic APCs for proper negative selection (260). Thymic DCs are also required for induction of negative selection in the murine cortex (264, 265).

Signaling differences in positive and negative selection

While both positively and negatively selecting ligands interact with the TCR, they induce qualitatively different signals within the cell. Impairment of extracellular signal-related kinase (ERK) activation in murine thymocytes results in a deficiency in positive selection but does not affect negative selection unless ERK signaling is completely blocked (266-274). ERK has a lower activation threshold than other TCR signaling kinases, and low affinity ligands have been shown to induce weak but sustained ERK signals associated with localization to the Golgi, while high affinity ligands induce strong, transient ERK signals at the plasma membrane (201, 271, 274, 275). Positive selection has been shown to require that the cell maintain sustained interactions with a pMHC complex, which may be necessary to maintain the low ERK signaling (276, 277). In contrast, attenuation of Jun amino-terminal kinase (JNK) or p38 signaling specifically inhibits negative selection but not positive selection (275, 278, 279). JNK and p38 have higher activation thresholds than ERK, and thus may require a stronger TCR signal strength for activation and mediation of negative selection (275). Further studies are required to identify how qualitatively different TCR signaling by negatively selecting ligands leads to apoptosis through the activation of the pro-apoptotic Bim, Bax, and Bak proteins (280, 281).

High affinity TCR:pMHC interactions do not always result in negative selection within the thymus, they can also induce regulatory T cell (T_{reg}) development (259, 282, 283). T_{reg} cell development is impaired in patients with mutations in the *AIRE* gene or other mutations that result in decreased AIRE expression, suggesting a role for mTEC derived TSAs for T_{reg} development (284-287). T_{reg} commitment requires CD28 co-stimulation, which is provided by thymic dendritic cells that have been activated by thymic stromal lymphopoietin (TSLP) produced by Hassall's corpuscles in the human thymus (288-291). Further stimulation with IL-2, produced by TECs or mature CD4+ SP cells, or IL-15, produced by B cells and macrophages, is also necessary for T_{reg} development (292, 293). The exact mechanism by which cells differentiate between T_{reg} and negative selection signals is yet unknown.

CD4/CD8 Lineage Commitment

Prior to egress from the thymus, DP thymocytes must down-regulate one of their co-receptors and commit to either the $CD4^+$ or $CD8^+$ T cell lineage. The CD4 and CD8 co-receptors bind to MHC-II and MHC-I molecules, respectively. CD4 or CD8 binding to the MHC serves to stabilize the MHC:TCR interaction and bring the Src family tyrosine kinase Lck in proximity to the TCR to participate in TCR signaling. As positive selection signals are received by cortical DP thymocytes expressing both co-receptors, the cells must have a way of differentiating what the MHC specificity of the TCR is. As expected, murine thymocytes transgenically expressing the MHC-II-specific AND TCR are efficiently selected into the $CD4^+$ lineage, but when the MHC-II molecule is mutated so as not to recognize CD4, cells are selected into the $CD8^+$ lineage (294). This study suggested that while MHC:TCR interactions alone are sufficient for positive selection, proper interaction between the MHC and CD4 or CD8 is necessary for lineage

commitment. Three models of lineage commitment have been proposed based on experiments in murine thymocytes: the stochastic model, the instructive model, and the signal duration/kinetic signaling model.

The stochastic model proposes that CD4 or CD8 expression is terminated independent of TCR specificity, so that one of the two co-receptors is randomly down-regulated. Thymocytes will only survive positive selection if the MHC specificity of the TCR matches that of the expressed co-receptor. Thus, according to this model, thymocytes expressing a MHC-I restricted TCR that down-regulated CD8 to commit to the CD4 lineage would not survive but could be rescued by forced expression of CD8. The model was supported by studies that found the production $CD4^+$ SP cells when a CD8 transgene was expressed in MHC-I restricted TCR transgenic mice, and similarly $CD8^+$ SP cells developed when CD4 was constitutively expressed in MHC-II restricted TCR transgenic or β_2-microglobulin deficient mice (295-297). Contrary to these findings, $CD4^+$ SP cells were not produced when CD8 was constitutively expressed with a different MHC-I restricted TCR (298-300). In another study, it was determined that expression of transgenic TCRs led to highly efficient selection of SP cells expressing the coordinated co-receptor, suggesting an instructive model of development (301).

The instructive model suggests that lineage is determined based on the difference in signal received by thymocytes depending on whether CD4 or CD8 is engaged by the MHC. This model was prompted by the finding that CD4 binds Lck with a higher affinity than CD8, and thus CD4:MHC-II binding recruits more Lck to the TCR complex (302-304). Expression of a hybrid protein containing the extracellular and transmembrane CD8 domains fused to the CD4 cytoplasmic domain in a MHC-I restricted transgenic mouse resulted in the production of MHC-I-restricted $CD4^+$ T cells (298, 305). Further, by altering Lck activity lineage commitment could

be altered in transgenic mice: constitutively active Lck induced $CD4^+$ T cell development with a MHC-I-restricted TCR, and catalytically inactive Lck induced $CD8^+$ T cell development with a MHC-II-restricted TCR (306, 307). However, another study showed that a CD4 protein that was unable to interact with Lck was still able to induce production of $CD4^+$ SP cells, suggesting that recruitment of Lck to the signaling complex by CD4 is not essential for $CD4^+$ T cell commitment (308).

The signal duration/kinetic signaling model suggests that lineage commitment is determined by the duration of signal received through MHC-I-restricted and MHC-II-restricted TCRs due to differential kinetics of CD8 and CD4 expression. In a seminal study, MHC-I-restricted TCR transgenic thymocytes incubated for a short period of time with a high affinity ligand developed into SP $CD8^+$ cells, as expected, but if the incubation period was extended the cells developed into SP $CD4^+$ cells (309). These results suggested that lineage commitment is determined by the duration of the TCR signal received, rather than the strength of signal. Further, lineage commitment can occur independent of MHC specificity if the TCR signal is either terminated (SP $CD8^+$ cells) or elongated (SP $CD4^+$ cells) (309-311).

Murine thymocytes transition through a $CD4^+CD8^{lo}$ transitional single positive (TSP) stage after receiving a positive selection signal (312-315). These TSP cells retain the ability to differentiate into both $CD4^+$ and $CD8^+$ SP cells in culture, putting into question both the stochastic and instructive models (313-316). Further studies have shown that CD8 transcription is terminated after positive selection of DP thymocytes regardless of whether the TCR recognizes antigen in MHC-I or MHC-II molecules (317-320). Thus, down-regulation of CD8 on a positively selected thymocyte would lead to an interruption in the TCR signal on MHC-I-restricted thymocytes, but have no affect on MHC-II-restricted thymocytes. To further confirm

that co-receptor down-regulation affects lineage commitment, studies were performed in which CD4 was expressed under the control of the CD8α enhancer and promoter, either as a transgene or as a knock-in at the CD8α locus (311, 318). In these mice, MHC-II-restricted thymocytes developed into cytotoxic T cells that expressed granzyme B and the $CD8^+$ T cell specific transcription factor Runx3.

Commitment to the CD4 or CD8 lineage is dependent on expression of the transcription factors ThPOK and Runx3, respectively. The requirement of ThPOK in CD4 lineage commitment was first identified through gene mapping of a spontaneous recessive mutation in mice that resulted in a loss of $CD4^+$ T cell development due to positively selected MHC-II-restricted cells being diverted to the CD8 lineage (321-324). Loss of ThPOK function through mutation or deletion leads to a decrease in SP $CD4^+$ cell development in a dose dependent manner (325, 326). Decreases in ThPOK expression were associated with increased expression of Runx3, perforin, and IFN-γ in murine TSP $CD4^+$ and SP $CD4^+$ cells, suggesting that ThPOK expression represses CD8 lineage gene expression (325). Conversely, retroviral expression of ThPOK is capable of diverting MHC-I-restricted cells to the CD4 lineage (323). ThPOK is expressed in mature CD4 SP but not CD8 SP (323, 324). However, analysis of TSP cells expressing GFP from the ThPOK locus revealed three levels of GFP expression (325, 326). As expected GFP^{hi} TSP cells were committed to the CD4 lineage and GFP^- TSP cells were committed to the CD8 lineage, but the GFP^{int} TSP population retained the ability to differentiate into both CD4 SP and CD8 SP cells (326). This study further showed that the *ThPOK* proximal enhancer is required for expression of ThPOK at high enough levels sufficient for commitment to the CD4 lineage, and that ThPOK may solidify commitment to the CD4 lineage through antagonism of silencers in both the *CD4* and *ThPOK* loci.

Runx3 appears to play a similar role in CD8 lineage commitment as ThPOK does in CD4 commitment. Runx3 protein is exclusively expressed in $CD8^+$ SP thymocytes, whereas Runx1 expression is higher in DN but present throughout development (325, 327, 328). Loss of Runx3 expression results in a decrease in CD8 SP production and an accumulation of DP cells with a mature $TCR\beta^{hi}HSA^{lo}$ phenotype, suggesting that repression of the *CD4* locus does not occur in these cells (327, 329-331). Further studies found that increased Runx binding at the CD4 silencer occurred in CD8 SP cells and that Runx binding sites are required for CD4 repression (328-330). Enhancers within the *CD8* gene locus also contain Runx binding sites, and Runx binding at the post-selection *CD8* gene enhancer E8I is restricted to CD8 SP cells, suggesting a role for Runx3 regulation of CD8 re-expression (328). ThPOK expression is increased in TSP or CD8 SP cells when binding of both Runx1 and Runx3 are inhibited, either through knockdown of these genes specifically or of their binding partner Cbfβ (332). This study also showed that Runx proteins bind silencer elements in the *ThPOK* locus, but did not differentiate between Runx1 and Runx3 binding. These data suggest a role for Runx proteins in regulating CD4, CD8, and ThPOK expression in CD8 SP thymocytes.

A final aspect of the kinetic signaling model over the signal duration model is the role of cytokines in determining lineage commitment. Specifically, the kinetic signaling model poses that cytokine signaling, particularly IL-7 receptor (IL-7R) signaling, is responsible for final commitment to the CD8 lineage (317). DP thymocytes are not responsive to IL-7R signaling due to high expression of suppressor of cytokine signaling-1 (SOCS1), a negative regulator of Jak3-kinase phosphorylation downstream of cytokine signaling, which is down-regulated upon positive selection (333, 334). Mice deficient in SOCS1 have increased numbers of CD8 SP thymocytes, whereas SOCS1 transgenic mice were deficient in CD8 SP thymocytes, suggesting a

role for cytokine signaling in the development of CD8 lineage commitment (334-336). Further, SOCS1 deficiency in MHC-II restricted thymocytes leads to the development of CD8 SP cells with effector function (336). IL-7 is needed in culture for CD8 SP development (317), and IL-7 signaling increases expression of CD8α transcription through targeting of the E8I enhancer (337). Importantly, IL-7 signaling is capable of inducing Runx3 expression from the distal promoter (335). Together these studies show that IL-7R signaling can induce CD8α and Runx3 expression in a TCR independent manner, and is necessary for CD8 lineage commitment.

Analysis of Ikaros Family Expression in Human T Cell Development and T-ALL

To begin to elucidate the differences in Ikaros family function in murine and human T cell development, we investigated the expression of Ikaros family members in human thymocytes and compared this to expression in pediatric T-ALL patients. We began by determining the mRNA and protein expression levels in populations of murine and human thymocytes from the DN2 to DP stages of development. Differences in expression patterns of Helios and Aiolos between the species prompted a more thorough analysis of human thymocytes. To be able to identify changes in Ikaros family expression in small populations of cells, we used multi-parameter flow cytometry to identify subpopulations of human thymocytes and determine stages in which β-selection, positive selection, and CD4/CD8 lineage commitment likely occur. Finally, we analyzed mRNA expression of the entire Ikaros family, as well as protein expression of Ikaros and Aiolos, in cases of pediatric T-ALL compared to normal thymic populations to identify changes in Ikaros family expression. Our data represent the most thorough investigation into the subpopulations of human thymic development, and expression of the Ikaros family in human T cell development and leukemogenesis.

Chapter 2. Expression and splicing of Ikaros family members in murine and human thymocytes

Abstract

The Ikaros family of transcription factors includes five highly homologous members that can homodimerize or heterodimerize in any combination. Dimerization is essential for their ability to bind DNA and function as transcription factors. Previous studies showed that eliminating the function of the entire family blocks lymphocyte development while deletion of individual family members has relatively minor defects. These data indicate that multiple family members function during T cell development, so we examined the changes in expression of each family member as thymocytes progressed from the $CD4^{-}CD8^{-}$ double negative (DN) to the $CD4^{+}CD8^{+}$ double positive (DP) developmental stage. Further, we compared the expression of each family member in murine and human thymocytes. In both species, Ikaros and Aiolos mRNA levels increased as thymocytes progressed through the DN to DP transition, but the corresponding increases in protein levels were only observed in mice. Further, Ikaros and Aiolos underwent extensive alternative splicing in mice, whereas only Ikaros was extensively spliced in humans. Helios mRNA and protein levels decreased during murine T cell development, but increased during human T cell development. These differences in the expression and splicing of Ikaros family members between human and murine thymocytes indicate that the Ikaros family of transcription factors regulates murine and human T cell development differently.

Introduction

T cell development in the thymus is a highly ordered process that includes intermittent periods of proliferation and selection with the purpose of producing a diverse repertoire of T cells. Early T cell progenitors entering the thymus lack CD4 and CD8 expression and are called $CD4^{-}CD8^{-}$ double negative (DN) thymocytes. In mice, DN thymocytes can be subdivided into at least four major populations (DN1-4) based on their expression of CD44 and CD25 (107). After the DN stage, murine thymocytes express CD8 to become immature single positive (ISP) $CD8^{+}$ thymocytes before expressing CD4 to become $CD4^{+}CD8^{+}$ double positive (DP) thymocytes (111). In humans, DN thymocytes are commonly divided into three subsets (DN1-3) based on their expression of CD34, CD38, and CD1a (109, 338, 339). After the DN3 stage, human thymocytes express CD4 to become ISP $CD4^{+}$ thymocytes and then CD8 to become DP thymocytes (110).

During early T cell development, thymocytes progress through a series of checkpoints. The first major checkpoints involve restricting the lineage potential of the cells to the T cell lineage and then to the αβ T cell lineage. Once committed to the αβ T cell lineage, thymocytes progress through the next major checkpoint, which occurs when TCRβ is expressed for the first time. TCRβ protein can be first detected in murine DN3 thymocytes (180) and human ISP thymocytes (117). The next major checkpoint occurs following expression of TCRα protein, which happens for the first time in DP thymocytes in mice and humans.

The Ikaros family of transcription factors is required for T cell development (16, 340). The members of this family of five proteins (Ikaros, Helios, Aiolos, Eos, and Pegasus) share two zinc finger domains that are highly homologous across the family members. The N-terminal domain includes the DNA-binding domain, and the C-terminal domain mediates dimerization.

Each family member can homodimerize or heterodimerize with any other family member, and dimerization is required for high affinity DNA binding and transcriptional activity (1-5). Because of the extensive dimerization that can occur among family members, it is important to consider the entire Ikaros family as a whole. A change in the expression of one family member has the potential to alter the functionality of the entire family.

Adding complexity to the study of the Ikaros family, each family member can undergo extensive alternative splicing that results in the deletion of zinc fingers in the DNA binding domain. Deletion of one or two zinc fingers can change the DNA sequences recognized by the Ikaros dimer (1, 6, 341). Deletion of three or more zinc fingers in the DNA binding motif results in a dominant-negative variant that can dimerize with other family members, but is unable to bind DNA (1).

The importance of the Ikaros family in hematopoiesis was demonstrated in mice expressing the dominant-negative isoform of Ikaros; these mice lacked T, B, and NK cells as well as their precursors (46). In contrast, mice lacking the Ikaros dimerization domain, which preserves the function of the other family members, had impaired B cell and fetal T cell development, but only mild deficits in postnatal T cell development (50). The differences in the phenotypes observed in these two mouse lines demonstrate that multiple Ikaros family members are critical for T cell development. To determine which family members might be required for T cell development, we analyzed how mRNA levels, protein levels, and alternative splicing of Ikaros family members change during early T cell development. In addition, we provide the first data directly comparing expression and splicing patterns of Ikaros family members in murine and human thymocytes.

Materials and Methods

Antibodies

The anti-mouse antibodies, anti-TER119-FITC, anti-CD4 FITC, anti-CD24-PE, anti-CD44-PE-Cy7, and anti-CD25-APCCy7, were purchased from eBioscience (San Diego, CA, USA). Anti-CD8-FITC, anti-CD8-AF647, and anti-CD4-Pacific Blue were purchased from BD Biosciences (San Jose, CA, USA). The anti-human antibodies, anti-CD1a-PerCP-Cy5.5, anti-CD1a-PECy5, anti-CD3-APCCy7, anti-CD4-Pacific Blue, anti-CD7-FITC, anti-CD8-BV785, anti-CD8-FITC, anti-CD34-PE, anti-CD34-PECy7, and anti-CD38-AF700 were purchased from Biolegend (San Diego, CA). Anti-Aiolos-PE was purchased from e-Biosciences, and anti-Mouse IgG1κ-PE and anti-Ikaros-PE were purchased from BD Biosciences. The anti-human/mouse antibody, anti-Helios-AF647, was purchased from eBioscience. The anti-Armenian Hamster IgG-AF647 control was purchased from Biolegend.

FACS-purification of murine thymocytes

Wild-type C57BL/6 mice were housed under specific pathogen-free conditions and used between the ages of 3-5 weeks. All experiments were performed in compliance with the University of Kansas Medical Center Institutional Animal Care and Use Committee. To obtain DN thymocytes, single cell suspensions of murine thymocytes were immunodepleted using magnetic beads conjugated to anti-CD4 and anti-CD8 (BD Biosciences). The remaining DN cells were labeled with anti-TER119, anti-CD4, anti-CD8, anti-CD25, and anti-CD44. Using a BD FACSAria IIIu (BD Biosciences), cells were gated on $TER119^{-}CD4^{-}CD8^{-}$ thymocytes and DN1, DN2, DN3, and DN4 populations were FACS-purified according to CD44 and CD25 expression.

To collect ISP thymocytes, total thymocytes were depleted using magnetic beads conjugated to anti-CD4. Remaining cells were labeled with anti-CD4, anti-CD8, and anti-CD24, and $CD8^{+}CD24^{+}$ ISP cells were FACS-purified. To obtain DP thymocytes, single cell suspensions of total murine thymocytes were labeled with anti-CD4 and anti-CD8, and were FACS-purified.

FACS-purification of human thymocytes

After obtaining consent from the parent or guardian, human thymus samples were obtained from children (0 – 18 years) that underwent corrective surgery at Children's Mercy Hospital (Kansas City, MO) for congenital cardiac defects. Tissue samples were obtained in compliance with the Institutional Review Boards at Children's Mercy Hospital and the University of Kansas Medical Center.

To obtain DN and ISP thymocytes, single cell suspensions of total thymocytes were immunodepleted using magnetic beads conjugated to anti-CD8 and anti-CD3 (BD Biosciences). The remaining cells were labeled with anti-CD1a, anti-CD3, anti-CD4, anti-CD8, anti-CD34, and anti-CD38. $CD4^{-}CD8^{-}$ DN cells were gated on $CD3^{-}CD34^{+}$ thymocytes. DN2 and DN3 populations were FACS-purified using a FACSAria IIIu (BD Biosciences) according to their expression of CD1a and CD38. For the ISP population, cells were gated on $CD4^{+}CD8^{-}$ thymocytes and $CD3^{-}$ ISP cells were FACS-purified. For DP thymocytes, single cell suspensions of human thymocytes were labeled with anti-CD4 and anti-CD8 and $CD4^{+}CD8^{+}$ thymocytes were FACS-purified.

Quantitative RT-PCR (qRT-PCR)

Total mRNA was isolated from FACS-purified thymocytes using the RNeasy Mini Kit or RNeasy Micro Kit (Qiagen, Valencia, CA), depending on total cell count. Isolated mRNA was converted to cDNA using the TaqMan® High Capacity RNA-to-cDNA™ kit (Applied Biosystems, Foster City, CA). For qRT-PCR, 2μL of cDNA was amplified using TaqMan® Gene Expression Assays for the Ikaros family members or GAPDH housekeeping gene (Ikaros: Mm01187878_m1, Hs00958473_m1; Helios: Mm00496108_m1; Aiolos: mM01306721_m1, Hs00232635_m1; Eos: Mm00496114_m1, Hs00223842_m1; Pegasus: Mm00731061_s1, Hs00223846_m1; GAPDH: Mm99999915_g1, Hs03929097_g1; Applied Biosystems), and was performed using a 7500 Fast Real-Time PCR System (Applied Biosystems). Relative expression levels of Ikaros family members were calculated relative to GAPDH using a relative quantification study in the 7500 Fast System Software. At least five independent experiments were performed for each subset, and in each experiment the samples were run in triplicate and averaged. Statistical significance was determined using the Log_2(Fold Change), or $-\Delta\Delta Ct$.

Western blot analysis

Cell lysates prepared from $2\text{-}3\times10^5$ cells of each murine thymocyte population or $4\text{-}5\times10^5$ cells of each human thymocyte population were separated by SDS-PAGE, transferred to nitrocellulose and probed with antibodies against murine Ikaros, murine Aiolos, murine p38 MAPK, human Ikaros, human Aiolos, or human p38 MAPK (all purchased from Santa Cruz Biotechnology, Inc., Dallas, TX). Bands were visualized using horseradish peroxidase-conjugated secondary antibodies (Santa Cruz Biotechnology, Inc.) and Pierce™ ECL Western Blotting Substrate (Life Technologies, Grand Island, NY), and detected using an ImageQuant

LAS-4000 gel imager (GE Healthcare Systems, Pittsburgh, PA). Protein levels of Ikaros and Aiolos were measured relative to p38 MAPK levels using the total densitometry for all protein isoforms as measured with MultiGauge Software (FujiFilm).

Intracellular staining

Intracellular staining was performed using the FoxP3/Transcription Factor Staining Buffer Set (eBioscience) according to the manufacturer's instructions. Single cell suspensions of murine thymocytes were labeled on their surface using anti-CD3, anti-CD4, anti-CD8, anti-CD24, anti-CD25, anti-CD44, and anti-TCRβ. Cells were washed three times with PBS before addition of the Fixation/Permeabilization working solution. Cells were washed twice with 1X Permeabilization Buffer before labeling with anti-Helios or isotype control. Single cell suspensions of human thymocytes were first labeled on their surface with anti-CD1a, anti-CD3, anti-CD4, anti-CD8, anti-CD34, and anti-CD38. After washing and fixation/permeabilization as described, cells were intracellularly labeled with either anti-Ikaros or anti-Aiolos and anti-Helios, or isotype control antibodies. Cells were analyzed using a BD LSR II (BD Biosciences), and data were analyzed with BD FACSDiva software (BD Biosciences) and FlowJo (TreeStar, Inc., Ashland, OR). Fold change was measured as the ratio of geometric fluorescence intensity between Ikaros family member and isotype control labeled cells.

Nested PCR

Isolated total mRNA was reverse transcribed to cDNA with AMV RT (Promega, Madison, WI) before amplification with Taq DNA Polymerase (Fisher Scientific, Pittsburgh, PA). Primary PCR reactions were performed using cloning primers specific to the 5′ UTR and

3′ UTR, and nested PCR reactions were then performed with primers that spanned all possible exon pairs (Tables 2-1 and 2-2). PCR products were run on a 2% agarose gel that was then stained with ethidium bromide and washed with water before visualization using an ImageQuant LAS-4000 gel imager (GE Healthcare Systems).

Helios variant cloning

Isolated total human mRNA was reverse transcribed and amplified with the AccuScript PFUUltra II RT-PCR Kit (Agilent Technologies, Inc., Santa Clara, CA) using the cloning primers listed for Helios in Table 2-1. PCR products were cut with EcoRI and XhoI (Promega), and purified from an agarose gel using the QIAquick Gel Extraction Kit (Qiagen), and cloned into the MIGR1 vector. cDNA was collected from positively transformed colonies using the IBI High Speed Plasmid Mini Kit (Midwest Scientific, Valley Park, MO) and sequenced by GENEWIZ, Inc. (South Plainfield, NJ).

Statistics

For most figures, statistics were performed using the one-way ANOVA with a Tukey posthoc test, and significance was defined as $p < 0.05$. For statistical analysis of the mRNA levels of Ikaros family members relative to Ikaros, the two-way ANOVA was used with a Bonferroni posthoc test, and significance was defined as $p < 0.05$.

Table 2-1. Nested PCR primers for murine Ikaros and Aiolos

Murine	Ikaros	Aiolos
5' Cloning	CGCCCGAATTCACATAACCTGAAGAC	GCCGGAATTCGGCGACATGGAAGATATAC
Exon 2 Forward	TCAGTGACACTCCAGATGAAGG	ACGCTCTGAATGACTACAGCTTGCC
Exon 3 Forward	TCAGGAGTTGGAGGCATTCG	TGAACTGCGACGTGTGCGGG
Exon 4 Forward	TACCCAGAAAGGCAACCTCC	AGATGCGCTCACGGGACACCT
Exon 5 Forward	TGGATATTGTGGCCGGAGC	GCCGTACAAGTGTGAGTTCTGCG
Exon 4 Reverse	GCAGGCATAGTTGCAAAGATGG	CCCGTGAGCGCATCTCTCCTTTG
Exon 5 Reverse	CCAAGTAGTTGTGGCATCGC	TCGGCAGCGTTCCTTGTGCT
Exon 6 Reverse	CTCTTACGTTTGGCGACATTGC	TCGGCTTTGATGTGTCTTGCCTCC
Exon 7 Reverse	CTCCGATGACACAGACTTGG	GGACAGACCTCGTTCAGAAGGCAAG
3' Cloning	TATTCTCGAGTGGGTTTAGCTCAGGTGG	TGTTGACCCTCGAGTTGAGGACAG

Table 2-2. Nested PCR primers for human Ikaros, Aiolos, and Helios

Human	Ikaros	Aiolos	Helios
5' Cloning	CGACGCACAAATCCACATAACCTGAG	GGCAGCGACATGGAAGATATAC	TGCACTTTGACTATGGAAACAGAGGC
Exon 1 Forward	CATGGATGCTGATGAGGGTC	CACTCAGGAGCAGTCTGTG	
Exon 2 Forward	TAAGCGATACTCCAGATGAGGG	AATGTGGACAGTGGAGAAGGC	TTGACCTCACCTCAAGCACACC
Exon 3 Forward	TCGGGAGTTGGAGGCATTCG	GTCTCATTCGATAGTAGCAGGC	ATTGAGAGCAGCGAGGTGGC
Exon 4 Forward	GGCACATCAAGCTGCATTCC	AGAAGAGATGCGCTCACGG	CTTCCACTGTAACCAGTGTGGAGC
Exon 5 Forward	TGGATATTGTGGCCGAAGC	GAGAAGTTCCCTTGAGGAGC	ACTGGAGGAACACAAGGAACGC
Exon 3 Reverse	CCATTCATTTCACAGGCACGC	TCATCTTTCCACTGGTTGGC	GGCCCAATGCAAACCATGCC
Exon 4 Reverse	AGGCGTAGTTGCAGAGGTGG	GTGAGCGCATCTCTTCTTTGG	GCGTCCCTTCTTCTACAGGC
Exon 5 Reverse	CCAAGTAGTTGTGGCAGCG	CCTCAAGGGAACTTCTCTGC	CTGCGCTGCTTGTAGCTTCG
Exon 6 Reverse	GACGTTACTTGCTAGTCTGTCC	GCTAATCTGTCCAGTACGAGAGC	GAGCTTCTCTATGACAGCAGGTCTC
Exon 7 Reverse	TTGTGCAGCTGGTACATCG	ACCGTTTGACATCTCAGCC	CCACTTCAGCGATTGTGCTTGG
3' Cloning	TTGTCTGGTCCAGTCCAGTCTATGC	GAGACCAGATATTCACTTCAGCAGG	GAGGAAAGGTGGGATTGTAAGTGC

Results

mRNA levels of Ikaros family members during early murine T cell development

We FACS-purified murine DN2, DN3, DN4, ISP, and DP thymocytes and analyzed the relative mRNA levels of each Ikaros family member in each cell population using qRT-PCR (Fig. 2-1A). Of the five family members, Aiolos mRNA levels increased most dramatically as thymocytes progressed from the DN2 to the DP stage; Aiolos mRNA levels in DP thymocytes were 27-fold higher than in DN3 thymocytes. Ikaros mRNA levels also increased during early T cell development and were 3.0-fold higher in DP thymocytes than in DN3 thymocytes. Pegasus mRNA levels were 1.6-fold higher in DN2 thymocytes than DN3 thymocytes, but increased to 4.1-fold higher in DP thymocytes than DN3 cells.

By contrast, Helios and Eos mRNA levels decreased as thymocytes progressed from the DN2 stage to the DP stage. Helios mRNA levels were 2.6-fold higher in DN2 thymocytes than DN3 cells and were similar in the DN3, DN4, ISP, and DP populations. Eos mRNA levels were comparable in DN2 and DN3 thymocytes, but were 10-fold higher in DN3 thymocytes than DP cells.

For the calculations in Fig. 2-1A, the mRNA levels of each Ikaros family member were first normalized to that of GAPDH before comparing cell populations. GAPDH can be induced in mature T cells (342), so it is unclear whether this is an appropriate control gene for these assays. In addition, because Ikaros family members dimerize with each, the ratio of family members is an important parameter. Hence, we directly compared the mRNA levels of each Ikaros family member to that of Ikaros itself (Fig. 2-1B). Ikaros was the predominant mRNA species in DN2 thymocytes; Ikaros mRNA levels were 7.3-

Figure 2-1. Ikaros, Aiolos, and Pegasus mRNA levels increase during early murine T cell development. mRNA isolated from murine DN2 ($CD4^{-}CD8^{-}CD44^{+}CD25^{hi}$), DN3 ($CD4^{-}CD8^{-}CD44^{-}CD25^{hi}$), DN4 ($CD4^{-}CD8^{-}CD44^{-}CD25^{-}$), ISP ($CD4^{-}CD8^{+}CD24^{+}$), and DP ($CD4^{+}CD8^{+}$) thymocyte populations was subjected to qRT-PCR. *A*) For each thymocyte population, the relative expression of each Ikaros family member was normalized to that of DN3 thymocytes and the $\log_2$ (Fold Change) is shown. (n = 7 independent samples; $*p < 0.05$, $**p < 0.01$, $***p < 0.001$ as compared to DN3) *B*) For each population, relative mRNA levels of the Ikaros family members were normalized to those of Ikaros.

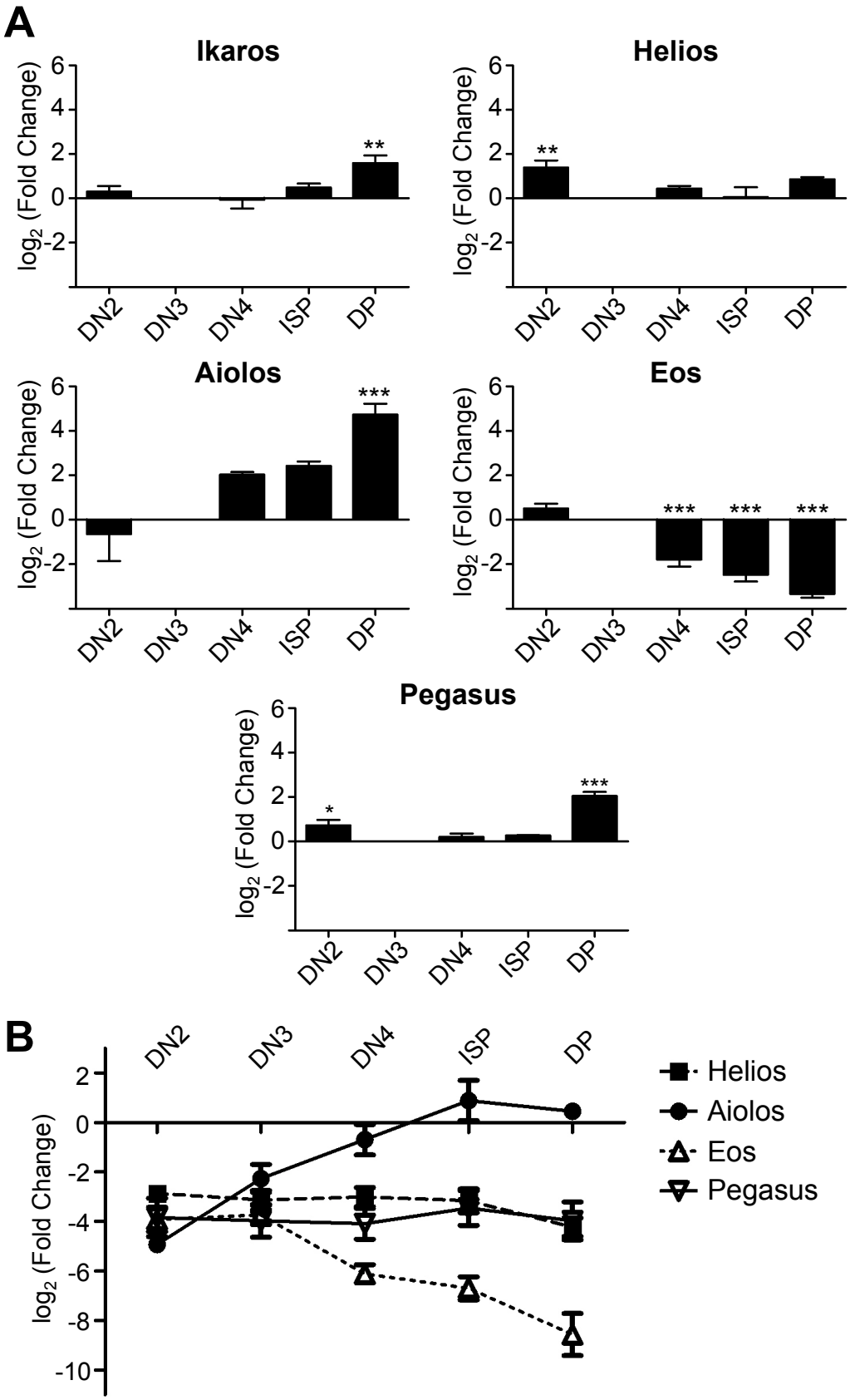
A
Ikaros
Helios
Aiolos
Eos
Pegasus
log2 (Fold Change)
DN2
DN3
DN4
ISP
DP
B
Helios
Aiolos
Eos
Pegasus

fold higher than Helios, 14-fold higher than Pegasus, 15-fold higher than Eos, and 30-fold higher than Aiolos ($p < 0.01$ for all family members compared to Ikaros). As thymocytes progressed through development, their Aiolos mRNA levels increased to such an extent that Ikaros and Aiolos mRNA levels were comparable in DN4, ISP, and DP thymocytes. Pegasus, Helios, and Eos mRNA levels remained significantly lower than Ikaros in all murine thymocyte populations tested ($p < 0.001$). Relative to Ikaros mRNA levels, Eos mRNA levels decreased throughout early T cell development; Eos mRNA levels at the DP stage were 380-fold lower than those of Ikaros ($p < 0.001$ for DP compared to DN2). Helios and Pegasus mRNA levels did not change significantly relative to Ikaros. These data suggest that the mRNA levels of some Ikaros family member are regulated independently. In addition, Ikaros and Aiolos are the predominant family members expressed in murine thymocytes, but the other family members are also present, particularly in early stages of T cell development.

Protein levels of Ikaros family members during murine T cell development

To determine whether the Ikaros family protein levels correlated with their mRNA levels, we analyzed Ikaros, Aiolos, and Helios protein levels (Fig. 2-2). According to the western blot analysis and consistent with previous reports (2), Ikaros and Aiolos protein levels were 2.5-fold and 11-fold higher in DP thymocytes than DN3 thymocytes, respectively (Fig. 2-2A). Helios protein levels were assessed by intracellular staining and flow cytometry (Fig. 2-2B) and found to be 2.3-fold higher in DN2 thymocytes than in DN3 thymocytes. Helios protein levels transiently increased in DN4 thymocytes before decreasing to levels just above the isotype control in DP thymocytes.

Figure 2-2. Ikaros and Aiolos protein levels increase and Helios protein levels decrease during early murine T cell development. *A*) Cell lysates prepared from FACS-purified murine DN2, DN3, DN4, ISP, and DP thymocytes were probed with antibodies against Ikaros, Aiolos, or p38 MAPK. Using densitometry, the sums of the splice variants were normalized to the quantity of p38 MAPK. The fold change in protein level relative to DN3 is shown. Data are representative of at least five independent experiments. *B*) Murine thymocytes were surface labeled with antibodies against CD4, CD8, CD24, CD25, CD44 and TCRβ before fixing, permeabilizing, and intracellular staining with either anti-Helios (dark line) or isotype control (shaded histogram). DN thymocytes were gated on surface $CD24^{+}TCR\beta^{-}$ cells before being gated based on CD25 and CD44 expression. For each population shown, the geometric mean fluorescence intensity (GMFI) of the anti-Helios staining was divided by the GMFI of the isotype control. Data are representative of six mice and three independent experiments. (*$p < 0.05$, **$p < 0.01$, ***$p < 0.001$ as compared to DN3).

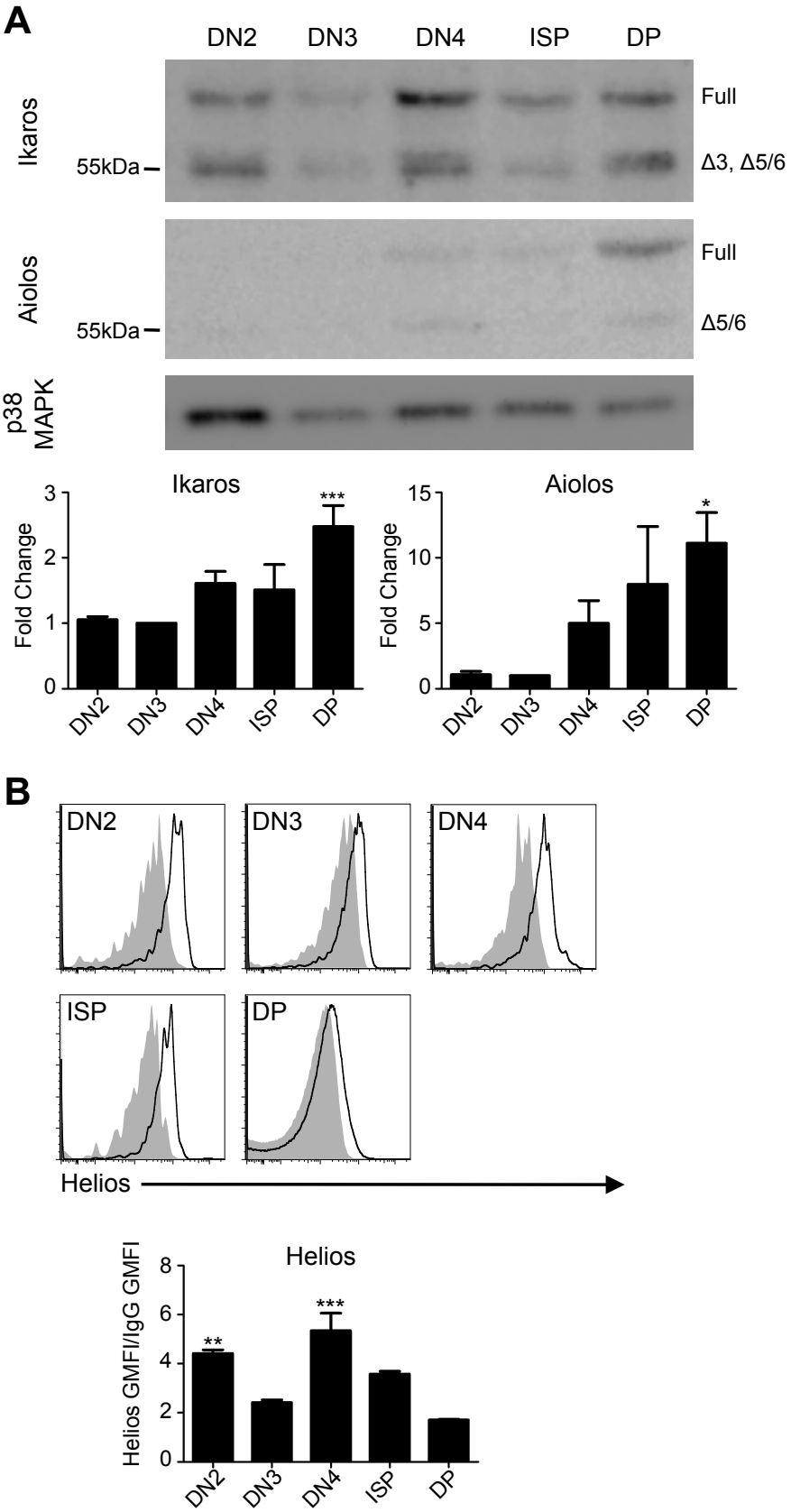
A
DN2
DN3
DN4
ISP
DP
Ikaros
55kDa
Full
Δ3, Δ5/6
Aiolos
55kDa
Full
Δ5/6
p38 MAPK
Ikaros
Fold Change
***
Aiolos
Fold Change
*
B
DN2
DN3
DN4
ISP
DP
Helios
Helios
Helios GMFI/IgG GMFI
**
***

In summary, Ikaros and Aiolos mRNA and protein levels increased as murine thymocytes progressed from the DN2 to the DP developmental stage. By contrast, Helios mRNA and protein levels decreased, except for a transient increase in protein levels at the DN4 stage.

Splice variants of Ikaros and Aiolos in murine thymocytes

When cell lysates were probed with anti-Ikaros, three bands were detected (Fig. 2-2A), suggesting the presence of alternative splice variants. To identify the bands, we performed nested RT-PCR using mRNA isolated from FACS-purified murine DN3, DN4, ISP, and DP thymocytes (Fig. 2-3). Using the nested PCR primers to amplify exons 2 through 7, bands corresponding to the molecular weights of full-length Ikaros (Ik-Full), Ikaros lacking exon 3 (Ik-Δ3), Ikaros lacking exons 5 and 6 (Ik-Δ5/6), and Ikaros lacking exons 3 and 5 (Ik-Δ3/5) were detected. To verify the identity of these splice variants, we performed nested PCR using primers that amplified each possible pair of exons; an example of the data generated by this approach is shown in Fig. 2-3C. Based on the nested PCR and the predicted molecular weights, Ik-Full, Ik-Δ5/6, and Ik-Δ3 are the most likely splice variants detected by western blot (Fig. 2-2A). These data are consistent with previous reports showing that Ik-Δ3 is a prominent splice variant in murine thymocytes (6, 343)

The splice variants detected for Ikaros at the protein and mRNA levels were similar in all thymocyte populations tested. In addition, the proportion of total Ikaros represented by each splice variant was comparable in each population. Ik-Δ3/5 was readily detected by nested PCR, but the protein product was not observed. The polyclonal anti-Ikaros antibodies used were raised against an unknown C-terminal epitope and the antibodies could recognize Ik-Δ3 and Ik-Δ5/6, so it is unlikely that the lack of Ik-Δ3/5 detection is due to lack of antibody recognition.

Figure 2-3. Ikaros and Aiolos mRNA undergo extensive splicing during early T cell development. *A*) The exon structure of Ikaros and Aiolos is shown along with the location of the four N-terminal DNA binding zinc fingers and the two C-terminal zinc fingers that mediate dimerization. The outer and inner primer pairs for the nested PCR are shown. *B* and *D*) Total mRNA isolated from DN3, DN4, ISP, and DP thymocytes was amplified using the outer primers shown in (*A*). The PCR product was reamplified using the inner primers shown in (*A*). The identity of the splice variants for Ikaros (*B*) and Aiolos (*D*) are shown. Data shown represent two independently derived sets of thymocytes, out of four independent experiments. *C*) To confirm splice variants, total mRNA isolated from DN3, DN4, ISP, and DP thymocytes was amplified using the outer primers shown in (*A*), and the PCR product was reamplified using all possible pairs of inner primers described in Table 2-1. A representative gel is shown for Ikaros expression in DP thymocytes.

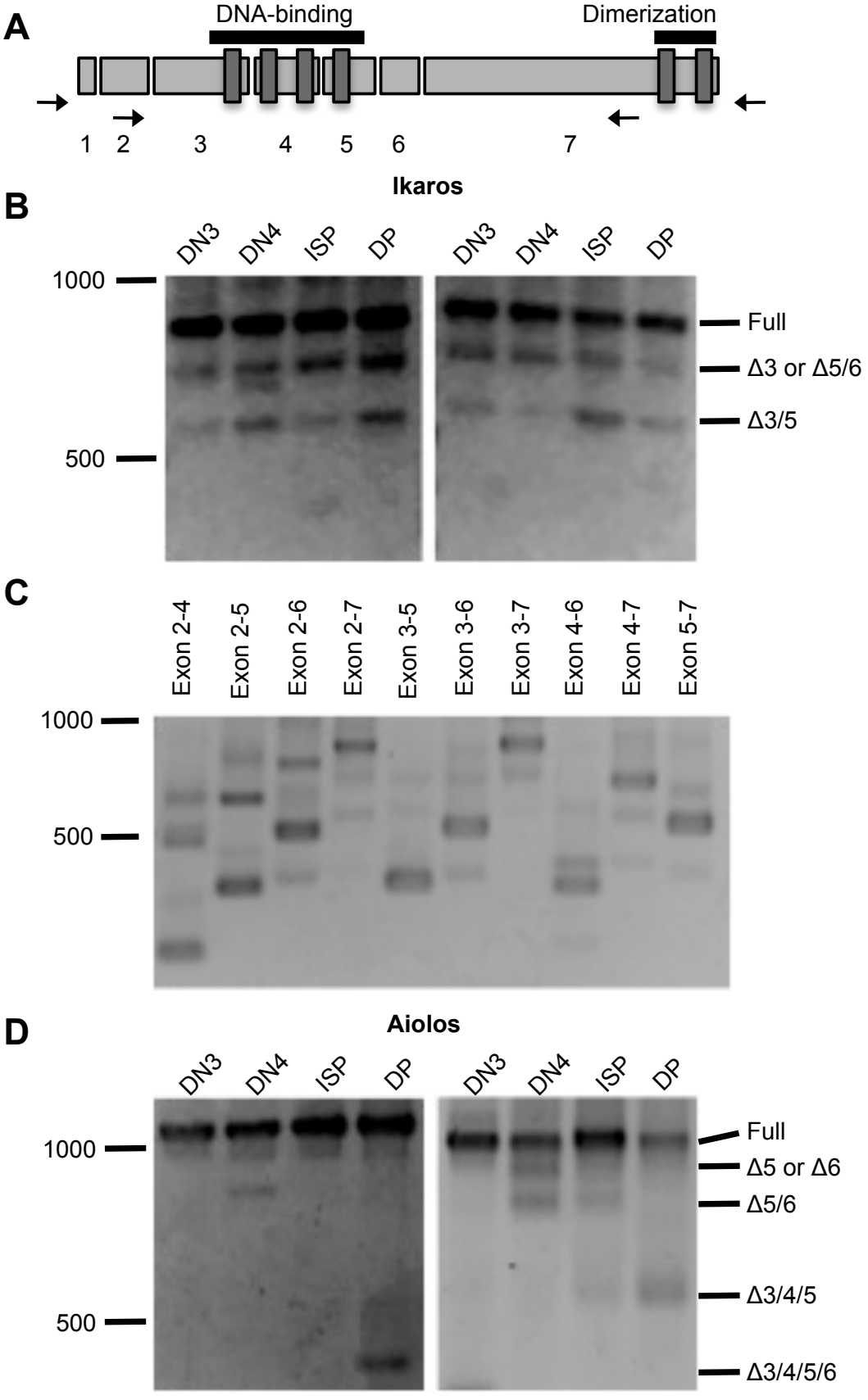
A
DNA-binding
Dimerization
1 2 3 4 5 6 7
B
Ikaros
DN3 DN4 ISP DP DN3 DN4 ISP DP
1000
500
Full
Δ3 or Δ5/6
Δ3/5
C
Exon 2-4
Exon 2-5
Exon 2-6
Exon 2-7
Exon 3-5
Exon 3-6
Exon 3-7
Exon 4-6
Exon 4-7
Exon 5-7
1000
500
D
Aiolos
DN3 DN4 ISP DP DN3 DN4 ISP DP
1000
500
Full
Δ5 or Δ6
Δ5/6
Δ3/4/5
Δ3/4/5/6

For Aiolos, two bands were detected by western blot. The ratio of the two bands changed from being nearly equivalent in DN4 thymocytes to being predominantly full-length in DP thymocytes. To identify the two bands, we performed nested PCR, using the same strategy as for Ikaros (Fig. 2-3D). While the splice variants detected at the protein level were consistent across thymocyte populations, the mRNA species detected were highly variable between thymocyte populations and between mice. Based on the molecular weights of the protein bands and the splice variants most consistently detected at the mRNA level, the most likely Aiolos isoforms observed at the protein level are full-length Aiolos and Ai-Δ5/6. In each mouse analyzed, Ai-Δ5/6 mRNA was detected in DN thymocytes and the band decreased in intensity in ISP and DP thymocytes. This observation is consistent with the protein data showing that, as a percentage of total Aiolos, Ai-Δ5/6 is more prevalent in DN4 thymocytes than DP thymocytes.

To summarize, Ikaros and Aiolos expression increased at the protein and mRNA levels as murine thymocytes progressed from the DN2 to the DP developmental stage. Three Ikaros and two Aiolos splice variants were detected at the protein level for each thymocyte population analyzed, although the ratio of the two Aiolos isoforms shifted as thymocytes progressed through development. For both Ikaros and Aiolos, multiple splice variants, including dominant negative splice variants, were detected at the mRNA level, but not the protein level, indicating that the mRNA was not translated, the antibodies could not detect the splice variant, or the splice variants were expressed at levels below the limits of detection.

mRNA levels of Ikaros family members during early human T cell development

mRNA was isolated from FACS-purified human DN2, DN3, ISP, and DP thymocytes and subjected to qRT-PCR. Ikaros, Aiolos, Helios, and Pegasus mRNA levels increased as

thymocytes progressed from the DN2 developmental stage to the DP stage, while Eos mRNA levels remained constant (Fig. 2-4A). As in mice, the most dramatic change detected was in Aiolos mRNA levels, which were 18-fold higher in DP thymocytes than DN2 thymocytes. Ikaros and Pegasus mRNA levels in DP thymocytes were 4.4-fold and 2.5-fold than in DN2 thymocytes, respectively. In contrast to murine thymocytes, in which Helios mRNA levels decreased during early T cell development, Helios mRNA levels increased in human thymocytes. Helios mRNA levels in DN3 thymocytes were 2.3-fold higher than in DN2 thymocytes and 10-fold higher in DP thymocytes than DN2 thymocytes.

We also compared the mRNA levels of each Ikaros family member to that of Ikaros (Fig. 2-4B). Ikaros mRNA was the most abundant family member expressed in all populations except the DP population. As thymocytes matured into the DP stage, the relative quantity of Helios increased from 9.0-fold less than Ikaros ($p < 0.05$) to 3.9-fold less than Ikaros and the difference between Ikaros and Helios mRNA levels at the DP stage was not statistically significant. Similarly, Aiolos mRNA levels increased from 20-fold lower than Ikaros to 5.2-fold lower than Ikaros and the change in the Ikaros to Aiolos ratio was statistically significant ($p < 0.05$). Conversely, Eos mRNA levels decreased from 14-fold less than Ikaros to 52-fold less than Ikaros, and Pegasus mRNA decreased from 3,500-fold less than Ikaros to more than 10,000-fold less than Ikaros. These data indicate that Ikaros, Aiolos, and Helios are significant contributors to the total quantity of Ikaros family mRNA, but Eos may also function in human thymocytes, particularly in DN cells.

Figure 2-4. Ikaros, Helios, Aiolos, and Pegasus mRNA levels increase during early human T cell development. mRNA isolated from human DN2 (CD4–CD8–CD3–CD34+CD38+CD1a–), DN3 (CD4–CD8–CD3–CD34+CD38+CD1a+), ISP (CD4+CD8–CD3–), and DP (CD4+CD8+) thymocytes was subjected to qRT-PCR. A) For each thymocyte population, the relative expression of each Ikaros family member was normalized to that of DN2 thymocytes and the log2 (Fold Change) is shown. (n = 5 independent samples; * $p < 0.05$, ** $p < 0.01$, *** $p < 0.001$ as compared to DN3) (B) For each population, relative mRNA levels of the Ikaros family members were normalized to that of Ikaros.

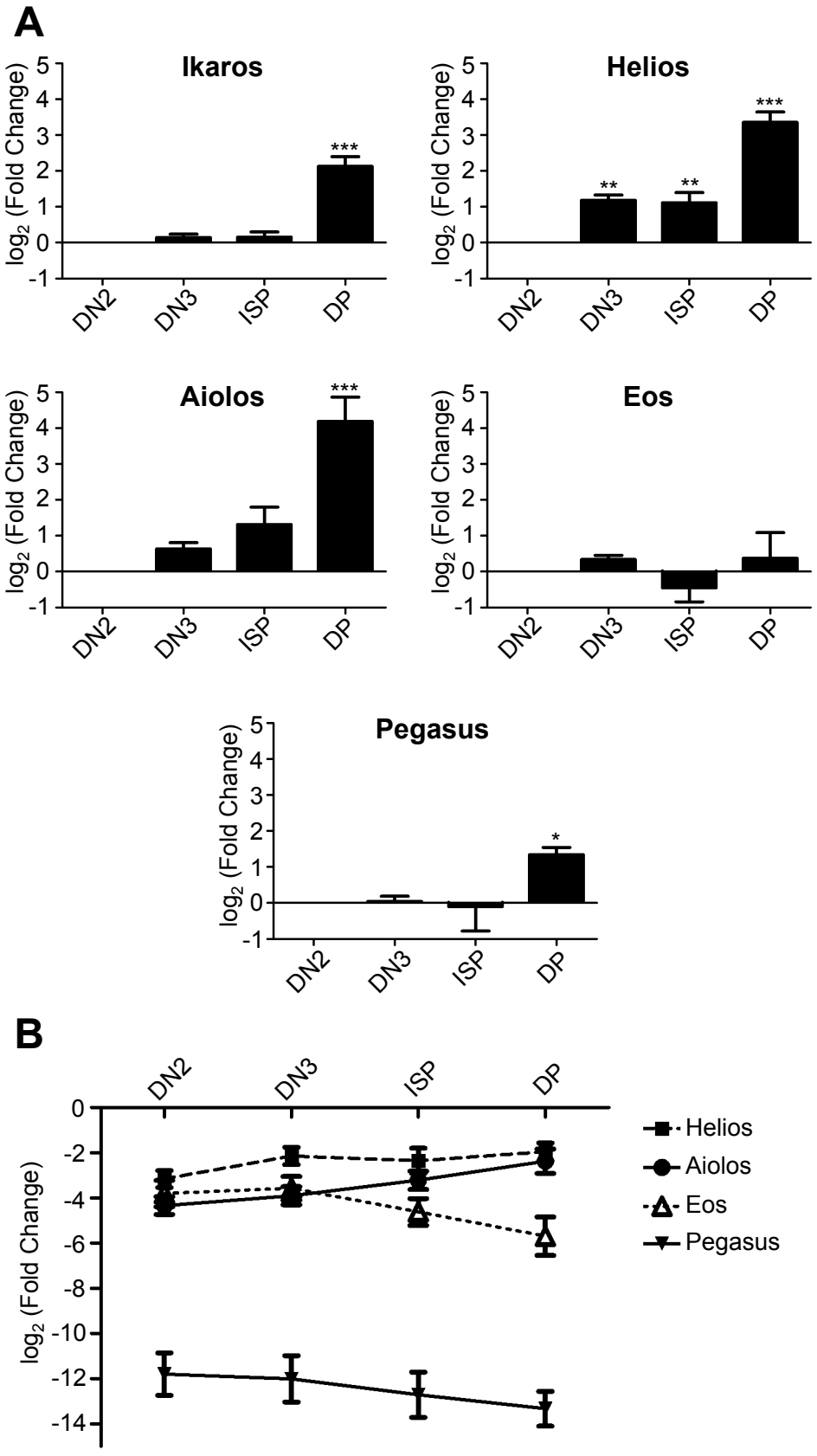
A
Ikaros
Helios
Aiolos
Eos
Pegasus
log2 (Fold Change)
DN2
DN3
ISP
DP
***
**
*
B
Helios
Aiolos
Eos
Pegasus

Protein levels of Ikaros family members during human T cell development

Despite statistically significant increases in Ikaros and Aiolos mRNA levels, western blot analysis showed that Ikaros and Aiolos protein levels remained similar across the thymocyte populations (Fig. 2-5A). However, subtle changes in protein levels were noted using intracellular staining and flow cytometry (Fig. 2-5B). For example, Aiolos protein levels were 1.9-fold higher in DP thymocytes than in DN2 cells. In DP thymocytes, a distinct subpopulation of cells with slightly higher Ikaros protein could be detected. Helios protein levels increased to a greater extent than Ikaros and Aiolos as thymocytes matured; Helios protein levels were 4.9-fold higher in DP thymocytes than the earlier developmental stages. These data suggest that post-transcriptional regulation of Ikaros and Aiolos is a critical factor in regulating protein levels, while Helios protein levels are more tightly linked to transcriptional control.

Splice variants of Ikaros and Aiolos in human thymocytes

Using western blot analysis, we detected three bands when cell lysates derived from DN2, DN3, ISP, and DP thymocytes were probed with anti-Ikaros (Fig. 2-5A), suggesting that multiple splice variants of Ikaros are expressed in human thymocytes. To identify the Ikaros splice variants, we used nested PCR (Fig. 2-6A). The pattern of Ikaros splicing was complex and varied across thymocyte populations and between individuals. In addition to the loss of intact exons, Ikaros splice variants can include the addition of sixty intronic base pairs following exon 2 and the deletion of thirty base pairs at the 3′ end of exon 6 (8-10). These additions and deletions resulted in the complex pattern seen in the nested PCR. The identity of each mRNA species in Fig. 2-6A was determined by calculating its molecular weight and verified using nested PCR primers that include each possible pair of exons, as shown in Fig. 2-6B. Because of

Figure 2-5. Helios protein levels, but not Ikaros and Aiolos protein levels, increase during early human T cell development. *A*) Cell lysates prepared from FACS-purified human DN2, DN3, ISP, and DP thymocytes were probed with antibodies against Ikaros, Aiolos, or p38 MAPK and quantified as described in the legend to Figure 2-2. Data are representative of three independent experiments. *B*) Human thymocytes were labeled with antibodies against CD4, CD8, CD34, CD38, and CD1a before fixing, permeabilizing, and staining with anti-Helios and either anti-Ikaros or anti-Aiolos (dark lines) or the appropriate isotype controls (shaded histogram). For each population shown, the geometric mean fluorescence intensity (GMFI) of the anti-Ikaros, anti-Aiolos, or anti-Helios staining was divided by the GMFI of the corresponding isotype control. Data were normalized to the DN2 population (*$p < 0.05$).

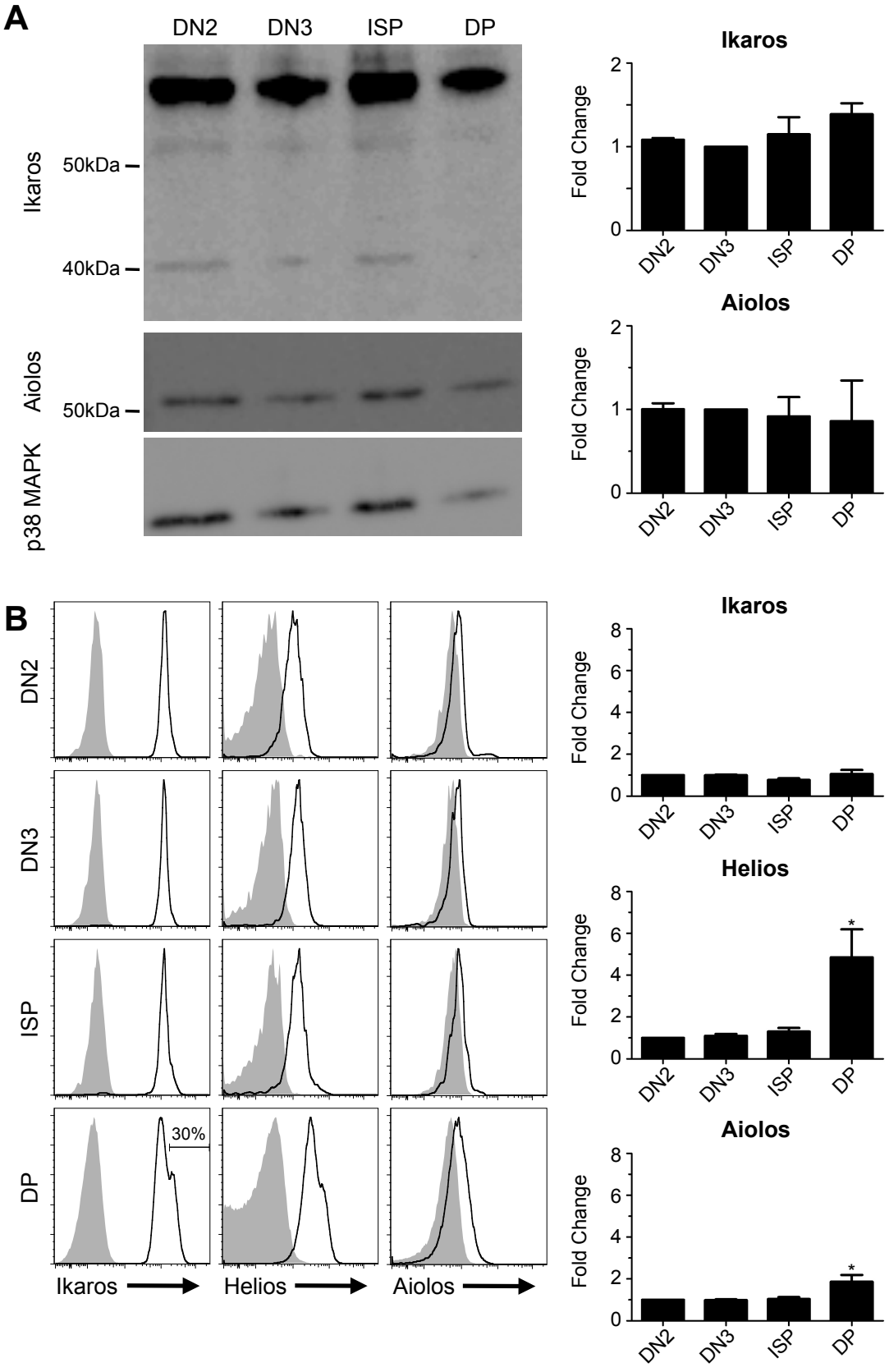
A
DN2
DN3
ISP
DP
Ikaros
50kDa
40kDa
Aiolos
50kDa
p38 MAPK
Ikaros
Fold Change
Aiolos
Fold Change
B
DN2
DN3
ISP
DP
30%
Ikaros
Helios
Aiolos
Ikaros
Fold Change
Helios
Fold Change
Aiolos
Fold Change

Figure 2-6. Ikaros and Helios, but not Aiolos, mRNA undergoes extensive alternative splicing in human thymocytes. Nested RT-PCR was performed on FACS-purified DN2, DN3, ISP, and DP human thymocytes to examine Ikaros (*A*), Aiolos (*C*), and Helios (*D*) alternative splicing, as described in the legend to Figure 2-3A. Two representative sample sets are shown from three independent experiments. *B*) A representative gel showing the results of nested RT-PCR for DN3 thymocytes using all possible pairs of inner primers shown in Table 2-2.

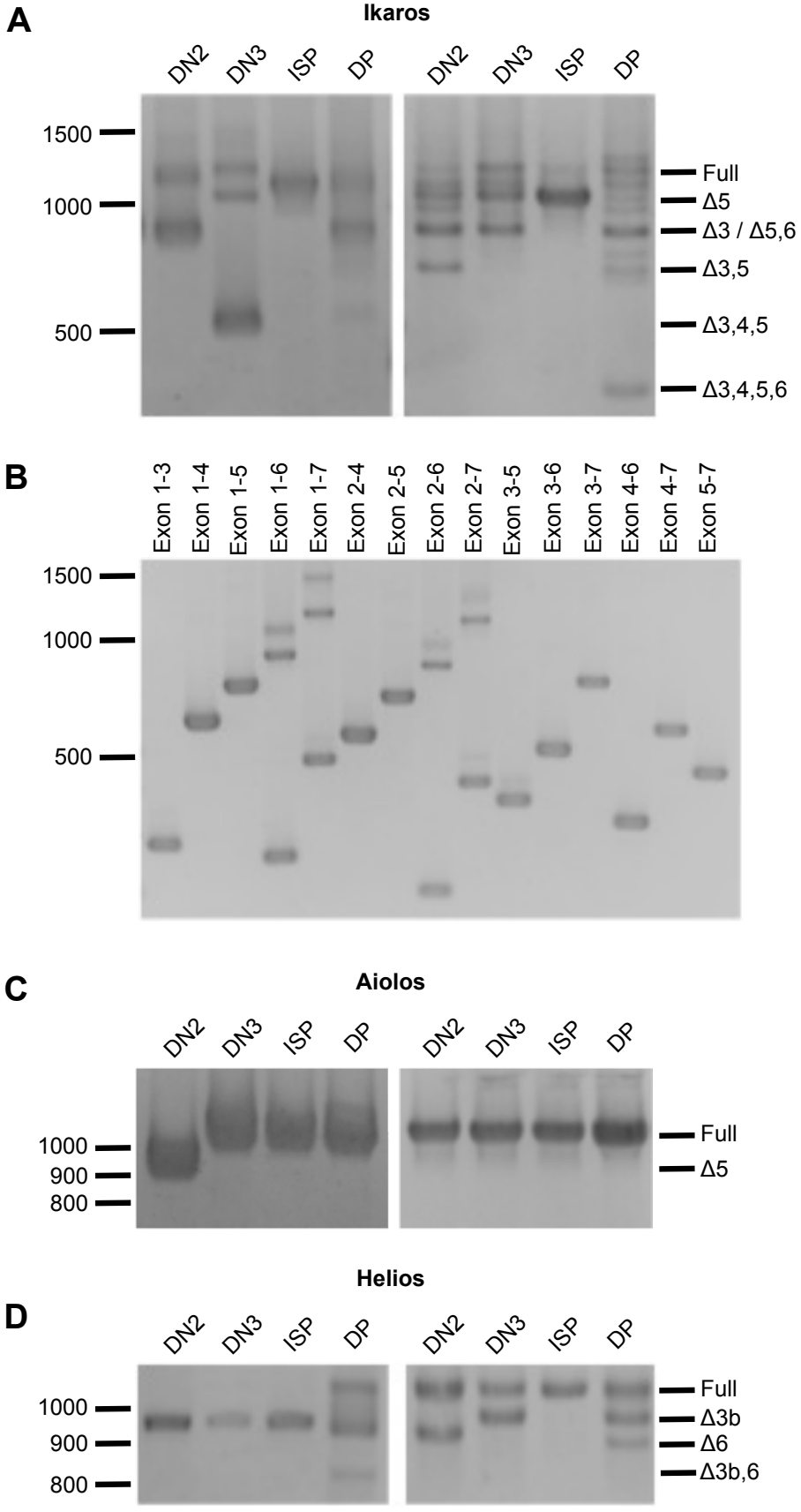
A
Ikaros
DN2
DN3
ISP
DP
DN2
DN3
ISP
DP
1500
1000
500
Full
Δ5
Δ3 / Δ5,6
Δ3,5
Δ3,4,5
Δ3,4,5,6
B
Exon 1-3
Exon 1-4
Exon 1-5
Exon 1-6
Exon 1-7
Exon 2-4
Exon 2-5
Exon 2-6
Exon 2-7
Exon 3-5
Exon 3-6
Exon 3-7
Exon 4-6
Exon 4-7
Exon 5-7
1500
1000
500
C
Aiolos
DN2
DN3
ISP
DP
DN2
DN3
ISP
DP
1000
900
800
Full
Δ5
Helios
D
DN2
DN3
ISP
DP
DN2
DN3
ISP
DP
1000
900
800
Full
Δ3b
Δ6
Δ3b,6

the complexity of Ikaros splicing and the fact that not all mRNA splice variants are translated at detectable levels, we are unable to definitively identify the two minor splice variants of Ikaros detected on the western blot. Possible splice variants represented by the band at 55 kD are Ik-Δ3 or Ik-Δ5/6. The band at 39 kD might be Ik-Δ3/4/5/6.

Unlike Ikaros, only one Aiolos band could be detected by western blot and this band was full-length Aiolos (Fig. 2-5A). Using nested RT-PCR, we detected one sample in which Aiolos lacked exon 5 (Ai-Δ5), but all the other samples only contained full-length Aiolos (Fig. 2-6C). Helios was also subjected to alternate mRNA splicing, as determined by nested RT-PCR (Fig. 2-6D). The splicing pattern varied between patients and between thymocyte populations, but samples containing full-length Helios (Helios-Full), Helios lacking the terminal seventy-eight bases of exon 3 (Hel-Δ3b), Helios lacking exon 6 (Hel-Δ6), and Helios lacking part of exon 3 and all of exon 6 (Hel-Δ3b/6) were detected. Hel-Δ3b is missing the first DNA-binding zinc finger, as previously reported (3). Hel-Δ6 and Hel-Δ3b/6 have not been previously reported, but we used high fidelity RT-PCR to amplify the mRNA from total human thymocytes and sequenced the cDNA as verification of its identity.

Discussion

We report the first comprehensive characterization of the expression and splicing patterns of the entire Ikaros family of transcription factors during the DN, ISP, and DP stages of murine and human T cell development. In both mice and humans, Ikaros and Aiolos mRNA levels increased as thymocytes differentiated from the DN2 to DP stages (Figs 2-1 and 2-4), but the corresponding increase in protein levels was only observed in mice (Fig. 2-2), suggesting that human Ikaros and Aiolos mRNA might be stored for rapid translation following a stimulus. Further, multiple Ikaros and Aiolos mRNA splice variants were detected in mice (Fig. 2-3), but only Ikaros underwent extensive alternative splicing in humans (Fig. 2-6). Another remarkable difference between mice and humans was that Helios mRNA and protein levels decreased during murine T cell development (Figs. 2-1 and 2-2), but increased during human T cell development (Figs. 2-4 and 2-5). Helios mRNA underwent alternative splicing in humans and we identified two novel splice variants (Hel-Δ6 and Hel-Δ3b/6). These differences in the expression and splicing of Ikaros family members between human and murine thymocytes indicate that the Ikaros family of transcription factors regulates murine and human T cell development differently.

The importance of small changes in expression levels among Ikaros family members was highlighted in a study by Dovat, *et. al.* (55), who transgenically expressed Helios in murine B cells, which express very low levels of endogenous Helios (5). Even though the transgenic expression resulted in a level of Helios that was approximately ten-fold lower than Ikaros, the mice developed B cell lymphoma characterized by increased Bcl-xL expression and B cell receptor-mediated proliferation.

The significance of changing the protein levels of any family member during T cell development is that the ratio of each family member to each other family member changes, thereby altering the composition of the Ikaros family dimers. In mice, DN2 thymocytes expressed Ikaros and Helios protein, suggesting that the predominant dimers in murine DN2 thymocytes are likely Ikaros-Ikaros homodimers and Ikaros-Helios heterodimers, the latter of which have been demonstrated to form in a murine thymocyte cell line (5, 30). As murine thymocytes progress toward the DP developmental stage, the dimer species likely switch to predominantly Ikaros- and Aiolos-containing homodimers and heterodimers, which are also known to occur in murine thymocyte cell lines (27). In humans, the only family member whose protein levels changed significantly during T cell development is Helios (Fig. 2-5). Our data would predict that dimers containing Ikaros and Helios are common in human DP thymocytes, whereas DN2 thymocytes would express primarily Ikaros- and Aiolos- containing dimers.

The Ikaros family members are derived from duplication events originating with a common gene (344). Consistent with this shared origin, the family members share a high degree of homology, particularly within the DNA binding sites, which are nearly perfectly conserved across family members and between humans and mice (2, 3). This homology means that Ikaros, Aiolos, and Helios can bind identical DNA sequences with comparable affinity, but the ability of each family member to drive transcription varies; Aiolos activity is greater than that of Ikaros, which is greater than Helios (2, 5). The observations that different Ikaros family members vary in their transcriptional potency despite comparable DNA binding suggests that the activity of each family member is determined by their ability to bind co-transcription factors.

A protein complex that has been linked to Ikaros function is the nucleosome remodeling and histone deacetylase (NuRD) complex. Ikaros, Aiolos, and Helios are all capable of

associating with the NuRD complex, but the nature of the Ikaros dimers present in the cells can regulate which genes are bound by the NuRD complex (27-30). Mi-2β, the catalytic core protein of the NuRD complex, primarily associates with genes that promote differentiation in the presence of Ikaros and genes associated with proliferation in the absence of Ikaros (27). The mechanism for this differential gene association is unknown, but may be related to the nature of the Ikaros dimers present in the cell.

An example of where differences in the expression of Ikaros family members may influence gene transcription is in the expression of CD4 and CD8α. In mice, Ikaros and Mi-2β bind the CD8α and CD4 genetic loci. Mi-2β binds the CD8α locus during early T cell development and is removed from the DNA when CD8 is expressed later in development (65). During the DP stage, Mi-2β associates with the CD4 locus and disruption of Mi-2β expression results in the inability to optimally express CD4 (66, 345). The role of Ikaros family members in Mi-2β-mediated regulation of CD4 and CD8 transcription is unclear, but Ikaros associates with the CD8α and CD4 loci in murine DN and DP thymocytes (65, 66, 346). This constitutive association of Ikaros with these loci suggests that other Ikaros family members may regulate Mi-2β recruitment or release. The increase in Aiolos expression we observed in murine thymocytes (Fig. 2-2) may affect Mi-2β binding to these loci. In support of this model, Ikaros$^{+/-}$Aiolos $^{-/-}$ mice have an increase in the number of CD4^{+}CD8$^{-/lo}$ cells with an immature phenotype (346). This population resembles the CD4^{+} ISP stage of human development. Thus, the opposing expression of CD4 and CD8 observed in human and murine ISP thymocytes may be related to the fact that Aiolos protein levels increase in murine thymocytes and Helios protein levels increase in human thymocytes.

Another mechanism by which Ikaros dimer composition might regulate T cell development is through control of Notch-dependent transcription. Ikaros, Aiolos, and Helios bind the same DNA consensus sequence (GGGAA) as the Notch-dependent transcriptional regulator RBP-Jκ (14, 43, 44, 60, 77). Based on this observation, it has been proposed that Ikaros might act as a competitive inhibitor of Notch-dependent transcription. In support of this model, murine thymocytes lacking Ikaros have elevated expression of Notch-dependent genes (44, 60). In addition, the increase in Aiolos protein levels in murine thymocytes correlates with the developmental stage at which cells reduce their ability to respond to Notch ligation (347).

In addition to the protein levels of Aiolos and Helios being markedly different between human and murine thymocytes, the splicing patterns of Ikaros and Aiolos were also different. In mice, three prominent variants of Ikaros were found: Ik-FL, Ik-Δ5/6, and Ik-Δ3 (Fig. 2-2). These variants were detected at the mRNA and protein levels and the relative quantity of each variant was comparable in each thymocyte population tested. By contrast, mRNA splicing of Ikaros in human thymocytes varied dramatically across the thymocyte populations and between patients (Fig. 2-6), but the major Ikaros isoform detected at the protein level was full-length. Some splice variants detected at the mRNA level in normal thymocytes had been previously reported to be aberrant splice variants in patients with acute lymphoblastic leukemia (8-10, 85, 90, 91, 100, 105). Our data suggest that these unusual splice variants occur naturally, although their relative abundance may be elevated in leukemia and they may be translated into protein in leukemia. For Aiolos, the opposite splicing pattern was noted; there was minimal splicing in human thymocytes (Fig. 2-6), but highly variable splicing in murine thymocytes (Fig. 2-3). This variability in splicing was detected primarily at the mRNA level and did not necessarily translate into detectable protein.

During human T cell development, there were marked changes in the mRNA levels of Ikaros and Aiolos that were not detected at the protein level (Figs. 2-4 and 2-5). This discrepancy between mRNA and protein levels was not observed in murine thymocytes nor was it observed for human Helios. These data indicate that the rates of synthesis or degradation of Ikaros and Aiolos proteins change during human T cell development. Recent studies have shown that the thalidomide derivatives lenalidomide and pomalidomide induce the degradation of Ikaros and Aiolos through activation of the CRBN-CRL4 E3 ubiquitin ligase (348-351). Importantly, Helios is resistant to CRBN-CRL4-mediated degradation (351), suggesting a possible mechanism for the selective increase in Helios protein levels.

In summary, we report the first comprehensive characterization of the expression and splicing of Ikaros family members during murine and human T cell development. In both species, members of the Ikaros family change their expression at the mRNA and protein levels in manners that are expected to profoundly alter the functionality of the family. In addition, there were notable differences in the expression and splicing patterns of Ikaros family members that clearly indicate that murine and human T cell development are regulated differently.

Chapter 3. Ikaros, Helios, and Aiolos protein levels increase in human thymocytes after β selection

Abstract

In human T cell development, the mechanisms that regulate cell fate decisions after TCRβ expression remain unclear. We defined the stages of T cell development that flank TCRβ expression and found distinct patterns of human T cell development. In half the subjects, T cell development progressed from the $CD4^{-}CD8^{-}$ double negative (DN) stage to the $CD4^{+}CD8^{+}$ double positive (DP) stage through an immature single positive (ISP) $CD4^{+}$ intermediate. However, in some patients, CD4 and CD8 were expressed simultaneously and the ISP population was small. In each group of patients, $CD3^{-}$ ISP and DP thymocytes were subdivided into ISP1, ISP2, DP1, DP2, DP3, DP4, and DP5 developmental stages according to their expression of CD28, CD44, CD1a, CD7, CD45RO, and CD38. The ISP2, DP2, and DP3 thymocyte populations proliferated more robustly than ISP1 and DP1 and expressed markers consistent with TCRβ expression. After the DP3 stage, proliferation returned to baseline levels. We then analyzed protein levels of Ikaros, Helios, and Aiolos, the three Ikaros family members most abundantly expressed in human thymocytes. Ikaros and Helios expression increased transiently at the ISP2, DP2, and DP3 populations. Aiolos expression also increased at the ISP2, DP2, and DP3 stages, but its expression remained elevated throughout the DP4 and DP5 stages. In summary, we propose a model of human T cell development that reflects the asynchronous nature of TCRβ expression and we define the subpopulations of thymocytes that are highly proliferative and express Ikaros family members.

Introduction

Human T cell precursors enter the thymus at a developmental stage in which the cells lack CD4 and CD8 expression and are called $CD4^{-}CD8^{-}$ double negative (DN) thymocytes. The DN thymocyte population can be subdivided into three subsets: DN1 ($CD34^{+}CD38^{-}CD1a^{-}$), DN2 ($CD34^{+}CD38^{+}CD1a^{-}$), and DN3 ($CD34^{+}CD38^{+}CD1a^{+}$). After the DN3 stage, the cells express CD4 and CD8 to become $CD4^{+}CD8^{+}$ double positive (DP) thymocytes. Finally, the cells mature into single positive (SP) $CD4^{+}$ or SP $CD8^{+}$ thymocytes and exit the thymus.

Rearrangement of the *TCRD* and *TCRG* genes occurs during the DN stages of human development, while *TCRA* rearrangement occurs in the DP stage (109). Between the rearrangement of *TCRG* and *TCRA* genomic loci, V(D)J recombination at the *TCRB* locus occurs and T cell receptor β chain (TCRβ) protein is expressed. Rearrangement of the *TCRB* genomic locus has been reported to begin as early as the DN3 stage, but TCRβ protein has not been detected until the immature single positive (ISP) developmental stage, the stage between the DN and DP populations (109, 115-117, 119). However, there are $TCR\beta^{-}$ DP thymocytes (116, 117, 119), indicating that the exact timing of β selection remains unclear.

In mice, successful expression of TCRβ leads to proliferation, survival, and differentiation (177-179), processes that must be tightly regulated to balance the expansion of $TCR\beta^{+}$ thymocytes with the prevention of leukemia. A family of transcription factors that is likely to regulate β selection is the Ikaros family. The Ikaros family consists of five family members (Ikaros, Helios, Aiolos, Eos, and Pegasus) that share a common structure with two zinc finger domains, an N-terminal DNA binding domain and a C-terminal dimerization domain. Protein dimerization is required for high affinity DNA binding. The dimerization domain allows

for the binding of any family member to any other family member, creating the potential for a mixture of homodimers and heterodimers within the same cell (1-5). Though the different family members have similar DNA recognition sites (2, 3), some family members are more potent transcriptional activators than others (2, 5).

Ikaros family functionality is critical for lymphocyte development as expression of dominant-negative Ikaros can block murine B and T cell development (16). Further, during murine B cell development, signals from the pre-B cell receptor drive Ikaros and Aiolos expression, resulting in loss of expression of the surrogate light chain and withdrawal from the cell cycle (2, 352, 353).

Based on these results, we postulated that the expression of Ikaros family members may correlate with TCRβ expression during human T cell development. Ikaros, Helios, and Aiolos mRNA levels increase as human thymocytes progress from the DN to the DP developmental stage (354). However, despite large increases in mRNA levels, only subtle changes in protein levels were observed. To investigate this observation in more detail, we first defined the human thymocyte subsets in which TCRβ is expressed and in which cell proliferation occurs. We then correlated these observations with changes in Ikaros, Helios, and Aiolos protein levels.

Materials and Methods

Antibodies

The anti-human antibodies, anti-CD1a-PerCP-Cy5.5, anti-CD1a-PE-Cy5, anti-CD3-Allophycocyanin (APC)-Cy7, anti-CD4-Pacific Blue, anti-CD4-PE-CF594, anti-CD7-FITC, anti-CD7-APC, anti-CD8-Brilliant Violet (BV) 785, anti-CD28-Pacific Blue, anti-CD34-BV605, anti-CD34-PE, anti-CD38-Alexa Fluor (AF) 700, anti-CD44-PE-Cy7, and anti-TCRγδ-FITC were purchased from Biolegend (San Diego, CA). Anti-Helios-AF647 was purchased from e-Biosciences (San Diego, CA), and Mouse IgG1κ-PE control, anti-Ikaros-PE, and anti-Aiolos-PE were purchased from BD Biosciences (San Jose, CA). The Armenian Hamster IgG-AF647 control was purchased from Biolegend.

Human thymocyte labeling

After obtaining consent from the parent or guardian, human thymus samples were obtained from children (0 – 18 years) that underwent corrective surgery at Children's Mercy Hospital (Kansas City, MO) for congenital cardiac defects. Deidentified tissue samples void of any clinical data were obtained in compliance with the Institutional Review Boards at our institutions.

Single cell suspensions of human thymocytes were labeled on their surface with anti-CD1a, anti-CD3, anti-CD4, anti-CD7, anti-CD8, anti-CD28, anti-CD34, anti-CD38, anti-CD44, anti-CD45RO, and anti-TCRγδ, as previously described (355). Cells were analyzed using a BD LSR II (BD Biosciences), and data was analyzed with BD FACSDiva software (BD Biosciences).

For labeling with 4',6′-diamidino-2-phenylindole (DAPI) staining, cells were surface labeled as indicated. After washing, cells were fixed in PBS with 2% paraformaldehyde and incubated over night at 4°C. Cells were washed and resuspended in PBS with 0.2% Tween and 1 μg/ml DAPI and analyzed, as previously described (356).

For intracellular staining, cells were first surface stained as indicated, washed, and incubated in Foxp3/Transcription Factor Staining Buffer Set (Affymetrix/eBioscience, San Diego, CA), according to the manufacturer's instructions. Permeabilized cells were labeled with anti-Helios and either anti-Ikaros or anti-Aiolos, or isotype control antibodies before analyzing using the BD LSR II. Data were analyzed using FlowJo (TreeStar, Inc., Ashland, OR). Relative expression of Ikaros, Helios, and Aiolos in each cell population was defined as the ratio of geometric mean fluorescence intensity of each Ikaros family member and the corresponding isotype control.

Statistical analysis

The Student *t* test was performed for experiments in which two groups were compared. For comparisons across groups, the repeated measure ANOVA (Fig. 3-4) or one-way ANOVA (Fig. 3-5) analyses with Tukey posthoc tests were performed using GraphPad Prism (GraphPad Software, Inc, La Jolla, CA), and significance was defined as $p < 0.05$.

Results

The DN to DP transition in human thymocytes occurs in two patterns

Before we can analyze the expression patterns of Ikaros, Helios, and Aiolos at β selection, we must first define the $CD3^-$ thymocyte subsets that express TCRβ. Because TCRβ protein can be first detected in the ISP $CD4^+$ population (109, 115-117, 119), we determined the percentage of SP $CD4^+$ thymocytes that lacked surface CD3 expression (Fig. 3-1A). Based on the analysis of 27 patients, we identified two groups of patients. The percentage of $CD4^+$ cells that were $CD3^-$ was 22% ± 2.0% in Group 1 (n = 14) and 3.6% ± 0.53% in Group 2 (n = 13).

To further explore the differences in T cell development between the groups, we gated on $CD3^-$ thymocytes and re-analyzed CD4 and CD8 expression (Fig. 3-1B). In group 1 samples, DN, ISP $CD4^+$, and DP thymocytes were readily detected. However, few ISP $CD4^+$ thymocytes were observed in group 2 patients. In two patients, there appeared to be an ISP $CD8^+$ population (called Group 3 in Fig. 3-1B). Because only two of the 27 patients were in group 3, the data from these individuals were excluded from further analysis. To quantify the difference in the developmental patterns between groups 1 and 2, we calculated the ratio of $CD3^-$ DN cells to $CD3^-$ ISP $CD4^+$ cells. This ratio was 0.88 ± 0.13 in Group 1 patients and 6.4 ± 1.7 in Group 2 patients ($p < 0.01$).

In summary, the up-regulation of CD4 and CD8 expression observed during the transition from the DN to DP developmental stage can occur in different sequences in different individuals. In some cases, CD4 is expressed first, resulting in an ISP $CD4^+$ population. In other cases, CD4 and CD8 expression occurs simultaneously. In rare cases, CD8 is expressed before CD4, resulting in an ISP $CD8^+$ population.

Figure 3-1. Up-regulation of CD4 and CD8 occurs in two patterns. *A*) TCRγδ$^-$ thymocytes were analyzed for CD4 and CD8 expression (*upper panels*). Thymocytes were gated on SP CD4$^+$ cells and analyzed for CD3 and CD4 expression. The percentages of SP CD4$^+$ thymocytes that were CD3$^-$ were calculated. Representative dot plots are shown for a thymus with a high ISP percentage (Group 1) and low ISP percentage (Group 2). The scattergram shows the percentages of SP CD4$^+$ thymocytes that were CD3$^-$ along with the line dividing patients in group 1 and group 2. *B*) Total thymocytes were gated on CD3$^-$ cells and expression of CD4 and CD8 expression is shown from a representative thymus from each group. The ratio of the percentages of DN to CD4$^+$ SP thymocytes within the CD3$^-$ population was calculated for groups 1 and 2. The lines indicate the mean ± SE of each group.

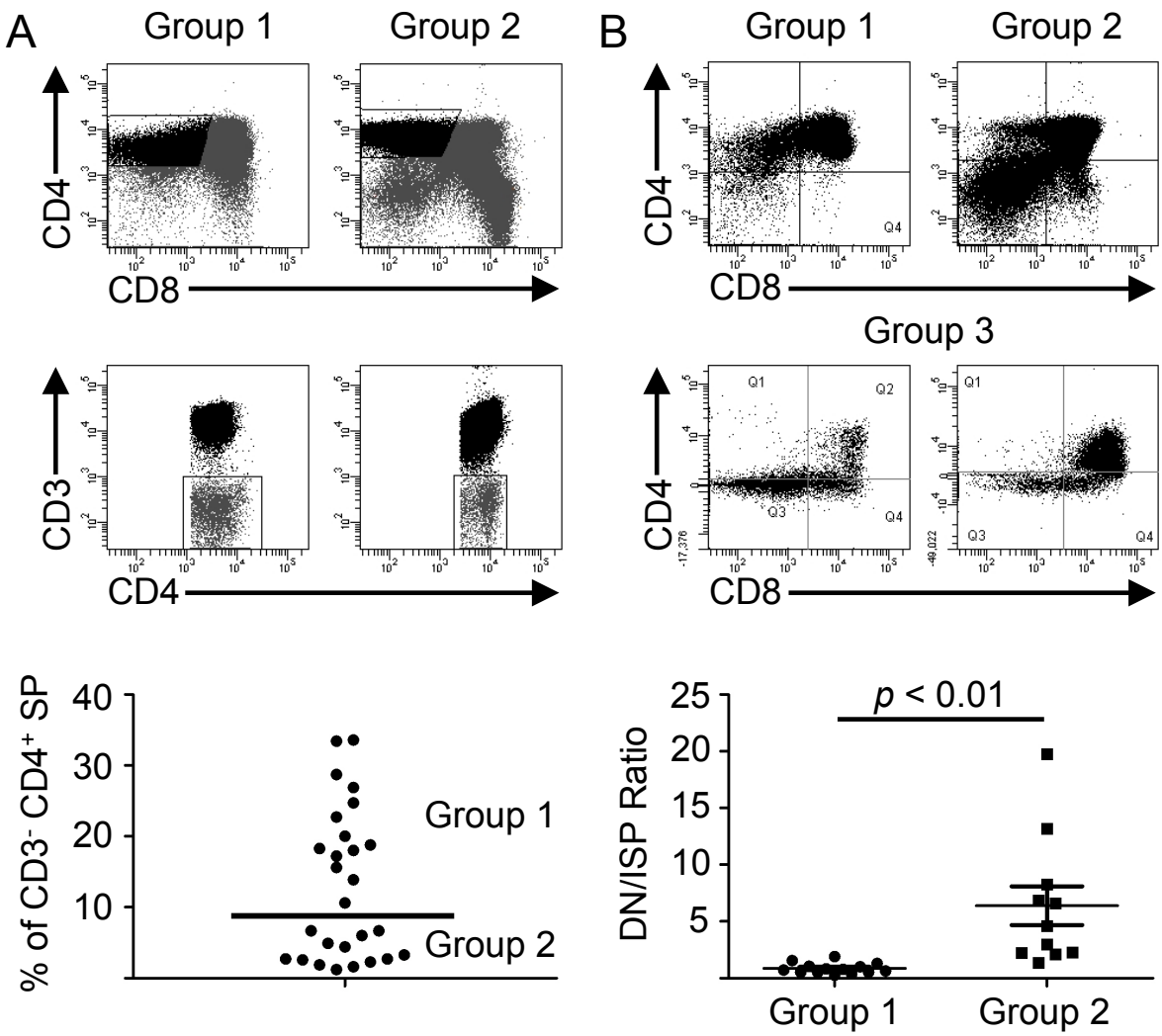
A
Group 1
Group 2
CD4
CD8
CD3
CD4
B
Group 1
Group 2
Group 3
CD4
CD8
Q1
Q2
Q3
Q4
% of CD3- CD4+ SP
40
30
20
10
Group 1
Group 2
p < 0.01
DN/ISP Ratio
25
20
15
10
5
Group 1
Group 2

ISP thymocytes can be subdivided based on CD44, CD1a, and CD28 expression

Next, we used CD44, CD1a, and CD28 to subdivide the ISP $CD4^+$ cells thymocytes. In both patient groups, CD28 expression correlated with the expression of CD44 and CD1a, so the ISP population could be subdivided into $CD44^+CD1a^+CD28^-$ cells (called ISP1 cells) and $CD44^{++}CD1a^{++}CD28^+$ cells (ISP2 cells) (Fig. 3-2A). Because CD28 has been shown to correlate with TCRβ expression (117), we propose that ISP1 thymocytes lack TCRβ protein and ISP2 thymocytes express TCRβ. The percentages of ISP $CD4^+$ cells that were ISP1 were 71% ± 4.2% in Group 1 patients and 47% ± 6.8% in Group 2 patients ($p < 0.01$) (Fig. 3-2B).

To further characterize the ISP1 and ISP2 populations, we analyzed CD7 and CD45RO expression (Fig. 3-2C). CD45RO expression increases as thymocytes progress toward the DP developmental stage (357). In group 1 patients, 93% ± 1.0% of ISP1 cells and 72% ± 4.8% of ISP2 cells were $CD7^{++}CD45RO^-$. The remaining ISP thymocytes were $CD7^+CD45RO^+$. In group 2 patients, nearly all ISP1 and ISP2 thymocytes were $CD7^{++}CD45RO^-$.

These data suggest that ISP thymocytes progress from $CD7^{++}CD45RO^-$ to $CD7^+CD45RO^+$ as they progress through development. To further test the developmental sequence of ISP1 and ISP2 thymocytes, we analyzed the expression of CD28, CD44, CD1a, CD28, CD7, and CD45RO on DN3 thymocytes, the stage immediately preceding the ISP stage (Fig. 3-2D). DN3 thymocytes from both groups of patients are uniformly $CD44^+CD1a^+CD28^-$ $CD7^{++}CD45RO^-$, similar to ISP1 $CD7^{++}CD45RO^-$ thymocytes.

$CD3^-$ DP thymocytes can be divided into five subsets

Our analysis of CD7 and CD45RO expression on the ISP population suggested that the $CD7^+CD45RO^+$ ISP population is the final stage before the DP population. To test this

Figure 3-2. CD1a and CD44 expression correlate with CD28 in ISP cells. *A*) ISP $CD4^+$ thymocytes were analyzed for CD28, CD44, and CD1a expression and divided into ISP1 and ISP2 subpopulations. *B*) The percentages of ISP thymocytes from each subject in groups 1 and 2 are shown. The line indicates the mean ± SE for each group. *C*) ISP1 and ISP2 thymocytes from group 1 and group 2 patients were analyzed for CD7 and CD45RO expression. *D*) DN3 thymocytes from group 1 (*left panels*) and group 2 (*right panels*) patients were analyzed for CD1a, CD44, CD28, CD7, and CD45RO expression.

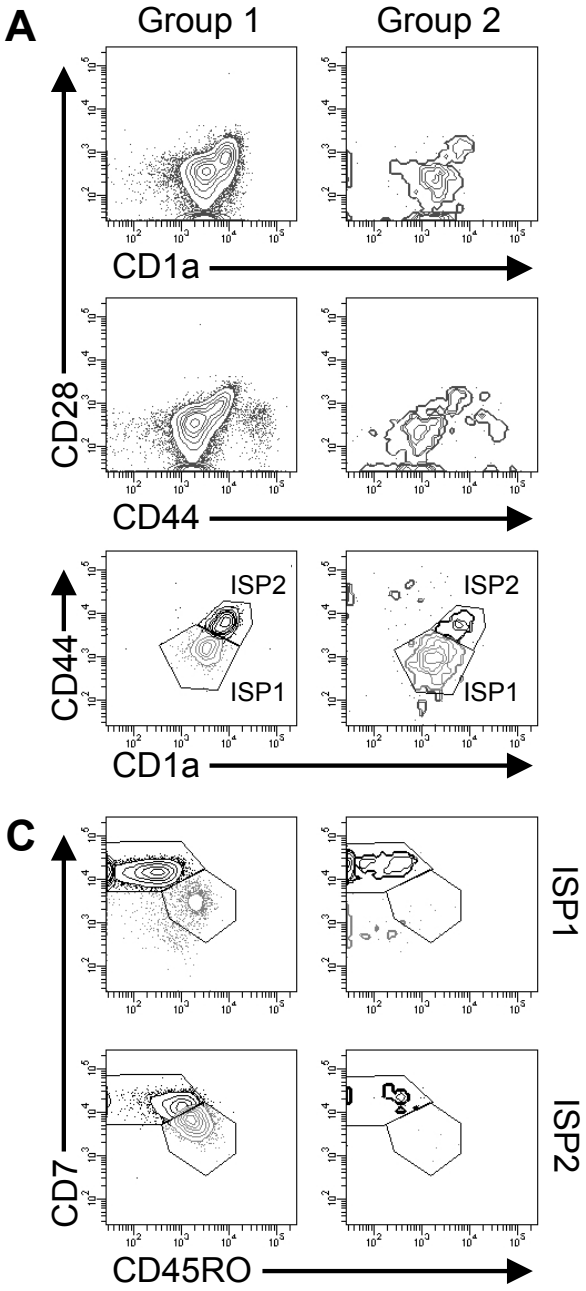
A
Group 1
Group 2
CD1a
CD28
CD44
ISP2
ISP1
CD44
CD1a
C
ISP1
ISP2
CD7
CD45RO

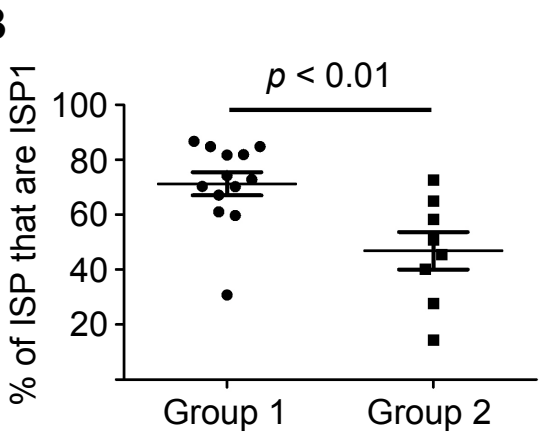
B
p < 0.01
% of ISP that are ISP1
100
80
60
40
20
Group 1
Group 2

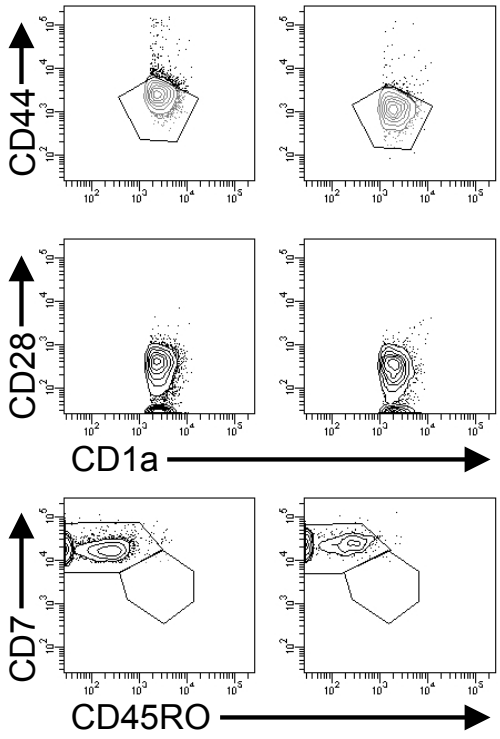
D
CD44
CD28
CD1a
CD7
CD45RO

hypothesis, we analyzed CD7 and CD45RO expression on $CD3^-$ and $CD3^{lo}$ DP thymocytes from patients in group 1 and group 2 (Fig. 3-3A). In both groups, 85% ± 1.9% of $CD3^-$ DP thymocytes were $CD7^+CD45RO^+$. Among $CD3^{lo}$ DP thymocytes, which represent the developmental stage after $CD3^-$ DP thymocytes, 95% ± 1.3% of the cells were $CD7^+CD45RO^+$.

Because a small percentage of DP thymocytes lack TCRβ expression (119), we further divided the $CD3^-$ DP subpopulations to define the subsets that express or lack TCRβ. As with the ISP1 and ISP2 thymocytes, we used CD44, CD1a, and CD28 to label $CD7^{++}CD45RO^-$ $CD3^-$ DP thymocytes (Fig. 3-3B). We called $CD44^+CD1a^+CD28^-CD7^{++}CD45RO^-$ DP thymocytes DP1 thymocytes and $CD44^{++}CD1a^{++}CD28^+CD7^{++}CD45RO^-$ DP thymocytes DP2 thymocytes, as shown in Fig. 3-3B.

Next, we used CD38 and CD45RO to subdivide the $CD7^+CD45RO^+CD3^-$ DP populations from each group (Fig. 3-3C, plot iii). As a comparison, we performed parallel analysis on DP1 and DP2 thymocytes (Fig. 3-3C, plot i). DP1 and DP2 thymocytes were uniformly $CD38^+$, but DP2 thymocytes expressed slightly higher CD45RO levels than DP1. Two populations of $CD7^+CD45RO^+$ thymocytes (plot iii) could be detected, one that is similar to DP2 thymocytes ($CD38^+CD45RO^{lo}$) and one with increased expression of CD38 and CD45RO ($CD38^{hi}CD45RO^{hi}$). We propose that the DP2 thymocytes mature into $CD38^+CD45RO^{lo}$ thymocytes. To determine whether this is a uniform population, we analyzed CD7 and CD44 expression. DP1 and DP2 had similar and high levels of CD7 and DP2 thymocytes expressed higher levels of CD44 than DP1 cells (Fig. 3-3C, plot ii). $CD38^+CD45RO^{lo}CD3^-$ DP thymocytes could be divided into $CD44^{hi}CD7^{hi}$ and $CD44^{lo}CD7^{lo}$ thymocytes (Fig. 3-3B, plot iv). The $CD44^{hi}CD7^{hi}$ thymocytes resembled DP2 thymocytes, so we called this subset DP3. We called the $CD44^{lo}CD7^{lo}$ cells DP4. In support of the conclusion that DP3 precedes DP4, the

Figure 3-3. CD3$^-$ DP cells can be divided into five subpopulations. *A*) CD3$^-$ and CD3^{lo} DP thymocytes were analyzed for CD7 and CD45RO expression. *B*) CD3$^-$CD7^{++}CD45RO$^-$ thymocytes were analyzed for CD44, CD1a, and CD28 expression and divided into DP1 (*lightly shaded cells*) and DP2 (*darkly shaded cells*) subsets. *C*) CD3$^-$CD7^{++}CD45RO$^-$ thymocytes (plots i and ii) and CD3$^-$CD7$^+$CD45RO$^+$ thymocytes (plots iii, iv, and v) were analyzed for expression of CD38, CD45RO, CD44, and CD7, as shown. Lightly shaded cells in plots i and ii reflect the shading in panel *B*. *D*) DP1, DP2, DP3, DP4, and DP5 thymocytes (as defined in panel *C*) were analyzed for CD28 and CD1a expression. *A*-*D*) Representative dot blots from a patient in group 1 (*upper panels*) and a patient from group 2 (*lower panels*) are shown in each panel. *E*) The percentages of CD3$^-$ DP thymocytes in each of the five subsets are shown.

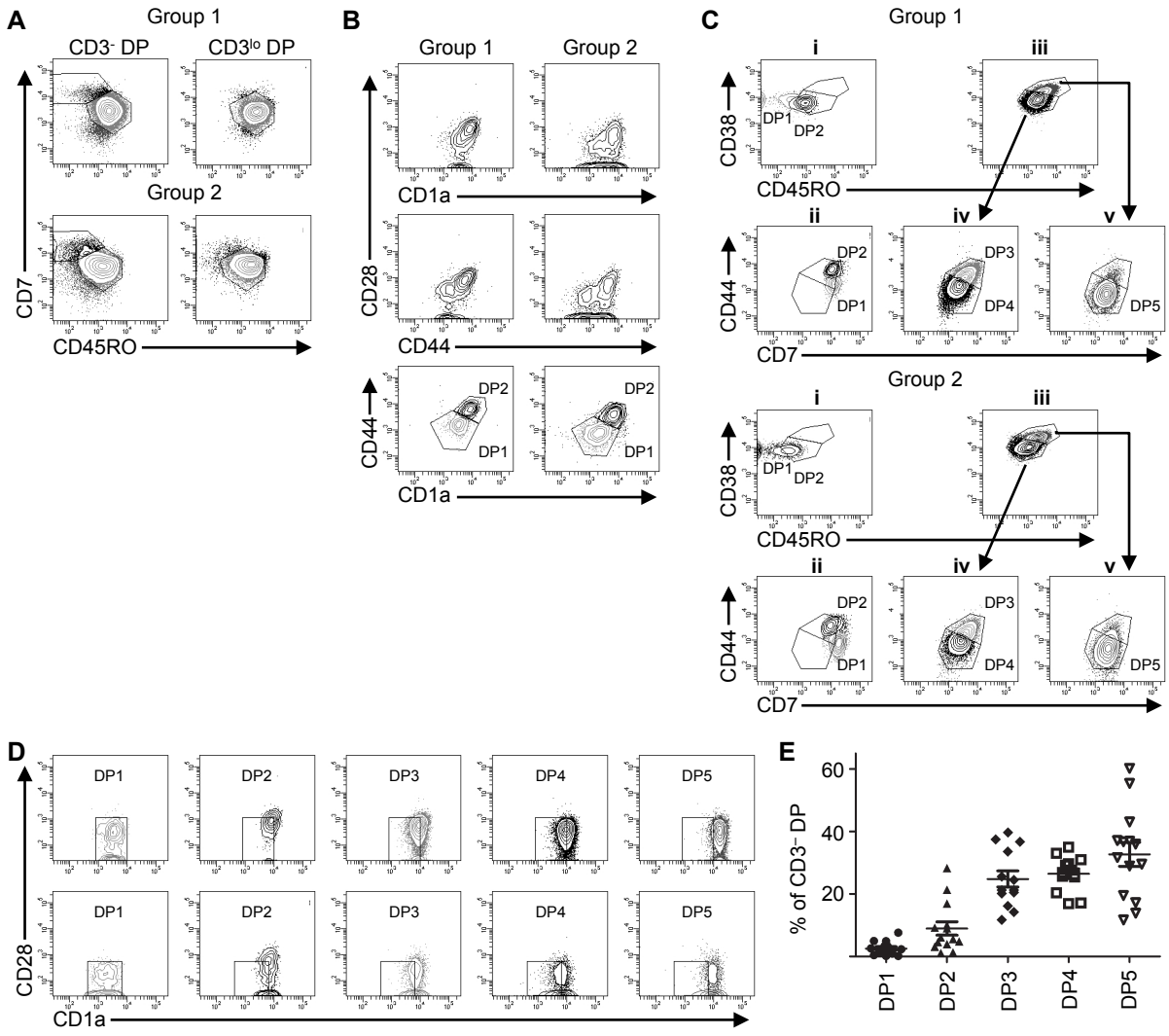
A
Group 1
CD3- DP
CD3lo DP
Group 2
CD7
CD45RO
B
Group 1
Group 2
CD1a
CD28
CD44
DP2
DP1
C
Group 1
i
iii
CD38
DP1
DP2
CD45RO
ii
iv
v
CD44
DP3
DP4
DP5
CD7
Group 2
D
DP1
DP2
DP3
DP4
DP5
CD28
CD1a
E
% of CD3- DP
60
40
20

$CD38^{hi}CD45RO^{hi}$ thymocytes from Fig. 3-3B, plot iii were mostly $CD44^{lo}CD7^{lo}$ and are called DP5.

For each subpopulation of $CD3^-$ DP thymocytes, we analyzed CD28 and CD1a expression (Fig. 3-3D). As thymocytes progressed from DP1 to DP5, CD1a expression increased and remained elevated. However, CD28 expression was transient and followed a similar pattern as CD44; surface protein levels were higher at the DP2 and DP3 stages than the other populations.

In summary, we defined five subsets of $CD3^-$ DP thymocytes and placed them into developmental sequence by comparing the expression of a set of surface markers with that of the developmental stages immediately preceding and following. We then calculated the percentage of $CD3^-$ DP thymocytes represented by each subset (Fig. 3-3E). Unlike ISP thymocytes in which there was a difference in the percentage of ISP1 and ISP2 subsets between the two groups of patients, there were no statistically significant differences between patient groups observed in the percentages of $CD3^-$ DP thymocytes within each of the five subsets (data not shown). Of the $CD45RO^+CD3^-$ DP thymocytes, the cells were equally distributed among the DP3, DP4, and DP5 developmental stages.

The rate of proliferation peaks during the ISP2 and DP2 stages

Expression of TCRβ triggers robust proliferation in murine thymocytes (177, 358). We used cell cycle analysis to determine which human DN, ISP, and DP thymocyte subsets were actively proliferating (Fig. 3-4). On average, fewer than 9% of DN2, DN3, and ISP1 thymocytes were in the S, G2, or M phase of the cell cycle. Likewise, 10% ± 3.4% of the DP1 thymocytes were in the S, G2, or M phase of the cell cycle. By contrast, 25% ± 4.5% of the ISP2 thymocytes

Figure 3-4. ISP2, DP2, and DP3 cells have increased proliferation. *A*) Thymocytes from the indicated cell populations were analyzed for DNA content using DAPI. The percentages of cells in the S, G2, or M phase of the cell cycle are shown. Representative data are shown as histograms. The bar graph shows the mean ± SE for five independent experiments.

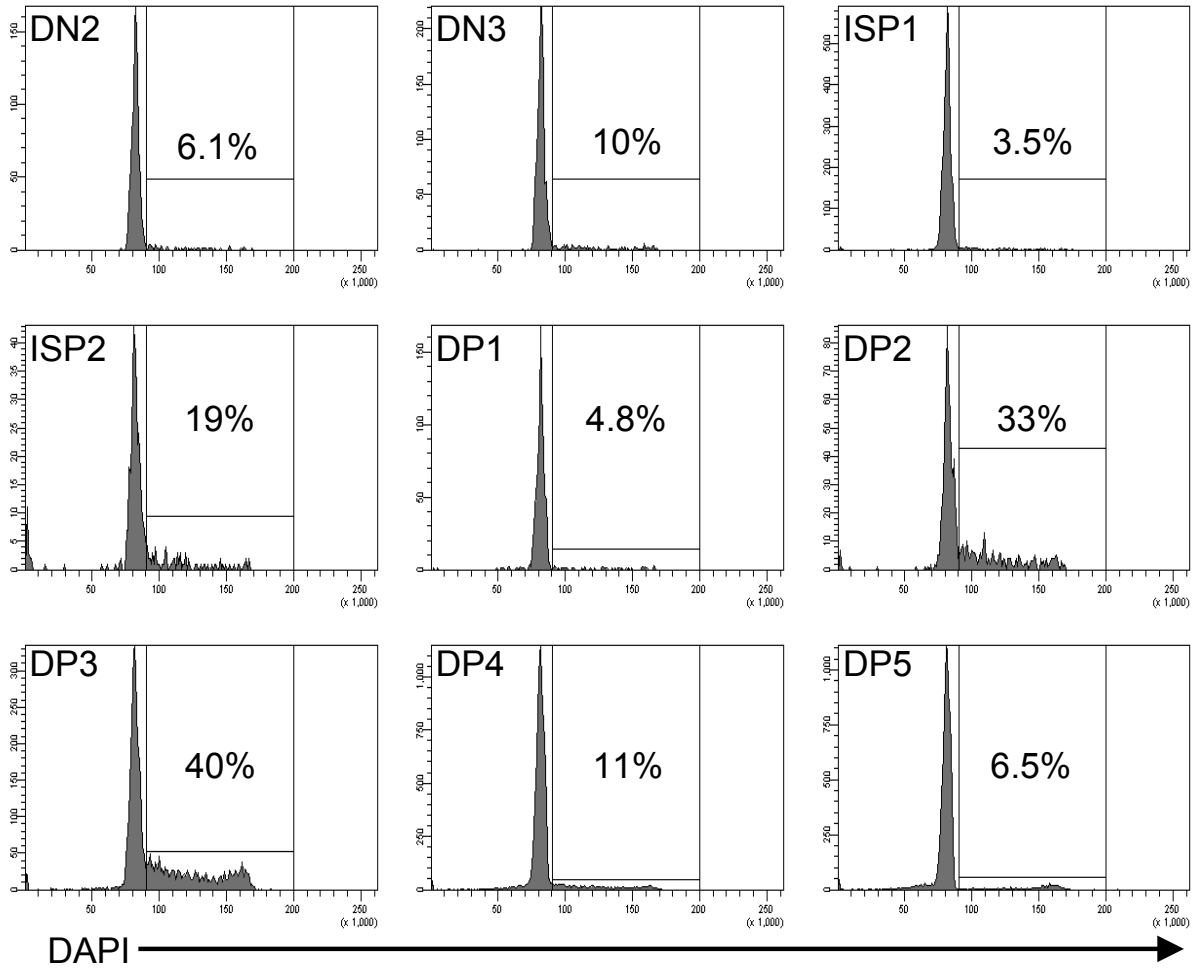
DN2
6.1%
DN3
10%
ISP1
3.5%
ISP2
19%
DP1
4.8%
DP2
33%
DP3
40%
DP4
11%
DP5
6.5%
DAPI

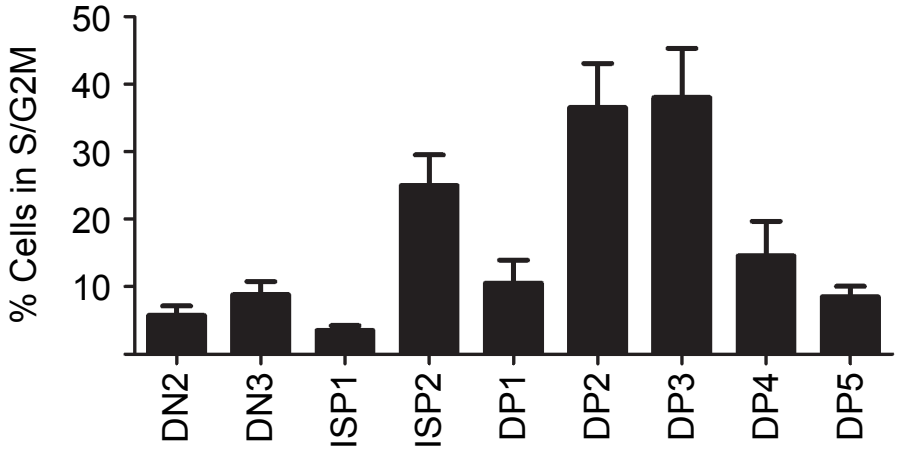
% Cells in S/G2M
50
40
30
20
10
DN2
DN3
ISP1
ISP2
DP1
DP2
DP3
DP4
DP5

were in the S, G2, or M phase of the cell cycle ($p < 0.001$, compared to ISP1). Further, 37% ± 6.6% and 38% ± 7.3% of the DP2 and DP3 thymocytes, respectively, were in the S, G2, or M phase of the cell cycle ($p < 0.01$, DP2 and DP3 thymocytes compared to DN, ISP1, and DP1 thymocytes).

Compared to the DP2 and DP3 populations, the percentages of thymocytes in the S, G2, or M phase were lower in the DP4 and DP5 stages; 15% ± 5.1% of DP4 thymocytes and 8.5% ± 1.5% of DP5 thymocytes were in the S, G2, or M phase of the cell cycle ($p < 0.01$, DP2 and DP3 thymocytes compared to DP4 and DP5 thymocytes). These data support the model in which TCRβ expression is an asynchronous process with some cells expressing TCRβ and entering the cell cycle during the ISP stage and some cells expressing TCRβ and entering the cell cycle during the DP stage. Further, these data suggest that proliferation is reduced in the populations immediately prior to surface CD3 expression. The stepwise reduction in the rate of proliferation seen in the DP3, DP4, and DP5 populations further supports our model that these stages represent sequential developmental stages.

TCRβ expression correlates with an increase in Ikaros, Helios, and Aiolos protein levels

Next, we used intracellular staining and flow cytometry to monitor the protein levels of Ikaros, Helios, and Aiolos in the $CD3^-$ thymocyte populations (Fig. 3-5). The protein levels of Ikaros, Helios, and Aiolos were higher in the ISP2 population, as compared to the ISP1 population. Helios protein levels increased 2.8-fold at this stage ($p < 0.05$), Aiolos increased 2.0-fold ($p < 0.05$), and Ikaros increased 1.9-fold ($p < 0.01$). Similarly, Ikaros protein levels in DP2 thymocytes were 1.9-fold higher than in DP1 cells ($p < 0.05$) and Aiolos protein levels were 1.8-fold higher in DP2 cells than DP1 cells ($p < 0.05$). Helios protein levels also trended higher in

Figure 3-4. Ikaros, Helios, and Aiolos protein levels increase with TCRβ expression. *A*) The indicated populations of thymocytes were intracellularly stained with anti-Helios, anti-Ikaros, or anti-Aiolos (dark lines), or the appropriate isotype controls (shaded histogram). The geometric mean fluorescence intensity (GMFI) of the anti-Ikaros, anti-Helios, or anti-Aiolos was normalized to the GMFI of the isotype control for each population, and the mean ± SE fold change relative to ISP1 is shown for four independent experiments.

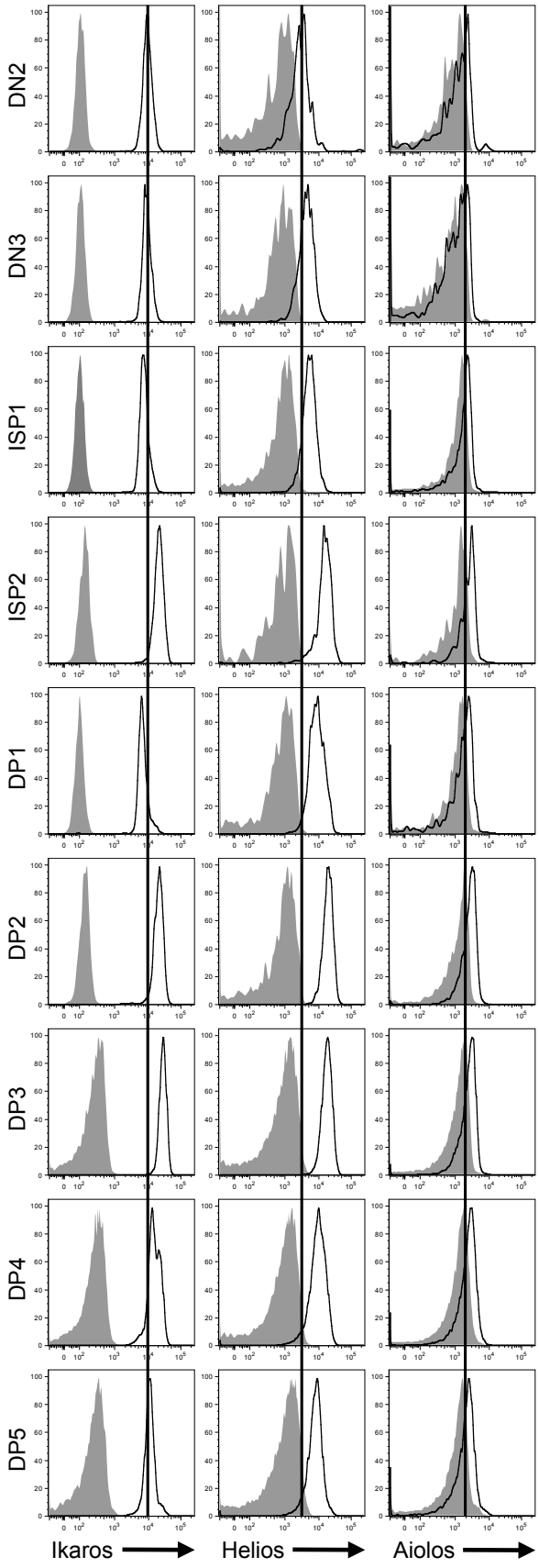
DN2
DN3
ISP1
ISP2
DP1
DP2
DP3
DP4
DP5
Ikaros
Helios
Aiolos

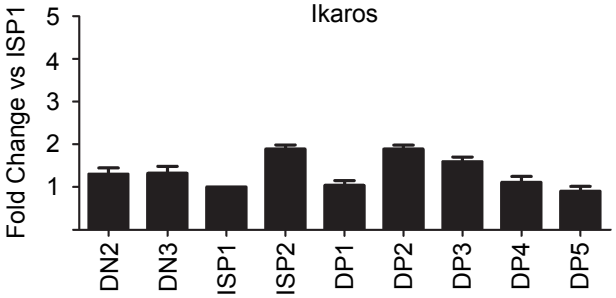
Ikaros
Fold Change vs ISP1
DN2
DN3
ISP1
ISP2
DP1
DP2
DP3
DP4
DP5

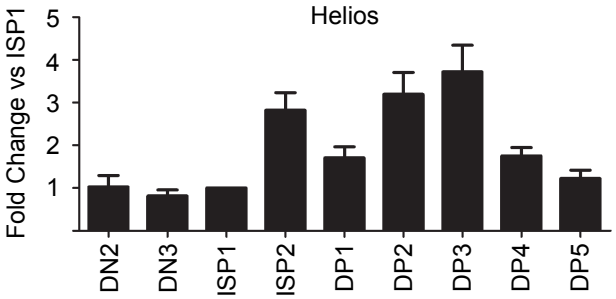
Helios
Fold Change vs ISP1
DN2
DN3
ISP1
ISP2
DP1
DP2
DP3
DP4
DP5

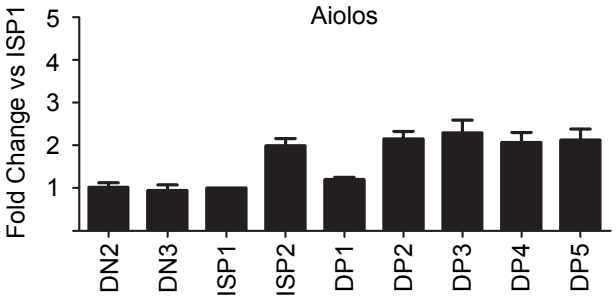
Aiolos
Fold Change vs ISP1
DN2
DN3
ISP1
ISP2
DP1
DP2
DP3
DP4
DP5

DP2 thymocytes than DP1, although this difference did not reach statistical significance until the DP3 stage ($p < 0.001$, DP3 vs. DP1). As thymocytes continued to mature, only Aiolos protein levels remained elevated. By contrast, Helios levels were 3.1-fold higher in DP3 thymocytes than DP5 cells ($p < 0.001$) and Ikaros levels were 1.8-fold higher in DP3 thymocytes than DP5 cells ($p < 0.05$), indicating that Ikaros and Helios undergo a transient increase in protein levels when TCRβ is expressed.

Discussion

The data presented here highlight the asynchronous manner by which human thymocytes express TCRβ protein. Using CD28 as a marker of TCRβ expression (117), we show that expression of TCRβ correlates with increases in the expression of CD1a, CD44, Ikaros, Helios, and Aiolos, but does not strictly correlate with CD4 and CD8 expression. Importantly, we identified CD1a and CD44 as markers that delineated populations of $TCR\beta^-$ and $TCR\beta^+$ cells in both the ISP and DP stages within the same thymus (Fig. 3-2A and 3-3B). Greater percentages of $CD1a^{++}CD44^{++}CD28^+$ ISP2 and DP2 cells were in the S, G2, or M phase of the cell cycle than $CD1a^+CD44^+CD28^-$ ISP1 and DP1 cells (Fig. 3-4), supporting the model that ISP2 and DP2 thymocytes express TCRβ. ISP2 and DP2 thymocytes also had higher expression of Ikaros, Helios, and Aiolos protein levels, as compared to ISP1 and DP1 cells.

Based on our analysis, we propose the model of human T cell development shown in Fig. 3-6. Because we are focusing on cells that lack surface TCRαβ or TCRγδ expression, we gated on $CD3^-$ live events before analyzing the remaining markers. In developing the model, several assumptions were made. Firstly, as thymocytes progress through the developmental stages, it is more likely that protein levels of surface markers change subtly than drastically. Secondly, once TCRβ is expressed, it is highly unlikely that it is lost. Lastly, $TCR\beta^+$ thymocytes proliferate at a greater rate than $TCR\beta^-$ cells, at least until rearrangement of the *TCRA* locus commences.

Based on these assumptions, we found three patterns of CD4 and CD8 expression in $CD3^-$ thymocytes (Fig. 3-1B): the canonical pattern in which CD4 is expressed prior to CD8, creating an ISP $CD4^+$ population (Group 1); a pattern in which CD4 and CD8 are expressed simultaneously (Group 2); and a third pattern that appeared in two patients in which CD8 is

Figure 3-6. A model of human T cell development through the $CD3^-$ developmental stages.

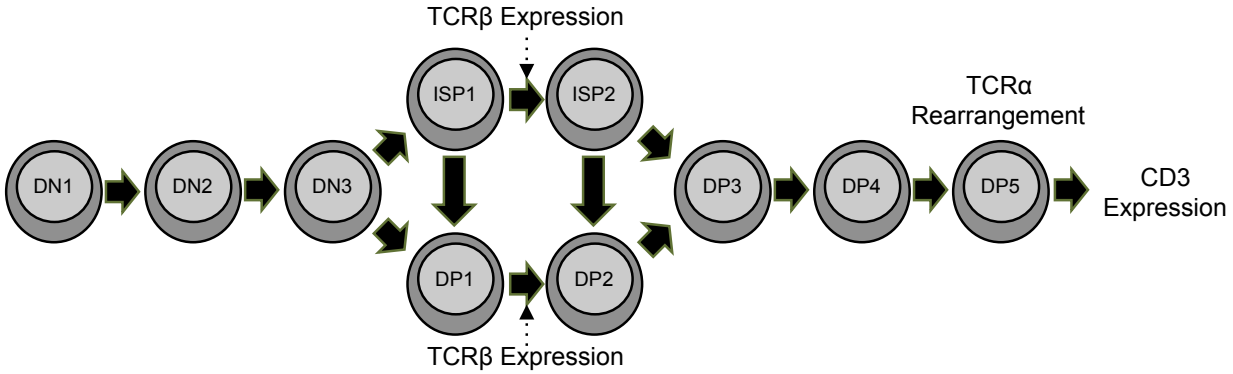

	DN3	ISP1	ISP2	DP1	DP2	DP3	DP4	DP5
CD4	−	+	+	+	+	+	+	+
CD8	−	−	−	+	+	+	+	+
CD1a	+	+	++	+	++	++	++	++
CD44	+	+	++	+	++	++	+	+
CD28	−	−	+	−	+	−/+	−	−
CD45RO	−	−	+	−	+	++	++	+++
CD7	++	++	++/+	++	++	++/+	+	+
CD38	+	+	+	+	+	+	+	++

expressed prior to CD4 (Group 3). While it might be expected that individual cells would take random paths from the DN to the DP stage, it was unexpected that most cells in an individual followed one of the three patterns. Because the tissue samples were collected without clinical data, we are unable to determine whether the age of the patient, comorbidities, or pre-surgery medications might influence the developmental pattern (359-361). The implications of these developmental patterns on physiology or pathophysiology are unknown; however, these observations imply that DN3 thymocytes could differentiate directly into ISP1 or DP1 thymocytes, as shown in Fig. 3-6, or an ISP $CD8^+$ population that is not shown in the figure.

Regardless of the pathway that thymocytes follow during the DN to DP transition, $TCR\beta^-$ and $TCR\beta^+$ subsets of ISP and DP thymocytes could be detected in each individual. ISP1 and DP1 cells appear to be pre-β selection cells based on their lack of CD28 expression (Figs. 3-2A and 3-3B) and low proliferation rate (Fig. 3-4). The presence of $TCR\beta^-$ DP thymocytes suggests that remodeling of the CD8 locus is not dependent on pre-TCR signals, as it is in murine thymocytes (65). Further, these data suggest that ISP1 cells could express TCRβ protein and differentiate into ISP2 cells. The newly formed ISP2 thymocytes likely differentiate into either DP2 or DP3 cells, depending on whether the cells up-regulate CD45RO before or after CD8.

If TCRβ expression fails to occur during the ISP $CD4^+$ stage, the cells likely differentiate into DP1 thymocytes. DP1 cells may retain the potential to successfully rearrange their *TCRB* locus, express TCRβ protein, and differentiate into DP2 thymocytes. However, if DP1 thymocytes fail to express TCRβ, the cells likely undergo apoptosis.

As in murine T cell development, TCRβ expression in human thymocytes triggers robust proliferation, as seen by a greater percentage of $CD3^-$ DP thymocytes in the S, G2, or M phase of

the cell cycle than DN thymocytes (115, 116, 118). We extend these observations by showing which subpopulations of ISP and DP thymocytes are the most rapidly dividing (Fig. 3-4). Specifically, more than 20% of ISP2, DP2, and DP3 thymocytes were in the S, G2, or M phase of the cell cycle, as compared to less than 10% of ISP1 and DP1 thymocytes. Proliferation was most robust in the DP2 and DP3 stages and then declined in the DP4 and DP5 stages, the final stages prior to the expression of TCRα and surface TCR. This is analogous to the proliferation that occurs after TCRβ expression in murine thymocytes. The first murine thymocytes that express TCRβ proliferate more robustly than TCRβ^{+} thymocytes at later stages (356, 362, 363). At the DP5 stage, thymocytes decrease their expression of CD44 and increase their expression of CD38 (Fig. 3-3C). CD38 is first expressed at the DN2 stage, the stage in which rearrangement of the *TCRD* and *TCRG* loci occurs (109). This suggests that *CD38* transcription may be regulated via similar mechanisms as RAG-1 or RAG-2. In chronic lymphocytic leukemia, CD38 expression is regulated by the E-box factor, E2A (364). E2A binds the RAG enhancer regulatory element in developing murine B cells (365) and human cancer cell lines (366). Thus, the increase in CD38 expression on DP5 cells may correlate with the onset of *TCRA* rearrangement.

With this detailed image of the developmental stages that surround TCRβ expression, we are now able to examine changes in the protein levels of Ikaros, Helios, and Aiolos at this critical point in human T cell development. It was previously shown that the mRNA levels of each of these molecules increased dramatically as human thymocytes progressed from the DN to the DP stages (354). However, previous data also showed that protein levels in total DP thymocytes were only slightly elevated, as compared to DN thymocytes. Using flow cytometry, we are now able to subdivide the ISP and DP populations and detect transient changes in protein expression that occur as thymocytes mature.

Protein levels of Ikaros, Helios, and Aiolos increased when thymocytes expressed TCRβ and proliferated (Fig. 3-5). The relative increase in Helios expression was greater than that of Ikaros and Aiolos, suggesting that the composition of Ikaros family dimers changes when thymocytes express TCRβ. More Ikaros family dimers likely contain Helios in ISP2, DP2, and DP3 thymocytes than ISP1 and DP1 cells. The other significant difference among family members is that the increase in Ikaros and Helios protein levels was transient; protein levels of these two family members were lower in DP4 and DP5 thymocytes than DP2 and DP3 thymocytes. By contrast, Aiolos protein remained elevated in DP4 and DP5 thymocytes. This observation indicates that more Ikaros family dimers contain Aiolos in DP4 and DP5 thymocytes than previous developmental stages.

The importance of small changes in the expression of Ikaros family members was demonstrated in a study in which transgenic mice were generated that express low levels of Helios (55). Expressing ten-fold lower levels of Helios than Ikaros resulted in B cell lymphoma. The mechanism by which changes in Ikaros family dimers influence gene transcription is unknown. Because of the high degree of homology within the DNA binding motifs of each family member, it is likely that all family members can bind the same DNA sequences with similar affinities. However, the relative potency of each family member is different. For example, Aiolos is a more potent transcriptional activator than Ikaros (2).

Helios expression is different in murine and human thymocytes (354). Specifically, Helios mRNA levels decrease as murine thymocytes progress from the DN to the DP stage while Helios mRNA levels increase in human thymocytes. Thus, it is difficult to draw conclusions regarding the function of Ikaros family members using data from the opposite species. However, loss of Ikaros in murine thymocytes obviates the need for TCRβ expression for differentiation

into DP thymocytes, even though Ikaros could not drive proliferation after TCRβ expression (367). In human thymocytes, Ikaros, Helios, and Aiolos were most abundantly expressed in the thymocyte populations that were most proliferative (Figs. 3-4 and 3-5), suggesting that the Ikaros family might promote proliferation in human $TCR\beta^{+}$ thymocytes. The decrease in Ikaros and Helios coupled with sustained Aiolos expression seen in DP4 and DP5 thymocytes might lead to the slowing of cell cycle progression and rearranging of the *TCRA* locus. More experiments are necessary to determine the function of Ikaros in human thymocytes.

Consistent with a role for Ikaros family members in pre-TCR-mediated proliferation and differentiation is the observation that pre-BCR-mediated Ikaros and Aiolos expression during murine B cell development induces exit from the cell cycle (352, 353, 368, 369). Further, exogenous expression of Ikaros in a pre-B cell line could halt cell division (369). In addition, expression of Ikaros in an Ikaros-deficient DN3-like murine thymoma cell line can induce differentiation and expression of TCRα (45, 370). This differentiation is independent of TCRβ expression as loss of Ikaros expression on a RAG-$1^{-/-}$ background induced differentiation to the DP stage and expression of TCRα germline transcripts (367).

In summary, we defined the stages of human T cell development flanking the expression of TCRβ to a greater level of detail than has been previously reported. Further, we show that Ikaros, Helios, and Aiolos protein levels fluctuate during this critical time in T cell development.

Chapter 4. Positive selection and lineage commitment of human thymocytes occur during the transitional single positive developmental stage

Abstract

Subdividing human thymocytes into fine populations enables us to define the developmental stages at which critical checkpoints occur. T cell precursors enter the thymus as $CD4^{-}CD8^{-}$ double negative (DN) thymocytes and then express both CD4 and CD8 to become $CD4^{+}CD8^{+}$ double positive (DP) thymocytes before maturing into either single positive (SP) $CD4^{+}$ or SP $CD8^{+}$ thymocytes. We used multi-parameter flow cytometry to define the populations in which positive selection and lineage commitment are most likely to occur and to analyze expression of Ikaros, Helios, and Aiolos, key transcription factors required for T cell development. After human thymocytes express CD3 and receive positive selection signals, the cells down-regulate expression of CD4 to become transitional single positive (TSP) $CD8^{+}$ thymocytes. At this stage, there was a transient increase in the Ikaros, Helios, and Aiolos protein levels. After the TSP $CD8^{+}$ developmental stage, some thymocytes re-express CD4 and become $CD3^{hi}$ DP thymocytes before down-regulating CD8 to become mature SP $CD4^{+}$ thymocytes. During $CD4^{+}$ T cell maturation, Helios expression declined and Aiolos expression transiently increased. For commitment to the $CD8^{+}$ T cell lineage, TSP $CD8^{+}$ thymocytes increase their expression of CD3 and maintain high levels of Aiolos protein as the cells complete their maturation. In summary, we defined the TSP $CD8^{+}$ developmental stage in human T cell development and propose that this stage is where CD4/CD8 lineage commitment occurs.

Introduction

Human T cell development is a multi-step process of selection, proliferation, and maturation that produces functional T cells able to participate in an immune response. Immature T cells enter the thymus as $CD4^{-}CD8^{-}$ double negative (DN) thymocytes and, during the DN developmental stage, begin rearranging the genomic loci encoding the T cell receptor (TCR) chains (109, 116). After the DN stage, thymocytes express CD4 to become immature single positive (ISP) $CD4^{+}$ thymocytes and then express CD8 to become double positive (DP) thymocytes. Rearrangement of the genomic locus encoding TCRβ is completed during the ISP or DP developmental stages and expression of TCRα can be detected within the DP stage (115-119, 354).

After expression of TCRα and TCRβ, thymocytes are subjected to positive and negative selection, ensuring the production of T cells that express a functional TCR with limited autoreactivity. Selection requires engagement of the TCR and leads to expression of activation markers, such as CD69 and CD5, and increased expression of CD3 (276, 371-374). Positive selection induces continued thymocyte maturation, including commitment to the single positive (SP) $CD4^{+}$ or SP $CD8^{+}$ lineages.

The lack of clarity regarding the cell populations in which developmental milestones occur have led to competing models of thymic selection and lineage commitment. Positive selection is proposed to occur at the DP developmental stage, when CD4 and CD8 are both available to bind major histocompatibility complex (MHC). A possible model of lineage commitment is that positive selection stochastically induces down-regulation of either CD4 or CD8. In this model, T cell maturation is dependent on the random chance that the remaining co-receptor has the same MHC specificity as the TCR. Alternatively, CD4 and CD8 may induce

distinct signals that drive lineage commitment and the down-regulation of the opposing co-receptor.

A third model of CD4/CD8 lineage commitment emerged from studies in murine models where a transitional single positive (TSP) $CD4^{+}CD8^{lo}$ thymocyte population has been described (312-315). According to this model, positive selection induces decreased CD8 expression (317-320). This model posits that down-regulation of CD8 interrupts the MHC/TCR interaction in MHC I-restricted thymocytes, while signaling is maintained in MHC II-restricted thymocytes, thereby differentiating between the two lineages. This model is supported by data showing that prolonged signaling after positive selection results in the preferential development of SP $CD4^{+}$ thymocytes whereas short-lived signals lead to the production of SP $CD8^{+}$ thymocytes (309, 311).

A family of proteins proposed to regulate positive selection and lineage commitment is the Ikaros family of transcription factors. This family regulates numerous steps of T cell development, including regulation of CD4 and CD8 expression, survival, and proliferation (2-4, 22, 46-48, 66, 340, 346, 367). Disrupting the function of the Ikaros family in murine thymocytes results in the accumulation of TSP $CD4^{+}$ thymocytes and increased proliferation and apoptosis (375). These data suggest that one or more Ikaros family members are critical for positive selection or lineage commitment.

In this chapter, we will provide the most detailed map of the developmental stages surrounding positive selection and lineage commitment yet reported in the human thymus. In addition, we will define how expression of Ikaros, Helios, and Aiolos changes during this time.

Materials and Methods

Human thymocytes

After obtaining consent from the parent or guardian, human thymus samples were obtained from children (0 – 18 years) who underwent corrective surgery at Children's Mercy Hospital (Kansas City, MO) for congenital cardiac defects. De-identified tissue samples void of any clinical data were obtained in compliance with the Institutional Review Boards at our institutions.

Antibodies, cell labeling, and flow cytometry

The anti-human antibodies, anti-CD1a-PerCP-Cy5.5, anti-CD3-APC-Cy7, anti-CD4-Pacific Blue, anti-CD7-APC, anti-CD7-FITC, anti-CD7-PE, anti-CD8α-BV785, anti-CD25-PerCPCy5.5, anti-CD28-Pacific Blue, anti-CD38-AF700, anti-CD44-PE-Cy7, anti-CD45RO-PECy5, anti-CD69-BV650, anti-FoxP3-PE, anti-FoxP3-AF647, anti-Helios-AF647, anti-TCRγδ-FITC, Armenian hamster IgG-AF647 control, and mouse IgG1κ-PE control were purchased from Biolegend (San Diego, CA). Anti-CD4-PE-eFlour 610, anti-CD8β-PECy7, and anti-CD44-PE were purchased from e-Biosciences (San Diego, CA), and anti-CD27-Horizon V500, anti-Ikaros-PE, anti-Aiolos-PE, and mouse IgG1κ-PE control were purchased from BD Biosciences (San Jose, CA). Armenian hamster IgG-AF647 was purchased from Biolegend.

Single cell suspensions of human thymocytes were labeled on their surface as previously described (355). For intracellular staining, surface-labeled cells were fixed and permeabilized using the Foxp3/Transcription Factor Staining Buffer Set (Affymetrix/eBioscience, San Diego, CA), according to the manufacturer's instructions. Cells were analyzed using a BD LSR II (BD Biosciences) and data were analyzed using BD FACSDiva software (BD Biosciences) or FlowJo

(TreeStar, Inc., Ashland, OR). Relative expression of Ikaros, Helios, and Aiolos in each cell population was defined as the ratio of the geometric mean fluorescence intensity of each Ikaros family member to the corresponding isotype control. Representative dot plots are shown from one thymus out of eleven analyzed for all surface markers except CD28. Representative dot plots of CD28 expression are shown for one thymus out of four analyzed.

Statistical analysis

For comparisons across groups, the paired t-test analysis or the repeated measure ANOVA analysis with Tukey posthoc test were performed using GraphPad Prism (GraphPad Software, Inc, La Jolla, CA), and significance was defined as $p < 0.05$.

Results

DP thymocytes can be divided into twelve subsets

We previously showed that thymocytes enter the $CD3^-$ DP developmental stage as $CD7^{++}CD45RO^-$ thymocytes and mature into $CD7^+CD45RO^+$ thymocytes (376). In addition, we showed that $CD3^-$ DP thymocytes progress from $CD38^{lo}CD45RO^{lo}$ to $CD38^{hi}CD45RO^{hi}$. To define the stages of human T cell development through the $CD3^+$ stages, we divided $TCR\gamma\delta^-$ DP thymocytes into $CD3^-$, $CD3^{lo}$, and $CD3^{hi}$ populations (Fig. 4-1A) and analyzed CD7, CD38, and CD45RO expression on each population (Fig. 4-1B). Consistent with our prior observations, the $CD3^-$ DP population included a small percentage of $CD7^{++}CD45RO^-$ thymocytes while all of the $CD3^+$ DP cells were $CD7^+CD45RO^+$. Further, the percentage of cells that were $CD38^{hi}CD45RO^{hi}$ increased as DP thymocytes increased their expression of CD3; 27 ± 4.6 % of $CD3^-$ DP thymocytes, 67 ± 4.5% of $CD3^{lo}$ DP thymocytes, and 78 ± 3.4% of $CD3^{hi}$ DP thymocytes were $CD38^{hi}CD45RO^{hi}$. These data support a model in which DP thymocytes progress from $CD7^{++}CD45RO^-$ to $CD7^+CD45RO^+$ and from $CD38^{lo}CD45RO^{lo}$ to $CD38^{hi}CD45RO^{hi}$.

We also previously showed that $CD3^-CD7^{++}CD45RO^-$ DP thymocytes could be divided into $CD44^{lo}$ DP1 and $CD44^{med}$ DP2 subsets and that $CD3^-CD7^+CD45RO^+$ DP thymocytes could be divided into DP3, DP4, and DP5 subsets (376) (Fig. 4-1C). Within the $CD3^{lo}$ DP thymocyte population, subsets of cells were identified with similar expression levels of CD38, CD45RO, CD44, and CD7 as DP3, DP4, and DP5 thymocytes, and so we labeled the $CD3^{lo}$ subsets DP6, DP7, and DP8, as shown in Fig. 4-1C. In addition, a population of cells (called DP9) was observed within the $CD38^{hi}CD45RO^{hi}$ subpopulation that expressed comparable levels of CD7 as DP8 thymocytes, but higher levels of CD44.

Figure 4-1. DP thymocytes can be divided into twelve populations. A) TCRγδ– thymocytes were gated on CD4+CD8+ DP cells and analyzed for CD3 expression. B) CD3–, CD3lo, and CD3hi DP thymocytes were analyzed for expression of CD7, CD45RO, and CD38. C) CD38loCD45ROlo and CD38hiCD45ROhi cells from (B) were analyzed for CD44 and CD7 expression. The DP3 through DP12 subsets are indicated. D) Expression of CD44, CD38, and CD45RO on total TCRγδ– thymocytes was compared to CD3 expression.

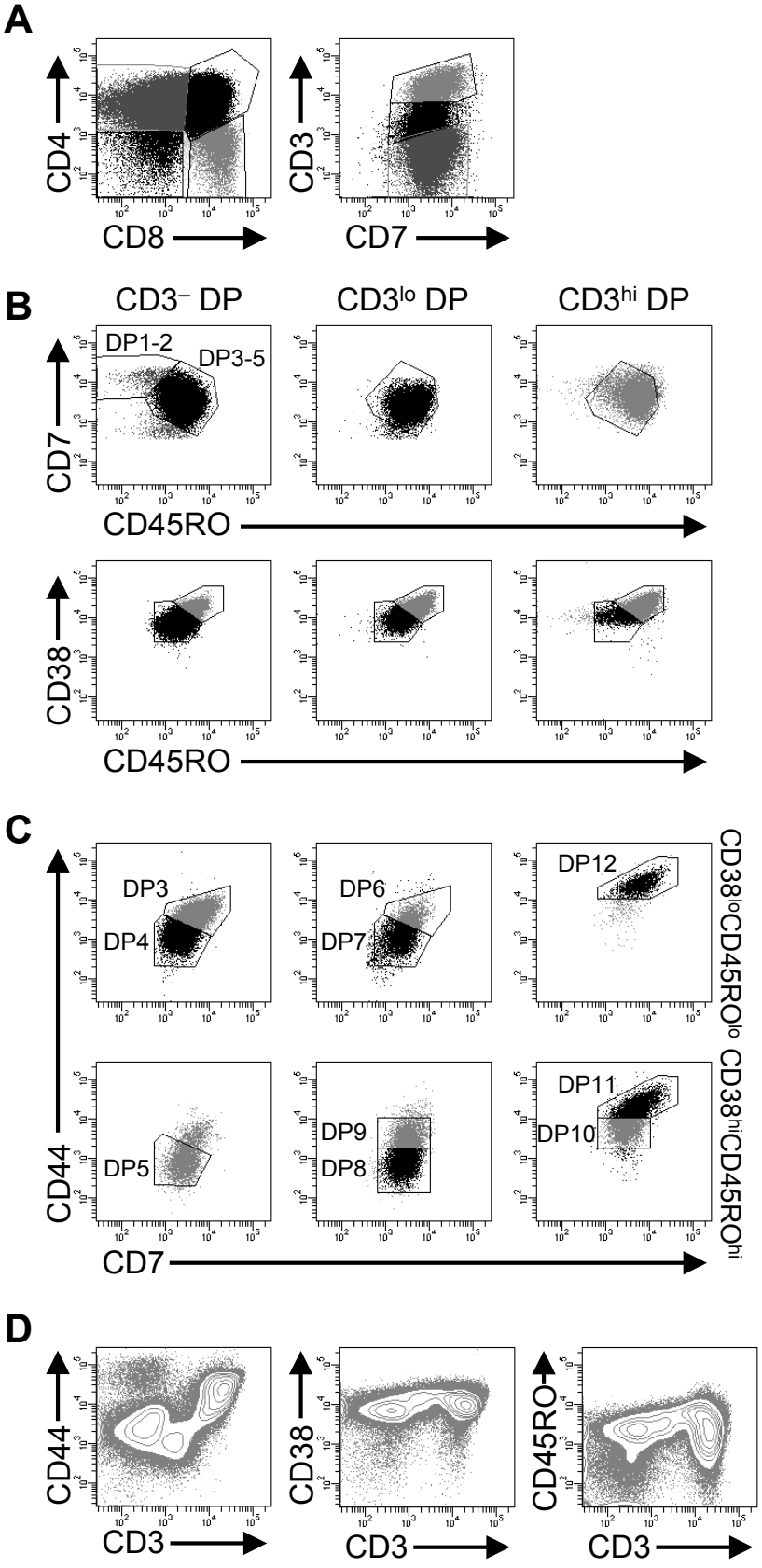
A
CD4
CD8
CD3
CD7
B
CD3⁻ DP
CD3lo DP
CD3hi DP
DP1-2
DP3-5
CD7
CD45RO
CD38
CD45RO
C
DP3
DP4
DP6
DP7
DP12
DP5
DP9
DP8
DP11
DP10
CD44
CD7
CD38loCD45ROlo
CD38hiCD45ROhi
D
CD44
CD3
CD38
CD3
CD45RO
CD3

These data suggest that CD44 expression declines as cells progress from the DP3 to the DP8 stage, but then increases at later stages. Consistent with this model, the lowest expression of CD44 among $CD3^{hi}$ DP thymocytes was found on a $CD38^{hi}CD45RO^{hi}$ subset that resembled the DP9 stage, and are thus called DP10 thymocytes (Fig. 4-1C). Further, subpopulations of $CD38^{hi}CD45RO^{hi}$ and $CD38^{lo}CD45RO^{lo}$ thymocytes were identified with higher CD44 expression than DP10 thymocytes and we labeled these cells DP11 and DP12, respectively.

An implication of our analysis of T cell development through the DP stages is that CD44 expression is high early in T cell development, declines transiently, and then returns to a high level. To test this model, we analyzed CD3 and CD44 expression on total thymocytes (Fig. 4-1D). Indeed, CD44 expression was higher on $CD3^{-}$ and $CD3^{hi}$ thymocytes than $CD3^{lo}$ thymocytes.

Another implication of our analysis is that CD38 and CD45RO expression increase as thymocytes progress through the $CD3^{-}$ and $CD3^{lo}$ stages and declines as cells reach maturity, as previously reported for CD45RO (357). Indeed, dot plots of total thymocytes analyzed for CD38 versus CD3 expression and CD45RO versus CD3 expression showed similar patterns (Fig. 4-1D); CD38 and CD45RO expression was highest among thymocytes with intermediate levels of CD3 and lowest among $CD3^{-}$ and $CD3^{hi}$ thymocytes. Consistent with this model is that DP12 thymocytes express high levels of CD44, but lower levels of CD38 and CD45RO than other DP thymocytes (Fig. 4-1B and C).

In summary, human DP thymocytes can be divided into at least twelve subpopulations based on their expression of CD3, CD7, CD38, CD44, and CD45RO. Five populations (DP1-5) do not express CD3 and were previously identified (376). There are four populations of $CD3^{lo}$ DP thymocytes (DP6-9) and three populations of $CD3^{hi}$ DP thymocytes (DP10-12).

Human thymocytes progress through a $CD8^+CD4^{lo}$ transitional single positive stage

In mice, thymocytes progress from the $CD3^{lo}$ DP developmental stage to the $CD4^+CD8^{lo}$ transitional single positive (TSP) stage (312-315). To determine whether a comparable developmental stage might exist in humans, we examined CD3 and CD7 expression within the SP $CD4^+$ and SP $CD8^+$ populations (Fig. 4-2). SP $CD4^+$ thymocytes could be divided into $CD3^-CD7^{hi}$, $CD3^{hi}CD7^{lo}$, and $CD3^{hi}CD7^{hi}$ subsets (Fig. 4-2A). The $CD3^-CD7^{hi}$ subset corresponds to the previously described immature single positive (ISP) developmental stage (377). Few, if any, $CD3^{lo}$ SP $CD4^+$ thymocytes were detected, making it unlikely that a TSP subpopulation exists within the SP $CD4^+$ population.

In contrast to the SP $CD4^+$ population, a $CD3^{lo}CD7^{lo}$ subset of SP $CD8^+$ thymocytes was detected (Fig. 4-2B), which is consistent with the phenotype expected for a TSP developmental stage. Cells within the putative TSP population had CD7, CD38, CD45RO, and CD44 expression levels that were similar to DP8 and DP9 thymocytes, and we refer to the TSP counterparts as TSP1 and TSP2 (Fig. 4-2C). The phenotypic similarities between DP8, DP9, TSP1, and TSP2 thymocytes suggest that these populations represent sequential stages of T cell development.

Positive selection is initiated prior to the down-regulation of CD4

To place the DP8, DP9, TSP1, and TSP2 in developmental sequence, we analyzed CD69 and CD27 expression on each subset of $CD3^{lo}$ thymocytes (Fig. 4-3A). At least 80% of DP6, DP7, and DP8 thymocytes lacked CD69 or CD27 expression, indicating that few of these cells

Figure 4-2. SP CD8$^+$ thymocytes include a CD3^{lo} subset. SP CD4$^+$ (*A*) and SP CD8$^+$ (*B*) thymocytes, as defined in Fig. 4-1A, were analyzed for CD3 and CD7 expression. *C)* CD3^{lo}CD7^{lo} SP CD8$^+$ thymocytes from *(B)* were analyzed for expression of CD38, CD45RO, CD44, and CD7.

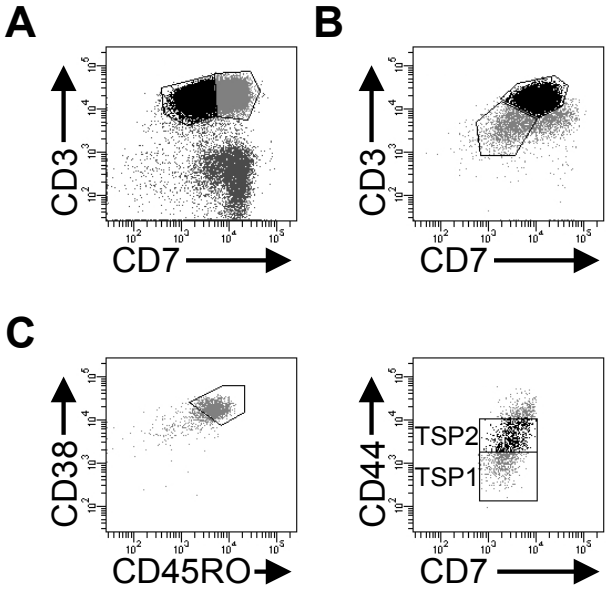
A
CD3
CD7
B
CD3
CD7
C
CD38
CD45RO
CD44
TSP2
TSP1
CD7

Figure 4-3. TSP $CD8^+$ cells are the most mature $CD3^{lo}$ thymocytes. *A)* CD69 and CD27 expression were analyzed on the $CD3^{lo}$ DP and TSP $CD8^+$ populations defined in Figs. 4-1 and 4-2. The bar graph shows the percentages (mean ± SE) of cells in each population that were $CD69^-CD27^-$, $CD69^+CD27^-$, $CD69^+CD27^+$, and $CD69^-CD27^+$ (n = 11). *B and C)* $CD3^{lo}$ thymocyte populations were analyzed for CD69 and CD28 (*B*) and CD27 and CD28 (*C*) expression. *D)* CD69 and CD27 expression were analyzed on $CD3^{lo}$ thymocytes and the $CD69^-CD27^-$, $CD69^+CD27^-$, and $CD69^+CD27^+$ populations were analyzed for CD4 and CD8 expression.

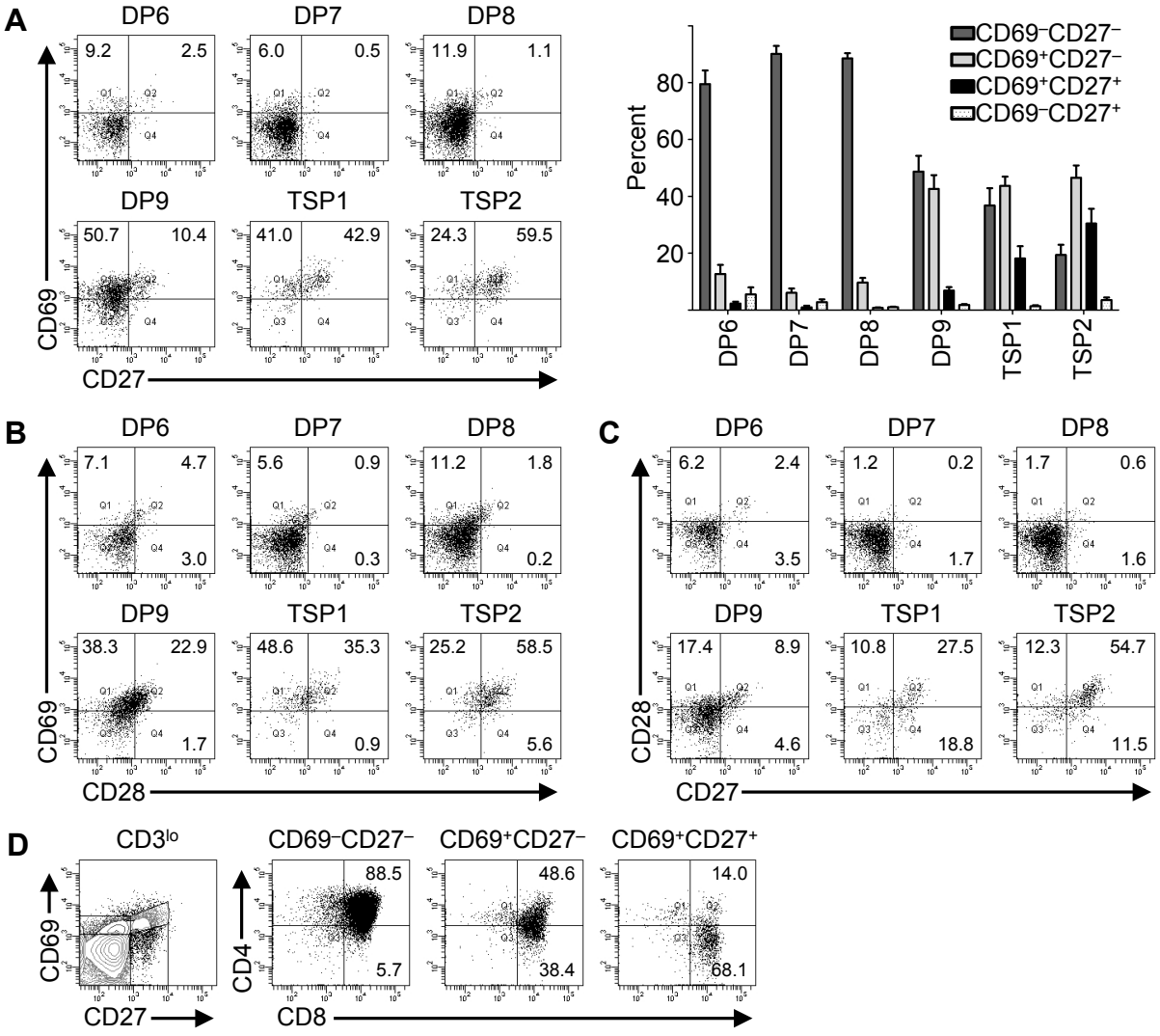
A
DP6
DP7
DP8
DP9
TSP1
TSP2
9.2
2.5
6.0
0.5
11.9
1.1
50.7
10.4
41.0
42.9
24.3
59.5
CD69
CD27
CD69⁻CD27⁻
CD69⁺CD27⁻
CD69⁺CD27⁺
CD69⁻CD27⁺
Percent
B
7.1
4.7
3.0
5.6
0.9
0.3
11.2
1.8
0.2
38.3
22.9
1.7
48.6
35.3
0.9
25.2
58.5
5.6
CD28
C
6.2
2.4
3.5
1.2
0.2
1.7
1.7
0.6
1.6
17.4
8.9
4.6
10.8
27.5
18.8
12.3
54.7
11.5
D
CD3lo
CD69⁻CD27⁻
CD69⁺CD27⁻
CD69⁺CD27⁺
88.5
5.7
48.6
38.4
14.0
68.1
CD4
CD8

had received signals leading to positive selection. By contrast, 43 ± 4.9% of DP9 thymocytes were $CD69^{+}CD27^{-}$ and 6.8 ± 1.2% of DP9 thymocytes were $CD69^{+}CD27^{+}$. The percentage of thymocytes that expressed CD69 and CD27 trended higher in TSP1 thymocytes than DP thymocytes, although the difference did not reach statistical significance. In TSP2 thymocytes, CD69 and CD27 expression was higher than DP9 thymocytes ($p < 0.001$) and TSP1 thymocytes ($p < 0.05$). These data indicate that more TSP thymocytes had received positive selection signals than DP9 thymocytes, suggesting a developmental progression from the DP9 developmental stage to the TSP1 and TSP2 stages. To test this developmental progression, we analyzed CD28 expression on each $CD3^{lo}$ thymocyte population (Fig. 4-3B). Only 47 ± 5.8% of $CD69^{+}$ DP9 and 41 ± 5.4% of $CD69^{+}$ TSP1 thymocytes expressed CD28, but 65 ± 3.7% of $CD69^{+}$ TSP2 thymocytes expressed CD28 ($p < 0.05$ for TSP2 compared to DP9 or TSP1). Nearly all $CD27^{+}$ DP9, TSP1, and TSP2 thymocytes expressed CD28 (Fig. 4-3C). In summary, analysis of the markers of thymic selection (such as CD69, CD28, and CD27) suggests that TSP2 thymocytes represent the final developmental stage prior to up-regulation of CD3.

To further support our model that thymocytes undergoing selection down-regulate CD4, total $CD3^{lo}$ thymocytes were analyzed for CD69 and CD27 expression (Fig. 4-3D). Among $CD69^{-}CD27^{-}$ $CD3^{lo}$ thymocytes, 83 ± 5.3% were DP thymocytes. The percentage of $CD3^{lo}$ thymocytes that were DP cells decreased to 45 ± 6.5% among $CD69^{+}CD27^{-}$ thymocytes and 23 ± 5.3% among $CD69^{+}CD27^{+}$ cells. The progressive decrease in the percentage of DP thymocytes was associated with a concomitant increase in the percentage of SP $CD8^{+}$ thymocytes.

In summary, these data indicate that up-regulation of CD69, CD27, and CD28 occur before CD3 expression reaches high levels. Further, as human thymocytes progress through the

stages of positive selection, the cells down-regulate surface expression of CD4 to become TSP $CD8^+$ thymocytes.

Commitment to the $CD4^+$ T cell lineage

DP9, TSP1, and TSP2 thymocytes were $CD3^{lo}CD7^{lo}$ and represent the final stages of T cell development prior to up-regulation of CD3. Among $CD3^{hi}$ DP thymocytes, DP10 thymocytes are $CD7^+$ and CD7 increases in the DP11 and DP12 subsets. As described above, $CD3^{hi}$ $CD4^+$ thymocytes can be divided into $CD7^{lo}$ and $CD7^{hi}$ subsets, suggesting that $CD3^{hi}CD7^{lo}$ SP $CD4^+$ thymocytes include the earliest stages of the $CD3^{hi}$ SP $CD4^+$ population. Because CD38 and CD45RO expression decrease as thymocytes mature (Fig. 4-1D), we compared the expression of these markers on $CD3^{hi}CD7^{lo}$ SP $CD4^+$ thymocytes and $CD3^{hi}$ DP thymocytes. A lower percentage of $CD3^{hi}CD7^{lo}$ SP $CD4^+$ thymocytes (51 ± 6.1%) were $CD38^{hi}CD45RO^{hi}$ than $CD3^{hi}$ DP thymocytes (78 ± 3.4%) ($p < 0.001$) (Fig. 4-4A), suggesting that the DP10 developmental stage precedes the $CD3^{hi}CD7^{lo}$ SP $CD4^+$ stage. Among $CD3^{hi}CD7^{lo}$ SP $CD4^+$ thymocytes, the $CD38^{hi}CD45RO^{hi}$ and $CD38^{lo}CD45RO^{lo}$ populations both contained a subset of cells that expressed comparable levels of CD44 as DP10 thymocytes and a subset that expressed higher levels of CD44 (data not shown). We labeled the $CD44^{med}$ and $CD44^{hi}$ subsets of $CD3^{hi}CD7^{lo}$ $CD4^+$ thymocytes MSP1 and MSP2, respectively, as shown in Fig. 4-4B.

Because CD38 and CD45RO expression decrease as thymocytes reach maturity (Fig. 4-1D), we analyzed these markers on the MSP1 and MSP2 populations. Among MSP1 thymocytes, 66 ± 6.7% of the cells were $CD38^{hi}CD45RO^{hi}$, but only 46 ± 6.2% of the MSP2

Figure 4-4. $CD3^{hi}$ DP thymocytes represent a transition from TSP $CD8^+$ cells to MSP $CD4^+$ cells. *A)* SP $CD4^+$ thymocytes were gated on $CD3^{hi}CD7^{lo}$ and $CD3^{hi}CD7^{hi}$ populations as indicated in Fig. 4-2A, and analyzed for CD38 and CD45RO expression. *B)* CD7 and CD44 expression were analyzed on total $CD3^{hi}CD7^{lo}$ SP $CD4^+$ cells and each $CD7^{hi}$ subset. MSP1-5 subpopulations are defined as indicated. *C and D)* CD69, CD27, CD28, and CD1a expression were analyzed on the $CD3^{hi}CD7^{lo}$ (*C*) and $CD3^{hi}CD7^{hi}$ (*D*) subpopulations of DP and SP $CD4^+$ thymocytes. *E)* The percentages (mean ± SE) of cells in each subpopulation that were $CD69^-$ $CD27^-$, $CD69^+CD27^-$, $CD69^+CD27^+$, and $CD69^-CD27^+$ thymocytes are shown (n = 11).

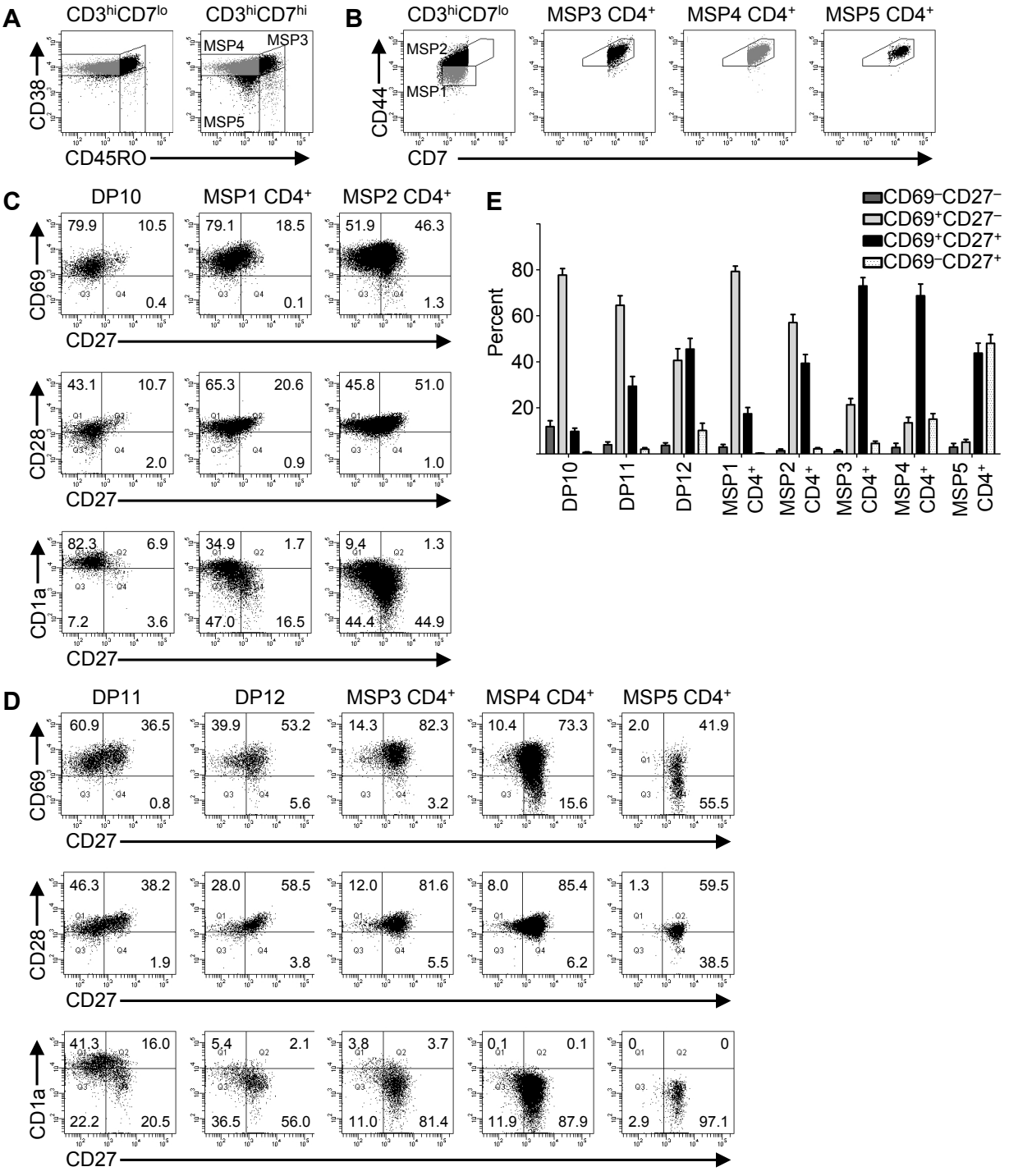
A
CD3hiCD7lo
CD3hiCD7hi
MSP4
MSP3
MSP5
CD38
CD45RO
B
CD3hiCD7lo
MSP3 CD4+
MSP4 CD4+
MSP5 CD4+
MSP2
MSP1
CD44
CD7
C
DP10
MSP1 CD4+
MSP2 CD4+
CD69
CD27
79.9 10.5 0.4
79.1 18.5 0.1
51.9 46.3 1.3
CD28
43.1 10.7 2.0
65.3 20.6 0.9
45.8 51.0 1.0
CD1a
82.3 6.9 7.2 3.6
34.9 1.7 47.0 16.5
9.4 1.3 44.4 44.9
E
CD69−CD27−
CD69+CD27−
CD69+CD27+
CD69−CD27+
Percent
80
60
40
20
DP10
DP11
DP12
MSP1 CD4+
MSP2 CD4+
MSP3 CD4+
MSP4 CD4+
MSP5 CD4+
D
DP11
DP12
MSP3 CD4+
MSP4 CD4+
MSP5 CD4+
CD69
CD27
60.9 36.5 0.8
39.9 53.2 5.6
14.3 82.3 3.2
10.4 73.3 15.6
2.0 41.9 55.5
CD28
46.3 38.2 1.9
28.0 58.5 3.8
12.0 81.6 5.5
8.0 85.4 6.2
1.3 59.5 38.5
CD1a
41.3 16.0 22.2 20.5
5.4 2.1 36.5 56.0
3.8 3.7 11.0 81.4
0.1 0.1 11.9 87.9
0 0 2.9 97.1

population were $CD38^{hi}CD45RO^{hi}$ ($p < 0.001$), supporting the hypothesis that the MSP1 $CD4^+$ developmental stage precedes the MSP2 $CD4^+$ stage. Consistent with a model in which DP10 thymocytes mature into MSP1 $CD4^+$ thymocytes and then MSP2 $CD4^+$ thymocytes, 10 ± 1.4% of DP10 thymocytes, 18 ± 2.7% of MSP1 $CD4^+$ thymocytes, and 42 ± 3.8% of MSP2 $CD4^+$ thymocytes expressed CD27 (Fig. 4-4C). To further test this model, we analyzed CD1a expression on DP10, MSP1 $CD4^+$, and MSP2 $CD4^+$ thymocytes because decreased CD1a expression is a marker of thymocyte maturation (378). The percentage of thymocytes that expressed CD1a was highest among DP10 thymocytes and lower in the MSP1 $CD4^+$ and MSP2 $CD4^+$ subsets. Whereas CD28 was only expressed in DP9 and TSP thymocytes that also expressed CD27 (Fig. 4-3C), all DP10, MSP1 $CD4^+$, and MSP2 $CD4^+$ expressed CD28, regardless of CD27 expression (Fig. 4-4C).

Next, we analyzed $CD3^{hi}CD7^{hi}$ DP and SP $CD4^+$ thymocytes. $CD3^{hi}CD7^{hi}$ DP thymocytes include the DP11 and DP12 subsets, which are distinguished based on expression of CD38 and CD45RO (Fig. 4-1). $CD3^{hi}CD7^{hi}$ SP $CD4^+$ thymocytes include cells that are $CD38^{hi}CD45RO^{hi}$ (MSP3), $CD38^{lo}CD45RO^{lo}$ (MSP4), and $CD38^{-}CD45RO^{-}$ (MSP5) (Fig. 4-4A). DP11, DP12, MSP3 $CD4^+$, MSP4 $CD4^+$, and MSP5 $CD4^+$ thymocytes express comparable and high levels of CD7 and CD44 (Fig. 4-4B), suggesting that these populations are among the final stages prior to thymic egress. To test this model, we analyzed CD69, CD27, CD1a, and CD28 expression on each population. Consistent with a model in which DP11 thymocytes are the least mature $CD3^{hi}CD7^{hi}$ cells, only 31 ± 4.1% of DP11 cells were $CD27^+$, while 56 ± 5.1% of DP12 cells and over 75% of each of the $CD3^{hi}CD7^{hi}$ SP $CD4^+$ populations were $CD27^+$. ($p <$ 0.001 for DP11 or DP12 compared to each of the $CD3^{hi}CD7^{hi}$ SP $CD4^+$ populations) (Fig. 4-4D and E). Further, CD1a expression was high on DP11 cells and decreased as cells matured

through the MSP $CD4^+$ stages. In agreement with MSP5 $CD4^+$ being the most mature population of $CD4^+$ thymocytes, these cells had all down-regulated CD1a expression and 48 ± 3.8% of cells were $CD69^-$.

In summary, we propose that $CD3^{hi}$ DP thymocytes represent the developmental stages between the TSP $CD8^+$ population and the MSP $CD4^+$ thymocytes. Further, these data suggest that DP10 thymocytes can differentiate into either MSP1 $CD4^+$ thymocytes or DP11 thymocytes, implying that down-regulation of CD8, CD38, and CD45RO and up-regulation of CD44 are asynchronous processes that occur between the TSP $CD8^+$ developmental stage and the MSP $CD4^+$ stages. In addition, the data shown here suggest that MSP5 $CD4^+$ thymocytes represent the final developmental stage before cells exit the thymus.

Commitment to the $CD8^+$ T cell lineage

Besides DP and SP $CD4^+$ thymocytes, the other population that included $CD3^{hi}CD7^{hi}$ thymocytes was the SP $CD8^+$ population (Fig. 4-2B). Like $CD3^{hi}$ $CD4^+$ thymocytes, $CD3^{hi}CD7^{hi}$ SP $CD8^+$ thymocytes could be divided into three populations, based on CD38 and CD45RO expression: $CD38^{hi}CD45RO^{hi}$ (MSP1 $CD8^+$), $CD38^{lo}CD45RO^{lo}$ (MSP2 $CD8^+$), and $CD38^-$ $CD45RO^-$ (MSP3 $CD8^+$) (Fig. 4-5A). Each subset expressed high levels of CD44 (Fig. 4-5B). To determine the developmental sequence of the MSP1 $CD8^+$, MSP2 $CD8^+$, and MSP3 $CD8^+$ populations, we analyzed CD69 and CD27 expression (Figs. 4-5C and 4-5D). Nearly all cells in these subsets expressed CD69, CD27, or both markers, but the percentage of cells that were $CD69^-CD27^+$ increased as thymocytes progressed through the MSP1, MSP2, and MSP3 stages. In addition, CD1a expression declined as thymocytes matured through the MSP $CD8^+$ subsets.

Figure 4-5. $CD3^{hi}$ SP $CD8^+$ cells can be subdivided into three populations. *A)* SP $CD8^+$ thymocytes were gated on the $CD3^{hi}CD7^{hi}$ population as shown in Fig. 4-2B and analyzed for CD38 and CD45RO expression. The MSP1, MSP2, and MSP3 $CD8^+$ subsets are defined as shown. *B)* Each subset of MSP $CD8^+$ thymocytes was analyzed for CD44 and CD7 expression. *C)* $CD8^+$ MSP1, MSP2, and MSP3 thymocytes were analyzed for their expression of CD69, CD27, CD28, and CD1a. *D)* The percentages (mean ± SE) of MSP $CD8^+$ thymocytes that were $CD69^-CD27^-$, $CD69^+CD27^-$, $CD69^+CD27^+$, and $CD69^-CD27^+$ thymocytes are shown (n = 11).

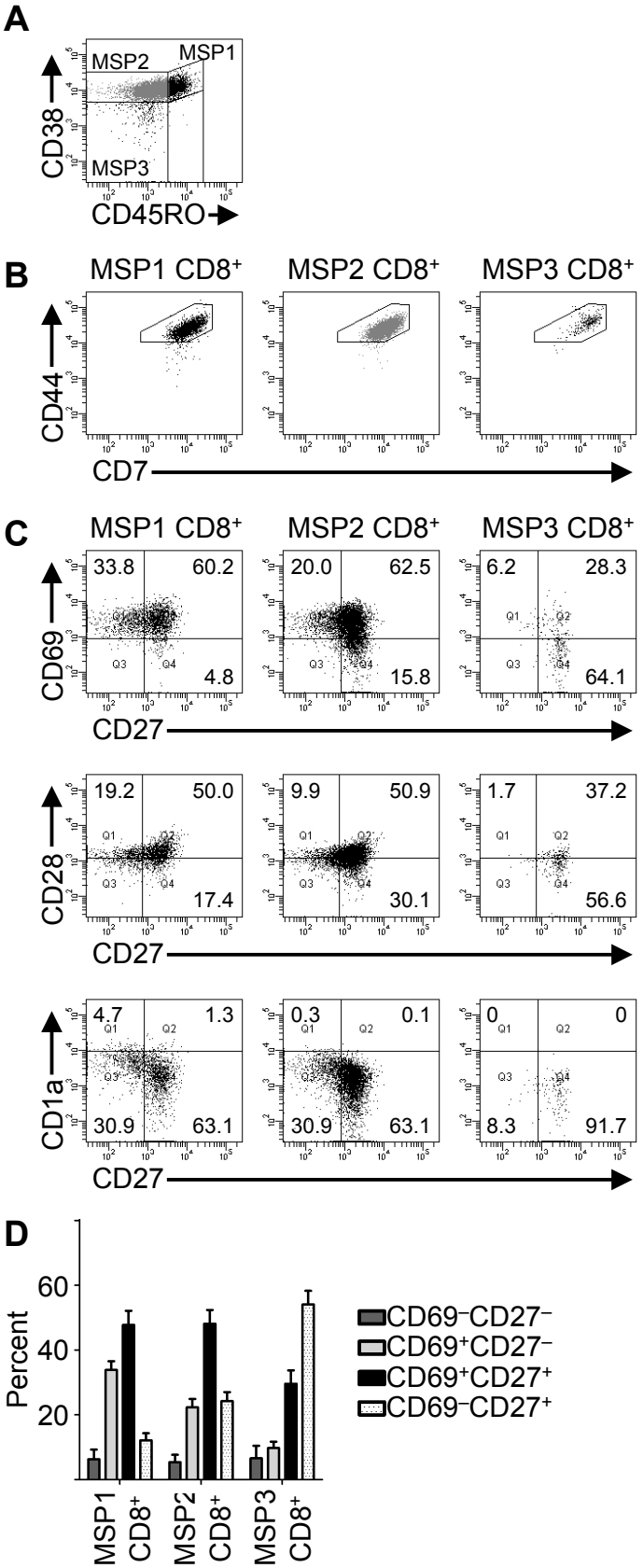
A
MSP2
MSP1
MSP3
CD38
CD45RO
B
MSP1 CD8+
MSP2 CD8+
MSP3 CD8+
CD44
CD7
C
MSP1 CD8+
MSP2 CD8+
MSP3 CD8+
CD69
CD27
33.8
60.2
4.8
20.0
62.5
15.8
6.2
28.3
64.1
CD28
CD27
19.2
50.0
17.4
9.9
50.9
30.1
1.7
37.2
56.6
CD1a
CD27
4.7
1.3
30.9
63.1
0.3
0.1
30.9
63.1
0
0
8.3
91.7
D
Percent
60
40
20
MSP1 CD8+
MSP2 CD8+
MSP3 CD8+
CD69−CD27−
CD69+CD27−
CD69+CD27+
CD69−CD27+

CD28 expression was comparable among MSP1, MSP2, and MSP3 $CD8^+$ thymocytes. These data suggest that $CD3^{hi}$ $CD8^+$ thymocytes progress from the MSP1 $CD8^+$ developmental stage through the MSP2 $CD8^+$ and MSP3 $CD8^+$ stages.

Differences in the protein levels of Ikaros, Helios and Aiolos across $CD3^+$ thymocyte subsets

Ikaros, Helios, and Aiolos protein levels increase when TCRβ is first expressed (376). For Ikaros and Helios, the increase in expression was transient whereas the increase in Aiolos was sustained throughout the $CD3^-$ DP populations. Consistent with this pattern, Ikaros and Helios protein levels were 1.6-fold (p<0.001) and 2.0-fold (p<0.001) higher, respectively, in DP6 thymocytes than in DP8 thymocytes, while Aiolos levels were comparable among the DP6, DP7, and DP8 subsets (Fig. 4-6).

As thymocytes progressed from the DP8 developmental stage to the TSP2 stage, Ikaros, Helios, and Aiolos protein levels increased by 2.3-fold, 2.5-fold, and 2.0-fold ($p < 0.001$ for each protein, comparing DP8 and TSP2 thymocytes). Then, levels of all three proteins were lower in DP10 and MSP1 $CD4^+$ thymocytes than TSP2 cells. The most dramatic difference between the TSP2 and MSP1 $CD4^+$ populations occurred with Helios, whose protein levels were 11-fold lower in MSP1 $CD4^+$ cells than TSP2 cells. Helios expression continued to decline as $CD4^+$ and $CD8^+$ thymocytes matured, except for subpopulations of MSP3 and MSP5 $CD4^+$ thymocytes. Because Helios is highly expressed in regulatory T cells (74, 379), we tested whether $Helios^{hi}$ MSP $CD4^+$ thymocytes co-expressed FoxP3 and CD25 (Fig. 4-7). Indeed, a subset of $Helios^{hi}$ MSP3 and MSP5 $CD4^+$ thymocytes expressed FoxP3 and CD25.

Among MSP $CD4^+$ thymocytes, Aiolos protein levels were 2.5-fold lower in MSP1 $CD4^+$ thymocytes than TSP2 cells, increased transiently during the MSP3 and MSP4 $CD4^+$ stages, and

Figure 4-6. Ikaros, Helios, and Aiolos expression patterns differ in developing $CD3^+$ thymocytes. $CD3^{lo}$ (*A*) and $CD3^{hi}$ (*B*) thymocyte populations were intracellularly stained with anti-Ikaros, anti-Helios, anti-Aiolos (dark lines), or an appropriate isotype control (shaded histogram). *C*) For each population in *A* and *B,* the geometric mean fluorescence intensity (GMFI) of anti-Ikaros, anti-Helios, or anti-Aiolos was normalized to the GMFI of the isotype control. Mean ± SE fold change relative to DP8 is shown for at least 5 independent experiments.

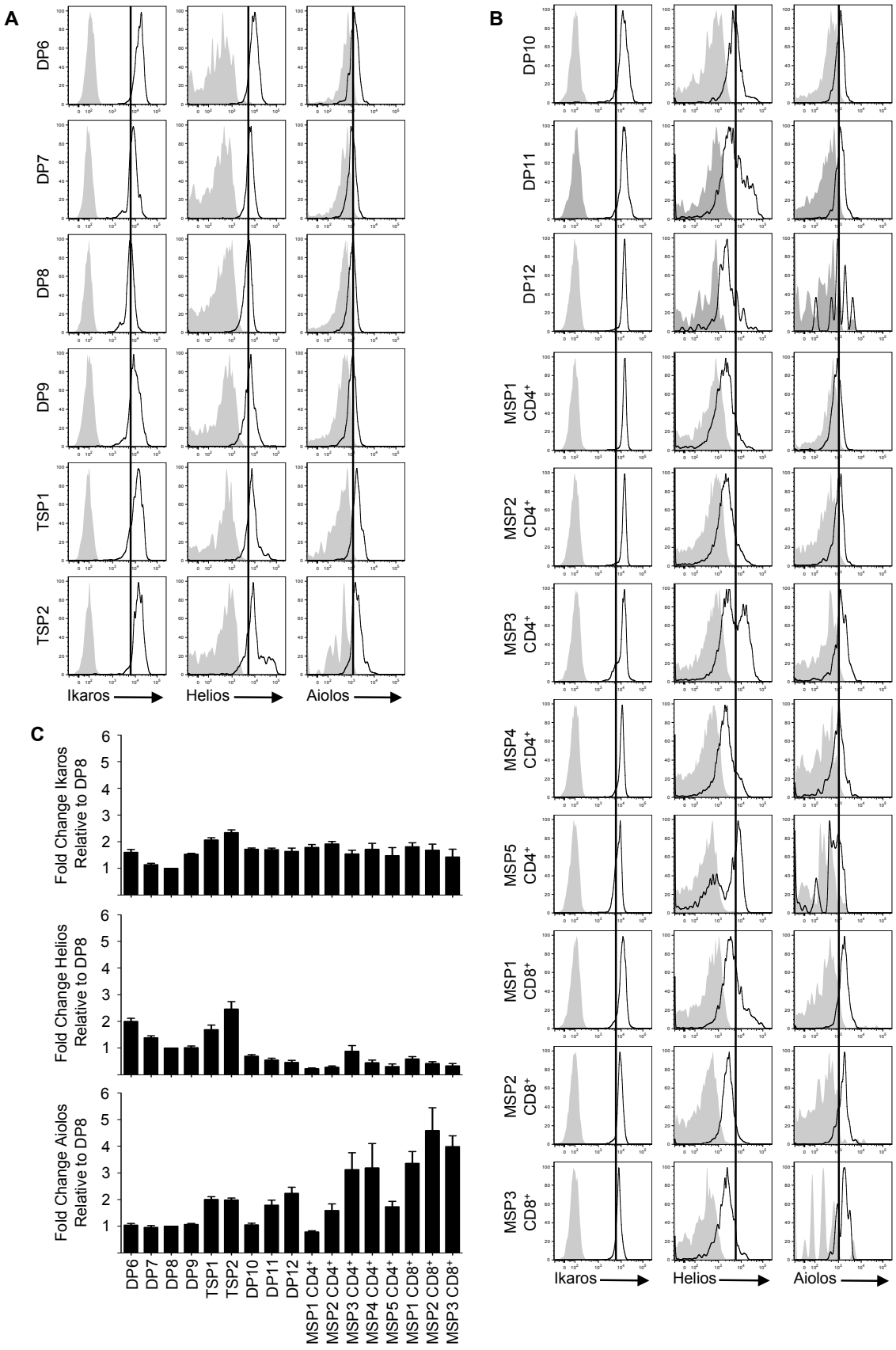
A
DP6
DP7
DP8
DP9
TSP1
TSP2
Ikaros
Helios
Aiolos
B
DP10
DP11
DP12
MSP1 CD4+
MSP2 CD4+
MSP3 CD4+
MSP4 CD4+
MSP5 CD4+
MSP1 CD8+
MSP2 CD8+
MSP3 CD8+
Ikaros
Helios
Aiolos
C
Fold Change Ikaros Relative to DP8
Fold Change Helios Relative to DP8
Fold Change Aiolos Relative to DP8
DP6
DP7
DP8
DP9
TSP1
TSP2
DP10
DP11
DP12
MSP1 CD4+
MSP2 CD4+
MSP3 CD4+
MSP4 CD4+
MSP5 CD4+
MSP1 CD8+
MSP2 CD8+
MSP3 CD8+

Figure 4-7. Helios^{hi} MSP CD4^{+} thymocytes are regulatory T cells. DP11, DP12, and MSP CD4^{+} thymocytes were analyzed for *A)* Helios and FoxP3 expression, and *B)* Helios and CD25 expression. Dot plots are from a single thymus that was analyzed.

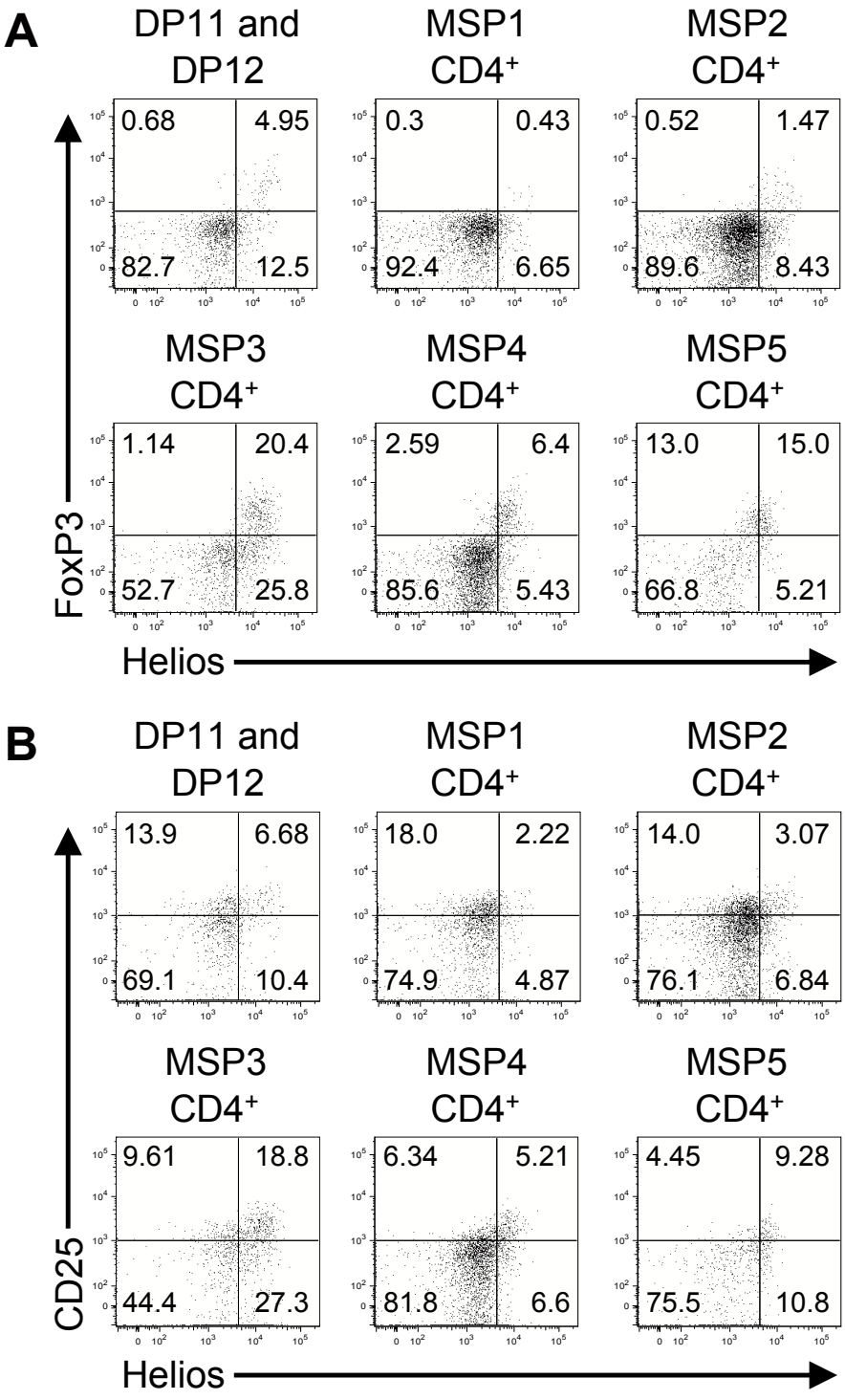
A
DP11 and DP12
MSP1 CD4+
MSP2 CD4+
0.68
4.95
82.7
12.5
0.3
0.43
92.4
6.65
0.52
1.47
89.6
8.43
MSP3 CD4+
MSP4 CD4+
MSP5 CD4+
1.14
20.4
52.7
25.8
2.59
6.4
85.6
5.43
13.0
15.0
66.8
5.21
FoxP3
Helios
B
DP11 and DP12
MSP1 CD4+
MSP2 CD4+
13.9
6.68
69.1
10.4
18.0
2.22
74.9
4.87
14.0
3.07
76.1
6.84
MSP3 CD4+
MSP4 CD4+
MSP5 CD4+
9.61
18.8
44.4
27.3
6.34
5.21
81.8
6.6
4.45
9.28
75.5
10.8
CD25
Helios

decreased again at the MSP5 $CD4^+$ stage. By contrast, Aiolos protein levels were higher in the MSP1 $CD8^+$ and MSP2 $CD8^+$ subsets than TSP2 thymocytes. ($p < 0.05$). In addition, Aiolos levels were 2.3-fold higher in the mature MSP3 $CD8^+$ cells than in the mature MSP5 $CD4^+$ cells ($p < 0.01$). Unlike Helios and Aiolos, Ikaros protein levels remained steady after the transient increase seen in the TSP subsets.

These data indicate that Ikaros, Helios, and Aiolos undergo a transient increase in protein levels during the TSP developmental stage. However, expression of Helios and Aiolos in populations varies: Ikaros expression remains steady, Helios expression declines, except for a subpopulation of MSP $CD4^+$ thymocytes, and Aiolos expression increases, particularly among $CD8^+$ T cells.

Discussion

The data presented here represent the highest resolution image to date of human T cell development beginning with detectable surface CD3 expression. The multi-parameter flow cytometry data revealed twelve subpopulations of DP thymocytes, five subpopulations of SP $CD8^+$ thymocytes, and five subpopulations of SP $CD4^+$ thymocytes. Each of these subpopulations can be further divided using additional markers. Our analysis focused on the stages of T cell development surrounding positive selection and lineage commitment and resulted in the model shown in Fig. 4-8.

Based on CD7, CD45RO, CD38, and CD44 expression, we found three pairs of DP subsets in which one half of each pair was $CD3^-$ and the other subset was $CD3^{lo}$. The $CD3^-$ fractions (DP3, DP4, and DP5) represent the final developmental stages that lack surface CD3 expression. We previously showed that these populations express TCRβ and DP3 thymocytes are the most highly proliferative population of $CD3^-$ thymocytes (376). Proliferation slows as thymocytes progress through the DP4 and DP5 thymocytes, suggesting that these populations are undergoing genomic rearrangement at the locus encoding TCRα. When TCRα is expressed, CD3 becomes detectable at the cell surface. Thymocytes expressing levels of CD7 and CD44 similar to those of the DP3, DP4, and DP5 developmental stages can express surface CD3, indicating that CD7 and CD44 down-regulation is independent of TCRα expression. Thus, DP3 thymocytes can differentiate into DP4 or DP6 thymocytes. Likewise, DP4 thymocytes can differentiate into DP5 thymocytes unless they express surface CD3, in which case they become DP7 thymocytes.

A small percentage of DP6, DP7, and DP8 thymocytes express CD69 (Fig. 4-3A), suggesting that thymocytes have the potential to become positively selected as soon as surface

Figure 4-8. A model of human T cell development through the $CD3^+$ stages.

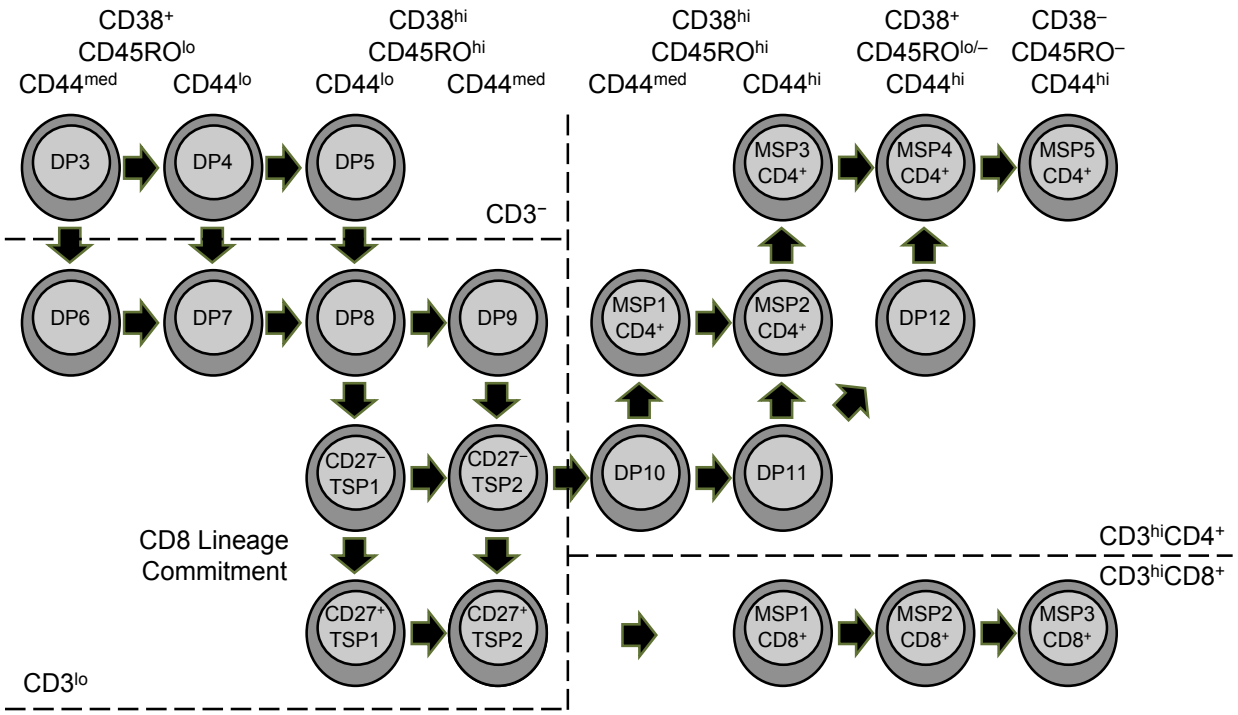
CD38+ CD45ROlo CD44med
CD44lo
CD38hi CD45ROhi CD44lo
CD44med
CD38hi CD45ROhi CD44med
CD44hi
CD38+ CD45RO lo/– CD44hi
CD38– CD45RO– CD44hi
DP3
DP4
DP5
MSP3 CD4+
MSP4 CD4+
MSP5 CD4+
CD3–
DP6
DP7
DP8
DP9
MSP1 CD4+
MSP2 CD4+
DP12
CD27– TSP1
CD27– TSP2
DP10
DP11
CD8 Lineage Commitment
CD3hiCD4+
CD3hiCD8+
CD27+ TSP1
CD27+ TSP2
MSP1 CD8+
MSP2 CD8+
MSP3 CD8+
CD3lo

CD3 is expressed. After positive selection, thymocytes down-regulate CD4 expression to become TSP $CD8^+$ thymocytes (Fig. 4-3C). We propose that the TSP $CD8^+$ population is analogous to the TSP $CD4^+$ thymocytes observed in mice (312-315). During murine T cell development, CD8 expression decreases after positive selection, resulting in the TSP $CD4^+$ population (317-320). In humans, maturation into the TSP $CD8^+$ population is associated with a transient increase in Ikaros, Helios, and Aiolos expression (Fig. 4-6). Studying all three proteins is important because Ikaros family members can homodimerize or heterodimerize with each other family member and dimerization is required for transcriptional activity (1-5). Because all three proteins increase their expression two- to three-fold, it is likely that the composition of the dimers does not change at the TSP stage, but the number of dimers increases.

Despite the likelihood that dimer composition does not change, data from murine models of T cell development indicate that Ikaros family members are important at the TSP stage (380). Specifically, expression of a dominant negative Ikaros isoform results in accumulation of $CD4^+CD8^{lo}$ TSP cells (381). One function of Ikaros at the TSP stage may be to inhibit transcription of TdT and pre-Tα (56, 382). However, it was suggested that higher levels of Ikaros resulted in the recruitment of an elongation-competent NuRD/P-TEFb complex to gene targets, rather than the repressive NuRD complex (40). Thus, increased Ikaros family expression at the TSP stage may be required for activation of genes for further maturation. In addition, Ikaros family members may affect the signal strength necessary for lineage commitment, as Ikaros and Aiolos can regulate the TCR signaling threshold in murine thymocytes and splenocytes (26, 51, 367, 383-385). Ikaros family members can also regulate CD4 and CD8 expression (65, 66, 346), a necessary step for lineage commitment.

The role of Ikaros in regulating signal strength and CD4/CD8 expression in the TSP stage implies that the TSP developmental stage might be the site of lineage commitment. TSP $CD8^+$ thymocytes express CD69 and many TSP $CD8^+$ thymocytes express CD27. Vanhecke, *et al.* previously showed that $CD27^+$ SP $CD4^+$ and SP $CD8^+$ thymocytes are committed to their respective lineages while $CD27^-$ SP $CD4^+$ cells could still differentiate into SP $CD8^+$ cells (386). This observation suggests that CD27 is a marker of thymocytes committed to the $CD4^+$ or $CD8^+$ lineage. Even though most TSP $CD8^+$ thymocytes expressed CD27, most DP10 thymocytes lacked CD27 expression. Although this observation might suggest that DP10 thymocytes are less mature than TSP thymocytes, the fact that TSP thymocytes have lower surface CD3 levels places the TSP developmental stage earlier than the DP10 stage. Thus, the TSP $CD8^+$ developmental stage most likely represents the decision point between the $CD4^+$ and $CD8^+$ lineages. $CD27^+$ TSP $CD8^+$ thymocytes likely retain their CD8 expression, up-regulate CD3 and mature into MSP1 $CD8^+$ thymocytes, while $CD27^-$ TSP $CD8^+$ thymocytes likely re-express CD4, becoming DP10 thymocytes (Fig. 4-8).

Because DP10 and MSP1 $CD4^+$ thymocytes express similar levels of CD38, CD45RO, CD7, CD44, CD3, CD69, and CD27 (Figs. 4-1 and 4-4), it is likely that DP10 thymocytes can differentiate directly into MSP1 $CD4^+$ thymocytes. Alternatively, DP10 thymocytes could up-regulate CD44, becoming DP11 thymocytes. DP11 thymocytes could differentiate into MSP2 $CD4^+$ thymocytes or DP12 thymocytes, depending on the sequence in which the cells down-regulate CD8, CD38, and CD45RO, and up-regulate CD27. DP12 thymocytes are most similar to MSP4 $CD4^+$ thymocytes, suggesting that DP12 thymocytes can directly mature into MSP4 $CD4^+$ cells.

As thymocytes continue to mature into naïve $CD4^+$ and $CD8^+$ T cells, their expression of Ikaros, Helios, and Aiolos change in manners that would be predicted to influence the composition of the dimers (Fig. 4-6). Specifically, Ikaros expression remains constant throughout the MSP subpopulations. Aiolos is more highly expressed in MSP $CD8^+$ thymocytes than most MSP $CD4^+$ thymocyte subsets. Helios expression declines as thymocyte mature, except for a subset of SP $CD4^+$ thymocytes, which are likely to be the regulatory T cell subset (Fig. 4-7) (74, 379). The function of Ikaros family members at these stages is unclear.

In summary, we used multi-parameter flow cytometry to define the stages of human T cell development in which positive selection and lineage commitment are most likely to occur. We observed a transient increase in Ikaros, Helios, and Aiolos expression when thymocytes undergo positive selection, and Aiolos is more highly expressed in subsets of mature SP $CD4^+$ and $CD8^+$ thymocytes than pre-selection thymocytes.

Chapter 5. Classifying pediatric T cell acute lymphoblastic leukemia patients according to Ikaros family expression

Abstract

Pediatric T cell acute lymphoblastic leukemia (T-ALL) is a highly heterogeneous disease in which the cells share phenotypic characteristics with normal human thymocytes. Attempts have been made to classify patients according to the stage of thymic development that the T-ALL cells most closely resemble. However, there is no consensus regarding the relevance of such a classification scheme. We obtained twenty-four blood or bone marrow samples from newly diagnosed pediatric T-ALL patients and used multi-parameter flow cytometry to demonstrate the extent of diversity of T-ALL samples, even among samples that appeared similar. To develop an alternate classification strategy, we examined the mRNA and protein levels of each member of the Ikaros family of transcription factors. Ikaros and Helios mRNA were the predominant family members expressed in normal human thymocytes and leukemic cells. By calculating the ratio of Ikaros to Helios mRNA, the T-ALL cases could be divided into three groups that were independent of the phenotype of the cells. However, the protein levels of Ikaros and Aiolos did not correlate with the mRNA levels and not all splice variants detected at the mRNA level were detected at the protein level. Future studies will be required to determine whether Ikaros family mRNA levels could be used as a prognostic indicator for pediatric T-ALL patients.

Introduction

Pediatric T cell acute lymphoblastic leukemia (T-ALL) is a heterogeneous disease in which the leukemic cells often resemble normal thymocyte populations. The phenotypic similarities between leukemic cells and normal thymocytes have led to the conclusion that patients might be classified according to the developmental stage that is most similar to the leukemic cells (78, 80). For example, cells from some T-ALL cases lack TCRβ expression and are thought to be derived from early T cell precursors. During normal human T cell development, early T cell precursors are $CD4^{-}CD8^{-}$ double negative (DN) thymocytes that express CD34. DN thymocytes can be divided into DN1, DN2, or DN3 cells, depending on their expression of CD38 and CD1a (108, 109). During the DN stages, the cells commit to either the αβ or γδ T cell lineage (130, 164). Cells from some T-ALL patients resemble uncommitted early T cell progenitors and likely emerge from the early DN stages. Cells from other patients express TCRγδ and resemble stages of γδ T cell development.

In other T-ALL cases, the leukemic cells express cytoplasmic TCRβ, but not surface CD3. During normal T cell development, cytoplasmic $TCR\beta^{+}$ cells are either immature single positive (ISP) $CD4^{+}$ thymocytes or a subpopulation of $CD4^{+}CD8^{+}$ double positive (DP) thymocytes (117, 119). ISP $CD4^{+}$ thymocytes are a transition between the DN and DP stages (110). During the DP stage, thymocytes express TCRα, undergo positive or negative selection, and differentiate into mature single positive cells that can egress from the thymus and function as mature naïve T cells.

There are conflicting data regarding the prognostic value of classifying pediatric T-ALL patients according to the phenotype of the leukemic cells. For example, some studies reported a

poor prognosis for patients whose cells express either CD34 or surface TCR (79, 82), while other studies found no differences in survival between groups (81, 83). In this study, we used multi-parameter flow cytometry to demonstrate the degree of heterogeneity among T-ALL patients, perhaps explaining the challenges faced when attempting to correlate the phenotype of the leukemic cells with clinical outcomes.

As an alternative classification strategy, we tested whether patients could be grouped according to their expression of Ikaros family members. The Ikaros family has been linked to T-ALL in mice (47-49) and humans (8, 10, 84-86, 88-91) and consists of five highly homologous transcription factors: Ikaros, Helios, Aiolos, Eos, and Pegasus. Each family member has two zinc finger domains. The four N-terminal zinc fingers mediate DNA binding, and the two C-terminal zinc fingers are required for dimerization. Transcriptional activity requires dimerization and each family member is capable of dimerizing with each other family member (1-5).

Adding complexity to the study of Ikaros is that some family members undergo alternative splicing that results in the deletion of one or more DNA binding zinc fingers. Loss of one or two zinc fingers can result in more promiscuous DNA binding, but deletion of three or more zinc fingers can create dominant negative isoforms that block the ability of other family members to bind DNA (1-4, 6, 341). Some reports indicate that alternative splicing is common in T-ALL while other reports find it to be rare (8, 10, 84-86, 88-92).

We compared mRNA and protein levels of each Ikaros family member in normal human thymocytes and cells from pediatric T-ALL patients. We identified patterns of Ikaros family mRNA levels that transcend surface phenotypes, suggesting that the key elements in investigating mechanisms of leukemogenesis lie in the function of Ikaros family proteins or the signaling pathways that regulate Ikaros family transcription.

Materials and Methods

Human tissue samples

Human thymus samples were obtained from children (0 – 18 years) that underwent corrective surgery at Children's Mercy Hospital (Kansas City, MO) for congenital cardiac defects after obtaining parent or guardian consent. Tissue samples were obtained in compliance with the Institutional Review Boards at Children's Mercy Hospital and the University of Kansas Medical Center.

Twenty-four blood or bone marrow samples were obtained from newly diagnosed pediatric T-ALL patients prior to the initiation of anti-cancer therapy. Samples from patients diagnosed at Children's Mercy Hospital were collected after obtaining parent or guardian consent. Leukemic cells were enriched by labeling the cells with anti-CD7-PE antibody and positively selecting with magnetic beads conjugated to anti-PE antibody (BD Biosciences, San Jose, CA). Other samples were obtained as frozen samples through the Children's Oncology Group (NCI Protocol AALL12B11). Each sample was divided into aliquots for flow cytometric, mRNA, and protein analysis.

Phenotypic analysis of T-ALL samples

The anti-human antibodies anti-CD1a-PerCP-Cy5.5, anti-CD1a-PECy5, anti-CD3-APCCy7, anti-CD3-APC-Alexa750, anti-CD4-Pacific Blue, anti-CD5-AF647, anti-CD7-PE, anti-CD8-BV785, anti-CD8-FITC, anti-CD27-HV500, anti-CD34-BV605, anti-CD34-PE, anti-CD34-PECy7, and anti-CD38-AF700, anti-CD44-PECy7, anti-CD45RO-PECy5, anti-CD69-BV650, anti-TCRγδ-FITC were purchased from Biolegend (San Diego, CA). Samples were

labeled with anti-CD1a, anti-CD3, anti-CD4, anti-CD5, anti-CD7, anti-CD8, anti-CD34, anti-CD38, and anti-TCRγδ antibodies. Most samples were also labeled with anti-CD27, anti-CD44, anti-CD45RO, and anti-CD69. Data were acquired using a BD LSR II (BD Biosciences) and analyzed using BD FACSDiva software (BD Biosciences).

FACS-purification of human thymocytes

DN2, DN3, and ISP thymocytes were obtained by depleting total thymocytes with magnetic beads conjugated to anti-CD8 and anti-CD3 (BD Biosciences). Remaining cells were divided into the DN2 ($CD3^-CD4^-CD8^-CD34^+CD38^+CD1a^-$), DN3 ($CD3^-CD4^-CD8^-CD34^+CD38^+CD1a^+$), and ISP ($CD3^-CD4^+CD8^-$) populations using a FACSAria IIIu (BD Biosciences). For total DN or DP thymocytes, cells were labeled with anti-CD4 and anti-CD8 and $CD4^-CD8^-$ or $CD4^+CD8^+$ thymocytes were FACS-purified.

Quantitative RT-PCR (qRT-PCR)

Total mRNA was isolated using the RNeasy Mini Kit or RNeasy Micro Kit (Qiagen, Valencia, CA), converted to cDNA using the TaqMan® High Capacity RNA-to-cDNA™ kit (Applied Biosystems, Foster City, CA), and amplified using TaqMan® Gene Expression Assays: Ikaros: Hs00958473_m1; Helios: Hs00212361_m1 ; Aiolos: Hs00232635_m1; Eos: Hs00223842_m1; Pegasus: Hs00223846_m1; and GAPDH: Hs03929097_g1 (Applied Biosystems). qRT-PCR was performed using a 7500 Fast Real-Time PCR System (Applied Biosystems). Each sample was run in triplicate. For normal thymocytes, at least five biological replicates were performed for each subset and each replicate was performed in triplicate. mRNA

levels of each Ikaros family member were calculated relative to GAPDH and statistical significance was determined using the Log_2(Fold Change).

Western blot analysis

Cell lysates prepared from 4-5×10^5 cells were separated by SDS-PAGE, transferred to nitrocellulose, and probed with antibodies against Ikaros, Aiolos, or p38 MAPK (all purchased from Santa Cruz Biotechnology, Inc., Dallas, TX). Bands were visualized using horseradish peroxidase-conjugated secondary antibodies (Santa Cruz Biotechnology, Inc.) and Pierce™ ECL Western Blotting Substrate (Life Technologies, Grand Island, NY), and detected using an ImageQuant LAS-4000 gel imager (GE Healthcare systems, Pittsburgh, PA).

Nested PCR

Total mRNA was reverse transcribed with AMV RT (Promega, Madison, WI) before amplification with Taq DNA Polymerase (Fisher Scientific, Pittsburgh, PA). Primary PCR reactions were performed using primers specific to the 5' UTR and 3' UTR (Table 5-1). The PCR products were re-amplified using primers that spanned all possible exon pairs. PCR products were separated on an agarose gel, visualized with ethidium bromide and analyzed using an ImageQuant LAS-4000 gel imager.

Statistics

For qRT-PCR data, statistics were performed using the one-way ANOVA with a Tukey posthoc test, and significance was defined as $p < 0.05$. For linear regression, whether the slope of the line was different than zero was determined and significance was defined as $p < 0.05$.

Statistical analysis was performed using GraphPad Prism (GraphPad Software, Inc, La Jolla, CA).

Table 5-1. Primers used for nested PCR.

Ikaros	
5’ UTR	CGACGCACAAATCCACATAACCTGAG
Exon 1 Forward	CATGGATGCTGATGAGGGTC
Exon 2 Forward	TAAGCGATACTCCAGATGAGGG
Exon 3 Forward	TCGGGAGTTGGAGGCATTCG
Exon 4 Forward	GGCACATCAAGCTGCATTCC
Exon 5 Forward	TGGATATTGTGGCCGAAGC
Exon 3 Reverse	CCATTCATTTCACAGGCACGC
Exon 4 Reverse	AGGCGTAGTTGCAGAGGTGG
Exon 5 Reverse	CCAAGTAGTTGTGGCAGCG
Exon 6 Reverse	GACGTTACTTGCTAGTCTGTCC
Exon 7 Reverse	TTGTGCAGCTGGTACATCG
3’ UTR	TTGTCTGGTCCAGTCCAGTCTATGC
Aiolos	
5’ UTR	GGCAGCGACATGGAAGATATAC
Exon 1 Forward	CACTCAGGAGCAGTCTGTG
Exon 2 Forward	AATGTGGACAGTGGAGAAGGC
Exon 3 Forward	GTCTCATTCGATAGTAGCAGGC
Exon 4 Forward	AGAAGAGATGCGCTCACGG
Exon 5 Forward	GAGAAGTTCCCTTGAGGAGC
Exon 3 Reverse	TCATCTTTCCACTGGTTGGC
Exon 4 Reverse	GTGAGCGCATCTCTTCTTTGG
Exon 5 Reverse	CCTCAAGGGAACTTCTCTGC
Exon 6 Reverse	GCTAATCTGTCCAGTACGAGAGC
Exon 7 Reverse	ACCGTTTGACATCTCAGCC
3’ UTR	GAGACCAGATATTCACTTCAGCAGG
Helios	
5’ UTR	TGCACTTTGACTATGGAAACAGAGGC
Exon 2 Forward	TTGACCTCACCTCAAGCACACC
Exon 3 Forward	ATTGAGAGCAGCGAGGTGGC
Exon 4 Forward	CTTCCACTGTAACCAGTGTGGAGC
Exon 5 Forward	ACTGGAGGAACACAAGGAACGC
Exon 3 Reverse	GGCCCAATGCAAACCATGCC
Exon 4 Reverse	GCGTCCCTTCTTCTACAGGC
Exon 5 Reverse	CTGCGCTGCTTGTAGCTTCG
Exon 6 Reverse	GAGCTTCTCTATGACAGCAGGTCTC
Exon 7 Reverse	CCACTTCAGCGATTGTGCTTGG
3’ UTR	GAGGAAAGGTGGGATTGTAAGTGC

Results

Cells from T-ALL patients with a CD3$^-$ DN phenotype

Multi-parameter flow cytometry was used to define the phenotypic characteristics of the cells from pediatric T-ALL patients. Cells from one patient (PATLGK) were mostly CD7$^-$ and were CD3$^-$CD4$^-$CD8$^-$CD34$^+$CD1a$^-$ (Fig. 5-1A), suggesting that they arose from an early developmental stage, possibly early thymic progenitors (387). However, these cells also expressed CD38, which is not typically observed until the DN2 developmental stage (108, 109).

Cells from five T-ALL patients were CD7$^+$ and CD3$^-$CD4$^-$CD8$^-$ (Fig. 5-1B). In each of these five patients, the majority of the cells were CD38$^+$CD1a$^-$, but the expression of CD38 and CD1a varied slightly among the patients. For example, cells from patient PASIZR were CD38^{lo} and resembled a DN1/DN2 transition state. By contrast, cells from patients PASIZW and PASKMA were CD1a^{lo}, consistent with a DN2/DN3 transition. Most CD3$^-$CD4$^-$CD8$^-$ T-ALL cells were CD44^{hi}CD27$^-$CD45RO$^-$, but had varying levels of CD5 and CD69 (Fig. 5-2A and 5-2B). In normal human thymocytes, CD5 is expressed on almost all cells and CD69 is not expressed until after cells express surface CD3 (388-390).

Pediatric T-ALL cells that lacked CD3, but expressed either CD4 or CD8

Six CD7$^+$CD3$^-$ leukemia samples expressed varying levels of CD4 or CD8 (Fig. 5-1C). We classified patient PAQAPZ as CD3$^-$ because the CD3$^-$ cells were CD8^{lo} and were likely the leukemic cells while the CD3$^+$ cells resembled normal peripheral T cells. Cells from three patients (PASTCF, PATHXN, and PAQYHW) were predominantly CD4$^+$ and the CD8 levels ranged from negative to high, phenotypes consistent with the ISP CD4$^+$ and DP developmental

Figure 5-1. Phenotypes of $CD3^-$ T-ALL cells. The indicated T-ALL samples were labeled for flow cytometry as described in *Materials and Methods*. *A*) CD7 and CD3 expression were analyzed (*Top panel*) and $CD7^-CD3^-$ cells were analyzed as shown in the remaining panels. *B* and *C*) Cells were analyzed as in '*A*' except $CD7^+CD3^-$ cells were analyzed as shown.

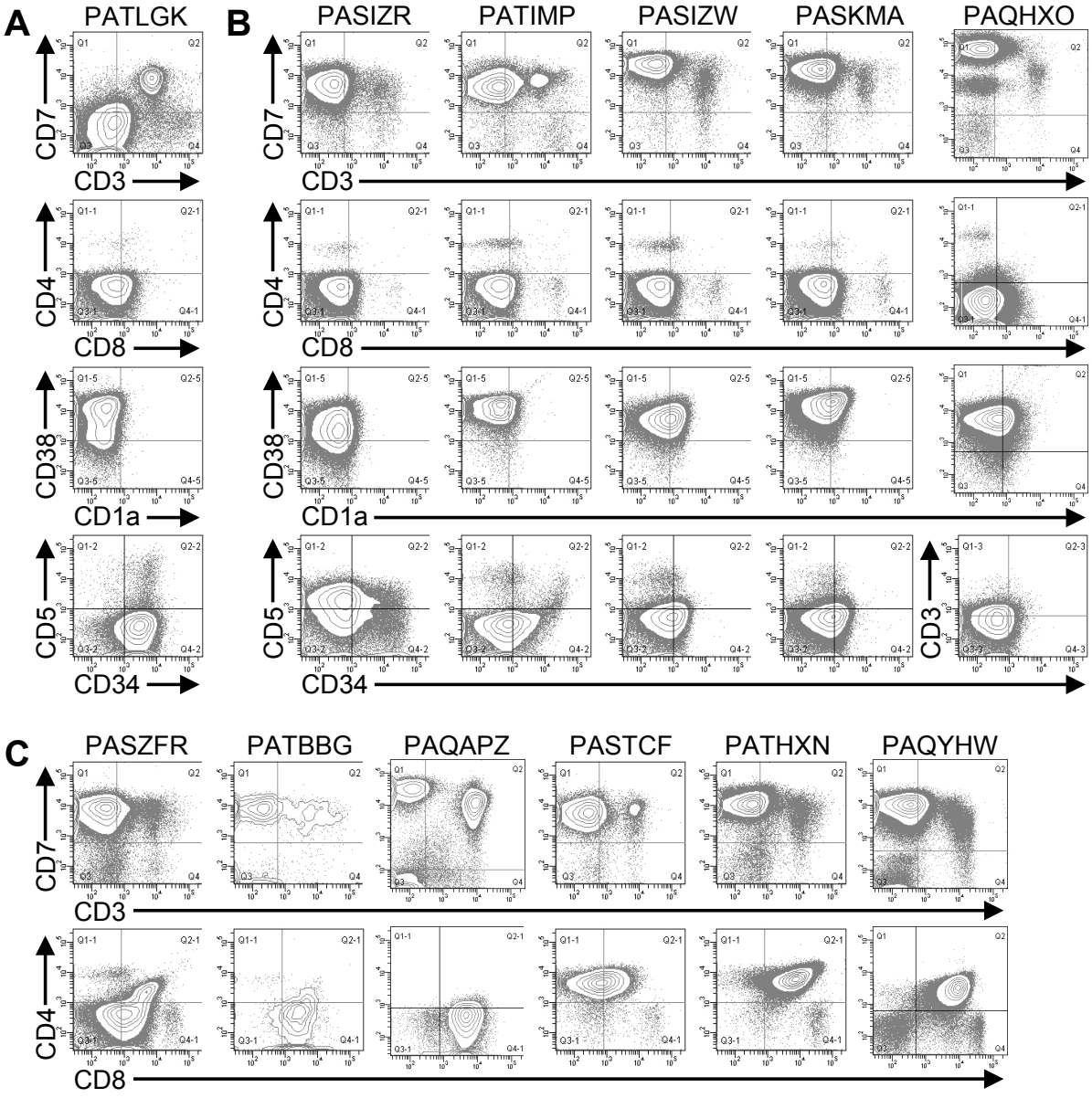
A
PATLGK
CD7
CD3
CD4
CD8
CD38
CD1a
CD5
CD34
B
PASIZR
PATIMP
PASIZW
PASKMA
PAQHXO
CD7
CD3
CD4
CD8
CD38
CD1a
CD5
CD34
CD3
C
PASZFR
PATBBG
PAQAPZ
PASTCF
PATHXN
PAQYHW
CD7
CD3
CD4
CD8

Figure 5-2. Phenotypes of CD3$^-$ T-ALL cells. *A*) CD7$^-$CD3$^-$ cells from Fig. 5-1 were analyzed as shown in the remaining panels. *B* and *C*) CD7$^+$CD3$^-$ cells from Fig. 5-1 were analyzed as shown in the remaining panels.

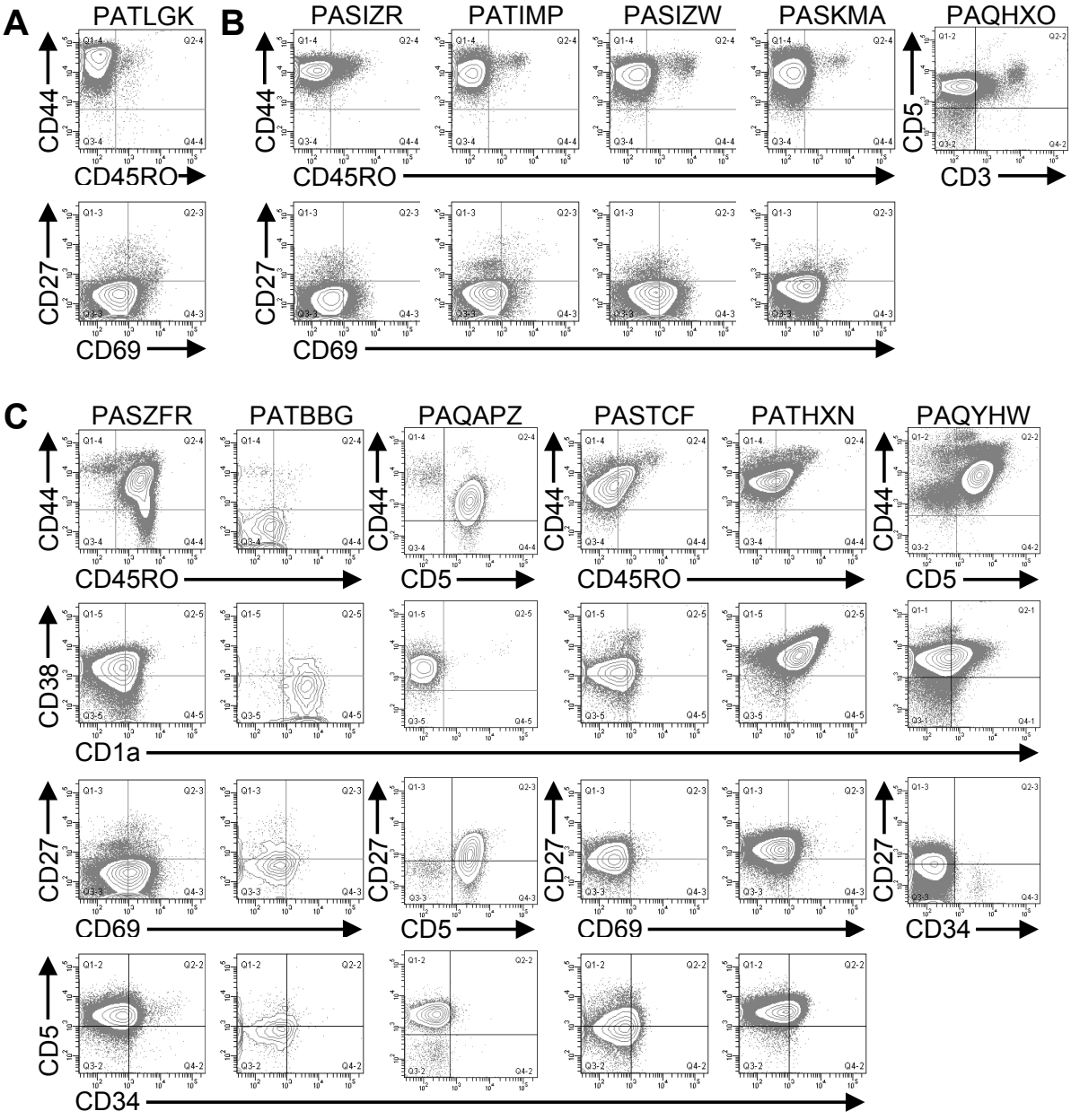
A
PATLGK
CD44
CD45RO
CD27
CD69
B
PASIZR
PATIMP
PASIZW
PASKMA
PAQHXO
CD44
CD45RO
CD5
CD3
CD27
CD69
C
PASZFR
PATBBG
PAQAPZ
PASTCF
PATHXN
PAQYHW
CD44
CD45RO
CD5
CD38
CD1a
CD27
CD69
CD34

stages. Three patients (PASZFR, PATBBG, and PAQAPZ) were $CD3^{-}CD4^{-}$ and expressed low levels of CD8, a phenotype that is rare among normal thymocytes (354).

Among the $CD7^{+}CD3^{-}$ leukemia samples, cells from patient PATBBG were unique in that they lacked CD44, CD45RO, and CD38 expression on their surface (Fig. 5-2C). Cells from the three patients that expressed ISP $CD4^{+}$ and DP markers had varying levels of CD45RO with the DP-like T-ALL cells expressing the highest levels of CD45RO (Fig. 5-2C); during normal T cell development, increased CD45RO expression correlates with progression to the DP developmental stage (391-393). Cells from patient PASZFR, which were $CD3^{-}CD4^{-}CD8^{lo}$, were also $CD45RO^{+}$ and had low levels of CD69. CD38 and CD1a expression was highly variable across the six samples and did not correlate with CD4 and CD8 expression. Cells from five of the six patients expressed CD27, even though CD27 is not normally expressed until the late stages of T cell development (390).

$CD3^{+}$ Pediatric T-ALL cells

Cells from the remaining twelve patients expressed CD3 on their surface (Fig. 5-3). Cells from four patients (PATCSS, PARSZP, PASIYP, and PASJNV) were $CD4^{-}CD8^{-}$, $CD4^{+}CD8^{-/lo}$, or $CD4^{+}CD8^{+}$ (Fig. 5-3A). Cells from each of these four samples expressed CD45RO and CD38, but variable levels of CD44 and CD1a (Fig. 5-4A). Three of these samples expressed low levels of CD27. Cells from patients PARSZP and PASJNV also expressed CD34.

Cells from three patients (PARVLA, PATCHB, and PASUVH) expressed TCRγδ (Fig. 5-3B). Cells from patient PATCHB lacked CD4 and CD8 expression, but the other two samples expressed CD4 and cells from patient PARVLA also expressed low levels of CD8. Cells from

Figure 5-3. Phenotypes of CD3$^+$ T-ALL cells. The indicated T-ALL samples were labeled and analyzed as described in the legend to Fig. 5-1, except all panels were gated on total CD7$^+$ cells.

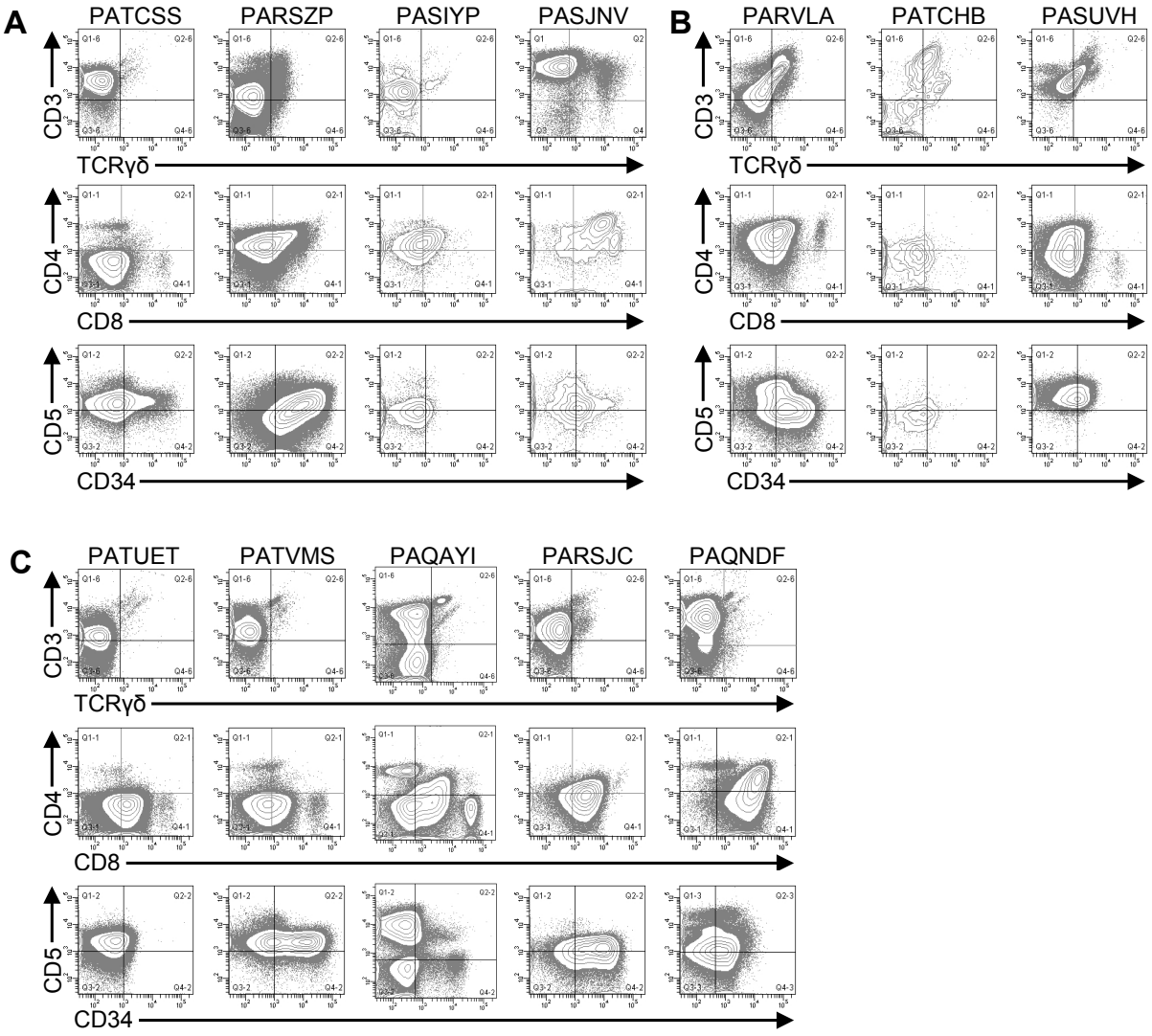
A
PATCSS
PARSZP
PASIYP
PASJNV
B
PARVLA
PATCHB
PASUVH
CD3
TCRγδ
CD4
CD8
CD5
CD34
C
PATUET
PATVMS
PAQAYI
PARSJC
PAQNDF

Figure 5-4. Phenotypes of CD3$^+$ T-ALL cells. T-ALL cells from Fig. 5-3 were analyzed using the markers shown, as described in the legend to Fig. 5-1.

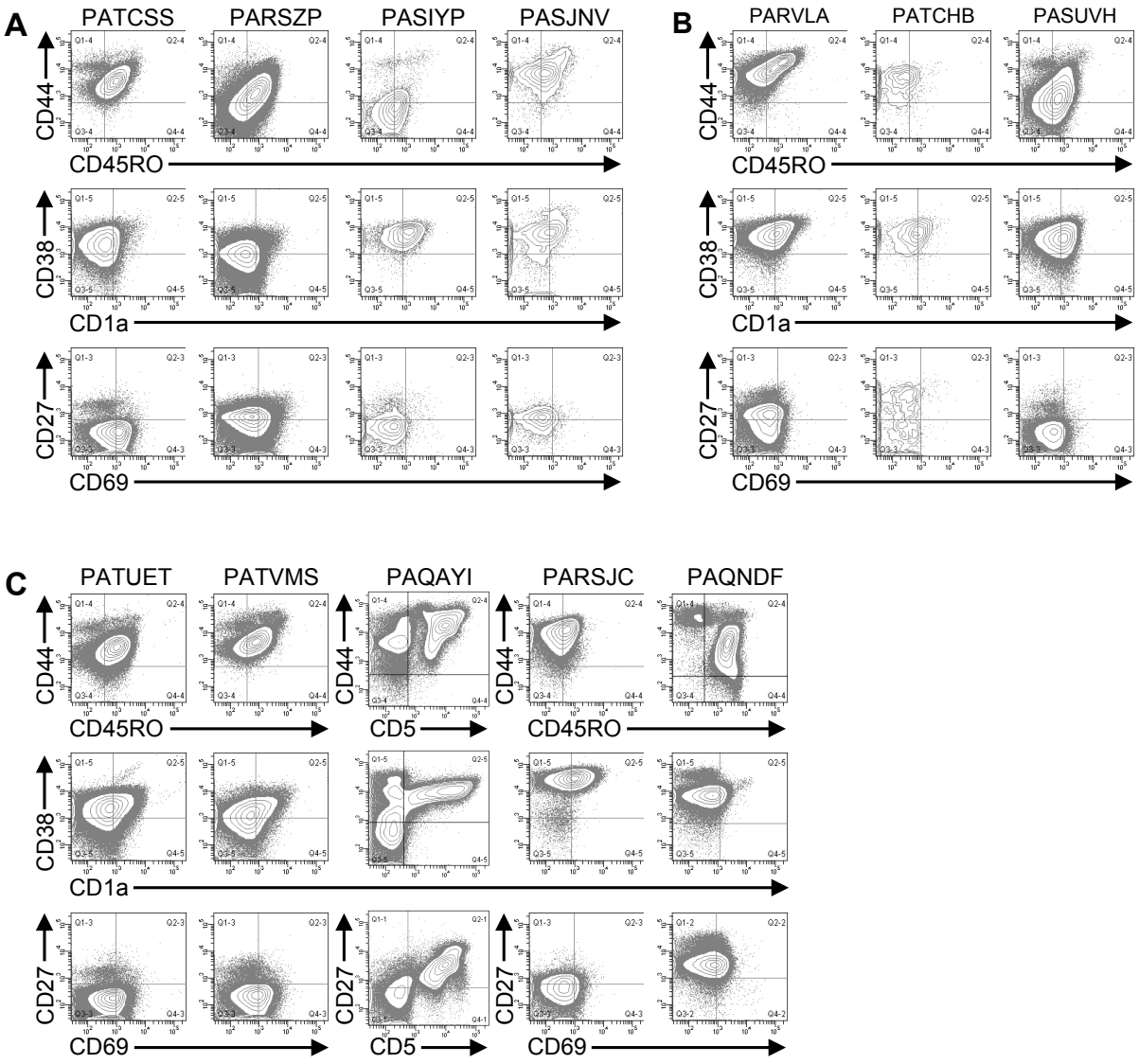
A
PATCSS
PARSZP
PASIYP
PASJNV
CD44
CD45RO
CD38
CD1a
CD27
CD69
B
PARVLA
PATCHB
PASUVH
CD44
CD45RO
CD38
CD1a
CD27
CD69
C
PATUET
PATVMS
PAQAYI
PARSJC
PAQNDF
CD44
CD45RO
CD5
CD38
CD1a
CD27
CD69

each of these three patients were primarily $CD38^{+}CD1a^{lo}CD69^{-}$ (Fig. 5-4B). Expression of CD44 and CD27 varied among these patients.

Cells from five patients were $CD3^{+}TCR\gamma\delta^{-}$ and primarily $CD8^{lo}CD4^{-}$ (Fig. 5-3C). Cells from two of these patients (PATVMS and PARSJC) could be subdivided into $CD34^{lo}$ and $CD34^{hi}$ subsets while cells from patient PAQNDF were uniformly $CD34^{lo}$. Cells from patients PATUET and PAQAYI were predominantly $CD34^{-}$. Most cells from these six patients expressed CD44, CD45RO, CD38, and CD1a (Fig. 5-4C). Cells from two patients expressed CD27 and three patients had low levels of CD69 expression.

In summary, the phenotyping data indicate that correlating the surface phenotype of the leukemic cells to normal thymocyte populations is rarely possible. In many cases, cells expressed combinations of markers that were inconsistent with any normal thymocyte populations. Further, none of the samples shared identical phenotypes.

mRNA levels of Ikaros family members vary among T-ALL cells

For each T-ALL sample, we determined the relative mRNA levels of each of the five Ikaros family members (Fig. 5-5A). Samples were grouped according to their expression of CD4, CD8 and TCRγδ and, where possible, the mRNA levels were compared to normal thymocytes within each phenotype. Of the seven T-ALL samples with a DN phenotype, Ikaros mRNA levels were elevated in five samples, Helios mRNA levels in four samples, Aiolos mRNA levels in five samples, and Pegasus mRNA levels in six samples, as compared to normal DN thymocytes. Two patients had low Ikaros mRNA levels, one had low Helios mRNA levels, one had low Aiolos mRNA levels, and six had low Eos mRNA levels.

Figure 5-5. Helios, Aiolos, and Eos mRNA levels correlate with each other but not surface phenotype in T-ALL. *A*) mRNA was isolated from each T-ALL sample and normal thymocytes and subjected to qRT-PCR. Relative mRNA levels for each Ikaros family member were calculated by normalizing each family member to the mRNA levels of GAPDH. Then, the relative mRNA levels were normalized to that of simultaneously run normal thymocytes. For T-ALL samples resembling normal DN, ISP, or DP thymocytes, the average of five normal thymocyte samples is shown by the solid line and the dashed line indicates the 95% confidence interval. *B*) For each patient, the relative mRNA levels of each Ikaros family member was compared pairwise using linear regression. The correlation coefficient (*R*) is shown for each pair. Statistical significance signifies whether the slope of the line is different than zero. (* $p < 0.05$, ** $p < 0.01$, *** $p < 0.001$). *C*) The fold change for the three pairs of Ikaros family members with the strongest correlations are shown. The line of best fit and 95% confidence intervals are shown for Helios, Aiolos, and Eos correlation. N.D. = not detected.

A

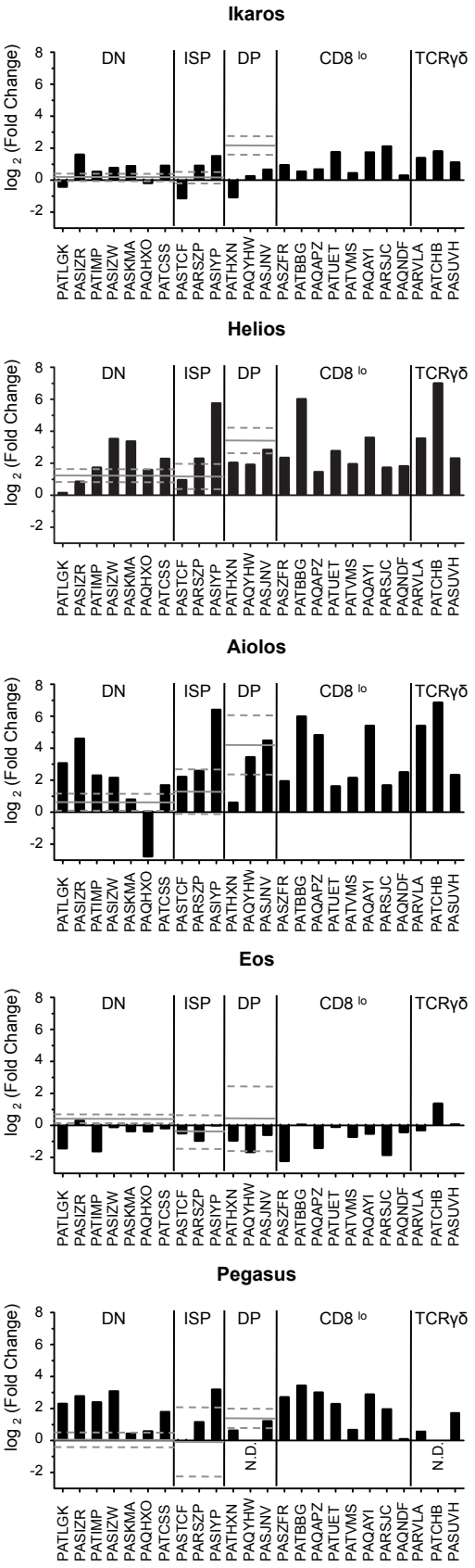

B

	Helios	Aiolos	Eos	Pegasus
Ikaros	0.34	0.42 *	0.37	0.31
Helios		0.90***	0.81***	0.61**
Aiolos			0.71***	0.61**
Eos				0.18
Pegasus				

C

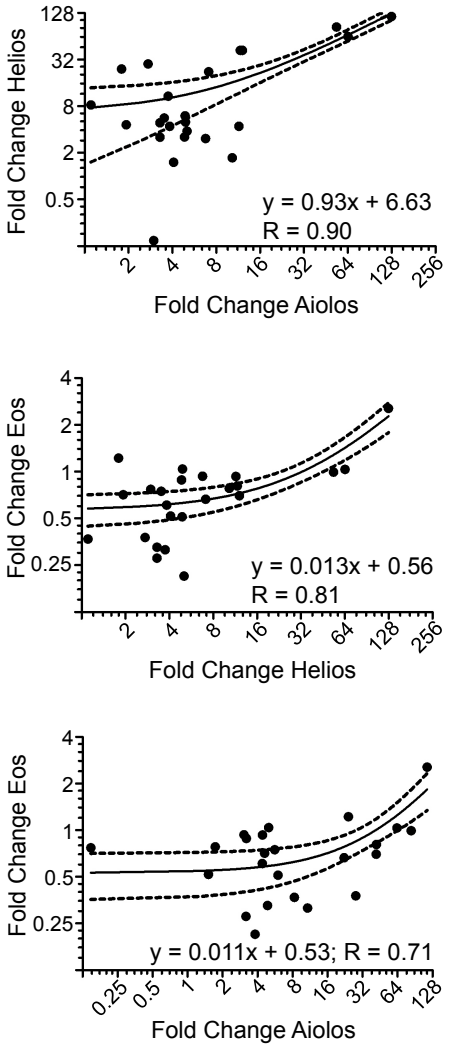

Among the three T-ALL samples with an ISP phenotype, one patient had elevated Ikaros, Helios, Aiolos, and Pegasus mRNA levels. One patient had elevated Ikaros and Helios mRNA levels. The third patient had low Ikaros mRNA levels. All three patients whose T-ALL cells were $CD4^+CD8^+$ had low Ikaros mRNA levels, as compared to normal DP thymocytes. Two of these patients had low Helios mRNA levels; one of these also had low Aiolos and Pegasus mRNA levels and the other had low Eos mRNA levels.

For patients whose cells were $CD8^{lo}$ or $TCR\gamma\delta^+$, we compared the expression of each Ikaros family member across the samples. Helios and Aiolos mRNA levels varied most dramatically in these patients; the samples that expressed the highest Helios and Aiolos mRNA levels had 47-fold and 38-fold more than samples with the lowest mRNA levels, respectively. By contrast, cells expressing the highest levels of Ikaros, Eos, and Pegasus had 3.5-fold, 12-fold, and 10-fold more mRNA, respectively, than cells expressing the lowest levels of these family members.

Next, we used linear regression to determine whether the mRNA levels of any Ikaros family member correlated with that of any other family member (Figs. 5-5B and 5-5C). There were strong correlations between the mRNA levels of Helios and Aiolos, Helios and Eos, and Aiolos and Eos. There were weak but statistically significant correlations between Helios and Pegasus and between Aiolos and Pegasus. Further, there was a very weak, but statistically significant correlation between Ikaros and Aiolos.

In conclusion, the mRNA levels of the Ikaros family members do not correlate with the surface phenotype of the T-ALL cells. However, the mRNA levels of Helios, Aiolos, and Eos correlated strongly with each other, suggesting that these genes are regulated similarly or these genes regulate each other.

The contribution of each Ikaros family member to the total Ikaros pool varies

Next, we calculated the percentage of total Ikaros family mRNA represented by each family member (Table 5-2 and Fig. 5-6). The majority (14/24) of T-ALL samples had a lower percentage of Ikaros family members represented by Ikaros than normal thymocytes. By contrast, Helios was overrepresented in 16/24 T-ALL samples, as compared to normal cells. Aiolos mRNA represented 1% or less of the total Ikaros mRNA in four T-ALL samples, but more than 20% of total Ikaros mRNA in three samples. Eos mRNA was underrepresented, as compared to normal thymocytes, in ten T-ALL samples. Pegasus represented less than 0.03% of total Ikaros mRNA in normal thymocytes, but more than 0.5% in four T-ALL samples and 2.1% in one case.

Next, we determined whether the T-ALL patients could be categorized based on the distribution of Ikaros mRNA levels. Because Ikaros and Helios accounted for most of the Ikaros family mRNA in nearly all T-ALL samples, we first calculated the ratio of Ikaros mRNA to Helios mRNA. Three groups of patients emerged, as shown in Table 5-2. Group I included samples in which the ratio of Ikaros to Helios mRNA levels was less than 0.5. Group II samples included those with an Ikaros to Helios ratio between 0.5 and 10. Group III included samples in which the Ikaros to Helios ratio exceeded 10. Group II could be subdivided into three subgroups based on the expression of Aiolos and Eos. Group IIA samples had minimal contribution from either Aiolos or Eos. Aiolos accounted for more than 10% of the total Ikaros mRNA in samples from Group IIB and Eos accounted for more than 20% of total Ikaros in samples in Group IIC.

The categorization of patients based on Ikaros family expression was independent of the surface phenotype of the cells. For example, most T-ALL groups included patients whose cells were $CD3^-$ and other patients whose cells were $CD3^+$.

Table 5-2. The contribution of each Ikaros family member to the total pool of Ikaros family mRNA.*

	Sample	Phenotype	Ikaros	Helios	Aiolos	Eos	Pegasus	Ik/Hel**
Normal thymocytes	DN2	$CD3^-CD4^-CD8^-$ $CD38^+CD1a^-$	80	9.8	3.5	6.5	0.03	8.2
	DN3	$CD3^-CD4^-CD8^-$ $CD38^+CD1a^+$	71	18	4.3	6.6	0.02	4
	ISP	$CD3^-CD4^+CD8^-$	72	17	7	3.8	0.02	4.2
	DP	$CD3^-CD4^+CD8^+$	67	19	12	1.6	0.01	3.4
Group I	PATCHB	$TCR\gamma\delta^+$ $CD4^-CD8^-$	12	65	14	8	N.D.	0.19
	PATBBG	$CD3^-CD4^-CD8^+$	13	69	13	4.4	0.39	0.18
	PASIYP	$CD3^+CD4^+CD8^+$	24	55	17	4.1	0.32	0.43
Group IIA	PATHXN	$CD3^-CD4^+CD8^+$	51	44	2.2	2.1	0.33	1.2
	PASIZW	$CD3^-CD4^-CD8^-$	52	44	2.6	0.95	0.33	1.2
	PASKMA	$CD3^-CD4^-CD8^-$	58	40	1	0.81	0.05	1.4
	PASZFR	$CD3^-CD4^-CD8^+$	64	24	4.4	6.1	2.1	2.7
	PATIMP	$CD3^-CD4^-CD8^-$	73	21	4.7	0.55	0.34	3.5
	PARSZP	$CD3^+CD4^+CD8^+$	74	20	3.4	2	0.21	3.6
	PATVMS	$CD3^+CD4^-CD8^+$	74	21	3.3	1.3	0.17	3.5
	PAQXHO	$CD3^-CD4^-CD8^-$	75	19	0.3	5	0.07	3.9
	PATCSS	$CD3^+CD4^-CD8^-$	77	20	1.8	1.4	0.28	3.8
	PATUET	$CD3^+CD4^-CD8^+$	81	16	1	0.87	0.23	4.9
Group IIB	PARVLA	$TCR\gamma\delta^+$ $CD4^+CD8^+$	40	26	23	11	0.23	1.6
	PAQYHW	$CD3^-CD4^+CD8^+$	44	20	34	2.3	N.D.	2.2
	PAQAPZ	$CD3^-CD4^-CD8^+$	56	12	24	6.6	1.2	4.7
	PASJNV	$CD3^+CD4^+CD8^+$	58	28	12	2.4	0.2	2.1
	PAQAYI	$CD3^+CD4^-CD8^+$	63	24	11	1.3	0.33	2.6
	PATLGK	$CD7^-CD3^-$ $CD4^-CD8^-$	71	13	15	1.1	0.58	5.5
	PAQNDF	$CD3^+CD4^{-/+}CD8^+$	71	15	12	2.8	0.01	4.8
Group IIC	PASTCF	$CD3^-CD4^+CD8^+$	39	21	9.6	30	0.35	1.9
	PASUVH	$TCR\gamma\delta^+$ $CD4^+CD8^-$	54	18	4.4	23	0.86	3.1
Group III	PASIZR	$CD3^-CD4^-CD8^-$	80	6	12	1.1	0.23	12
	PARSJC	$CD3^+CD4^-CD8^+$	91	7.3	0.95	0.58	0.19	13

*The $2^{-\Delta CT}$ for each family member was calculated based on the difference in the CT values for each Ikaros family member and GAPDH. The sum of the $2^{-\Delta CT}$ of the family was normalized to 100% for each sample.

**Ik/Hel is the relative mRNA levels of Ikaros divided by that of Helios.

Figure 5-6. A graphical representation of the proportion of Ikaros family mRNA represented by each family member. The percentage of total Ikaros family mRNA was calculated as described in Table 5-2. Each bar indicates 100% of the Ikaros family mRNA in each normal and T-ALL sample. Each segment within each bar indicates the portion of the total represented by each family member.

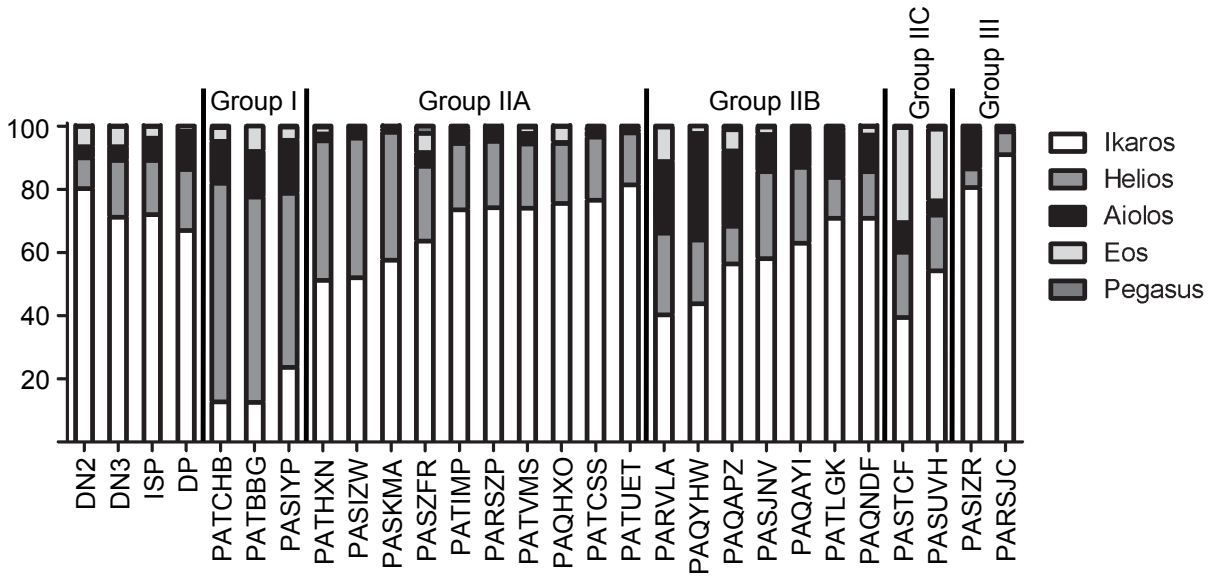
Group I
Group IIA
Group IIB
Group IIC
Group III
100
80
60
40
20
Ikaros
Helios
Aiolos
Eos
Pegasus
DN2
DN3
ISP
DP
PATCHB
PATBBG
PASIYP
PATHXN
PASIZW
PASKMA
PASZFR
PATIMP
PARSZP
PATVMS
PAQHXO
PATCSS
PATUET
PARVLA
PAQYHW
PAQAPZ
PASJNV
PAQAYI
PATLGK
PAQNDF
PASTCF
PASUVH
PASIZR
PARSJC

Protein levels and alternative splicing of Ikaros, Aiolos, and Helios in T-ALL

We used western blot analysis to examine Ikaros and Aiolos protein levels and splicing in cells from each T-ALL patient and in normal DN thymocytes (Fig. 5-7). Ikaros protein levels in one patient were similar to that of normal DN thymocytes, but the Ikaros levels were less than half of normal in the remaining samples. The patient with the highest Ikaros protein levels, PAQNDF, had lower Ikaros mRNA levels than 18 of the other 23 samples. Similarly, most T-ALL samples expressed less full-length Aiolos protein than normal DN thymocytes.

Low molecular weight bands were detected when membranes were probed with anti-Ikaros and anti-Aiolos, suggestive of the presence of alternative splice variants. We performed nested PCR using the primer pairs illustrated in Fig. 5-8A to determine whether Ikaros, Helios, and Aiolos might undergo alternative splicing in normal thymocytes and T-ALL cells. A complex pattern of Ikaros splice variants was detected in normal and leukemic cells, consistent with our previous observations (354) and that different isoforms can lack exons, lack portions of exons, or include intronic sequences (8-10). In contrast to Ikaros, few T-ALL samples expressed multiple splice variants of Aiolos and Helios.

To verify the identity of the splice variants, nested RT-PCR was performed using primers that span each combination of exons (a sample of which is shown in Fig. 5-8E). For Ikaros, the most abundant proteins detected by western blot are most likely full-length Ikaros and Ikaros lacking exon 3 (Ik-Δ3). In addition, numerous other splice variants were detected at the mRNA level; the most prevalent of which are shown in Fig. 5-8B.

For Aiolos, full-length mRNA was detected in most samples (Fig. 5-8C). Other splice variants detected lacked exon 2 (Ai-Δ2), exon 3 (Ai-Δ3), or exon 4 (Ai-Δ4) or a combination of two or more exon deletions, such as Ai-Δ5/6 and Ai-Δ4/5/6. Helios lacking a portion of exon 3

Figure 5-7. Most T-ALL samples express low levels of Ikaros and Aiolos protein. Cell lysates were separated by SDS-PAGE, transferred to nitrocellulose, and probed with anti-Ikaros, anti-Aiolos, or p38 MAPK. *A*) Bands corresponding to full-length Ikaros and Aiolos along with major splice variants are shown. *B*) Densitometry was performed using the images shown in '*A*' and the relative protein levels of full-length Ikaros and Aiolos protein was normalized to that of the p38 MAPK loading control and then to normal DN thymocytes.

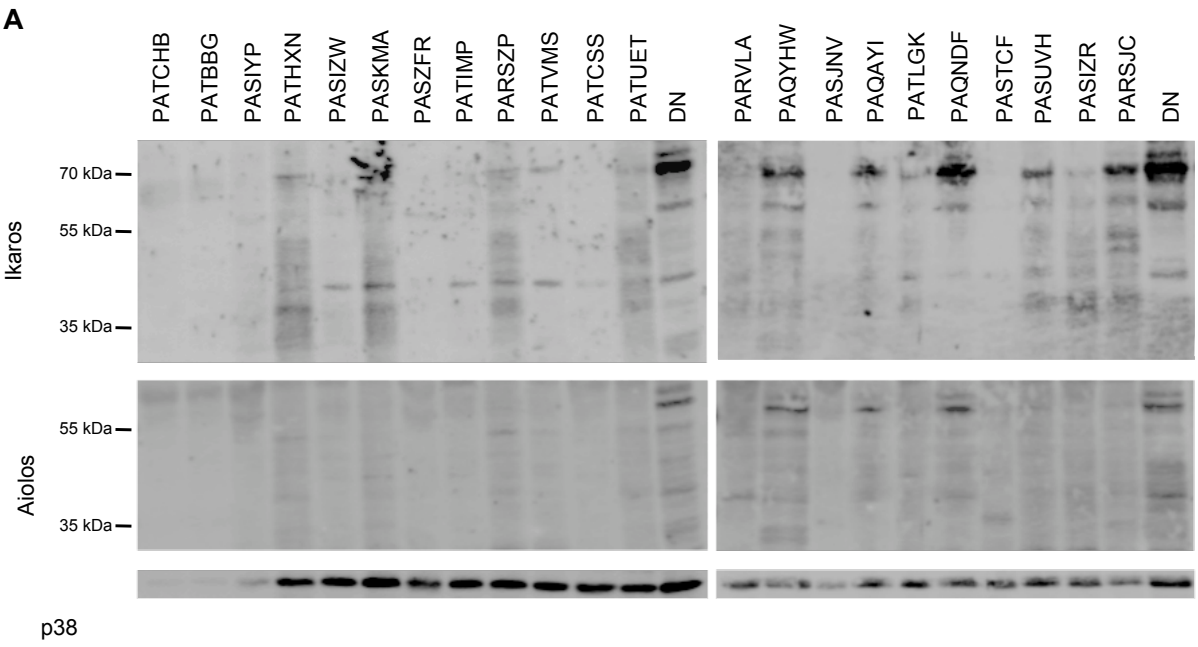
A
PATCHB
PATBBG
PASIYP
PATHXN
PASIZW
PASKMA
PASZFR
PATIMP
PARSZP
PATVMS
PATCSS
PATUET
DN
PARVLA
PAQYHW
PASJNV
PAQAYI
PATLGK
PAQNDF
PASTCF
PASUVH
PASIZR
PARSJC
DN
Ikaros
70 kDa
55 kDa
35 kDa
Aiolos
55 kDa
35 kDa
p38

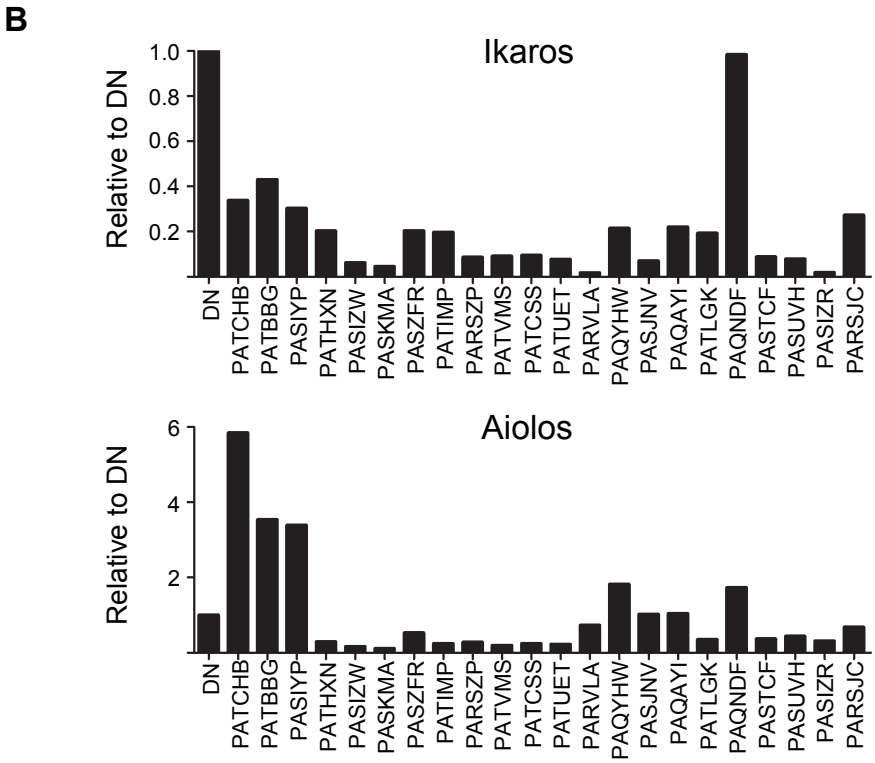
B
Ikaros
Relative to DN
1.0
0.8
0.6
0.4
0.2
DN
PATCHB
PATBBG
PASIYP
PATHXN
PASIZW
PASKMA
PASZFR
PATIMP
PARSZP
PATVMS
PATCSS
PATUET
PARVLA
PAQYHW
PASJNV
PAQAYI
PATLGK
PAQNDF
PASTCF
PASUVH
PASIZR
PARSJC
Aiolos
Relative to DN
6
4
2
DN
PATCHB
PATBBG
PASIYP
PATHXN
PASIZW
PASKMA
PASZFR
PATIMP
PARSZP
PATVMS
PATCSS
PATUET
PARVLA
PAQYHW
PASJNV
PAQAYI
PATLGK
PAQNDF
PASTCF
PASUVH
PASIZR
PARSJC

Figure 5-8. Ikaros mRNA undergoes extensive alternative splicing in normal thymocytes and in T-ALL. *A*) A schematic of the exon structure of Ikaros, Aiolos, and Helios with the position of the nested PCR primers shown. Nested PCR was performed using mRNA isolated from the indicated normal thymocyte populations and each T-ALL sample for Ikaros *(B*), Aiolos (*C*), and Helios (*D*). *E*) mRNA obtained from cells from one sample shown in *(B*) was amplified with each possible pair of Ikaros nested PCR primers found in Table 5-1.

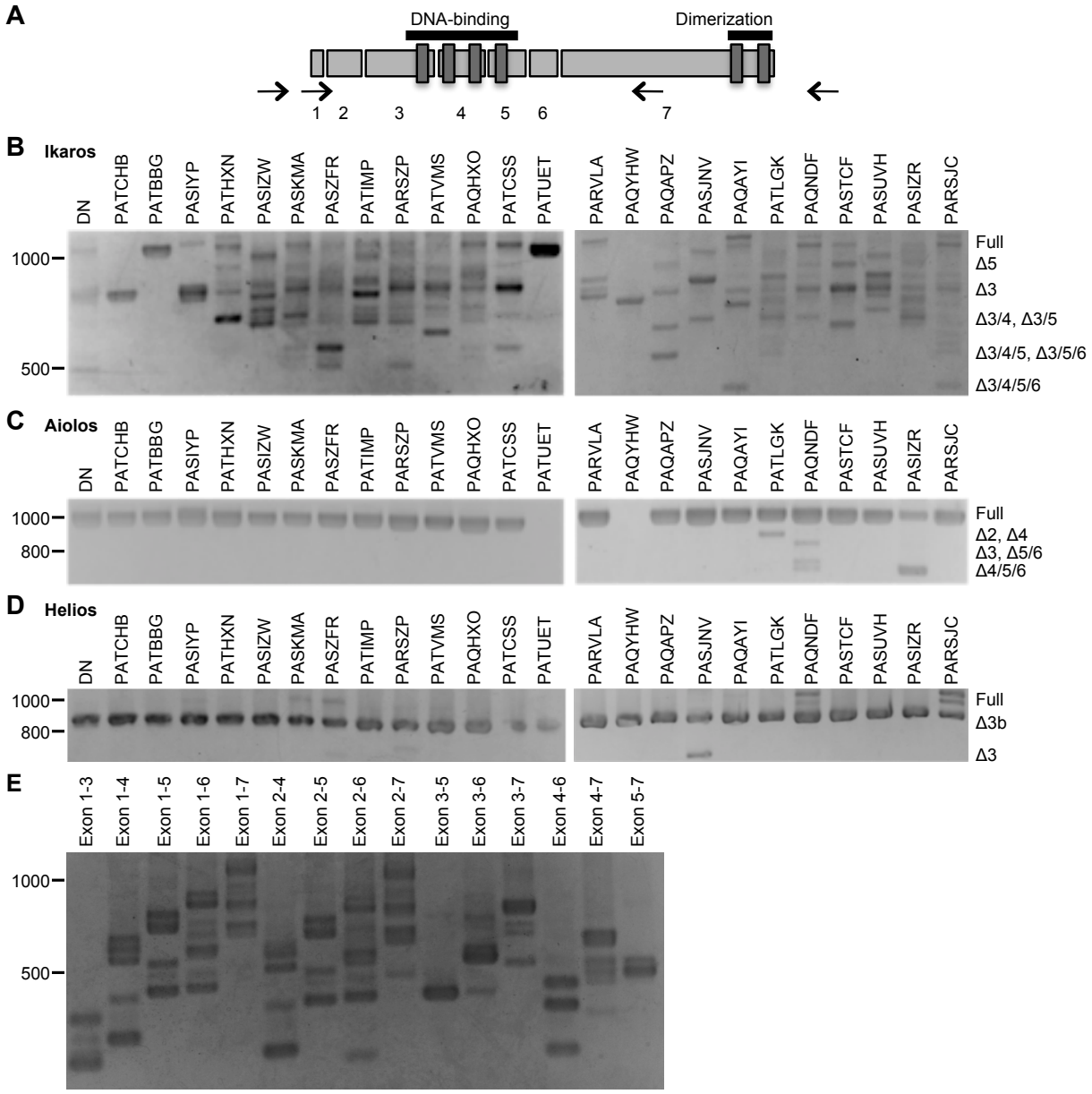
A
DNA-binding
Dimerization
1 2 3 4 5 6 7
B Ikaros
DN PATCHB PATBBG PASIYP PATHXN PASIZW PASKMA PASZFR PATIMP PARSZP PATVMS PAQHXO PATCSS PATUET PARVLA PAQYHW PAQAPZ PASJNV PAQAYI PATLGK PAQNDF PASTCF PASUVH PASIZR PARSJC
1000
500
Full
Δ5
Δ3
Δ3/4, Δ3/5
Δ3/4/5, Δ3/5/6
Δ3/4/5/6
C Aiolos
DN PATCHB PATBBG PASIYP PATHXN PASIZW PASKMA PASZFR PATIMP PARSZP PATVMS PAQHXO PATCSS PATUET PARVLA PAQYHW PAQAPZ PASJNV PAQAYI PATLGK PAQNDF PASTCF PASUVH PASIZR PARSJC
1000
800
Full
Δ2, Δ4
Δ3, Δ5/6
Δ4/5/6
D Helios
DN PATCHB PATBBG PASIYP PATHXN PASIZW PASKMA PASZFR PATIMP PARSZP PATVMS PAQHXO PATCSS PATUET PARVLA PAQYHW PAQAPZ PASJNV PAQAYI PATLGK PAQNDF PASTCF PASUVH PASIZR PARSJC
1000
800
Full
Δ3b
Δ3
E
Exon 1-3 Exon 1-4 Exon 1-5 Exon 1-6 Exon 1-7 Exon 2-4 Exon 2-5 Exon 2-6 Exon 2-7 Exon 3-5 Exon 3-6 Exon 3-7 Exon 4-6 Exon 4-7 Exon 5-7
1000
500

(Hel-Δ3b) was the most evident splice variant observed (Fig. 5-8D), but some samples expressed full-length Helios and Helios lacking the entire third exon (Hel-Δ3).

Based on these data, we conclude that the mRNA and protein levels of Ikaros and Aiolos do not directly correlate, which is consistent with our previous observations in normal human thymocytes (354). Further, many splice variants are not translated at detectable levels. For most splice variants detected, the isoforms also exist in normal thymocytes.

Discussion

The multi-parameter phenotypic analysis of cells from pediatric T-ALL patients revealed great heterogeneity among patients. Even when analyzing a limited number of markers, leukemic cells resembled normal human thymocyte populations in only nine of the 24 samples studied. For the majority of the samples, the phenotype deviated significantly from that of known normal human thymocyte populations. For example, cells from some T-ALL patients were $CD8^{lo}$ with little or no CD4 expression. The $CD3^{-}CD4^{-}CD8^{lo}$ T-ALL cells are similar to the ISP population observed during murine T cell development and a population of human thymocytes found in a fraction of patients (Fig. 3-1) (376). The $CD3^{+}CD8^{lo}$ leukemia cells expressed lower levels of CD8 than mature SP $CD8^{+}$ thymocytes and they did not express CD69 or CD27, making it unlikely that these are mature thymocytes. Among the T-ALL samples were those in which the cells expressed markers representing conflicting stages of development. For example, some cells co-expressed CD3 and CD34; in normal thymocytes, CD34 expression is terminated prior to CD3 expression.

Collectively, our data indicate that correlating T-ALL cells to normal developmental stages is rarely possible. In addition, each T-ALL sample had a unique phenotype. These two features make classifying T-ALL patients a challenging endeavor, as seen by the difficulty in using phenotype as a prognostic indicator (82, 83, 394).

As an alternate method to classify T-ALL patients, we focused on the Ikaros family of transcription factors, which was previously implicated in leukemogenesis. ChIP-seq data showed that the Ikaros family can bind 4,500-7,120 sites in the genome and regulate several hundred genes (27, 43, 54), making these transcription factors key regulators of cell fate decisions in developing lymphocytes. The importance of the Ikaros family in leukemogenesis

has been most clearly demonstrated in mice, where expression of dominant negative isoforms of Ikaros or Helios resulted in T cell malignancies (47-49). Disease onset in these mice was dependent on the reduced functionality of the entire Ikaros family, as deletion of individual family members did not cause disease (50-52). This observation highlights the importance of studying the entire family. In humans, correlative studies have suggested the presence of dominant negative isoforms of Ikaros in T-ALL patients, but the percentage of patients harboring these splice variants is controversial (8-10, 85, 90, 91, 100, 105). Our data indicate that alternative mRNA splicing of Ikaros is common in normal thymocytes and T-ALL cells, but not all splice variants are translated into protein products (Figs. 5-7 and 5-8).

The mRNA levels of each Ikaros family member varied widely across T-ALL samples, but the greatest disparity was in Aiolos and Helios expression (Fig. 5-5A). The samples with the highest Aiolos and Helios mRNA levels were 780-fold and 120-fold greater, respectively, than the samples with the lowest mRNA levels. This level of variability is in contrast to the 18-fold and 10-fold changes in Aiolos and Helios mRNA levels, respectively, that normally occur as thymocytes progress from the DN to the DP stages. By contrast, samples with the highest mRNA levels of Ikaros, Eos, and Pegasus only contained 8.6- to 11-fold more than the samples with the lowest levels.

Based on these data, we propose the classification of T-ALL patients using the strategy shown in Fig. 5-6 and Table 5-2. For most patients, Ikaros and Helios mRNA were the primary Ikaros family member transcripts detected, so the ratio of Ikaros mRNA levels to Helios mRNA levels was used to divide the samples into three groups. The largest group of patients had Ikaros to Helios ratios similar to those of normal thymocytes. Within this group, the mRNA levels of Aiolos and Eos varied in a manner that provided a means to subdivide these patients.

The importance of Ikaros family mRNA levels in leukemogenesis may arise from the function of the Ikaros family proteins. Because of the limited number of cells we could obtain from the patients, we were only able to analyze Ikaros and Aiolos protein levels. For both proteins, the protein levels did not correlate with mRNA levels and the protein levels were lower than in normal thymocytes for most patients (Figs. 5-5 and 5-7). The reduction of Ikaros family proteins may be linked to leukemogenesis, as it is in mice (47-51, 55, 395).

In addition to a general reduction of Ikaros family expression, the ratio of Ikaros to Aiolos protein varied across the T-ALL samples, suggesting the dimer composition may vary among patients. For example, patient PATCHB had high Aiolos levels and low Ikaros levels whereas patient PAQNDF had the opposite pattern. Even small changes in the ratio among Ikaros family members can have profound biological effects, as seen by the development of lymphoma when Helios was expressed at low levels in murine B cells (55).

While Ikaros family protein levels have direct implications in leukemogenesis, the mechanisms that control Ikaros family transcription might control other genes that regulate the development of T-ALL. For example, c-myc, IRF4, Runx1, and TAL-1 can regulate Ikaros expression and are activated in some T-ALL patients (76, 352, 396-403). In addition, there are Ikaros binding sites within the promoters of Ikaros, Aiolos, Eos, and Pegasus (75, 76) and the correlations in the expression of some Ikaros family members we observed (Fig. 5-5) supports a model in which Ikaros family members may regulate the transcription of themselves and other family members. Further, the Ikaros binding site is shared by all family members and by the Notch-dependent transcription factor RBP-Jκ (44, 59, 60, 404). Because half of pediatric T-ALL patients have an activating mutation in Notch (405), it would be expected that Ikaros family mRNA levels would be altered in these patients.

In summary, we used multi-parameter flow cytometry to demonstrate the tremendous variability among pediatric T-ALL samples. Further, we performed the first comprehensive analysis of the expression of the entire Ikaros family of transcription factors reported in pediatric T-ALL. More research is needed to extend these observations and determine whether the patterns of Ikaros mRNA or protein levels correlate to clinical outcomes.

Chapter 6. Conclusions

These studies present the most comprehensive characterization of subpopulations of human thymocytes and Ikaros family expression during human T cell development. In Chapter II, we quantified mRNA and protein expression of Ikaros family members in murine and human thymocytes. These results highlighted differences in expression between the species, which has implications for the different developmental pathways seen between murine and human thymocytes. In Chapters III-IV, we used multi-parameter flow cytometry to identify subpopulations of human thymocytes, focusing on those populations that were undergoing the key αβT cell selection steps of β-selection, positive selection, and CD4/CD8 lineage commitment. Analysis of Ikaros, Helios, and Aiolos protein levels in these subpopulations showed that these family members have differential expression at the time of selection and in the ensuing populations. Finally, in Chapter V we compared surface marker and Ikaros family expression in cases of pediatric T-ALL to normal thymic populations. T-ALLs showed extensive diversity in protein expression that did not correspond to that seen in normal thymic populations. However, we were able to identify groups of T-ALL patients by the ratio of Ikaros family mRNA levels within the leukemic cells. Further studies are needed to determine how the changes in Ikaros family members during development affect gene expression, cell survival, proliferation, and potential development of T-ALL.

Stages of Human T cell Development

β-selection has been proposed to occur as early as the DN3 stage and as late as the DP stage of human T cell development (109, 115-117, 119). Studies looking at TCRβ protein expression focused on analysis of a single stage of development, either TSP or DP, but not both stages

within the same thymus. We showed that within a single thymus, β-selection occurs in ISP thymocytes but there is also a population of unselected DP1 thymocytes (Figs. 3-2 and 3-3). Further studies will be necessary to determine if these DP1 cells are still in the process of rearranging their *TCRB* loci and capable of successfully undergoing β-selection to differentiate to the DP2 stage. It is intriguing to hypothesize that cells in the DP1 stage have undergone extensive rearrangements of both *TCRB* loci without successful TCRβ production, and are thus likely to die due to unsuccessful TCRβ production. As TCRγδ cells differentiate into DP cells in the human thymus (151), these $CD3^-$ DP1 cells could also be TCRγδ precursor cells. However, since complete *TCRB* rearrangements are rare in TCRγδ cells, and the expression of surface markers and Ikaros family members in DP1 cells are similar to ISP1 cells (Figs. 3-2 to 3-5), we propose that these cells are differentiating along the αβT cell lineage pathway.

Through analysis of CD69, CD28, and CD27 expression, we showed that positive selection is initiated in DP9 cells, the last subpopulation of $CD3^{lo}$ DP thymocytes. It has been established that after positive selection, murine thymocytes stop transcription of CD8 and transition through a TSP $CD4^+$ population (312-315, 317-320), but a corresponding population of human thymocytes had not yet been described. We show that in human thymocytes, DP9 cells have lower CD4 expression than earlier DP populations, and CD4 expression continues to decline as cells move to a $CD3^{lo}$ $CD4^{lo/-}CD8^+$ TSP population. TSP $CD8^+$ cells are the most mature $CD3^{lo}$ thymocytes, with 77±3.8% of TSP2 cells having completed positive selection as measured by CD69 expression (Fig. 3-3). Further studies are needed to determine if TSP $CD8^+$ have similar properties as murine TSP $CD4^+$, such as termination of CD4 transcription and potential to differentiate into both MSP $CD8^+$ and MSP $CD4^+$ cells.

Differences in the kinetics of CD28 and CD27 expression after positive selection give new insights into the timing of CD4/CD8 lineage commitment in the human thymus. We propose that CD27 expression is a marker of lineage commitment in human thymocytes. *Vanhecke*, *et al.* previously showed that $CD27^+$ MSP $CD4^+$ and MSP $CD8^+$ cells are lineage committed, whereas $CD27^-$ MSP $CD4^+$ cells retained some potential to differentiate into $CD8^+$ cells in a human-mouse fetal thymic organ culture system (386). CD28 expression is induced by positive selection of human thymocytes, and is up-regulated after CD69 is expressed (Fig. 4-3B). In DP9 and TSP cells, CD28 and CD27 expression appear to be simultaneous (Fig. 4-3C). In contrast, whereas all DP10, MSP1 $CD4^+$ and MSP2 $CD4^+$ cells express CD28, CD27 expression is minimal or absent on these cells (Fig. 4-4C). These data suggest that while CD28 expression is a consequence of positive selection signaling, another signal is necessary for CD27 expression.

According to the signal instruction model of lineage commitment, the down-regulation of CD4 in human DP9 and TSP cells would disrupt the TCR signal for MHC-II restricted cells, but allow for extended signaling in MHC-I restricted cells. This would explain why some TSP $CD8^+$ cells express CD28 and CD27 at the same time: they are MHC-I restricted cells undergoing lineage commitment immediately after positive selection. In contrast, MHC-II restricted cells do not receive a lineage commitment signal until after CD4 has been re-expressed on the surface. Thus, DP10 and $CD4^+$ MSP1 cells have up-regulated CD28 expression, but have not received proper lineage commitment signals for CD27 expression. Our results suggest that CD8 lineage commitment occurs in the TSP population, prior to CD3 up-regulation, but CD4 lineage commitment does not occur until after CD3 up-regulation and differentiation to the $CD4^+$ MSP2 stage.

Expression of Ikaros Family Members During Key Selection Steps in Human αβT Cell Development

Ikaros family expression remains constant at human γδT cell lineage commitment

Sequencing of the β gene locus in human γδ T cells suggests that commitment to the γδ lineage happens before complete β gene rearrangement occurs in the ISP stage (109, 116, 162). Similarly, commitment to the γδ lineage is accomplished in murine thymocytes by the end of the DN3 stage, when complete β gene rearrangement occurs in this species (154, 406, 407). Though γδ lineage commitment occurs with similar timing relative to β rearrangement in both species, Notch signaling has differential affects on the selection of the αβ versus γδ lineage between the two species. Notch signaling is necessary for differentiation along the αβ lineage in murine thymocytes, whereas strong Notch signals induce human thymocytes to develop along the γδ lineage (112, 114, 130, 144, 164, 347, 408, 409).

Differences in the response to Notch signaling between the species may be due to regulation of Notch target genes by Ikaros family members. Ikaros, Aiolos, Helios, and Eos are all capable of competing with the Notch transcriptional regulator RBP-Jκ for binding at DNA with the shared consensus sequence GGGAA (14, 43, 44, 60, 77). Though the Ikaros family members bind similar DNA sequences, their differential expression can affect what genes are targeted and the levels of transcription (1, 2, 5, 6, 14, 15, 27, 54, 55). Thus differences in Ikaros family expression between murine and human thymocytes may result in altered targeting to and competitive binding to Notch target genes.

Analysis of early human thymocytes revealed that expression of Ikaros, Helios, and Aiolos proteins does not change prior to β-selection in the ISP stage (Figs. 2-5 and 3-5). However, Helios levels decrease in murine thymocytes at the early DN3 stage (Fig. 2-2). Thus, there is a

smaller proportion of Helios containing dimers in murine thymocytes at the γδ lineage commitment stage than in earlier stages. Overexpression of Helios in murine hematopoietic progenitor cells leads to a significant increase in the number of γδ T cells produced by these cells in reconstituted mice (48), suggesting that the decreased Helios levels in murine thymocytes are important for suppression of the γδ lineage fate. These data suggest that the differential changes in Helios expression in early murine and human thymocytes are regulating the affects of Notch signaling on the γδ lineage decision. Further studies are needed to determine the specific Notch target genes and Ikaros family dimers that are necessary for regulating γδ lineage commitment in murine and human thymocytes.

Ikaros, Helios, and Aiolos levels increase after β-selection

We identified changes in Ikaros, Helios, and Aiolos levels that correspond to β-selection. We used CD1a, CD28, and CD44 expression to identify β-selected thymocytes within the ISP and $CD7^{++}CD45RO^{-}$ $CD3^{-}$ DP populations, showing that cellular proliferation increased with β-selection of human thymocytes (Figs. 3-2 to 3-4). Expression of all three Ikaros family members is higher in β-selected ISP2 and DP2 cells than in pre-β-selection ISP1 and DP1 cells (Fig. 3-5). There is a larger increase in Helios protein expression after β-selection relative to that of Ikaros and Aiolos, suggesting that dimer formation in the cells will differ from pre-selection cells. Further, in the most mature $CD3^{-}$ DP populations, Ikaros and Helios protein levels decline while Aiolos protein levels remain elevated. These data suggest that the dimer make-up will change as thymocyte progress through β-selection, with more Helios containing dimers present in ISP2, DP2, and DP3 cells, and more Aiolos containing dimers present in the DP4 and DP5 cells. Changes in dimer make-up within these populations will likely affect which target

sites are bound and the strength of transcriptional activation or repression (2, 5, 27, 55). The overall increase in Ikaros family proteins levels may also affect whether dimers recruit the suppressive NuRD complex or the elongation-competent NuRD/P-TEFb complex (40).

Interestingly, Aiolos and Helios protein levels also increase in DN4 murine thymocytes, after β-selection (Fig. 2-5). Whereas Ikaros levels in murine DN4 cells were 1.6-fold higher than DN3 cells, Helios levels increased 5.3-fold and Aiolos levels increased 5.0-fold in DN4 thymocytes. The increase in Helios protein was transient, with levels declining in the ISP and DP stages, but Aiolos protein expression continued to increase through the DP stage. The sustained increase in Aiolos levels in post-β-selected murine and human thymocytes may regulate CD8 expression, and be responsible for the difference in co-receptor expression at the ISP stage in human and murine thymocytes.

Murine DN thymocytes up-regulate CD8 to become ISP $CD8^+$ cells, whereas human DN thymocytes express CD4 to become $CD4^+$ ISP cells (110, 111). In murine thymocytes, Ikaros is associated with both the CD4 and CD8α loci throughout T cell development (65, 66, 346), but the NuRD complex transitions from being associated with the CD8α locus in the DN stage to being associated with the CD4 locus in the DP stage (65, 66, 345). Aiolos protein levels increase just prior to CD8 expression in both murine and human thymocytes (Figs. 2-2 and 3-5), and may be responsible for drawing NuRD away from the CD8 locus to allow transcription. In support of this, loss of Aiolos in $Ikaros^{+/-}$ murine thymocytes leads to an inability to properly up-regulate CD8 expression (346). Further, Aiolos is capable of recruiting NuRD to the CD4 locus (27), and the high levels of Aiolos in murine ISP thymocytes may result in recruitment of the PTEF-b/NuRD complex to the CD4 locus to promote transcriptional elongation. Further studies are

needed to determine what NuRD and Ikaros family complexes are associated with the CD4 and CD8 loci in different stages of human thymic development.

Ikaros is up-regulated after positive selection

A role for the Ikaros family in regulating positive selection has been suggested by experiments in transgenic mice. Both Ikaros null mice and mice expressing a dominant negative Ikaros isoform had an accumulation of TSP $CD4^+$ cells, which underwent increased proliferation and apoptosis (380, 381). Ikaros is the only family member whose protein levels increased in DP9 cells when CD69 is first expressed, and the levels slowly increased in subsequent stages where a higher percentage of cells had undergone positive selection (Fig. 4-6).

The timing of the Ikaros peak in the TSP populations is intriguing, as it may have implications on the strength of signal necessary for productive CD8 lineage commitment. Ikaros has been shown to regulate TCR signaling thresholds in murine thymocytes and splenocytes (367, 383). The increased Ikaros protein levels in positively selected cells may serve to ensure that only stronger TCR signaling events induce lineage commitment at the TSP stage.

Aiolos protein levels increase after CD8 and CD4 lineage commitment

CD27 expression is associated with commitment to the CD8 and CD4 lineage in human thymocytes (386). CD27 expression is up-regulated on a portion of TSP $CD8^+$ thymocytes but not on DP10 and MSP1 $CD4^+$ cells, suggesting that CD8 lineage commitment occurs at the TSP stage but commitment to the CD4 lineage does not occur until CD27 is expressed in MSP2 $CD4^+$ thymocytes. In contrast to Ikaros, Aiolos protein levels did not increase in CD3 expressing cells until CD8 lineage commitment occurs in the TSP population (Fig. 4-6). Consistent with Aiolos

expression being associated with lineage commitment, protein levels were not elevated in DP10 and MSP1 $CD4^+$ cells, but increased in MSP2 $CD4^+$ thymocytes. Aiolos levels were highest in the phenotypically similar MSP3-4 $CD4^+$ and MSP1-2 $CD8^+$ populations. These data suggest that Aiolos is up-regulated coincident with CD27 expression in response to lineage commitment signals in human thymocytes, and is supported by initial data from a single thymus (data not shown). Further analysis of Aiolos protein levels in $CD27^-$ and $CD27^+$ TSP and MSP2 $CD4^+$ cells is necessary to confirm a correlation between Aiolos and CD27 expression. Aiolos may play multiple roles during CD4/CD8 lineage commitment, including regulation of TCR signal strength, survival, and proliferation (26, 51, 384, 385). Also, if increased Aiolos expression is required for CD8 expression as we propose, then increased Aiolos levels in lineage committed TSP cells could maintain CD8 expression and prevent diversion back to SP $CD4^+$ cells (65, 66, 346).

Helios is up-regulated in cells potentially undergoing negative selection and T_{reg} development

Strongly reactive TCR transgenic $CD4^+$ murine thymocytes up-regulate Helios expression in response to negatively selecting ligands (410). Helios expression is also elevated in T_{reg} cells, which are produced in the thymus when cells with strongly reactive TCRs are not negatively selected (74, 379). In contrast, positively selecting ligands induce down-regulation of Helios protein expression from the DP to the SP stage of murine development (410). Identifying human thymocytes with strongly reactive TCRs is complicated by the fact that Helios expression can be induced by TCR signaling, as seen in activation of peripheral T cells (411) and thymic β-selection (Fig. 3-5).

Within human thymocyte populations, Helios levels show a general decline after β-selection, as seen in the positively selected murine thymocytes (Fig. 4-6) (410). However, there is a transient increase in Helios expression in the TSP populations. Whereas it appears that all of the TSP cells have some increase in Helios expression, a population of Helios^{hi} cells also develops and is particularly notable in the TSP2 and the MSP1 CD8^{+} populations (Fig. 4-6A and B). These Helios^{hi} cells may be strongly reactive thymocytes that are in the process of negative selection, as they express the highest Helios levels of any thymocytes.

A population of cells with increased Helios expression also develops in the MSP3 CD4^{+} stage of human development (Fig. 4-6B). These cells have slightly lower Helios levels than the Helios^{hi} TSP cells, and almost half of the population also expresses FoxP3, suggesting they are thymic derived T_{reg} cells (Fig. 4-6D). The presence of Helios^{+}FoxP3^{-} cells in this population has two implications. These cells could be precursors to the Helios^{+}FoxP3^{+} T_{reg} cells, suggesting that Helios levels increase prior to FoxP3 levels in the process of T_{reg} development. Alternatively, the Helios^{+}FoxP3^{-} cells could be strongly reactive CD4^{+} SP cells that have not received signals necessary for T_{reg} development and are undergoing negative selection.

Pediatric T-ALL Cells Can Be Grouped by the Ratio of Ikaros Family Members

The ineffectiveness of current treatments for a portion of patients suggests that not all T-ALL cells are the same, and phenotypic markers are needed to categorize T-ALL patients for proper treatment strategies. T-ALL patients are most commonly categorized according to their expression of CD4, CD8, and components of the TCR complex (78, 80). Through multi-parameter flow cytometry we looked at expression of the surface markers we used for identifying subpopulations of human thymocytes (Figs. 5-1 to 5-4). Our original intent was to use

expression of surface markers on T-ALL cells to identify the corresponding thymic subpopulation from which they were derived, but analysis revealed extensive heterogeneity among T-ALL samples that precluded our ability to accomplish this.

Surprisingly, there was also a great deal of heterogeneity in the expression of Ikaros family members in the T-ALL samples compared to one another and normal thymic populations. Each T-ALL sample had mRNA levels of at least one Ikaros family member that fell outside the 95% confidence interval for those of normal thymic populations (Fig. 5-5). Changes in Ikaros family dimer make-up can lead to altered DNA binding, recruitment of repressive or activating chromatin remodeling complexes, and gene activation (2, 5, 27, 55). During normal human thymocyte development, Ikaros is the predominant mRNA species of the family, being expressed at 3.9-fold or higher levels than the other family members (Fig. 2-1). However, we found that in one third of the T-ALL patients, either Helios, Aiolos, or Eos mRNA levels were at least fifty percent of Ikaros levels, and in three of these cases Helios mRNA levels were higher than those of Ikaros (Fig. 5-5). Through analysis of the ratio of the mRNA levels of Ikaros family members to one another, we were able to identify groups of T-ALL patients. (Table 5-1 and Fig. 5-6). These groupings could have implications for direct involvement of Ikaros family members, as well as for altered function of other proteins that regulate transcription of Ikaros family members. In particular, c-myc, IRF4, Runx1, and TAL-1 can be activated in some T-ALL patients and also regulate expression of some Ikaros family members (76, 352, 396-403). Unfortunately, outcomes data were not available for the T-ALL samples analyzed, so correlations between our groupings and disease progression could not be made.

Although mRNA levels of at least one Ikaros family member were often elevated in the analyzed T-ALL samples, Ikaros and Aiolos protein levels were lower than normal thymic

populations (Fig. 5-7). Though we did not identify dominant negative isoforms of Ikaros or Aiolos proteins in the T-ALL patients, the low levels of both Ikaros and Aiolos may sufficiently alter Ikaros family function to contribute to the development of T-ALL. Alternatively, if Helios protein levels mirror mRNA levels in T-ALL cells, then there will be a large pool of Helios homodimers that can have profound impact on activation or repression of Ikaros family target genes. Unfortunately, insufficient sample size precluded analysis of Helios protein levels in the T-ALL patients, so these need to be determined in future studies.

Our analysis of mRNA and protein levels in murine and human DP thymocytes suggests that different mechanisms control Ikaros and Aiolos protein levels in the two species, and this may explain the low protein levels in T-ALL cells. As was expected, protein expression of Ikaros family members mirrored increases in mRNA levels in murine DP thymocytes (Figs. 2-1 and 2-2). However, despite a 4.4-fold increase in Ikaros mRNA levels and a 18-fold increase in Aiolos mRNA levels, no increase in protein was seen in total human DP thymocytes by Western blot analysis (Figs. 2-4 and 2-5). There was no increase in Ikaros protein and only a 1.9-fold increase in Aiolos in total DP thymocytes as measured by flow cytometry (Fig. 2-5). In contrast, Helios protein levels increased 4.9-fold in total DP thymocytes, corresponding to a 10-fold increase in mRNA (Figs. 2-4 and 2-5).

The low protein levels relative to mRNA found in both DP thymocytes and T-ALL cells could be due to increased degradation of Ikaros and Aiolos proteins or decreased translation of Ikaros and Aiolos mRNA. Proteasomal degradation of both Ikaros and Aiolos, but not Helios, is induced by the thalidomide derivatives lenalidomide and pomalidomide (348-351), suggesting that a mechanism to regulate degradation of Ikaros and Aiolos, separate from Helios, may occur. Another possibility is that mRNA, particularly that of Aiolos, is being sequestered by miRNAs

or subcellular localization for rapid protein translation upon stimulation. Analysis of Aiolos protein levels in $CD3^+$ SP cells revealed that Aiolos protein expression increased in TSP and MSP populations (Fig. 4-6). Thus, Aiolos mRNA may be amassed for rapid translation after stimulation, but further studies are needed to determine the mechanism of the sequestration and the exact signal received by positively selected thymocytes that induces translation. Identification of how Ikaros and Aiolos protein levels are being regulated in human DP cells and T-ALL may provide for new therapeutic targets.

Using Surface Marker Expression to Understand T Cell Development

Our identification of subpopulations of human thymocytes relied on the assumption that the expression levels of surface markers changes gradually as cells develop from one stage to the next. Thus, each population only differs from the one before or after it by subtle changes in one or two surface markers. However, not all surface markers change sequentially, resulting in parallel pathways within our proposed model of development in which populations have subtle changes in one surface marker as they move horizontally, and another marker as they move vertically (Figs. 3-6 and 4-7). Of note is that changes in expression of some of these markers appear to be independent of pre-TCR or TCR signaling. For instance, DP3, DP4, and DP5 thymocytes are $CD3^-$ but have similar expression of CD7, CD38, CD44, and CD45RO as the $CD3^{lo}$ DP6, DP7, and DP8 thymocytes, respectively (Fig. 4-1). Changes in these surface markers may then be a result of different signals received by cytokine and chemokine signaling or cell-cell interactions as cells move through the thymus. Further studies are needed to determine the functional significance of the changes in expression of CD7, CD38, CD44, and CD45RO during development.

Of particular note in our phenotyping of human thymocytes was the fluctuation of CD44 expression (Fig. 4-1D). Early thymocytes express high levels of CD44, which participates in homing of progenitor cells to the thymus (412). CD44 surface expression decreases in the DN2 stage, and remains low until a transient increase after β selection (Figs. 3-2 and 3-3). CD44 expression then increases again with positive selection, returning to high levels in the most mature thymocytes (Figs. 6-1,-2,-4, and -5).

CD44 is able to bind both hyaluronan and fibronectin, and expression of these proteins is limited to the capsule, septae, vessels, and Hassall's corpuscles in the post-natal human thymus (413, 414). CD44 ligation is capable of inducing motility, proliferation, apoptosis, or protection from apoptosis in T cells depending on the splice variant of CD44 being expressed and the amount of CD3 co-stimulation (412, 415-422). As $CD3^-$ thymocytes reside in the cortex (423), the $CD44^+CD3^-$ cells would encounter ligand at the subcortical and intralobular septael areas. The subcortical area is populated by actively dividing thymocytes that have just completed β selection (423), and, in the case of human thymocytes, have just up-regulated CD44 expression (Figs. 3-2 and 3-3). Activation of murine DN3, DN4, and DP thymocytes with sub-threshold levels of anti-CD3 antibody and anti-CD44 antibody promoted proliferation and survival (412). Thus, it is possible that CD44 engagement on human ISP2, DP2, and DP3 thymocytes near the subcortical and septael areas of the cortex may help promote the proliferation and survival seen after β selection. To support this theory, CD44 expression decreases as the rate of proliferation decreases in DP4 and DP5 thymocytes (Figs. 3-2 to 3-4). As CD44 expression decreases on these cells, it would also decrease the adherency of the cells, allowing for movement away from the subcortical region and towards the medulla for continued differentiation (424).

The increased CD44 expression after positive selection may play a role in negative selection. Cross-linking of CD44 and CD3 induces increased apoptosis of DP and SP murine thymocytes (412, 419). CD44 is associated with the protein tyrosine kinase Lck in T cells, and cross-linking of CD44 and CD3 results in higher levels of Lck phosphorylation than CD3 cross-linking alone (412, 419, 424, 425). Thus, binding of CD44 on $CD3^{hi}$ thymocytes to ligands on Hassall's corpuscles in the medulla may result in augmented signals that affect negative selection.

Conclusions and Implications

These studies were conducted to determine if altered expression of Ikaros family members contributes to the development of T-ALL through an analysis of normal thymic development. In Chapter 2, we identified differences in Ikaros family mRNA and protein expression between murine and human thymocyte development. In Chapters 3 and 4, we used multi-parameter flow cytometry to identify 27 subpopulations of human thymic development. Further, we showed that Ikaros, Aiolos, and Helios protein levels are differentially regulated after β-selection, positive selection, and lineage commitment of human thymocytes. Finally, in Chapter 5 we addressed Ikaros family expression in cases of pediatric T-ALL, finding that T-ALL samples could be grouped according to the ratios of Ikaros family mRNA expression, but that Ikaros and Aiolos protein levels were low in T-ALL compared to normal thymocytes.

Our data suggest that changes in the ratio of Ikaros family members, and thus dimer make-up, are important for human thymocyte development and leukemogenesis. Further analysis of the subpopulations we identified is needed to determine their functional significance and confirm the timing of selection steps as we have proposed them. These data can then be used to identify Ikaros family targets at key stages of human thymic development, identify the Ikaros family

members associated with these targets, and determine if Ikaros family dimer formation and target binding are altered in T-ALL. Further, determination of the mechanisms regulating protein levels of Ikaros and Aiolos may provide therapeutic targets for T-ALL and other leukemias.

References

1. Sun L, Liu A, Georgopoulos K. Zinc finger-mediated protein interactions modulate Ikaros activity, a molecular control of lymphocyte development. EMBO J. 1996;15(19):5358-69. Epub 1996/10/01. PubMed PMID: 8895580; PMCID: 452279.

2. Morgan B, Sun L, Avitahl N, Andrikopoulos K, Ikeda T, Gonzales E, Wu P, Neben S, Georgopoulos K. Aiolos, a lymphoid restricted transcription factor that interacts with Ikaros to regulate lymphocyte differentiation. EMBO J. 1997;16(8):2004-13. Epub 1997/04/15. doi: 10.1093/emboj/16.8.2004. PubMed PMID: 9155026; PMCID: 1169803.

3. Hahm K, Cobb BS, McCarty AS, Brown KE, Klug CA, Lee R, Akashi K, Weissman IL, Fisher AG, Smale ST. Helios, a T cell-restricted Ikaros family member that quantitatively associates with Ikaros at centromeric heterochromatin. Genes Dev. 1998;12(6):782-96. Epub 1998/04/29. PubMed PMID: 9512513; PMCID: 316626.

4. Perdomo J, Holmes M, Chong B, Crossley M. Eos and pegasus, two members of the Ikaros family of proteins with distinct DNA binding activities. J Biol Chem. 2000;275(49):38347-54. Epub 2000/09/09. doi: 10.1074/jbc.M005457200. PubMed PMID: 10978333.

5. Kelley CM, Ikeda T, Koipally J, Avitahl N, Wu L, Georgopoulos K, Morgan BA. Helios, a novel dimerization partner of Ikaros expressed in the earliest hematopoietic progenitors. Current biology : CB. 1998;8(9):508-15. Epub 1998/05/20. PubMed PMID: 9560339.

6. Molnar A, Georgopoulos K. The Ikaros gene encodes a family of functionally diverse zinc finger DNA-binding proteins. Mol Cell Biol. 1994;14(12):8292-303. Epub 1994/12/01. PubMed PMID: 7969165; PMCID: 359368.

7. Molnar A, Wu P, Largespada DA, Vortkamp A, Scherer S, Copeland NG, Jenkins NA, Bruns G, Georgopoulos K. The Ikaros gene encodes a family of lymphocyte-restricted zinc finger DNA binding proteins, highly conserved in human and mouse. J Immunol. 1996;156(2):585-92. Epub 1996/01/15. PubMed PMID: 8543809.

8. Sun L, Crotty ML, Sensel M, Sather H, Navara C, Nachman J, Steinherz PG, Gaynon PS, Seibel N, Mao C, Vassilev A, Reaman GH, Uckun FM. Expression of dominant-negative Ikaros isoforms in T-cell acute lymphoblastic leukemia. Clin Cancer Res. 1999;5(8):2112-20. Epub 1999/09/03. PubMed PMID: 10473095.

9. Sun L, Goodman PA, Wood CM, Crotty ML, Sensel M, Sather H, Navara C, Nachman J, Steinherz PG, Gaynon PS, Seibel N, Vassilev A, Juran BD, Reaman GH, Uckun FM. Expression of aberrantly spliced oncogenic ikaros isoforms in childhood acute lymphoblastic leukemia. J Clin Oncol. 1999;17(12):3753-66. Epub 1999/11/30. PubMed PMID: 10577847.

10. Sun L, Heerema N, Crotty L, Wu X, Navara C, Vassilev A, Sensel M, Reaman GH, Uckun FM. Expression of dominant-negative and mutant isoforms of the antileukemic transcription factor Ikaros in infant acute lymphoblastic leukemia. Proc Natl Acad Sci U S A. 1999;96(2):680-5. Epub 1999/01/20. PubMed PMID: 9892693; PMCID: 15196.

11. Payne KJ, Nicolas JH, Zhu JY, Barsky LW, Crooks GM. Cutting edge: predominant expression of a novel Ikaros isoform in normal human hemopoiesis. J Immunol. 2001;167(4):1867-70. Epub 2001/08/08. PubMed PMID: 11489963.

12. Cobb BS, Morales-Alcelay S, Kleiger G, Brown KE, Fisher AG, Smale ST. Targeting of Ikaros to pericentromeric heterochromatin by direct DNA binding. Genes Dev. 2000;14(17):2146-60. Epub 2000/09/06. PubMed PMID: 10970879; PMCID: 316893.

13. Koipally J, Heller EJ, Seavitt JR, Georgopoulos K. Unconventional potentiation of gene expression by Ikaros. J Biol Chem. 2002;277(15):13007-15. Epub 2002/01/19. doi: 10.1074/jbc.M111371200
M111371200 [pii]. PubMed PMID: 11799125.

14. Schjerven H, McLaughlin J, Arenzana TL, Frietze S, Cheng D, Wadsworth SE, Lawson GW, Bensinger SJ, Farnham PJ, Witte ON, Smale ST. Selective regulation of lymphopoiesis and leukemogenesis by individual zinc fingers of Ikaros. Nat Immunol. 2013;14(10):1073-83. Epub 2013/09/10. doi: 10.1038/ni.2707. PubMed PMID: 24013668; PMCID: 3800053.

15. Caballero R, Setien F, Lopez-Serra L, Boix-Chornet M, Fraga MF, Ropero S, Megias D, Alaminos M, Sanchez-Tapia EM, Montoya MC, Esteller M, Gonzalez-Sarmiento R, Ballestar E. Combinatorial effects of splice variants modulate function of Aiolos. J Cell Sci. 2007;120(Pt 15):2619-30. Epub 2007/07/25. doi: 120/15/2619 [pii]
10.1242/jcs.007344. PubMed PMID: 17646674.

16. Cortes M, Wong E, Koipally J, Georgopoulos K. Control of lymphocyte development by the Ikaros gene family. Curr Opin Immunol. 1999;11(2):167-71. Epub 1999/05/14. doi: S0952791599800284 [pii]. PubMed PMID: 10322160.

17. Ronni T, Payne KJ, Ho S, Bradley MN, Dorsam G, Dovat S. Human Ikaros function in activated T cells is regulated by coordinated expression of its largest isoforms. J Biol Chem. 2007;282(4):2538-47. Epub 2006/12/01. doi: M605627200 [pii] 10.1074/jbc.M605627200. PubMed PMID: 17135265.

18. Dovat S, Ronni T, Russell D, Ferrini R, Cobb BS, Smale ST. A common mechanism for mitotic inactivation of C2H2 zinc finger DNA-binding domains. Genes Dev. 2002;16(23):2985-90. Epub 2002/12/05. doi: 10.1101/gad.1040502. PubMed PMID: 12464629; PMCID: 187490.

19. Ma H, Qazi S, Ozer Z, Zhang J, Ishkhanian R, Uckun FM. Regulatory phosphorylation of Ikaros by Bruton's tyrosine kinase. PLoS One. 2013;8(8):e71302. doi: 10.1371/journal.pone.0071302. PubMed PMID: 23977012; PMCID: PMC3747153.

20. Gurel Z, Ronni T, Ho S, Kuchar J, Payne KJ, Turk CW, Dovat S. Recruitment of ikaros to pericentromeric heterochromatin is regulated by phosphorylation. J Biol Chem. 2008;283(13):8291-300. Epub 2008/01/29. doi: M707906200 [pii] 10.1074/jbc.M707906200. PubMed PMID: 18223295; PMCID: 2276389.

21. Uckun FM, Ma H, Zhang J, Ozer Z, Dovat S, Mao C, Ishkhanian R, Goodman P, Qazi S. Serine phosphorylation by SYK is critical for nuclear localization and transcription factor function of Ikaros. Proc Natl Acad Sci U S A. 2012;109(44):18072-7. doi: 10.1073/pnas.1209828109. PubMed PMID: 23071339; PMCID: PMC3497833.

22. Gomez-del Arco P, Maki K, Georgopoulos K. Phosphorylation controls Ikaros's ability to negatively regulate the G(1)-S transition. Mol Cell Biol. 2004;24(7):2797-807. Epub 2004/03/17. PubMed PMID: 15024069; PMCID: 371126.

23. Li Z, Song C, Ouyang H, Lai L, Payne KJ, Dovat S. Cell cycle-specific function of Ikaros in human leukemia. Pediatric blood & cancer. 2012;59(1):69-76. doi: 10.1002/pbc.23406. PubMed PMID: 22106042; PMCID: PMC3292658.

24. Song C, Li Z, Erbe AK, Savic A, Dovat S. Regulation of Ikaros function by casein kinase 2 and protein phosphatase 1. World J Biol Chem. 2011;2(6):126-31. doi: 10.4331/wjbc.v2.i6.126. PubMed PMID: 21765978; PMCID: PMC3135859.

25. Popescu M, Gurel Z, Ronni T, Song C, Hung KY, Payne KJ, Dovat S. Ikaros stability and pericentromeric localization are regulated by protein phosphatase 1. J Biol Chem. 2009;284(20):13869-80. Epub 2009/03/14. doi: M900209200 [pii] 10.1074/jbc.M900209200. PubMed PMID: 19282287; PMCID: 2679487.

26. Romero F, Martinez AC, Camonis J, Rebollo A. Aiolos transcription factor controls cell death in T cells by regulating Bcl-2 expression and its cellular localization. EMBO J. 1999;18(12):3419-30. Epub 1999/06/16. doi: 10.1093/emboj/18.12.3419. PubMed PMID: 10369681; PMCID: 1171421.

27. Zhang J, Jackson AF, Naito T, Dose M, Seavitt J, Liu F, Heller EJ, Kashiwagi M, Yoshida T, Gounari F, Petrie HT, Georgopoulos K. Harnessing of the nucleosome-remodeling-deacetylase complex controls lymphocyte development and prevents leukemogenesis. Nat

Immunol. 2012;13(1):86-94. Epub 2011/11/15. doi: 10.1038/ni.2150. PubMed PMID: 22080921; PMCID: 3868219.

28. Kim J, Sif S, Jones B, Jackson A, Koipally J, Heller E, Winandy S, Viel A, Sawyer A, Ikeda T, Kingston R, Georgopoulos K. Ikaros DNA-binding proteins direct formation of chromatin remodeling complexes in lymphocytes. Immunity. 1999;10(3):345-55. Epub 1999/04/16. doi: S1074-7613(00)80034-5 [pii]. PubMed PMID: 10204490.

29. O'Neill DW, Schoetz SS, Lopez RA, Castle M, Rabinowitz L, Shor E, Krawchuk D, Goll MG, Renz M, Seelig HP, Han S, Seong RH, Park SD, Agalioti T, Munshi N, Thanos D, Erdjument-Bromage H, Tempst P, Bank A. An ikaros-containing chromatin-remodeling complex in adult-type erythroid cells. Mol Cell Biol. 2000;20(20):7572-82. Epub 2000/09/26. PubMed PMID: 11003653; PMCID: 86310.

30. Sridharan R, Smale ST. Predominant interaction of both Ikaros and Helios with the NuRD complex in immature thymocytes. J Biol Chem. 2007;282(41):30227-38. Epub 2007/08/08. doi: M702541200 [pii]
10.1074/jbc.M702541200. PubMed PMID: 17681952.

31. Tong JK, Hassig CA, Schnitzler GR, Kingston RE, Schreiber SL. Chromatin deacetylation by an ATP-dependent nucleosome remodelling complex. Nature. 1998;395(6705):917-21. doi: 10.1038/27699. PubMed PMID: 9804427.

32. Xue Y, Wong J, Moreno GT, Young MK, Cote J, Wang W. NURD, a novel complex with both ATP-dependent chromatin-remodeling and histone deacetylase activities. Mol Cell. 1998;2(6):851-61. PubMed PMID: 9885572.

33. Zhang Y, LeRoy G, Seelig HP, Lane WS, Reinberg D. The dermatomyositis-specific autoantigen Mi2 is a component of a complex containing histone deacetylase and nucleosome remodeling activities. Cell. 1998;95(2):279-89. PubMed PMID: 9790534.

34. Bandyopadhyay S, Dure M, Paroder M, Soto-Nieves N, Puga I, Macian F. Interleukin 2 gene transcription is regulated by Ikaros-induced changes in histone acetylation in anergic T cells. Blood. 2007;109(7):2878-86. Epub 2006/12/07. doi: blood-2006-07-037754 [pii] 10.1182/blood-2006-07-037754. PubMed PMID: 17148585; PMCID: 1852212.

35. Baine I, Basu S, Ames R, Sellers RS, Macian F. Helios induces epigenetic silencing of IL2 gene expression in regulatory T cells. J Immunol. 2013;190(3):1008-16. doi: 10.4049/jimmunol.1200792. PubMed PMID: 23275607; PMCID: PMC3558938.

36. Pan F, Yu H, Dang EV, Barbi J, Pan X, Grosso JF, Jinasena D, Sharma SM, McCadden EM, Getnet D, Drake CG, Liu JO, Ostrowski MC, Pardoll DM. Eos mediates Foxp3-dependent gene silencing in CD4+ regulatory T cells. Science. 2009;325(5944):1142-6. doi: 10.1126/science.1176077. PubMed PMID: 19696312; PMCID: PMC2859703.

37. Thomas RM, Chunder N, Chen C, Umetsu SE, Winandy S, Wells AD. Ikaros enforces the costimulatory requirement for IL2 gene expression and is required for anergy induction in CD4+ T lymphocytes. J Immunol. 2007;179(11):7305-15. PubMed PMID: 18025173.

38. Quintana FJ, Jin H, Burns EJ, Nadeau M, Yeste A, Kumar D, Rangachari M, Zhu C, Xiao S, Seavitt J, Georgopoulos K, Kuchroo VK. Aiolos promotes TH17 differentiation by directly silencing Il2 expression. Nat Immunol. 2012;13(8):770-7. Epub 2012/07/04. doi: ni.2363 [pii] 10.1038/ni.2363. PubMed PMID: 22751139.

39. Schwickert TA, Tagoh H, Gultekin S, Dakic A, Axelsson E, Minnich M, Ebert A, Werner B, Roth M, Cimmino L, Dickins RA, Zuber J, Jaritz M, Busslinger M. Stage-specific control of early B cell development by the transcription factor Ikaros. Nat Immunol. 2014;15(3):283-93. doi: 10.1038/ni.2828. PubMed PMID: 24509509.

40. Bottardi S, Mavoungou L, Pak H, Daou S, Bourgoin V, Lakehal YA, Affar el B, Milot E. The IKAROS interaction with a complex including chromatin remodeling and transcription elongation activities is required for hematopoiesis. PLoS Genet. 2014;10(12):e1004827. doi: 10.1371/journal.pgen.1004827. PubMed PMID: 25474253; PMCID: PMC4256266.

41. Bottardi S, Mavoungou L, Bourgoin V, Mashtalir N, Affar el B, Milot E. Direct protein interactions are responsible for Ikaros-GATA and Ikaros-Cdk9 cooperativeness in hematopoietic cells. Mol Cell Biol. 2013;33(16):3064-76. doi: 10.1128/MCB.00296-13. PubMed PMID: 23732910; PMCID: PMC3753914.

42. Oravecz A, Apostolov A, Polak K, Jost B, Le Gras S, Chan S, Kastner P. Ikaros mediates gene silencing in T cells through Polycomb repressive complex 2. Nat Commun. 2015;6:8823. doi: 10.1038/ncomms9823. PubMed PMID: 26549758; PMCID: PMC4667618.

43. Geimer Le Lay AS, Oravecz A, Mastio J, Jung C, Marchal P, Ebel C, Dembele D, Jost B, Le Gras S, Thibault C, Borggrefe T, Kastner P, Chan S. The tumor suppressor Ikaros shapes the repertoire of notch target genes in T cells. Science signaling. 2014;7(317):ra28. Epub 2014/03/20. doi: 10.1126/scisignal.2004545. PubMed PMID: 24643801.

44. Kleinmann E, Geimer Le Lay AS, Sellars M, Kastner P, Chan S. Ikaros represses the transcriptional response to Notch signaling in T-cell development. Mol Cell Biol. 2008;28(24):7465-75. Epub 2008/10/15. doi: MCB.00715-08 [pii] 10.1128/MCB.00715-08. PubMed PMID: 18852286; PMCID: 2593445.

45. Collins B, Clambey ET, Scott-Browne J, White J, Marrack P, Hagman J, Kappler JW. Ikaros promotes rearrangement of TCR alpha genes in an Ikaros null thymoma cell line. Eur J Immunol. 2013;43(2):521-32. Epub 2012/11/23. doi: 10.1002/eji.201242757. PubMed PMID: 23172374; PMCID: 3923402.

46. Georgopoulos K, Bigby M, Wang JH, Molnar A, Wu P, Winandy S, Sharpe A. The Ikaros gene is required for the development of all lymphoid lineages. Cell. 1994;79(1):143-56. Epub 1994/10/07. doi: 0092-8674(94)90407-3 [pii]. PubMed PMID: 7923373.

47. Winandy S, Wu P, Georgopoulos K. A dominant mutation in the Ikaros gene leads to rapid development of leukemia and lymphoma. Cell. 1995;83(2):289-99. Epub 1995/10/20. doi: 0092-8674(95)90170-1 [pii]. PubMed PMID: 7585946.

48. Zhang Z, Swindle CS, Bates JT, Ko R, Cotta CV, Klug CA. Expression of a non-DNA-binding isoform of Helios induces T-cell lymphoma in mice. Blood. 2007;109(5):2190-7. Epub 2006/11/18. doi: 10.1182/blood-2005-01-031930. PubMed PMID: 17110463; PMCID: 1801072.

49. Papathanasiou P, Perkins AC, Cobb BS, Ferrini R, Sridharan R, Hoyne GF, Nelms KA, Smale ST, Goodnow CC. Widespread failure of hematolymphoid differentiation caused by a recessive niche-filling allele of the Ikaros transcription factor. Immunity. 2003;19(1):131-44. Epub 2003/07/23. doi: S1074761303001687 [pii]. PubMed PMID: 12871645.

50. Wang JH, Nichogiannopoulou A, Wu L, Sun L, Sharpe AH, Bigby M, Georgopoulos K. Selective defects in the development of the fetal and adult lymphoid system in mice with an Ikaros null mutation. Immunity. 1996;5(6):537-49. Epub 1996/12/01. doi: S1074-7613(00)80269-1 [pii]. PubMed PMID: 8986714.

51. Wang JH, Avitahl N, Cariappa A, Friedrich C, Ikeda T, Renold A, Andrikopoulos K, Liang L, Pillai S, Morgan BA, Georgopoulos K. Aiolos regulates B cell activation and maturation to effector state. Immunity. 1998;9(4):543-53. Epub 1998/11/07. PubMed PMID: 9806640.

52. Cai Q, Dierich A, Oulad-Abdelghani M, Chan S, Kastner P. Helios deficiency has minimal impact on T cell development and function. J Immunol. 2009;183(4):2303-11. doi: 10.4049/jimmunol.0901407. PubMed PMID: 19620299.

53. Alinikula J, Kohonen P, Nera KP, Lassila O. Concerted action of Helios and Ikaros controls the expression of the inositol 5-phosphatase SHIP. Eur J Immunol. 2010;40(9):2599-607. Epub 2010/07/06. doi: 10.1002/eji.200940002. PubMed PMID: 20602434.

54. Ferreiros-Vidal I, Carroll T, Taylor B, Terry A, Liang Z, Bruno L, Dharmalingam G, Khadayate S, Cobb BS, Smale ST, Spivakov M, Srivastava P, Petretto E, Fisher AG, Merkenschlager M. Genome-wide identification of Ikaros targets elucidates its contribution to mouse B-cell lineage specification and pre-B-cell differentiation. Blood. 2013;121(10):1769-82. doi: 10.1182/blood-2012-08-450114. PubMed PMID: 23303821.

55. Dovat S, Montecino-Rodriguez E, Schuman V, Teitell MA, Dorshkind K, Smale ST. Transgenic expression of Helios in B lineage cells alters B cell properties and promotes

lymphomagenesis. J Immunol. 2005;175(6):3508-15. Epub 2005/09/09. PubMed PMID: 16148093.

56. Trinh LA, Ferrini R, Cobb BS, Weinmann AS, Hahm K, Ernst P, Garraway IP, Merkenschlager M, Smale ST. Down-regulation of TDT transcription in CD4(+)CD8(+) thymocytes by Ikaros proteins in direct competition with an Ets activator. Genes Dev. 2001;15(14):1817-32. Epub 2001/07/19. doi: 10.1101/gad.905601. PubMed PMID: 11459831; PMCID: 312741.

57. Sabbattini P, Lundgren M, Georgiou A, Chow C, Warnes G, Dillon N. Binding of Ikaros to the lambda5 promoter silences transcription through a mechanism that does not require heterochromatin formation. EMBO J. 2001;20(11):2812-22. Epub 2001/06/02. doi: 10.1093/emboj/20.11.2812. PubMed PMID: 11387214; PMCID: 125479.

58. Reynaud D, Demarco IA, Reddy KL, Schjerven H, Bertolino E, Chen Z, Smale ST, Winandy S, Singh H. Regulation of B cell fate commitment and immunoglobulin heavy-chain gene rearrangements by Ikaros. Nat Immunol. 2008;9(8):927-36. Epub 2008/06/24. doi: ni.1626 [pii]
10.1038/ni.1626. PubMed PMID: 18568028; PMCID: 2699484.

59. Kathrein KL, Chari S, Winandy S. Ikaros directly represses the notch target gene Hes1 in a leukemia T cell line: implications for CD4 regulation. J Biol Chem. 2008;283(16):10476-84. Epub 2008/02/22. doi: M709643200 [pii]
10.1074/jbc.M709643200. PubMed PMID: 18287091; PMCID: 2447659.

60. Chari S, Winandy S. Ikaros regulates Notch target gene expression in developing thymocytes. J Immunol. 2008;181(9):6265-74. Epub 2008/10/23. doi: 181/9/6265 [pii]. PubMed PMID: 18941217; PMCID: 2778602.

61. Lo K, Landau NR, Smale ST. LyF-1, a transcriptional regulator that interacts with a novel class of promoters for lymphocyte-specific genes. Mol Cell Biol. 1991;11(10):5229-43. Epub 1991/10/01. PubMed PMID: 1922043; PMCID: 361569.

62. Ernst P, Hahm K, Smale ST. Both LyF-1 and an Ets protein interact with a critical promoter element in the murine terminal transferase gene. Mol Cell Biol. 1993;13(5):2982-92. Epub 1993/05/01. PubMed PMID: 8474456; PMCID: 359691.

63. Georgopoulos K, Moore DD, Derfler B. Ikaros, an early lymphoid-specific transcription factor and a putative mediator for T cell commitment. Science. 1992;258(5083):808-12. Epub 1992/10/30. PubMed PMID: 1439790.

64. Lee HC, Shibata H, Ogawa S, Maki K, Ikuta K. Transcriptional regulation of the mouse IL-7 receptor alpha promoter by glucocorticoid receptor. J Immunol. 2005;174(12):7800-6. PubMed PMID: 15944284.

65. Harker N, Garefalaki A, Menzel U, Ktistaki E, Naito T, Georgopoulos K, Kioussis D. Pre-TCR signaling and CD8 gene bivalent chromatin resolution during thymocyte development. J Immunol. 2011;186(11):6368-77. Epub 2011/04/26. doi: 10.4049/jimmunol.1003567. PubMed PMID: 21515796.

66. Naito T, Gomez-Del Arco P, Williams CJ, Georgopoulos K. Antagonistic interactions between Ikaros and the chromatin remodeler Mi-2beta determine silencer activity and Cd4 gene expression. Immunity. 2007;27(5):723-34. Epub 2007/11/06. doi: S1074-7613(07)00489-X [pii] 10.1016/j.immuni.2007.09.008. PubMed PMID: 17980631.

67. Gomez-del Arco P, Kashiwagi M, Jackson AF, Naito T, Zhang J, Liu F, Kee B, Vooijs M, Radtke F, Redondo JM, Georgopoulos K. Alternative promoter usage at the Notch1 locus supports ligand-independent signaling in T cell development and leukemogenesis. Immunity. 2010;33(5):685-98. doi: 10.1016/j.immuni.2010.11.008. PubMed PMID: 21093322; PMCID: PMC3072037.

68. Ma S, Pathak S, Mandal M, Trinh L, Clark MR, Lu R. Ikaros and Aiolos inhibit pre-B-cell proliferation by directly suppressing c-Myc expression. Mol Cell Biol. 2010;30(17):4149-58. Epub 2010/06/23. doi: MCB.00224-10 [pii]
10.1128/MCB.00224-10. PubMed PMID: 20566697; PMCID: 2937562.

69. Yoshida T, Ng SY, Zuniga-Pflucker JC, Georgopoulos K. Early hematopoietic lineage restrictions directed by Ikaros. Nat Immunol. 2006;7(4):382-91. Epub 2006/03/07. doi: ni1314 [pii]
10.1038/ni1314. PubMed PMID: 16518393.

70. Sugimoto N, Oida T, Hirota K, Nakamura K, Nomura T, Uchiyama T, Sakaguchi S. Foxp3-dependent and -independent molecules specific for CD25+CD4+ natural regulatory T cells revealed by DNA microarray analysis. Int Immunol. 2006;18(8):1197-209. Epub 2006/06/15. doi: dxl060 [pii]

10.1093/intimm/dxl060. PubMed PMID: 16772372.

71. Quirion MR, Gregory GD, Umetsu SE, Winandy S, Brown MA. Cutting edge: Ikaros is a regulator of Th2 cell differentiation. J Immunol. 2009;182(2):741-5. Epub 2009/01/07. doi: 182/2/741 [pii]. PubMed PMID: 19124715; PMCID: 2718557.

72. Yap WH, Yeoh E, Tay A, Brenner S, Venkatesh B. STAT4 is a target of the hematopoietic zinc-finger transcription factor Ikaros in T cells. FEBS Lett. 2005;579(20):4470-8. Epub 2005/08/06. doi: S0014-5793(05)00860-4 [pii] 10.1016/j.febslet.2005.07.018. PubMed PMID: 16081070.

73. Getnet D, Grosso JF, Goldberg MV, Harris TJ, Yen HR, Bruno TC, Durham NM, Hipkiss EL, Pyle KJ, Wada S, Pan F, Pardoll DM, Drake CG. A role for the transcription factor Helios in human CD4(+)CD25(+) regulatory T cells. Mol Immunol. 2010;47(7-8):1595-600. Epub 2010/03/17. doi: S0161-5890(10)00039-8 [pii] 10.1016/j.molimm.2010.02.001. PubMed PMID: 20226531; PMCID: 3060613.

74. Thornton AM, Korty PE, Tran DQ, Wohlfert EA, Murray PE, Belkaid Y, Shevach EM. Expression of Helios, an Ikaros transcription factor family member, differentiates thymic-derived from peripherally induced Foxp3+ T regulatory cells. J Immunol. 2010;184(7):3433-41. doi: 10.4049/jimmunol.0904028. PubMed PMID: 20181882; PMCID: PMC3725574.

75. Ghadiri A, Duhamel M, Fleischer A, Reimann A, Dessauge F, Rebollo A. Critical function of Ikaros in controlling Aiolos gene expression. FEBS Lett. 2007;581(8):1605-16. Epub 2007/03/27. doi: 10.1016/j.febslet.2007.03.025. PubMed PMID: 17383641.

76. Yoshida T, Landhuis E, Dose M, Hazan I, Zhang J, Naito T, Jackson AF, Wu J, Perotti EA, Kaufmann C, Gounari F, Morgan BA, Georgopoulos K. Transcriptional regulation of the Ikzf1 locus. Blood. 2013;122(18):3149-59. Epub 2013/09/05. doi: 10.1182/blood-2013-01-474916. PubMed PMID: 24002445; PMCID: 3814732.

77. Tun T, Hamaguchi Y, Matsunami N, Furukawa T, Honjo T, Kawaichi M. Recognition sequence of a highly conserved DNA binding protein RBP-J kappa. Nucleic acids research. 1994;22(6):965-71. Epub 1994/03/25. PubMed PMID: 8152928; PMCID: 307916.

78. Asnafi V, Beldjord K, Boulanger E, Comba B, Le Tutour P, Estienne MH, Davi F, Landman-Parker J, Quartier P, Buzyn A, Delabesse E, Valensi F, Macintyre E. Analysis of TCR, pT alpha, and RAG-1 in T-acute lymphoblastic leukemias improves understanding of early human T-lymphoid lineage commitment. Blood. 2003;101(7):2693-703. Epub 2002/11/26. doi: 10.1182/blood-2002-08-2438. PubMed PMID: 12446444.

79. Asnafi V, Buzyn A, Thomas X, Huguet F, Vey N, Boiron JM, Reman O, Cayuela JM, Lheritier V, Vernant JP, Fiere D, Macintyre E, Dombret H. Impact of TCR status and genotype on outcome in adult T-cell acute lymphoblastic leukemia: a LALA-94 study. Blood. 2005;105(8):3072-8. Epub 2005/01/08. doi: 10.1182/blood-2004-09-3666. PubMed PMID: 15637138.

80. Bene MC, Castoldi G, Knapp W, Ludwig WD, Matutes E, Orfao A, van't Veer MB. Proposals for the immunological classification of acute leukemias. European Group for the Immunological Characterization of Leukemias (EGIL). Leukemia. 1995;9(10):1783-6. Epub 1995/10/01. PubMed PMID: 7564526.

81. van Grotel M, Meijerink JP, van Wering ER, Langerak AW, Beverloo HB, Buijs-Gladdines JG, Burger NB, Passier M, van Lieshout EM, Kamps WA, Veerman AJ, van Noesel MM, Pieters R. Prognostic significance of molecular-cytogenetic abnormalities in pediatric T-ALL is not explained by immunophenotypic differences. Leukemia. 2008;22(1):124-31. Epub 2007/10/12. doi: 10.1038/sj.leu.2404957. PubMed PMID: 17928886.

82. van Grotel M, van den Heuvel-Eibrink MM, van Wering ER, van Noesel MM, Kamps WA, Veerman AJ, Pieters R, Meijerink JP. CD34 expression is associated with poor survival in pediatric T-cell acute lymphoblastic leukemia. Pediatric blood & cancer. 2008;51(6):737-40. Epub 2008/08/07. doi: 10.1002/pbc.21707. PubMed PMID: 18683236.

83. Pui CH, Hancock ML, Head DR, Rivera GK, Look AT, Sandlund JT, Behm FG. Clinical significance of CD34 expression in childhood acute lymphoblastic leukemia. Blood. 1993;82(3):889-94. Epub 1993/08/01. PubMed PMID: 7687897.

84. Maser RS, Choudhury B, Campbell PJ, Feng B, Wong KK, Protopopov A, O'Neil J, Gutierrez A, Ivanova E, Perna I, Lin E, Mani V, Jiang S, McNamara K, Zaghlul S, Edkins S, Stevens C, Brennan C, Martin ES, Wiedemeyer R, Kabbarah O, Nogueira C, Histen G, Aster J, Mansour M, Duke V, Foroni L, Fielding AK, Goldstone AH, Rowe JM, Wang YA, Look AT, Stratton MR, Chin L, Futreal PA, DePinho RA. Chromosomally unstable mouse tumours have genomic alterations similar to diverse human cancers. Nature. 2007;447(7147):966-71. Epub 2007/05/23. doi: nature05886 [pii]
10.1038/nature05886. PubMed PMID: 17515920; PMCID: 2714968.

85. Marcais A, Jeannet R, Hernandez L, Soulier J, Sigaux F, Chan S, Kastner P. Genetic inactivation of Ikaros is a rare event in human T-ALL. Leuk Res. 2010;34(4):426-9. Epub 2009/10/03. doi: 10.1016/j.leukres.2009.09.012. PubMed PMID: 19796813.

86. Kuiper RP, Schoenmakers EF, van Reijmersdal SV, Hehir-Kwa JY, van Kessel AG, van Leeuwen FN, Hoogerbrugge PM. High-resolution genomic profiling of childhood ALL reveals novel recurrent genetic lesions affecting pathways involved in lymphocyte differentiation and cell cycle progression. Leukemia. 2007;21(6):1258-66. Epub 2007/04/20. doi: 10.1038/sj.leu.2404691. PubMed PMID: 17443227.

87. Takanashi M, Yagi T, Imamura T, Tabata Y, Morimoto A, Hibi S, Ishii E, Imashuku S. Expression of the Ikaros gene family in childhood acute lymphoblastic leukaemia. Br J Haematol. 2002;117(3):525-30. PubMed PMID: 12028018.

88. Mullighan CG, Miller CB, Radtke I, Phillips LA, Dalton J, Ma J, White D, Hughes TP, Le Beau MM, Pui CH, Relling MV, Shurtleff SA, Downing JR. BCR-ABL1 lymphoblastic leukaemia is characterized by the deletion of Ikaros. Nature. 2008;453(7191):110-4. Epub 2008/04/15. doi: nature06866 [pii] 10.1038/nature06866. PubMed PMID: 18408710.

89. Meleshko AN, Movchan LV, Belevtsev MV, Savitskaja TV. Relative expression of different Ikaros isoforms in childhood acute leukemia. Blood cells, molecules & diseases. 2008;41(3):278-83. Epub 2008/08/05. doi: 10.1016/j.bcmd.2008.06.006. PubMed PMID: 18675565.

90. Ruiz A, Jiang J, Kempski H, Brady HJ. Overexpression of the Ikaros 6 isoform is restricted to t(4;11) acute lymphoblastic leukaemia in children and infants and has a role in B-cell survival. Br J Haematol. 2004;125(1):31-7. Epub 2004/03/16. PubMed PMID: 15015965.

91. Nakase K, Ishimaru F, Avitahl N, Dansako H, Matsuo K, Fujii K, Sezaki N, Nakayama H, Yano T, Fukuda S, Imajoh K, Takeuchi M, Miyata A, Hara M, Yasukawa M, Takahashi I, Taguchi H, Matsue K, Nakao S, Niho Y, Takenaka K, Shinagawa K, Ikeda K, Niiya K, Harada M. Dominant negative isoform of the Ikaros gene in patients with adult B-cell acute lymphoblastic leukemia. Cancer Res. 2000;60(15):4062-5. Epub 2000/08/17. PubMed PMID: 10945610.

92. Reyes-Leon A, Juarez-Velazquez R, Medrano-Hernandez A, Cuenca-Roldan T, Salas-Labadia C, Del Pilar Navarrete-Meneses M, Rivera-Luna R, Lopez-Hernandez G, Paredes-Aguilera R, Perez-Vera P. Expression of Ik6 and Ik8 Isoforms and Their Association with Relapse and Death in Mexican Children with Acute Lymphoblastic Leukemia. PLoS One. 2015;10(7):e0130756. Epub 2015/07/02. doi: 10.1371/journal.pone.0130756. PubMed PMID: 26131904; PMCID: 4488851.

93. Asanuma S, Yamagishi M, Kawanami K, Nakano K, Sato-Otsubo A, Muto S, Sanada M, Yamochi T, Kobayashi S, Utsunomiya A, Iwanaga M, Yamaguchi K, Uchimaru K, Ogawa S, Watanabe T. Adult T-cell leukemia cells are characterized by abnormalities of Helios expression that promote T cell growth. Cancer science. 2013;104(8):1097-106. Epub 2013/04/23. doi: 10.1111/cas.12181. PubMed PMID: 23600753.

94. Fujii K, Ishimaru F, Nakase K, Tabayashi T, Kozuka T, Naoki K, Miyahara M, Toki H, Kitajima K, Harada M, Tanimoto M. Over-expression of short isoforms of Helios in patients with adult T-cell leukaemia/lymphoma. Br J Haematol. 2003;120(6):986-9. Epub 2003/03/22. PubMed PMID: 12648068.

95. Nakase K, Ishimaru F, Fujii K, Tabayashi T, Kozuka T, Sezaki N, Matsuo Y, Harada M. Overexpression of novel short isoforms of Helios in a patient with T-cell acute lymphoblastic leukemia. Exp Hematol. 2002;30(4):313-7. Epub 2002/04/09. PubMed PMID: 11937265.

96. Tabayashi T, Ishimaru F, Takata M, Kataoka I, Nakase K, Kozuka T, Tanimoto M. Characterization of the short isoform of Helios overexpressed in patients with T-cell malignancies. Cancer science. 2007;98(2):182-8. Epub 2007/02/14. PubMed PMID: 17297655.

97. Asai D, Imamura T, Suenobu S, Saito A, Hasegawa D, Deguchi T, Hashii Y, Matsumoto K, Kawasaki H, Hori H, Iguchi A, Kosaka Y, Kato K, Horibe K, Yumura-Yagi K, Hara J, Oda M, Japan Association of Childhood Leukemia S. IKZF1 deletion is associated with a poor outcome in pediatric B-cell precursor acute lymphoblastic leukemia in Japan. Cancer medicine. 2013;2(3):412-9. Epub 2013/08/10. doi: 10.1002/cam4.87. PubMed PMID: 23930217; PMCID: 3699852.

98. Mullighan CG, Goorha S, Radtke I, Miller CB, Coustan-Smith E, Dalton JD, Girtman K, Mathew S, Ma J, Pounds SB, Su X, Pui CH, Relling MV, Evans WE, Shurtleff SA, Downing JR. Genome-wide analysis of genetic alterations in acute lymphoblastic leukaemia. Nature. 2007;446(7137):758-64. Epub 2007/03/09. doi: nature05690 [pii] 10.1038/nature05690. PubMed PMID: 17344859.

99. Iacobucci I, Iraci N, Messina M, Lonetti A, Chiaretti S, Valli E, Ferrari A, Papayannidis C, Paoloni F, Vitale A, Storlazzi CT, Ottaviani E, Guadagnuolo V, Durante S, Vignetti M, Soverini S, Pane F, Foa R, Baccarani M, Muschen M, Perini G, Martinelli G. IKAROS deletions dictate a unique gene expression signature in patients with adult B-cell acute lymphoblastic leukemia. PLoS One. 2012;7(7):e40934. Epub 2012/08/01. doi: 10.1371/journal.pone.0040934 PONE-D-12-01514 [pii]. PubMed PMID: 22848414; PMCID: 3405023.

100. Klein F, Feldhahn N, Herzog S, Sprangers M, Mooster JL, Jumaa H, Muschen M. BCR-ABL1 induces aberrant splicing of IKAROS and lineage infidelity in pre-B lymphoblastic leukemia cells. Oncogene. 2006;25(7):1118-24. Epub 2005/10/06. doi: 10.1038/sj.onc.1209133. PubMed PMID: 16205638.

101. Mullighan CG, Su X, Zhang J, Radtke I, Phillips LA, Miller CB, Ma J, Liu W, Cheng C, Schulman BA, Harvey RC, Chen IM, Clifford RJ, Carroll WL, Reaman G, Bowman WP, Devidas M, Gerhard DS, Yang W, Relling MV, Shurtleff SA, Campana D, Borowitz MJ, Pui CH, Smith M, Hunger SP, Willman CL, Downing JR. Deletion of IKZF1 and prognosis in acute lymphoblastic leukemia. N Engl J Med. 2009;360(5):470-80. Epub 2009/01/09. doi: NEJMoa0808253 [pii]
10.1056/NEJMoa0808253. PubMed PMID: 19129520; PMCID: 2674612.

102. Nakayama H, Ishimaru F, Avitahl N, Sezaki N, Fujii N, Nakase K, Ninomiya Y, Harashima A, Minowada J, Tsuchiyama J, Imajoh K, Tsubota T, Fukuda S, Sezaki T, Kojima K, Hara M, Takimoto H, Yorimitsu S, Takahashi I, Miyata A, Taniguchi S, Tokunaga Y, Gondo H, Niho Y, Harada M, et al. Decreases in Ikaros activity correlate with blast crisis in patients with

chronic myelogenous leukemia. Cancer Res. 1999;59(16):3931-4. Epub 1999/08/27. PubMed PMID: 10463586.

103. Yagi T, Hibi S, Takanashi M, Kano G, Tabata Y, Imamura T, Inaba T, Morimoto A, Todo S, Imashuku S. High frequency of Ikaros isoform 6 expression in acute myelomonocytic and monocytic leukemias: implications for up-regulation of the antiapoptotic protein Bcl-XL in leukemogenesis. Blood. 2002;99(4):1350-5. Epub 2002/02/07. PubMed PMID: 11830486.

104. Billot K, Soeur J, Chereau F, Arrouss I, Merle-Beral H, Huang ME, Mazier D, Baud V, Rebollo A. Deregulation of Aiolos expression in chronic lymphocytic leukemia is associated with epigenetic modifications. Blood. 2011;117(6):1917-27. Epub 2010/12/09. doi: 10.1182/blood-2010-09-307140. PubMed PMID: 21139082.

105. Nuckel H, Frey UH, Sellmann L, Collins CH, Duhrsen U, Siffert W. The IKZF3 (Aiolos) transcription factor is highly up-regulated and inversely correlated with clinical progression in chronic lymphocytic leukaemia. Br J Haematol. 2009;144(2):268-70. doi: 10.1111/j.1365-2141.2008.07442.x. PubMed PMID: 19016725.

106. Duhamel M, Arrouss I, Merle-Beral H, Rebollo A. The Aiolos transcription factor is up-regulated in chronic lymphocytic leukemia. Blood. 2008;111(6):3225-8. doi: 10.1182/blood-2007-09-113191. PubMed PMID: 18184862.

107. Godfrey DI, Kennedy J, Suda T, Zlotnik A. A developmental pathway involving four phenotypically and functionally distinct subsets of CD3-CD4-CD8- triple-negative adult mouse thymocytes defined by CD44 and CD25 expression. J Immunol. 1993;150(10):4244-52. Epub 1993/05/15. PubMed PMID: 8387091.

108. Staal FJ, Weerkamp F, Langerak AW, Hendriks RW, Clevers HC. Transcriptional control of t lymphocyte differentiation. Stem Cells. 2001;19(3):165-79. Epub 2001/05/22. doi: 10.1634/stemcells.19-3-165. PubMed PMID: 11359942.

109. Dik WA, Pike-Overzet K, Weerkamp F, de Ridder D, de Haas EF, Baert MR, van der Spek P, Koster EE, Reinders MJ, van Dongen JJ, Langerak AW, Staal FJ. New insights on human T cell development by quantitative T cell receptor gene rearrangement studies and gene expression profiling. J Exp Med. 2005;201(11):1715-23. Epub 2005/06/02. doi: 10.1084/jem.20042524. PubMed PMID: 15928199; PMCID: 2213269.

110. Takeuchi Y, Fujii Y, Okumura M, Inada K, Nakahara K, Matsuda H. Characterization of CD4+ single positive cells that lack CD3 in the human thymus. Cellular immunology. 1993;151(2):481-90. Epub 1993/10/15. doi: 10.1006/cimm.1993.1257. PubMed PMID: 8104713.

111. Nikolic-Zugic J, Bevan MJ. Thymocytes expressing CD8 differentiate into CD4+ cells following intrathymic injection. Proc Natl Acad Sci U S A. 1988;85(22):8633-7. Epub 1988/11/01. PubMed PMID: 3141930; PMCID: 282513.

112. Washburn T, Schweighoffer E, Gridley T, Chang D, Fowlkes BJ, Cado D, Robey E. Notch activity influences the alphabeta versus gammadelta T cell lineage decision. Cell. 1997;88(6):833-43. Epub 1997/03/21. PubMed PMID: 9118226.

113. Garbe AI, Krueger A, Gounari F, Zuniga-Pflucker JC, von Boehmer H. Differential synergy of Notch and T cell receptor signaling determines alphabeta versus gammadelta lineage fate. J Exp Med. 2006;203(6):1579-90. doi: 10.1084/jem.20060474. PubMed PMID: 16754723; PMCID: PMC2118312.

114. Wolfer A, Wilson A, Nemir M, MacDonald HR, Radtke F. Inactivation of Notch1 impairs VDJbeta rearrangement and allows pre-TCR-independent survival of early alpha beta Lineage Thymocytes. Immunity. 2002;16(6):869-79. Epub 2002/07/18. PubMed PMID: 12121668.

115. Blom B, Verschuren MC, Heemskerk MH, Bakker AQ, van Gastel-Mol EJ, Wolvers-Tettero IL, van Dongen JJ, Spits H. TCR gene rearrangements and expression of the pre-T cell receptor complex during human T-cell differentiation. Blood. 1999;93(9):3033-43. PubMed PMID: 10216100.

116. Joachims ML, Chain JL, Hooker SW, Knott-Craig CJ, Thompson LF. Human alpha beta and gamma delta thymocyte development: TCR gene rearrangements, intracellular TCR beta expression, and gamma delta developmental potential--differences between men and mice. J Immunol. 2006;176(3):1543-52. Epub 2006/01/21. PubMed PMID: 16424183; PMCID: 1592528.

117. Taghon T, Van de Walle I, De Smet G, De Smedt M, Leclercq G, Vandekerckhove B, Plum J. Notch signaling is required for proliferation but not for differentiation at a well-defined beta-selection checkpoint during human T-cell development. Blood. 2009;113(14):3254-63. Epub 2008/10/25. doi: 10.1182/blood-2008-07-168906. PubMed PMID: 18948571.

118. Ramiro AR, Trigueros C, Marquez C, San Millan JL, Toribio ML. Regulation of pre-T cell receptor (pT alpha-TCR beta) gene expression during human thymic development. J Exp Med. 1996;184(2):519-30. PubMed PMID: 8760805; PMCID: PMC2192728.

119. Carrasco YR, Trigueros C, Ramiro AR, de Yebenes VG, Toribio ML. Beta-selection is associated with the onset of CD8beta chain expression on CD4(+)CD8alphaalpha(+) pre-T cells during human intrathymic development. Blood. 1999;94(10):3491-8. Epub 1999/11/24. PubMed PMID: 10552959.

120. Galy A, Verma S, Barcena A, Spits H. Precursors of CD3+CD4+CD8+ cells in the human thymus are defined by expression of CD34. Delineation of early events in human thymic development. J Exp Med. 1993;178(2):391-401. PubMed PMID: 7688021; PMCID: PMC2191105.

121. Kraft DL, Weissman IL, Waller EK. Differentiation of CD3-4-8- human fetal thymocytes in vivo: characterization of a CD3-4+8- intermediate. J Exp Med. 1993;178(1):265-77. PubMed PMID: 8315382; PMCID: PMC2191096.

122. Sanchez MJ, Muench MO, Roncarolo MG, Lanier LL, Phillips JH. Identification of a common T/natural killer cell progenitor in human fetal thymus. J Exp Med. 1994;180(2):569-76. PubMed PMID: 7519241; PMCID: PMC2191594.

123. Res P, Martinez-Caceres E, Cristina Jaleco A, Staal F, Noteboom E, Weijer K, Spits H. CD34+CD38dim cells in the human thymus can differentiate into T, natural killer, and dendritic cells but are distinct from pluripotent stem cells. Blood. 1996;87(12):5196-206. PubMed PMID: 8652833.

124. Marquez C, Trigueros C, Franco JM, Ramiro AR, Carrasco YR, Lopez-Botet M, Toribio ML. Identification of a common developmental pathway for thymic natural killer cells and dendritic cells. Blood. 1998;91(8):2760-71. PubMed PMID: 9531586.

125. Weijer K, Uittenbogaart CH, Voordouw A, Couwenberg F, Seppen J, Blom B, Vyth-Dreese FA, Spits H. Intrathymic and extrathymic development of human plasmacytoid dendritic cell precursors in vivo. Blood. 2002;99(8):2752-9. PubMed PMID: 11929763.

126. Marquez C, Trigueros C, Fernandez E, Toribio ML. The development of T and non-T cell lineages from CD34+ human thymic precursors can be traced by the differential expression of CD44. J Exp Med. 1995;181(2):475-83. PubMed PMID: 7530757; PMCID: PMC2191886.

127. Spits H, Blom B, Jaleco AC, Weijer K, Verschuren MC, van Dongen JJ, Heemskerk MH, Res PC. Early stages in the development of human T, natural killer and thymic dendritic cells. Immunol Rev. 1998;165:75-86. PubMed PMID: 9850853.

128. Stewart CA, Walzer T, Robbins SH, Malissen B, Vivier E, Prinz I. Germ-line and rearranged Tcrd transcription distinguish bona fide NK cells and NK-like gammadelta T cells. Eur J Immunol. 2007;37(6):1442-52. doi: 10.1002/eji.200737354. PubMed PMID: 17492716.

129. Biassoni R, Verdiani S, Cambiaggi A, Romeo PH, Ferrini S, Moretta L. Human CD3-CD16+ natural killer cells express the hGATA-3 T cell transcription factor and an unrearranged 2.3-kb TcR delta transcript. Eur J Immunol. 1993;23(5):1083-7. doi: 10.1002/eji.1830230516. PubMed PMID: 8386664.

130. Van de Walle I, De Smet G, De Smedt M, Vandekerckhove B, Leclercq G, Plum J, Taghon T. An early decrease in Notch activation is required for human TCR-alphabeta lineage differentiation at the expense of TCR-gammadelta T cells. Blood. 2009;113(13):2988-98. Epub 2008/12/06. doi: 10.1182/blood-2008-06-164871. PubMed PMID: 19056690.

131. Van de Walle I, Waegemans E, De Medts J, De Smet G, De Smedt M, Snauwaert S, Vandekerckhove B, Kerre T, Leclercq G, Plum J, Gridley T, Wang T, Koch U, Radtke F, Taghon T. Specific Notch receptor-ligand interactions control human TCR-alphabeta/gammadelta development by inducing differential Notch signal strength. J Exp Med. 2013;210(4):683-97. doi: 10.1084/jem.20121798. PubMed PMID: 23530123; PMCID: PMC3620353.

132. La Motte-Mohs RN, Herer E, Zuniga-Pflucker JC. Induction of T-cell development from human cord blood hematopoietic stem cells by Delta-like 1 in vitro. Blood. 2005;105(4):1431-9. doi: 10.1182/blood-2004-04-1293. PubMed PMID: 15494433.

133. De Smedt M, Hoebeke I, Plum J. Human bone marrow CD34+ progenitor cells mature to T cells on OP9-DL1 stromal cell line without thymus microenvironment. Blood cells, molecules & diseases. 2004;33(3):227-32. doi: 10.1016/j.bcmd.2004.08.007. PubMed PMID: 15528136.

134. De Smedt M, Reynvoet K, Kerre T, Taghon T, Verhasselt B, Vandekerckhove B, Leclercq G, Plum J. Active form of Notch imposes T cell fate in human progenitor cells. J Immunol. 2002;169(6):3021-9. PubMed PMID: 12218117.

135. De Smedt M, Hoebeke I, Reynvoet K, Leclercq G, Plum J. Different thresholds of Notch signaling bias human precursor cells toward B-, NK-, monocytic/dendritic-, or T-cell lineage in thymus microenvironment. Blood. 2005;106(10):3498-506. doi: 10.1182/blood-2005-02-0496. PubMed PMID: 16030192.

136. Halkias J, Melichar HJ, Taylor KT, Robey EA. Tracking migration during human T cell development. Cell Mol Life Sci. 2014;71(16):3101-17. doi: 10.1007/s00018-014-1607-2. PubMed PMID: 24682469.

137. Van de Walle I, De Smet G, Gartner M, De Smedt M, Waegemans E, Vandekerckhove B, Leclercq G, Plum J, Aster JC, Bernstein ID, Guidos CJ, Kyewski B, Taghon T. Jagged2 acts as a Delta-like Notch ligand during early hematopoietic cell fate decisions. Blood. 2011;117(17):4449-59. doi: 10.1182/blood-2010-06-290049. PubMed PMID: 21372153; PMCID: PMC3673751.

138. Neves H, Weerkamp F, Gomes AC, Naber BA, Gameiro P, Becker JD, Lucio P, Clode N, van Dongen JJ, Staal FJ, Parreira L. Effects of Delta1 and Jagged1 on early human hematopoiesis: correlation with expression of notch signaling-related genes in CD34+ cells. Stem Cells. 2006;24(5):1328-37. doi: 10.1634/stemcells.2005-0207. PubMed PMID: 16410393.

139. Nwabo Kamdje AH, Mosna F, Bifari F, Lisi V, Bassi G, Malpeli G, Ricciardi M, Perbellini O, Scupoli MT, Pizzolo G, Krampera M. Notch-3 and Notch-4 signaling rescue from apoptosis human B-ALL cells in contact with human bone marrow-derived mesenchymal stromal cells. Blood. 2011;118(2):380-9. doi: 10.1182/blood-2010-12-326694. PubMed PMID: 21602525.

140. Liotta F, Angeli R, Cosmi L, Fili L, Manuelli C, Frosali F, Mazzinghi B, Maggi L, Pasini A, Lisi V, Santarlasci V, Consoloni L, Angelotti ML, Romagnani P, Parronchi P, Krampera M, Maggi E, Romagnani S, Annunziato F. Toll-like receptors 3 and 4 are expressed by human bone marrow-derived mesenchymal stem cells and can inhibit their T-cell modulatory activity by

impairing Notch signaling. Stem Cells. 2008;26(1):279-89. doi: 10.1634/stemcells.2007-0454. PubMed PMID: 17962701.

141. Li L, Milner LA, Deng Y, Iwata M, Banta A, Graf L, Marcovina S, Friedman C, Trask BJ, Hood L, Torok-Storb B. The human homolog of rat Jagged1 expressed by marrow stroma inhibits differentiation of 32D cells through interaction with Notch1. Immunity. 1998;8(1):43-55. PubMed PMID: 9462510.

142. Matsuoka Y, Nakatsuka R, Sumide K, Kawamura H, Takahashi M, Fujioka T, Uemura Y, Asano H, Sasaki Y, Inoue M, Ogawa H, Takahashi T, Hino M, Sonoda Y. Prospectively Isolated Human Bone Marrow Cell-Derived MSCs Support Primitive Human CD34-Negative Hematopoietic Stem Cells. Stem Cells. 2015;33(5):1554-65. doi: 10.1002/stem.1941. PubMed PMID: 25537923.

143. Garcia-Peydro M, de Yebenes VG, Toribio ML. Notch1 and IL-7 receptor interplay maintains proliferation of human thymic progenitors while suppressing non-T cell fates. J Immunol. 2006;177(6):3711-20. PubMed PMID: 16951331.

144. Magri M, Yatim A, Benne C, Balbo M, Henry A, Serraf A, Sakano S, Gazzolo L, Levy Y, Lelievre JD. Notch ligands potentiate IL-7-driven proliferation and survival of human thymocyte precursors. Eur J Immunol. 2009;39(5):1231-40. Epub 2009/04/08. doi: 10.1002/eji.200838765. PubMed PMID: 19350552.

145. Wiekmeijer AS, Pike-Overzet K, H IJ, Brugman MH, Wolvers-Tettero IL, Lankester AC, Bredius RG, van Dongen JJ, Fibbe WE, Langerak AW, van der Burg M, Staal FJ. Identification

of checkpoints in human T-cell development using severe combined immunodeficiency stem cells. J Allergy Clin Immunol. 2015. doi: 10.1016/j.jaci.2015.08.022. PubMed PMID: 26441229.

146. Vroom TM, Scholte G, Ossendorp F, Borst J. Tissue distribution of human gamma delta T cells: no evidence for general epithelial tropism. J Clin Pathol. 1991;44(12):1012-7. PubMed PMID: 1838746; PMCID: PMC494970.

147. Falini B, Flenghi L, Pileri S, Pelicci P, Fagioli M, Martelli MF, Moretta L, Ciccone E. Distribution of T cells bearing different forms of the T cell receptor gamma/delta in normal and pathological human tissues. J Immunol. 1989;143(8):2480-8. PubMed PMID: 2477444.

148. Groh V, Porcelli S, Fabbi M, Lanier LL, Picker LJ, Anderson T, Warnke RA, Bhan AK, Strominger JL, Brenner MB. Human lymphocytes bearing T cell receptor gamma/delta are phenotypically diverse and evenly distributed throughout the lymphoid system. J Exp Med. 1989;169(4):1277-94. PubMed PMID: 2564416; PMCID: PMC2189233.

149. Borst J, van Dongen JJ, Bolhuis RL, Peters PJ, Hafler DA, de Vries E, van de Griend RJ. Distinct molecular forms of human T cell receptor gamma/delta detected on viable T cells by a monoclonal antibody. J Exp Med. 1988;167(5):1625-44. PubMed PMID: 2966845; PMCID: PMC2188932.

150. Bordessoule D, Gaulard P, Mason DY. Preferential localisation of human lymphocytes bearing gamma delta T cell receptors to the red pulp of the spleen. J Clin Pathol. 1990;43(6):461-4. PubMed PMID: 2143201; PMCID: PMC502497.

151. Van Coppernolle S, Vanhee S, Verstichel G, Snauwaert S, van der Spek A, Velghe I, Sinnesael M, Heemskerk MH, Taghon T, Leclercq G, Plum J, Langerak AW, Kerre T, Vandekerckhove B. Notch induces human T-cell receptor gammadelta+ thymocytes to differentiate along a parallel, highly proliferative and bipotent CD4 CD8 double-positive pathway. Leukemia. 2012;26(1):127-38. doi: 10.1038/leu.2011.324. PubMed PMID: 22051534.

152. Offner F, Van Beneden K, Debacker V, Vanhecke D, Vandekerckhove B, Plum J, Leclercq G. Phenotypic and functional maturation of TCR gammadelta cells in the human thymus. J Immunol. 1997;158(10):4634-41. PubMed PMID: 9144475.

153. Leduc I, Hempel WM, Mathieu N, Verthuy C, Bouvier G, Watrin F, Ferrier P. T cell development in TCR beta enhancer-deleted mice: implications for alpha beta T cell lineage commitment and differentiation. J Immunol. 2000;165(3):1364-73. PubMed PMID: 10903739.

154. Livak F, Tourigny M, Schatz DG, Petrie HT. Characterization of TCR gene rearrangements during adult murine T cell development. J Immunol. 1999;162(5):2575-80. Epub 1999/03/11. PubMed PMID: 10072498.

155. Dudley EC, Girardi M, Owen MJ, Hayday AC. Alpha beta and gamma delta T cells can share a late common precursor. Current biology : CB. 1995;5(6):659-69. PubMed PMID: 7552177.

156. Winoto A, Baltimore D. Separate lineages of T cells expressing the alpha beta and gamma delta receptors. Nature. 1989;338(6214):430-2. doi: 10.1038/338430a0. PubMed PMID: 2927503.

157. Kang J, Baker J, Raulet DH. Evidence that productive rearrangements of TCR gamma genes influence the commitment of progenitor cells to differentiate into alpha beta or gamma delta T cells. Eur J Immunol. 1995;25(9):2706-9. doi: 10.1002/eji.1830250946. PubMed PMID: 7589149.

158. Haks MC, Lefebvre JM, Lauritsen JP, Carleton M, Rhodes M, Miyazaki T, Kappes DJ, Wiest DL. Attenuation of gammadeltaTCR signaling efficiently diverts thymocytes to the alphabeta lineage. Immunity. 2005;22(5):595-606. doi: 10.1016/j.immuni.2005.04.003. PubMed PMID: 15894277.

159. Hayes SM, Li L, Love PE. TCR signal strength influences alphabeta/gammadelta lineage fate. Immunity. 2005;22(5):583-93. doi: 10.1016/j.immuni.2005.03.014. PubMed PMID: 15894276.

160. Zarin P, Wong GW, Mohtashami M, Wiest DL, Zuniga-Pflucker JC. Enforcement of gammadelta-lineage commitment by the pre-T-cell receptor in precursors with weak gammadelta-TCR signals. Proc Natl Acad Sci U S A. 2014;111(15):5658-63. doi: 10.1073/pnas.1312872111. PubMed PMID: 24706811; PMCID: PMC3992653.

161. Margolis D, Yassai M, Hletko A, McOlash L, Gorski J. Concurrent or sequential delta and beta TCR gene rearrangement during thymocyte development: individual thymi follow distinct pathways. J Immunol. 1997;159(2):529-33. PubMed PMID: 9218565.

162. Sherwood AM, Desmarais C, Livingston RJ, Andriesen J, Haussler M, Carlson CS, Robins H. Deep sequencing of the human TCRgamma and TCRbeta repertoires suggests that TCRbeta rearranges after alphabeta and gammadelta T cell commitment. Science translational

medicine. 2011;3(90):90ra61. Epub 2011/07/08. doi: 10.1126/scitranslmed.3002536. PubMed PMID: 21734177; PMCID: 4179204.

163. Couedel C, Lippert E, Bernardeau K, Bonneville M, Davodeau F. Allelic exclusion at the TCR delta locus and commitment to gamma delta lineage: different modalities apply to distinct human gamma delta subsets. J Immunol. 2004;172(9):5544-52. PubMed PMID: 15100297.

164. Garcia-Peydro M, de Yebenes VG, Toribio ML. Sustained Notch1 signaling instructs the earliest human intrathymic precursors to adopt a gammadelta T-cell fate in fetal thymus organ culture. Blood. 2003;102(7):2444-51. Epub 2003/06/28. doi: 10.1182/blood-2002-10-3261. PubMed PMID: 12829602.

165. Saint-Ruf C, Panigada M, Azogui O, Debey P, von Boehmer H, Grassi F. Different initiation of pre-TCR and gammadeltaTCR signalling. Nature. 2000;406(6795):524-7. doi: 10.1038/35020093. PubMed PMID: 10952314.

166. Ramiro AR, Navarro MN, Carreira A, Carrasco YR, de Yebenes VG, Carrillo G, San Millan JL, Rubin B, Toribio ML. Differential developmental regulation and functional effects on pre-TCR surface expression of human pTalpha(a) and pTalpha(b) spliced isoforms. J Immunol. 2001;167(9):5106-14. PubMed PMID: 11673521.

167. Aifantis I, Borowski C, Gounari F, Lacorazza HD, Nikolich-Zugich J, von Boehmer H. A critical role for the cytoplasmic tail of pTalpha in T lymphocyte development. Nat Immunol. 2002;3(5):483-8. doi: 10.1038/ni779. PubMed PMID: 11927911.

168. Carrasco YR, Navarro MN, de Yebenes VG, Ramiro AR, Toribio ML. Regulation of surface expression of the human pre-T cell receptor complex. Semin Immunol. 2002;14(5):325-34. PubMed PMID: 12220933.

169. Carrasco YR, Ramiro AR, Trigueros C, de Yebenes VG, Garcia-Peydro M, Toribio ML. An endoplasmic reticulum retention function for the cytoplasmic tail of the human pre-T cell receptor (TCR) alpha chain: potential role in the regulation of cell surface pre-TCR expression levels. J Exp Med. 2001;193(9):1045-58. PubMed PMID: 11342589; PMCID: PMC2193431.

170. Carrasco YR, Navarro MN, Toribio ML. A role for the cytoplasmic tail of the pre-T cell receptor (TCR) alpha chain in promoting constitutive internalization and degradation of the pre-TCR. J Biol Chem. 2003;278(16):14507-13. doi: 10.1074/jbc.M204944200. PubMed PMID: 12473666.

171. Pang SS, Berry R, Chen Z, Kjer-Nielsen L, Perugini MA, King GF, Wang C, Chew SH, La Gruta NL, Williams NK, Beddoe T, Tiganis T, Cowieson NP, Godfrey DI, Purcell AW, Wilce MC, McCluskey J, Rossjohn J. The structural basis for autonomous dimerization of the pre-T-cell antigen receptor. Nature. 2010;467(7317):844-8. doi: 10.1038/nature09448. PubMed PMID: 20944746.

172. Irving BA, Alt FW, Killeen N. Thymocyte development in the absence of pre-T cell receptor extracellular immunoglobulin domains. Science. 1998;280(5365):905-8. PubMed PMID: 9572735.

173. Mahtani-Patching J, Neves JF, Pang DJ, Stoenchev KV, Aguirre-Blanco AM, Silva-Santos B, Pennington DJ. PreTCR and TCRgammadelta signal initiation in thymocyte

progenitors does not require domains implicated in receptor oligomerization. Science signaling. 2011;4(182):ra47. doi: 10.1126/scisignal.2001765. PubMed PMID: 21775286; PMCID: PMC3475409.

174. Mallis RJ, Bai K, Arthanari H, Hussey RE, Handley M, Li Z, Chingozha L, Duke-Cohan JS, Lu H, Wang JH, Zhu C, Wagner G, Reinherz EL. Pre-TCR ligand binding impacts thymocyte development before alphabetaTCR expression. Proc Natl Acad Sci U S A. 2015;112(27):8373-8. doi: 10.1073/pnas.1504971112. PubMed PMID: 26056289; PMCID: PMC4500245.

175. Bruno L, Res P, Dessing M, Cella M, Spits H. Identification of a committed T cell precursor population in adult human peripheral blood. J Exp Med. 1997;185(5):875-84. PubMed PMID: 9120393; PMCID: PMC2196171.

176. Long H, Gaffney P, Mortari F, Miller JS. CD3 gamma, CD3 delta, and CD3 zeta mRNA in adult human marrow hematopoietic progenitors correlates with surface CD2 and CD7 expression. Exp Hematol. 1996;24(12):1402-8. PubMed PMID: 8913286.

177. Michie AM, Zuniga-Pflucker JC. Regulation of thymocyte differentiation: pre-TCR signals and beta-selection. Semin Immunol. 2002;14(5):311-23. Epub 2002/09/11. PubMed PMID: 12220932.

178. Aifantis I, Gounari F, Scorrano L, Borowski C, von Boehmer H. Constitutive pre-TCR signaling promotes differentiation through Ca2+ mobilization and activation of NF-kappaB and NFAT. Nat Immunol. 2001;2(5):403-9. Epub 2001/04/27. doi: 10.1038/87704. PubMed PMID: 11323693.

179. Fehling HJ, Krotkova A, Saint-Ruf C, von Boehmer H. Crucial role of the pre-T-cell receptor alpha gene in development of alpha beta but not gamma delta T cells. Nature. 1995;375(6534):795-8. Epub 1995/06/29. doi: 10.1038/375795a0. PubMed PMID: 7596413.

180. Hoffman ES, Passoni L, Crompton T, Leu TM, Schatz DG, Koff A, Owen MJ, Hayday AC. Productive T-cell receptor beta-chain gene rearrangement: coincident regulation of cell cycle and clonality during development in vivo. Genes Dev. 1996;10(8):948-62. PubMed PMID: 8608942.

181. Aifantis I, Buer J, von Boehmer H, Azogui O. Essential role of the pre-T cell receptor in allelic exclusion of the T cell receptor beta locus. Immunity. 1997;7(5):601-7. PubMed PMID: 9390684.

182. Swat W, Shinkai Y, Cheng HL, Davidson L, Alt FW. Activated Ras signals differentiation and expansion of CD4+8+ thymocytes. Proc Natl Acad Sci U S A. 1996;93(10):4683-7. PubMed PMID: 8643464; PMCID: PMC39339.

183. Iritani BM, Alberola-Ila J, Forbush KA, Perimutter RM. Distinct signals mediate maturation and allelic exclusion in lymphocyte progenitors. Immunity. 1999;10(6):713-22. PubMed PMID: 10403646.

184. Gartner F, Alt FW, Monroe R, Chu M, Sleckman BP, Davidson L, Swat W. Immature thymocytes employ distinct signaling pathways for allelic exclusion versus differentiation and expansion. Immunity. 1999;10(5):537-46. PubMed PMID: 10367899.

185. Michie AM, Soh JW, Hawley RG, Weinstein IB, Zuniga-Pflucker JC. Allelic exclusion and differentiation by protein kinase C-mediated signals in immature thymocytes. Proc Natl Acad Sci U S A. 2001;98(2):609-14. doi: 10.1073/pnas.021288598. PubMed PMID: 11149941; PMCID: PMC14635.

186. Uematsu Y, Ryser S, Dembic Z, Borgulya P, Krimpenfort P, Berns A, von Boehmer H, Steinmetz M. In transgenic mice the introduced functional T cell receptor beta gene prevents expression of endogenous beta genes. Cell. 1988;52(6):831-41. PubMed PMID: 3258191.

187. Anderson SJ, Abraham KM, Nakayama T, Singer A, Perlmutter RM. Inhibition of T-cell receptor beta-chain gene rearrangement by overexpression of the non-receptor protein tyrosine kinase p56lck. EMBO J. 1992;11(13):4877-86. PubMed PMID: 1334460; PMCID: PMC556965.

188. Anderson SJ, Levin SD, Perlmutter RM. Protein tyrosine kinase p56lck controls allelic exclusion of T-cell receptor beta-chain genes. Nature. 1993;365(6446):552-4. doi: 10.1038/365552a0. PubMed PMID: 8413611.

189. Jackson AM, Krangel MS. A role for MAPK in feedback inhibition of Tcrb recombination. J Immunol. 2006;176(11):6824-30. PubMed PMID: 16709842.

190. Eyquem S, Chemin K, Fasseu M, Bories JC. The Ets-1 transcription factor is required for complete pre-T cell receptor function and allelic exclusion at the T cell receptor beta locus. Proc Natl Acad Sci U S A. 2004;101(44):15712-7. doi: 10.1073/pnas.0405546101. PubMed PMID: 15496469; PMCID: PMC524847.

191. O'Shea CC, Thornell AP, Rosewell IR, Hayes B, Owen MJ. Exit of the pre-TCR from the ER/cis-Golgi is necessary for signaling differentiation, proliferation, and allelic exclusion in immature thymocytes. Immunity. 1997;7(5):591-9. PubMed PMID: 9390683.

192. Kisielow P, Bluthmann H, Staerz UD, Steinmetz M, von Boehmer H. Tolerance in T-cell-receptor transgenic mice involves deletion of nonmature CD4+8+ thymocytes. Nature. 1988;333(6175):742-6. doi: 10.1038/333742a0. PubMed PMID: 3260350.

193. Ober BT, Hu Q, Opferman JT, Hagevik S, Chiu N, Wang CR, Ashton-Rickardt PG. Affinity of thymic self-peptides for the TCR determines the selection of CD8(+) T lymphocytes in the thymus. Int Immunol. 2000;12(9):1353-63. PubMed PMID: 10967031.

194. Alam SM, Davies GM, Lin CM, Zal T, Nasholds W, Jameson SC, Hogquist KA, Gascoigne NR, Travers PJ. Qualitative and quantitative differences in T cell receptor binding of agonist and antagonist ligands. Immunity. 1999;10(2):227-37. PubMed PMID: 10072075.

195. Alam SM, Travers PJ, Wung JL, Nasholds W, Redpath S, Jameson SC, Gascoigne NR. T-cell-receptor affinity and thymocyte positive selection. Nature. 1996;381(6583):616-20. doi: 10.1038/381616a0. PubMed PMID: 8637599.

196. Juang J, Ebert PJ, Feng D, Garcia KC, Krogsgaard M, Davis MM. Peptide-MHC heterodimers show that thymic positive selection requires a more restricted set of self-peptides than negative selection. J Exp Med. 2010;207(6):1223-34. doi: 10.1084/jem.20092170. PubMed PMID: 20457759; PMCID: PMC2882826.

197. Naeher D, Daniels MA, Hausmann B, Guillaume P, Luescher I, Palmer E. A constant affinity threshold for T cell tolerance. J Exp Med. 2007;204(11):2553-9. doi: 10.1084/jem.20070254. PubMed PMID: 17938233; PMCID: PMC2118488.

198. Savage PA, Davis MM. A kinetic window constricts the T cell receptor repertoire in the thymus. Immunity. 2001;14(3):243-52. PubMed PMID: 11290334.

199. Gronski MA, Boulter JM, Moskophidis D, Nguyen LT, Holmberg K, Elford AR, Deenick EK, Kim HO, Penninger JM, Odermatt B, Gallimore A, Gascoigne NR, Ohashi PS. TCR affinity and negative regulation limit autoimmunity. Nat Med. 2004;10(11):1234-9. doi: 10.1038/nm1114. PubMed PMID: 15467726.

200. Williams CB, Engle DL, Kersh GJ, Michael White J, Allen PM. A kinetic threshold between negative and positive selection based on the longevity of the T cell receptor-ligand complex. J Exp Med. 1999;189(10):1531-44. PubMed PMID: 10330432; PMCID: PMC2193645.

201. Daniels MA, Teixeiro E, Gill J, Hausmann B, Roubaty D, Holmberg K, Werlen G, Hollander GA, Gascoigne NR, Palmer E. Thymic selection threshold defined by compartmentalization of Ras/MAPK signalling. Nature. 2006;444(7120):724-9. doi: 10.1038/nature05269. PubMed PMID: 17086201.

202. Fruh K, Gossen M, Wang K, Bujard H, Peterson PA, Yang Y. Displacement of housekeeping proteasome subunits by MHC-encoded LMPs: a newly discovered mechanism for modulating the multicatalytic proteinase complex. EMBO J. 1994;13(14):3236-44. PubMed PMID: 8045254; PMCID: PMC395220.

203. Nandi D, Jiang H, Monaco JJ. Identification of MECL-1 (LMP-10) as the third IFN-gamma-inducible proteasome subunit. J Immunol. 1996;156(7):2361-4. PubMed PMID: 8786291.

204. Groettrup M, Kraft R, Kostka S, Standera S, Stohwasser R, Kloetzel PM. A third interferon-gamma-induced subunit exchange in the 20S proteasome. Eur J Immunol. 1996;26(4):863-9. doi: 10.1002/eji.1830260421. PubMed PMID: 8625980.

205. Aki M, Shimbara N, Takashina M, Akiyama K, Kagawa S, Tamura T, Tanahashi N, Yoshimura T, Tanaka K, Ichihara A. Interferon-gamma induces different subunit organizations and functional diversity of proteasomes. J Biochem. 1994;115(2):257-69. PubMed PMID: 8206875.

206. Gaczynska M, Rock KL, Goldberg AL. Gamma-interferon and expression of MHC genes regulate peptide hydrolysis by proteasomes. Nature. 1993;365(6443):264-7. doi: 10.1038/365264a0. PubMed PMID: 8396732.

207. Driscoll J, Brown MG, Finley D, Monaco JJ. MHC-linked LMP gene products specifically alter peptidase activities of the proteasome. Nature. 1993;365(6443):262-4. doi: 10.1038/365262a0. PubMed PMID: 8371781.

208. Murata S, Sasaki K, Kishimoto T, Niwa S, Hayashi H, Takahama Y, Tanaka K. Regulation of CD8+ T cell development by thymus-specific proteasomes. Science. 2007;316(5829):1349-53. doi: 10.1126/science.1141915. PubMed PMID: 17540904.

209. Florea BI, Verdoes M, Li N, van der Linden WA, Geurink PP, van den Elst H, Hofmann T, de Ru A, van Veelen PA, Tanaka K, Sasaki K, Murata S, den Dulk H, Brouwer J, Ossendorp FA, Kisselev AF, Overkleeft HS. Activity-based profiling reveals reactivity of the murine thymoproteasome-specific subunit beta5t. Chem Biol. 2010;17(8):795-801. doi: 10.1016/j.chembiol.2010.05.027. PubMed PMID: 20797608; PMCID: PMC3039300.

210. Sasaki K, Takada K, Ohte Y, Kondo H, Sorimachi H, Tanaka K, Takahama Y, Murata S. Thymoproteasomes produce unique peptide motifs for positive selection of CD8(+) T cells. Nat Commun. 2015;6:7484. doi: 10.1038/ncomms8484. PubMed PMID: 26099460; PMCID: PMC4557289.

211. Benjamin RJ, Madrigal JA, Parham P. Peptide binding to empty HLA-B27 molecules of viable human cells. Nature. 1991;351(6321):74-7. doi: 10.1038/351074a0. PubMed PMID: 2027387.

212. Rehm A, Rohr A, Seitz C, Wonigeit K, Ziegler A, Uchanska-Ziegler B. Structurally diverse forms of HLA-B27 molecules are displayed in vivo in a cell type-dependent manner. Hum Immunol. 2000;61(4):408-18. PubMed PMID: 10715518.

213. Rouse RV, Parham P, Grumet FC, Weissman IL. Expression of HLA antigens by human thymic epithelial cells. Hum Immunol. 1982;5(1):21-34. PubMed PMID: 6956563.

214. Heinrichs H, Wernet P, Ziegler A. Expression of major histocompatibility antigens on human thymocytes studied using monoclonal antibodies. Immunogenetics. 1980;11(6):629-35. PubMed PMID: 6242892.

215. Xing Y, Jameson SC, Hogquist KA. Thymoproteasome subunit-beta5T generates peptide-MHC complexes specialized for positive selection. Proc Natl Acad Sci U S A. 2013;110(17):6979-84. doi: 10.1073/pnas.1222244110. PubMed PMID: 23569244; PMCID: PMC3637736.

216. Nitta T, Murata S, Sasaki K, Fujii H, Ripen AM, Ishimaru N, Koyasu S, Tanaka K, Takahama Y. Thymoproteasome shapes immunocompetent repertoire of CD8+ T cells. Immunity. 2010;32(1):29-40. doi: 10.1016/j.immuni.2009.10.009. PubMed PMID: 20045355.

217. Nedjic J, Aichinger M, Emmerich J, Mizushima N, Klein L. Autophagy in thymic epithelium shapes the T-cell repertoire and is essential for tolerance. Nature. 2008;455(7211):396-400. doi: 10.1038/nature07208. PubMed PMID: 18701890.

218. Ziegler A, Muller CA, Bockmann RA, Uchanska-Ziegler B. Low-affinity peptides and T-cell selection. Trends Immunol. 2009;30(2):53-60. doi: 10.1016/j.it.2008.11.004. PubMed PMID: 19201651.

219. Stoeckle C, Quecke P, Ruckrich T, Burster T, Reich M, Weber E, Kalbacher H, Driessen C, Melms A, Tolosa E. Cathepsin S dominates autoantigen processing in human thymic dendritic cells. J Autoimmun. 2012;38(4):332-43. doi: 10.1016/j.jaut.2012.02.003. PubMed PMID: 22424724.

220. Bromme D, Li Z, Barnes M, Mehler E. Human cathepsin V functional expression, tissue distribution, electrostatic surface potential, enzymatic characterization, and chromosomal localization. Biochemistry. 1999;38(8):2377-85. doi: 10.1021/bi982175f. PubMed PMID: 10029531.

221. Nakagawa T, Roth W, Wong P, Nelson A, Farr A, Deussing J, Villadangos JA, Ploegh H, Peters C, Rudensky AY. Cathepsin L: critical role in Ii degradation and CD4 T cell selection in the thymus. Science. 1998;280(5362):450-3. PubMed PMID: 9545226.

222. Riese RJ, Mitchell RN, Villadangos JA, Shi GP, Palmer JT, Karp ER, De Sanctis GT, Ploegh HL, Chapman HA. Cathepsin S activity regulates antigen presentation and immunity. J Clin Invest. 1998;101(11):2351-63. doi: 10.1172/JCI1158. PubMed PMID: 9616206; PMCID: PMC508824.

223. Shi GP, Villadangos JA, Dranoff G, Small C, Gu L, Haley KJ, Riese R, Ploegh HL, Chapman HA. Cathepsin S required for normal MHC class II peptide loading and germinal center development. Immunity. 1999;10(2):197-206. PubMed PMID: 10072072.

224. Honey K, Nakagawa T, Peters C, Rudensky A. Cathepsin L regulates CD4+ T cell selection independently of its effect on invariant chain: a role in the generation of positively selecting peptide ligands. J Exp Med. 2002;195(10):1349-58. PubMed PMID: 12021314; PMCID: PMC2193748.

225. Nakagawa TY, Brissette WH, Lira PD, Griffiths RJ, Petrushova N, Stock J, McNeish JD, Eastman SE, Howard ED, Clarke SR, Rosloniec EF, Elliott EA, Rudensky AY. Impaired invariant chain degradation and antigen presentation and diminished collagen-induced arthritis in cathepsin S null mice. Immunity. 1999;10(2):207-17. PubMed PMID: 10072073.

226. Hsieh CS, deRoos P, Honey K, Beers C, Rudensky AY. A role for cathepsin L and cathepsin S in peptide generation for MHC class II presentation. J Immunol. 2002;168(6):2618-25. PubMed PMID: 11884425.

227. Cheunsuk S, Lian ZX, Yang GX, Gershwin ME, Gruen JR, Bowlus CL. Prss16 is not required for T-cell development. Mol Cell Biol. 2005;25(2):789-96. doi: 10.1128/MCB.25.2.789-796.2005. PubMed PMID: 15632078; PMCID: PMC543420.

228. Gommeaux J, Gregoire C, Nguessan P, Richelme M, Malissen M, Guerder S, Malissen B, Carrier A. Thymus-specific serine protease regulates positive selection of a subset of CD4+ thymocytes. Eur J Immunol. 2009;39(4):956-64. doi: 10.1002/eji.200839175. PubMed PMID: 19283781.

229. Viret C, Leung-Theung-Long S, Serre L, Lamare C, Vignali DA, Malissen B, Carrier A, Guerder S. Thymus-specific serine protease controls autoreactive CD4 T cell development and autoimmune diabetes in mice. J Clin Invest. 2011;121(5):1810-21. doi: 10.1172/JCI43314. PubMed PMID: 21505262; PMCID: PMC3083765.

230. Viret C, Lamare C, Guiraud M, Fazilleau N, Bour A, Malissen B, Carrier A, Guerder S. Thymus-specific serine protease contributes to the diversification of the functional endogenous CD4 T cell receptor repertoire. J Exp Med. 2011;208(1):3-11. doi: 10.1084/jem.20100027. PubMed PMID: 21173102; PMCID: PMC3023141.

231. Sansom SN, Shikama-Dorn N, Zhanybekova S, Nusspaumer G, Macaulay IC, Deadman ME, Heger A, Ponting CP, Hollander GA. Population and single-cell genomics reveal the Aire dependency, relief from Polycomb silencing, and distribution of self-antigen expression in thymic epithelia. Genome Res. 2014;24(12):1918-31. doi: 10.1101/gr.171645.113. PubMed PMID: 25224068; PMCID: PMC4248310.

232. Anderson MS, Venanzi ES, Klein L, Chen Z, Berzins SP, Turley SJ, von Boehmer H, Bronson R, Dierich A, Benoist C, Mathis D. Projection of an immunological self shadow within the thymus by the aire protein. Science. 2002;298(5597):1395-401. doi: 10.1126/science.1075958. PubMed PMID: 12376594.

233. Gotter J, Brors B, Hergenhahn M, Kyewski B. Medullary epithelial cells of the human thymus express a highly diverse selection of tissue-specific genes colocalized in chromosomal clusters. J Exp Med. 2004;199(2):155-66. doi: 10.1084/jem.20031677. PubMed PMID: 14734521; PMCID: PMC2211762.

234. St-Pierre C, Brochu S, Vanegas JR, Dumont-Lagace M, Lemieux S, Perreault C. Transcriptome sequencing of neonatal thymic epithelial cells. Sci Rep. 2013;3:1860. doi: 10.1038/srep01860. PubMed PMID: 23681267; PMCID: PMC3656389.

235. Finnish-German AC. An autoimmune disease, APECED, caused by mutations in a novel gene featuring two PHD-type zinc-finger domains. Nat Genet. 1997;17(4):399-403. doi: 10.1038/ng1297-399. PubMed PMID: 9398840.

236. Nagamine K, Peterson P, Scott HS, Kudoh J, Minoshima S, Heino M, Krohn KJ, Lalioti MD, Mullis PE, Antonarakis SE, Kawasaki K, Asakawa S, Ito F, Shimizu N. Positional cloning of the APECED gene. Nat Genet. 1997;17(4):393-8. doi: 10.1038/ng1297-393. PubMed PMID: 9398839.

237. Ramsey C, Winqvist O, Puhakka L, Halonen M, Moro A, Kampe O, Eskelin P, Pelto-Huikko M, Peltonen L. Aire deficient mice develop multiple features of APECED phenotype and

show altered immune response. Hum Mol Genet. 2002;11(4):397-409. PubMed PMID: 11854172.

238. Kuroda N, Mitani T, Takeda N, Ishimaru N, Arakaki R, Hayashi Y, Bando Y, Izumi K, Takahashi T, Nomura T, Sakaguchi S, Ueno T, Takahama Y, Uchida D, Sun S, Kajiura F, Mouri Y, Han H, Matsushima A, Yamada G, Matsumoto M. Development of autoimmunity against transcriptionally unrepressed target antigen in the thymus of Aire-deficient mice. J Immunol. 2005;174(4):1862-70. PubMed PMID: 15699112.

239. Anderson MS, Venanzi ES, Chen Z, Berzins SP, Benoist C, Mathis D. The cellular mechanism of Aire control of T cell tolerance. Immunity. 2005;23(2):227-39. doi: 10.1016/j.immuni.2005.07.005. PubMed PMID: 16111640.

240. Org T, Chignola F, Hetenyi C, Gaetani M, Rebane A, Liiv I, Maran U, Mollica L, Bottomley MJ, Musco G, Peterson P. The autoimmune regulator PHD finger binds to non-methylated histone H3K4 to activate gene expression. EMBO Rep. 2008;9(4):370-6. doi: 10.1038/sj.embor.2008.11. PubMed PMID: 18292755; PMCID: PMC2261226.

241. Chakravarty S, Zeng L, Zhou MM. Structure and site-specific recognition of histone H3 by the PHD finger of human autoimmune regulator. Structure. 2009;17(5):670-9. doi: 10.1016/j.str.2009.02.017. PubMed PMID: 19446523; PMCID: PMC2923636.

242. Waterfield M, Khan IS, Cortez JT, Fan U, Metzger T, Greer A, Fasano K, Martinez-Llordella M, Pollack JL, Erle DJ, Su M, Anderson MS. The transcriptional regulator Aire coopts the repressive ATF7ip-MBD1 complex for the induction of immunotolerance. Nat Immunol. 2014;15(3):258-65. doi: 10.1038/ni.2820. PubMed PMID: 24464130; PMCID: PMC4172453.

243. Abramson J, Giraud M, Benoist C, Mathis D. Aire's partners in the molecular control of immunological tolerance. Cell. 2010;140(1):123-35. doi: 10.1016/j.cell.2009.12.030. PubMed PMID: 20085707.

244. Liiv I, Rebane A, Org T, Saare M, Maslovskaja J, Kisand K, Juronen E, Valmu L, Bottomley MJ, Kalkkinen N, Peterson P. DNA-PK contributes to the phosphorylation of AIRE: importance in transcriptional activity. Biochim Biophys Acta. 2008;1783(1):74-83. doi: 10.1016/j.bbamcr.2007.09.003. PubMed PMID: 17997173; PMCID: PMC2225445.

245. Pitkanen J, Doucas V, Sternsdorf T, Nakajima T, Aratani S, Jensen K, Will H, Vahamurto P, Ollila J, Vihinen M, Scott HS, Antonarakis SE, Kudoh J, Shimizu N, Krohn K, Peterson P. The autoimmune regulator protein has transcriptional transactivating properties and interacts with the common coactivator CREB-binding protein. J Biol Chem. 2000;275(22):16802-9. doi: 10.1074/jbc.M908944199. PubMed PMID: 10748110.

246. Giraud M, Jmari N, Du L, Carallis F, Nieland TJ, Perez-Campo FM, Bensaude O, Root DE, Hacohen N, Mathis D, Benoist C. An RNAi screen for Aire cofactors reveals a role for Hnrnpl in polymerase release and Aire-activated ectopic transcription. Proc Natl Acad Sci U S A. 2014;111(4):1491-6. doi: 10.1073/pnas.1323535111. PubMed PMID: 24434558; PMCID: PMC3910647.

247. Zumer K, Plemenitas A, Saksela K, Peterlin BM. Patient mutation in AIRE disrupts P-TEFb binding and target gene transcription. Nucleic acids research. 2011;39(18):7908-19. doi: 10.1093/nar/gkr527. PubMed PMID: 21724609; PMCID: PMC3185428.

248. Saare M, Rebane A, Rajashekar B, Vilo J, Peterson P. Autoimmune regulator is acetylated by transcription coactivator CBP/p300. Exp Cell Res. 2012;318(14):1767-78. doi: 10.1016/j.yexcr.2012.04.013. PubMed PMID: 22659170.

249. Mathieu AL, Verronese E, Rice GI, Fouyssac F, Bertrand Y, Picard C, Chansel M, Walter JE, Notarangelo LD, Butte MJ, Nadeau KC, Csomos K, Chen DJ, Chen K, Delgado A, Rigal C, Bardin C, Schuetz C, Moshous D, Reumaux H, Plenat F, Phan A, Zabot MT, Balme B, Viel S, Bienvenu J, Cochat P, van der Burg M, Caux C, Kemp EH, Rouvet I, Malcus C, Meritet JF, Lim A, Crow YJ, Fabien N, Menetrier-Caux C, De Villartay JP, Walzer T, Belot A. PRKDC mutations associated with immunodeficiency, granuloma, and autoimmune regulator-dependent autoimmunity. J Allergy Clin Immunol. 2015;135(6):1578-88 e5. doi: 10.1016/j.jaci.2015.01.040. PubMed PMID: 25842288; PMCID: PMC4487867.

250. Derbinski J, Gabler J, Brors B, Tierling S, Jonnakuty S, Hergenhahn M, Peltonen L, Walter J, Kyewski B. Promiscuous gene expression in thymic epithelial cells is regulated at multiple levels. J Exp Med. 2005;202(1):33-45. doi: 10.1084/jem.20050471. PubMed PMID: 15983066; PMCID: PMC2212909.

251. Takaba H, Morishita Y, Tomofuji Y, Danks L, Nitta T, Komatsu N, Kodama T, Takayanagi H. Fezf2 Orchestrates a Thymic Program of Self-Antigen Expression for Immune Tolerance. Cell. 2015;163(4):975-87. doi: 10.1016/j.cell.2015.10.013. PubMed PMID: 26544942.

252. Taubert R, Schwendemann J, Kyewski B. Highly variable expression of tissue-restricted self-antigens in human thymus: implications for self-tolerance and autoimmunity. Eur J Immunol. 2007;37(3):838-48. doi: 10.1002/eji.200636962. PubMed PMID: 17323415.

253. Derbinski J, Schulte A, Kyewski B, Klein L. Promiscuous gene expression in medullary thymic epithelial cells mirrors the peripheral self. Nat Immunol. 2001;2(11):1032-9. doi: 10.1038/ni723. PubMed PMID: 11600886.

254. Yamano T, Nedjic J, Hinterberger M, Steinert M, Koser S, Pinto S, Gerdes N, Lutgens E, Ishimaru N, Busslinger M, Brors B, Kyewski B, Klein L. Thymic B Cells Are Licensed to Present Self Antigens for Central T Cell Tolerance Induction. Immunity. 2015;42(6):1048-61. doi: 10.1016/j.immuni.2015.05.013. PubMed PMID: 26070482.

255. Bonasio R, Scimone ML, Schaerli P, Grabie N, Lichtman AH, von Andrian UH. Clonal deletion of thymocytes by circulating dendritic cells homing to the thymus. Nat Immunol. 2006;7(10):1092-100. doi: 10.1038/ni1385. PubMed PMID: 16951687.

256. Li J, Park J, Foss D, Goldschneider I. Thymus-homing peripheral dendritic cells constitute two of the three major subsets of dendritic cells in the steady-state thymus. J Exp Med. 2009;206(3):607-22. doi: 10.1084/jem.20082232. PubMed PMID: 19273629; PMCID: PMC2699131.

257. Volkmann A, Zal T, Stockinger B. Antigen-presenting cells in the thymus that can negatively select MHC class II-restricted T cells recognizing a circulating self antigen. J Immunol. 1997;158(2):693-706. PubMed PMID: 8992985.

258. Baba T, Nakamoto Y, Mukaida N. Crucial contribution of thymic Sirp alpha+ conventional dendritic cells to central tolerance against blood-borne antigens in a CCR2-dependent manner. J Immunol. 2009;183(5):3053-63. doi: 10.4049/jimmunol.0900438. PubMed PMID: 19675159.

259. Atibalentja DF, Byersdorfer CA, Unanue ER. Thymus-blood protein interactions are highly effective in negative selection and regulatory T cell induction. J Immunol. 2009;183(12):7909-18. doi: 10.4049/jimmunol.0902632. PubMed PMID: 19933868; PMCID: PMC3507440.

260. Gallegos AM, Bevan MJ. Central tolerance to tissue-specific antigens mediated by direct and indirect antigen presentation. J Exp Med. 2004;200(8):1039-49. doi: 10.1084/jem.20041457. PubMed PMID: 15492126; PMCID: PMC2211843.

261. Millet V, Naquet P, Guinamard RR. Intercellular MHC transfer between thymic epithelial and dendritic cells. Eur J Immunol. 2008;38(5):1257-63. doi: 10.1002/eji.200737982. PubMed PMID: 18412162.

262. Koble C, Kyewski B. The thymic medulla: a unique microenvironment for intercellular self-antigen transfer. J Exp Med. 2009;206(7):1505-13. doi: 10.1084/jem.20082449. PubMed PMID: 19564355; PMCID: PMC2715082.

263. Skogberg G, Lundberg V, Berglund M, Gudmundsdottir J, Telemo E, Lindgren S, Ekwall O. Human thymic epithelial primary cells produce exosomes carrying tissue-restricted antigens. Immunology and cell biology. 2015;93(8):727-34. doi: 10.1038/icb.2015.33. PubMed PMID: 25776846; PMCID: PMC4575951.

264. McCaughtry TM, Baldwin TA, Wilken MS, Hogquist KA. Clonal deletion of thymocytes can occur in the cortex with no involvement of the medulla. J Exp Med. 2008;205(11):2575-84. doi: 10.1084/jem.20080866. PubMed PMID: 18936237; PMCID: PMC2571932.

265. Melichar HJ, Ross JO, Herzmark P, Hogquist KA, Robey EA. Distinct temporal patterns of T cell receptor signaling during positive versus negative selection in situ. Science signaling. 2013;6(297):ra92. doi: 10.1126/scisignal.2004400. PubMed PMID: 24129702; PMCID: PMC4078262.

266. Alberola-Ila J, Hogquist KA, Swan KA, Bevan MJ, Perlmutter RM. Positive and negative selection invoke distinct signaling pathways. J Exp Med. 1996;184(1):9-18. PubMed PMID: 8691153; PMCID: PMC2192689.

267. Dower NA, Stang SL, Bottorff DA, Ebinu JO, Dickie P, Ostergaard HL, Stone JC. RasGRP is essential for mouse thymocyte differentiation and TCR signaling. Nat Immunol. 2000;1(4):317-21. doi: 10.1038/79766. PubMed PMID: 11017103.

268. O'Shea CC, Crompton T, Rosewell IR, Hayday AC, Owen MJ. Raf regulates positive selection. Eur J Immunol. 1996;26(10):2350-5. doi: 10.1002/eji.1830261012. PubMed PMID: 8898944.

269. Pages G, Guerin S, Grall D, Bonino F, Smith A, Anjuere F, Auberger P, Pouyssegur J. Defective thymocyte maturation in p44 MAP kinase (Erk 1) knockout mice. Science. 1999;286(5443):1374-7. PubMed PMID: 10558995.

270. Swan KA, Alberola-Ila J, Gross JA, Appleby MW, Forbush KA, Thomas JF, Perlmutter RM. Involvement of p21ras distinguishes positive and negative selection in thymocytes. EMBO J. 1995;14(2):276-85. PubMed PMID: 7835338; PMCID: PMC398081.

271. Werlen G, Hausmann B, Palmer E. A motif in the alphabeta T-cell receptor controls positive selection by modulating ERK activity. Nature. 2000;406(6794):422-6. doi: 10.1038/35019094. PubMed PMID: 10935640.

272. Delgado P, Fernandez E, Dave V, Kappes D, Alarcon B. CD3delta couples T-cell receptor signalling to ERK activation and thymocyte positive selection. Nature. 2000;406(6794):426-30. doi: 10.1038/35019102. PubMed PMID: 10935641.

273. Bommhardt U, Scheuring Y, Bickel C, Zamoyska R, Hunig T. MEK activity regulates negative selection of immature CD4+CD8+ thymocytes. J Immunol. 2000;164(5):2326-37. PubMed PMID: 10679067.

274. Mariathasan S, Zakarian A, Bouchard D, Michie AM, Zuniga-Pflucker JC, Ohashi PS. Duration and strength of extracellular signal-regulated kinase signals are altered during positive versus negative thymocyte selection. J Immunol. 2001;167(9):4966-73. PubMed PMID: 11673503.

275. Gong Q, Cheng AM, Akk AM, Alberola-Ila J, Gong G, Pawson T, Chan AC. Disruption of T cell signaling networks and development by Grb2 haploid insufficiency. Nat Immunol. 2001;2(1):29-36. doi: 10.1038/83134. PubMed PMID: 11135575.

276. Wilkinson RW, Anderson G, Owen JJ, Jenkinson EJ. Positive selection of thymocytes involves sustained interactions with the thymic microenvironment. J Immunol. 1995;155(11):5234-40. PubMed PMID: 7594535.

277. Kisielow P, Miazek A. Positive selection of T cells: rescue from programmed cell death and differentiation require continual engagement of the T cell receptor. J Exp Med. 1995;181(6):1975-84. PubMed PMID: 7759993; PMCID: PMC2192069.

278. Dong C, Yang DD, Tournier C, Whitmarsh AJ, Xu J, Davis RJ, Flavell RA. JNK is required for effector T-cell function but not for T-cell activation. Nature. 2000;405(6782):91-4. doi: 10.1038/35011091. PubMed PMID: 10811224.

279. Rincon M, Whitmarsh A, Yang DD, Weiss L, Derijard B, Jayaraj P, Davis RJ, Flavell RA. The JNK pathway regulates the In vivo deletion of immature CD4(+)CD8(+) thymocytes. J Exp Med. 1998;188(10):1817-30. PubMed PMID: 9815259; PMCID: PMC2212412.

280. Bouillet P, Purton JF, Godfrey DI, Zhang LC, Coultas L, Puthalakath H, Pellegrini M, Cory S, Adams JM, Strasser A. BH3-only Bcl-2 family member Bim is required for apoptosis of autoreactive thymocytes. Nature. 2002;415(6874):922-6. doi: 10.1038/415922a. PubMed PMID: 11859372.

281. Rathmell JC, Lindsten T, Zong WX, Cinalli RM, Thompson CB. Deficiency in Bak and Bax perturbs thymic selection and lymphoid homeostasis. Nat Immunol. 2002;3(10):932-9. doi: 10.1038/ni834. PubMed PMID: 12244308.

282. Apostolou I, Sarukhan A, Klein L, von Boehmer H. Origin of regulatory T cells with known specificity for antigen. Nat Immunol. 2002;3(8):756-63. doi: 10.1038/ni816. PubMed PMID: 12089509.

283. Jordan MS, Boesteanu A, Reed AJ, Petrone AL, Holenbeck AE, Lerman MA, Naji A, Caton AJ. Thymic selection of CD4+CD25+ regulatory T cells induced by an agonist self-peptide. Nat Immunol. 2001;2(4):301-6. doi: 10.1038/86302. PubMed PMID: 11276200.

284. Poliani PL, Facchetti F, Ravanini M, Gennery AR, Villa A, Roifman CM, Notarangelo LD. Early defects in human T-cell development severely affect distribution and maturation of thymic stromal cells: possible implications for the pathophysiology of Omenn syndrome. Blood. 2009;114(1):105-8. doi: 10.1182/blood-2009-03-211029. PubMed PMID: 19414857; PMCID: PMC2710940.

285. Kekalainen E, Tuovinen H, Joensuu J, Gylling M, Franssila R, Pontynen N, Talvensaari K, Perheentupa J, Miettinen A, Arstila TP. A defect of regulatory T cells in patients with autoimmune polyendocrinopathy-candidiasis-ectodermal dystrophy. J Immunol. 2007;178(2):1208-15. PubMed PMID: 17202386.

286. Laakso SM, Laurinolli TT, Rossi LH, Lehtoviita A, Sairanen H, Perheentupa J, Kekalainen E, Arstila TP. Regulatory T cell defect in APECED patients is associated with loss of naive FOXP3(+) precursors and impaired activated population. J Autoimmun. 2010;35(4):351-7. doi: 10.1016/j.jaut.2010.07.008. PubMed PMID: 20805020.

287. Poliani PL, Fontana E, Roifman CM, Notarangelo LD. zeta Chain-associated protein of 70 kDa (ZAP70) deficiency in human subjects is associated with abnormalities of thymic stromal

cells: Implications for T-cell tolerance. J Allergy Clin Immunol. 2013;131(2):597-600 e1-2. doi: 10.1016/j.jaci.2012.11.002. PubMed PMID: 23245794.

288. Hanabuchi S, Ito T, Park WR, Watanabe N, Shaw JL, Roman E, Arima K, Wang YH, Voo KS, Cao W, Liu YJ. Thymic stromal lymphopoietin-activated plasmacytoid dendritic cells induce the generation of FOXP3+ regulatory T cells in human thymus. J Immunol. 2010;184(6):2999-3007. doi: 10.4049/jimmunol.0804106. PubMed PMID: 20173030; PMCID: PMC3325785.

289. Watanabe N, Wang YH, Lee HK, Ito T, Wang YH, Cao W, Liu YJ. Hassall's corpuscles instruct dendritic cells to induce CD4+CD25+ regulatory T cells in human thymus. Nature. 2005;436(7054):1181-5. doi: 10.1038/nature03886. PubMed PMID: 16121185.

290. Salomon B, Lenschow DJ, Rhee L, Ashourian N, Singh B, Sharpe A, Bluestone JA. B7/CD28 costimulation is essential for the homeostasis of the CD4+CD25+ immunoregulatory T cells that control autoimmune diabetes. Immunity. 2000;12(4):431-40. PubMed PMID: 10795741.

291. Tai X, Cowan M, Feigenbaum L, Singer A. CD28 costimulation of developing thymocytes induces Foxp3 expression and regulatory T cell differentiation independently of interleukin 2. Nat Immunol. 2005;6(2):152-62. doi: 10.1038/ni1160. PubMed PMID: 15640801.

292. Caramalho I, Nunes-Silva V, Pires AR, Mota C, Pinto AI, Nunes-Cabaco H, Foxall RB, Sousa AE. Human regulatory T-cell development is dictated by Interleukin-2 and -15 expressed in a non-overlapping pattern in the thymus. J Autoimmun. 2015;56:98-110. doi: 10.1016/j.jaut.2014.11.002. PubMed PMID: 25481744.

293. Nazzal D, Gradolatto A, Truffault F, Bismuth J, Berrih-Aknin S. Human thymus medullary epithelial cells promote regulatory T-cell generation by stimulating interleukin-2 production via ICOS ligand. Cell Death Dis. 2014;5:e1420. doi: 10.1038/cddis.2014.377. PubMed PMID: 25210803; PMCID: PMC4540205.

294. Riberdy JM, Mostaghel E, Doyle C. Disruption of the CD4-major histocompatibility complex class II interaction blocks the development of CD4(+) T cells in vivo. Proc Natl Acad Sci U S A. 1998;95(8):4493-8. PubMed PMID: 9539765; PMCID: PMC22517.

295. Davis CB, Killeen N, Crooks ME, Raulet D, Littman DR. Evidence for a stochastic mechanism in the differentiation of mature subsets of T lymphocytes. Cell. 1993;73(2):237-47. PubMed PMID: 8097431.

296. Itano A, Kioussis D, Robey E. Stochastic component to development of class I major histocompatibility complex-specific T cells. Proc Natl Acad Sci U S A. 1994;91(1):220-4. PubMed PMID: 7904067; PMCID: PMC42918.

297. Leung RK, Thomson K, Gallimore A, Jones E, Van den Broek M, Sierro S, Alsheikhly AR, McMichael A, Rahemtulla A. Deletion of the CD4 silencer element supports a stochastic mechanism of thymocyte lineage commitment. Nat Immunol. 2001;2(12):1167-73. doi: 10.1038/ni733. PubMed PMID: 11694883.

298. Seong RH, Chamberlain JW, Parnes JR. Signal for T-cell differentiation to a CD4 cell lineage is delivered by CD4 transmembrane region and/or cytoplasmic tail. Nature. 1992;356(6371):718-20. doi: 10.1038/356718a0. PubMed PMID: 1533274.

299. Robey EA, Fowlkes BJ, Gordon JW, Kioussis D, von Boehmer H, Ramsdell F, Axel R. Thymic selection in CD8 transgenic mice supports an instructive model for commitment to a CD4 or CD8 lineage. Cell. 1991;64(1):99-107. PubMed PMID: 1898873.

300. Borgulya P, Kishi H, Muller U, Kirberg J, von Boehmer H. Development of the CD4 and CD8 lineage of T cells: instruction versus selection. EMBO J. 1991;10(4):913-8. PubMed PMID: 1901264; PMCID: PMC452734.

301. Itano A, Robey E. Highly efficient selection of CD4 and CD8 lineage thymocytes supports an instructive model of lineage commitment. Immunity. 2000;12(4):383-9. PubMed PMID: 10795736.

302. Wiest DL, Yuan L, Jefferson J, Benveniste P, Tsokos M, Klausner RD, Glimcher LH, Samelson LE, Singer A. Regulation of T cell receptor expression in immature CD4+CD8+ thymocytes by p56lck tyrosine kinase: basis for differential signaling by CD4 and CD8 in immature thymocytes expressing both coreceptor molecules. J Exp Med. 1993;178(5):1701-12. PubMed PMID: 8228817; PMCID: PMC2191226.

303. Campbell KS, Buder A, Deuschle U. Interactions between the amino-terminal domain of p56lck and cytoplasmic domains of CD4 and CD8 alpha in yeast. Eur J Immunol. 1995;25(8):2408-12. doi: 10.1002/eji.1830250842. PubMed PMID: 7664803.

304. Zamoyska R, Derham P, Gorman SD, von Hoegen P, Bolen JB, Veillette A, Parnes JR. Inability of CD8 alpha' polypeptides to associate with p56lck correlates with impaired function in vitro and lack of expression in vivo. Nature. 1989;342(6247):278-81. doi: 10.1038/342278a0. PubMed PMID: 2509945.

305. Itano A, Salmon P, Kioussis D, Tolaini M, Corbella P, Robey E. The cytoplasmic domain of CD4 promotes the development of CD4 lineage T cells. J Exp Med. 1996;183(3):731-41. PubMed PMID: 8642277; PMCID: PMC2192343.

306. Sharp LL, Hedrick SM. Commitment to the CD4 lineage mediated by extracellular signal-related kinase mitogen-activated protein kinase and lck signaling. J Immunol. 1999;163(12):6598-605. PubMed PMID: 10586054.

307. Hernandez-Hoyos G, Sohn SJ, Rothenberg EV, Alberola-Ila J. Lck activity controls CD4/CD8 T cell lineage commitment. Immunity. 2000;12(3):313-22. PubMed PMID: 10755618.

308. Killeen N, Littman DR. Helper T-cell development in the absence of CD4-p56lck association. Nature. 1993;364(6439):729-32. doi: 10.1038/364729a0. PubMed PMID: 8355789.

309. Yasutomo K, Doyle C, Miele L, Fuchs C, Germain RN. The duration of antigen receptor signalling determines CD4+ versus CD8+ T-cell lineage fate. Nature. 2000;404(6777):506-10. doi: 10.1038/35006664. PubMed PMID: 10761920.

310. Iwata M, Kuwata T, Mukai M, Tozawa Y, Yokoyama M. Differential induction of helper and killer T cells from isolated CD4+CD8+ thymocytes in suspension culture. Eur J Immunol. 1996;26(9):2081-6. doi: 10.1002/eji.1830260918. PubMed PMID: 8814250.

311. Adoro S, McCaughtry T, Erman B, Alag A, Van Laethem F, Park JH, Tai X, Kimura M, Wang L, Grinberg A, Kubo M, Bosselut R, Love P, Singer A. Coreceptor gene imprinting governs thymocyte lineage fate. EMBO J. 2012;31(2):366-77. doi: 10.1038/emboj.2011.388. PubMed PMID: 22036949; PMCID: PMC3261554.

312. Dalheimer SL, Zeng L, Draves KE, Hassaballa A, Jiwa NN, Parrish TD, Clark EA, Yankee TM. Gads-deficient thymocytes are blocked at the transitional single positive CD4+ stage. Eur J Immunol. 2009;39(5):1395-404. doi: 10.1002/eji.200838692. PubMed PMID: 19337995; PMCID: PMC2768049.

313. Lundberg K, Heath W, Kontgen F, Carbone FR, Shortman K. Intermediate steps in positive selection: differentiation of CD4+8int TCRint thymocytes into CD4-8+TCRhi thymocytes. J Exp Med. 1995;181(5):1643-51. PubMed PMID: 7722444; PMCID: PMC2191983.

314. Suzuki H, Punt JA, Granger LG, Singer A. Asymmetric signaling requirements for thymocyte commitment to the CD4+ versus CD8+ T cell lineages: a new perspective on thymic commitment and selection. Immunity. 1995;2(4):413-25. PubMed PMID: 7719943.

315. Lucas B, Germain RN. Unexpectedly complex regulation of CD4/CD8 coreceptor expression supports a revised model for CD4+CD8+ thymocyte differentiation. Immunity. 1996;5(5):461-77. PubMed PMID: 8934573.

316. Kydd R, Lundberg K, Vremec D, Harris AW, Shortman K. Intermediate steps in thymic positive selection. Generation of CD4-8+ T cells in culture from CD4+8+, CD4int8+, and CD4+8int thymocytes with up-regulated levels of TCR-CD3. J Immunol. 1995;155(8):3806-14. PubMed PMID: 7561086.

317. Brugnera E, Bhandoola A, Cibotti R, Yu Q, Guinter TI, Yamashita Y, Sharrow SO, Singer A. Coreceptor reversal in the thymus: signaled CD4+8+ thymocytes initially terminate

CD8 transcription even when differentiating into CD8+ T cells. Immunity. 2000;13(1):59-71. PubMed PMID: 10933395.

318. Sarafova SD, Erman B, Yu Q, Van Laethem F, Guinter T, Sharrow SO, Feigenbaum L, Wildt KF, Ellmeier W, Singer A. Modulation of coreceptor transcription during positive selection dictates lineage fate independently of TCR/coreceptor specificity. Immunity. 2005;23(1):75-87. doi: 10.1016/j.immuni.2005.05.011. PubMed PMID: 16039581.

319. Cibotti R, Bhandoola A, Guinter TI, Sharrow SO, Singer A. CD8 coreceptor extinction in signaled CD4(+)CD8(+) thymocytes: coordinate roles for both transcriptional and posttranscriptional regulatory mechanisms in developing thymocytes. Mol Cell Biol. 2000;20(11):3852-9. PubMed PMID: 10805728; PMCID: PMC85715.

320. Bosselut R, Guinter TI, Sharrow SO, Singer A. Unraveling a revealing paradox: Why major histocompatibility complex I-signaled thymocytes "paradoxically" appear as CD4+8lo transitional cells during positive selection of CD8+ T cells. J Exp Med. 2003;197(12):1709-19. doi: 10.1084/jem.20030170. PubMed PMID: 12810689; PMCID: PMC2193957.

321. Keefe R, Dave V, Allman D, Wiest D, Kappes DJ. Regulation of lineage commitment distinct from positive selection. Science. 1999;286(5442):1149-53. PubMed PMID: 10550051.

322. Dave VP, Allman D, Keefe R, Hardy RR, Kappes DJ. HD mice: a novel mouse mutant with a specific defect in the generation of CD4(+) T cells. Proc Natl Acad Sci U S A. 1998;95(14):8187-92. PubMed PMID: 9653162; PMCID: PMC20951.

323. He X, He X, Dave VP, Zhang Y, Hua X, Nicolas E, Xu W, Roe BA, Kappes DJ. The zinc finger transcription factor Th-POK regulates CD4 versus CD8 T-cell lineage commitment. Nature. 2005;433(7028):826-33. doi: 10.1038/nature03338. PubMed PMID: 15729333.

324. Sun G, Liu X, Mercado P, Jenkinson SR, Kypriotou M, Feigenbaum L, Galera P, Bosselut R. The zinc finger protein cKrox directs CD4 lineage differentiation during intrathymic T cell positive selection. Nat Immunol. 2005;6(4):373-81. doi: 10.1038/ni1183. PubMed PMID: 15750595.

325. Egawa T, Littman DR. ThPOK acts late in specification of the helper T cell lineage and suppresses Runx-mediated commitment to the cytotoxic T cell lineage. Nat Immunol. 2008;9(10):1131-9. doi: 10.1038/ni.1652. PubMed PMID: 18776905; PMCID: PMC2666788.

326. Muroi S, Naoe Y, Miyamoto C, Akiyama K, Ikawa T, Masuda K, Kawamoto H, Taniuchi I. Cascading suppression of transcriptional silencers by ThPOK seals helper T cell fate. Nat Immunol. 2008;9(10):1113-21. doi: 10.1038/ni.1650. PubMed PMID: 18776907.

327. Egawa T, Tillman RE, Naoe Y, Taniuchi I, Littman DR. The role of the Runx transcription factors in thymocyte differentiation and in homeostasis of naive T cells. J Exp Med. 2007;204(8):1945-57. doi: 10.1084/jem.20070133. PubMed PMID: 17646406; PMCID: PMC2118679.

328. Sato T, Ohno S, Hayashi T, Sato C, Kohu K, Satake M, Habu S. Dual functions of Runx proteins for reactivating CD8 and silencing CD4 at the commitment process into CD8 thymocytes. Immunity. 2005;22(3):317-28. doi: 10.1016/j.immuni.2005.01.012. PubMed PMID: 15780989.

329. Taniuchi I, Osato M, Egawa T, Sunshine MJ, Bae SC, Komori T, Ito Y, Littman DR. Differential requirements for Runx proteins in CD4 repression and epigenetic silencing during T lymphocyte development. Cell. 2002;111(5):621-33. PubMed PMID: 12464175.

330. Ehlers M, Laule-Kilian K, Petter M, Aldrian CJ, Grueter B, Wurch A, Yoshida N, Watanabe T, Satake M, Steimle V. Morpholino antisense oligonucleotide-mediated gene knockdown during thymocyte development reveals role for Runx3 transcription factor in CD4 silencing during development of CD4-/CD8+ thymocytes. J Immunol. 2003;171(7):3594-604. PubMed PMID: 14500656.

331. Zamisch M, Tian L, Grenningloh R, Xiong Y, Wildt KF, Ehlers M, Ho IC, Bosselut R. The transcription factor Ets1 is important for CD4 repression and Runx3 up-regulation during CD8 T cell differentiation in the thymus. J Exp Med. 2009;206(12):2685-99. doi: 10.1084/jem.20092024. PubMed PMID: 19917777; PMCID: PMC2806616.

332. Setoguchi R, Tachibana M, Naoe Y, Muroi S, Akiyama K, Tezuka C, Okuda T, Taniuchi I. Repression of the transcription factor Th-POK by Runx complexes in cytotoxic T cell development. Science. 2008;319(5864):822-5. doi: 10.1126/science.1151844. PubMed PMID: 18258917.

333. Yu Q, Park JH, Doan LL, Erman B, Feigenbaum L, Singer A. Cytokine signal transduction is suppressed in preselection double-positive thymocytes and restored by positive selection. J Exp Med. 2006;203(1):165-75. doi: 10.1084/jem.20051836. PubMed PMID: 16390939; PMCID: PMC2118084.

334. Chong MM, Cornish AL, Darwiche R, Stanley EG, Purton JF, Godfrey DI, Hilton DJ, Starr R, Alexander WS, Kay TW. Suppressor of cytokine signaling-1 is a critical regulator of interleukin-7-dependent CD8+ T cell differentiation. Immunity. 2003;18(4):475-87. PubMed PMID: 12705851.

335. Park JH, Adoro S, Guinter T, Erman B, Alag AS, Catalfamo M, Kimura MY, Cui Y, Lucas PJ, Gress RE, Kubo M, Hennighausen L, Feigenbaum L, Singer A. Signaling by intrathymic cytokines, not T cell antigen receptors, specifies CD8 lineage choice and promotes the differentiation of cytotoxic-lineage T cells. Nat Immunol. 2010;11(3):257-64. doi: 10.1038/ni.1840. PubMed PMID: 20118929; PMCID: PMC3555225.

336. Catlett IM, Hedrick SM. Suppressor of cytokine signaling 1 is required for the differentiation of CD4+ T cells. Nat Immunol. 2005;6(7):715-21. doi: 10.1038/ni1211. PubMed PMID: 15924143.

337. Park JH, Adoro S, Lucas PJ, Sarafova SD, Alag AS, Doan LL, Erman B, Liu X, Ellmeier W, Bosselut R, Feigenbaum L, Singer A. 'Coreceptor tuning': cytokine signals transcriptionally tailor CD8 coreceptor expression to the self-specificity of the TCR. Nat Immunol. 2007;8(10):1049-59. doi: 10.1038/ni1512. PubMed PMID: 17873878.

338. Terstappen LW, Huang S, Safford M, Lansdorp PM, Loken MR. Sequential generations of hematopoietic colonies derived from single nonlineage-committed CD34+CD38- progenitor cells. Blood. 1991;77(6):1218-27. Epub 1991/03/15. PubMed PMID: 1705833.

339. Terstappen LW, Huang S, Picker LJ. Flow cytometric assessment of human T-cell differentiation in thymus and bone marrow. Blood. 1992;79(3):666-77. Epub 1992/02/01. PubMed PMID: 1370641.

340. Schmitt C, Tonnelle C, Dalloul A, Chabannon C, Debre P, Rebollo A. Aiolos and Ikaros: regulators of lymphocyte development, homeostasis and lymphoproliferation. Apoptosis : an international journal on programmed cell death. 2002;7(3):277-84. Epub 2002/05/09. PubMed PMID: 11997672.

341. Schjerven H, McLaughlin J, Arenzana TL, Frietze S, Cheng D, Wadsworth SE, Lawson GW, Bensinger SJ, Farnham PJ, Witte ON, Smale ST. Selective regulation of lymphopoiesis and leukemogenesis by individual zinc fingers of Ikaros. Nat Immunol. 2013. doi: 10.1038/ni.2707. PubMed PMID: 24013668.

342. Sabath DE, Broome HE, Prystowsky MB. Glyceraldehyde-3-phosphate dehydrogenase mRNA is a major interleukin 2-induced transcript in a cloned T-helper lymphocyte. Gene. 1990;91(2):185-91. Epub 1990/07/16. PubMed PMID: 2145197.

343. Hahm K, Ernst P, Lo K, Kim GS, Turck C, Smale ST. The lymphoid transcription factor LyF-1 is encoded by specific, alternatively spliced mRNAs derived from the Ikaros gene. Mol Cell Biol. 1994;14(11):7111-23. Epub 1994/11/01. PubMed PMID: 7935426; PMCID: 359245.

344. John LB, Yoong S, Ward AC. Evolution of the Ikaros gene family: implications for the origins of adaptive immunity. J Immunol. 2009;182(8):4792-9. doi: 10.4049/jimmunol.0802372. PubMed PMID: 19342657.

345. Williams CJ, Naito T, Arco PG, Seavitt JR, Cashman SM, De Souza B, Qi X, Keables P, Von Andrian UH, Georgopoulos K. The chromatin remodeler Mi-2beta is required for CD4 expression and T cell development. Immunity. 2004;20(6):719-33. Epub 2004/06/11. doi: 10.1016/j.immuni.2004.05.005
S1074761304001372 [pii]. PubMed PMID: 15189737.

346. Harker N, Naito T, Cortes M, Hostert A, Hirschberg S, Tolaini M, Roderick K, Georgopoulos K, Kioussis D. The CD8alpha gene locus is regulated by the Ikaros family of proteins. Mol Cell. 2002;10(6):1403-15. Epub 2002/12/31. doi: S1097276502007116 [pii]. PubMed PMID: 12504015.

347. Xiong J, Armato MA, Yankee TM. Immature single-positive CD8+ thymocytes represent the transition from Notch-dependent to Notch-independent T-cell development. Int Immunol. 2011;23(1):55-64. Epub 2010/12/15. doi: 10.1093/intimm/dxq457. PubMed PMID: 21148236; PMCID: 3031305.

348. Fischer ES, Bohm K, Lydeard JR, Yang H, Stadler MB, Cavadini S, Nagel J, Serluca F, Acker V, Lingaraju GM, Tichkule RB, Schebesta M, Forrester WC, Schirle M, Hassiepen U, Ottl J, Hild M, Beckwith RE, Harper JW, Jenkins JL, Thoma NH. Structure of the DDB1-CRBN E3 ubiquitin ligase in complex with thalidomide. Nature. 2014;512(7512):49-53. Epub 2014/07/22. doi: 10.1038/nature13527. PubMed PMID: 25043012.

349. Kronke J, Hurst SN, Ebert BL. Lenalidomide induces degradation of IKZF1 and IKZF3. Oncoimmunology. 2014;3(7):e941742. Epub 2015/01/23. doi: 10.4161/21624011.2014.941742. PubMed PMID: 25610725; PMCID: 4292522.

350. Gandhi AK, Kang J, Havens CG, Conklin T, Ning Y, Wu L, Ito T, Ando H, Waldman MF, Thakurta A, Klippel A, Handa H, Daniel TO, Schafer PH, Chopra R. Immunomodulatory agents lenalidomide and pomalidomide co-stimulate T cells by inducing degradation of T cell repressors Ikaros and Aiolos via modulation of the E3 ubiquitin ligase complex CRL4(CRBN.). Br J Haematol. 2014;164(6):811-21. Epub 2013/12/18. doi: 10.1111/bjh.12708. PubMed PMID: 24328678; PMCID: 4232904.

351. Kronke J, Udeshi ND, Narla A, Grauman P, Hurst SN, McConkey M, Svinkina T, Heckl D, Comer E, Li X, Ciarlo C, Hartman E, Munshi N, Schenone M, Schreiber SL, Carr SA, Ebert BL. Lenalidomide causes selective degradation of IKZF1 and IKZF3 in multiple myeloma cells. Science. 2014;343(6168):301-5. Epub 2013/12/03. doi: 10.1126/science.1244851. PubMed PMID: 24292625; PMCID: 4077049.

352. Ma S, Pathak S, Trinh L, Lu R. Interferon regulatory factors 4 and 8 induce the expression of Ikaros and Aiolos to down-regulate pre-B-cell receptor and promote cell-cycle withdrawal in pre-B-cell development. Blood. 2008;111(3):1396-403. Epub 2007/11/01. doi: blood-2007-08-110106 [pii]
10.1182/blood-2007-08-110106. PubMed PMID: 17971486; PMCID: 2214771.

353. Thompson EC, Cobb BS, Sabbattini P, Meixlsperger S, Parelho V, Liberg D, Taylor B, Dillon N, Georgopoulos K, Jumaa H, Smale ST, Fisher AG, Merkenschlager M. Ikaros DNA-binding proteins as integral components of B cell developmental-stage-specific regulatory circuits. Immunity. 2007;26(3):335-44. Epub 2007/03/17. doi: S1074-7613(07)00179-3 [pii] 10.1016/j.immuni.2007.02.010. PubMed PMID: 17363301.

354. Mitchell JL, Seng A, Yankee TM. Expression and splicing of Ikaros family members in murine and human thymocytes. Molecular immunology. 2015:in revision.

355. Xiong J, Parker BL, Dalheimer SL, Yankee TM. Interleukin-7 supports survival of T-cell receptor-beta-expressing CD4(-) CD8(-) double-negative thymocytes. Immunology. 2013;138(4):382-91. doi: 10.1111/imm.12050. PubMed PMID: 23215679.

356. Zeng L, Dalheimer SL, Yankee TM. Gads-/- mice reveal functionally distinct subsets of TCRbeta+ CD4-CD8- double-negative thymocytes. J Immunol. 2007;179(2):1013-21. Epub 2007/07/10. PubMed PMID: 17617593.

357. Fujii Y, Okumura M, Inada K, Nakahara K, Matsuda H. CD45 isoform expression during T cell development in the thymus. Eur J Immunol. 1992;22(7):1843-50. doi: 10.1002/eji.1830220725. PubMed PMID: 1378021.

358. von Boehmer H, Aifantis I, Feinberg J, Lechner O, Saint-Ruf C, Walter U, Buer J, Azogui O. Pleiotropic changes controlled by the pre-T-cell receptor. Curr Opin Immunol. 1999;11(2):135-42. PubMed PMID: 10322152.

359. Varas A, Jimenez E, Sacedon R, Rodriguez-Mahou M, Maroto E, Zapata AG, Vicente A. Analysis of the human neonatal thymus: evidence for a transient thymic involution. J Immunol. 2000;164(12):6260-7. PubMed PMID: 10843679.

360. Weerkamp F, de Haas EF, Naber BA, Comans-Bitter WM, Bogers AJ, van Dongen JJ, Staal FJ. Age-related changes in the cellular composition of the thymus in children. J Allergy Clin Immunol. 2005;115(4):834-40. doi: 10.1016/j.jaci.2004.10.031. PubMed PMID: 15806007.

361. Murphy M, Epstein LB. Down syndrome (trisomy 21) thymuses have a decreased proportion of cells expressing high levels of TCR alpha, beta and CD3. A possible mechanism for diminished T cell function in Down syndrome. Clin Immunol Immunopathol. 1990;55(3):453-67. PubMed PMID: 1692775.

362. Penit C, Lucas B, Vasseur F. Cell expansion and growth arrest phases during the transition from precursor (CD4-8-) to immature (CD4+8+) thymocytes in normal and genetically modified mice. J Immunol. 1995;154(10):5103-13. PubMed PMID: 7730616.

363. Webb LM, Vigorito E, Wymann MP, Hirsch E, Turner M. Cutting edge: T cell development requires the combined activities of the p110gamma and p110delta catalytic isoforms of phosphatidylinositol 3-kinase. J Immunol. 2005;175(5):2783-7. PubMed PMID: 16116162.

364. Saborit-Villarroya I, Vaisitti T, Rossi D, D'Arena G, Gaidano G, Malavasi F, Deaglio S. E2A is a transcriptional regulator of CD38 expression in chronic lymphocytic leukemia. Leukemia. 2011;25(3):479-88. Epub 2011/01/08. doi: 10.1038/leu.2010.291. PubMed PMID: 21212793.

365. Hsu LY, Lauring J, Liang HE, Greenbaum S, Cado D, Zhuang Y, Schlissel MS. A conserved transcriptional enhancer regulates RAG gene expression in developing B cells. Immunity. 2003;19(1):105-17. Epub 2003/07/23. PubMed PMID: 12871643.

366. Chen Z, Xiao Y, Zhang J, Li J, Liu Y, Zhao Y, Ma C, Luo J, Qiu Y, Huang G, Korteweg C, Gu J. Transcription factors E2A, FOXO1 and FOXP1 regulate recombination activating gene

expression in cancer cells. PLoS One. 2011;6(5):e20475. Epub 2011/06/10. doi: 10.1371/journal.pone.0020475. PubMed PMID: 21655267; PMCID: 3105062.

367. Winandy S, Wu L, Wang JH, Georgopoulos K. Pre-T cell receptor (TCR) and TCR-controlled checkpoints in T cell differentiation are set by Ikaros. J Exp Med. 1999;190(8):1039-48. Epub 1999/10/19. PubMed PMID: 10523602; PMCID: 2195663.

368. Mandal M, Powers SE, Ochiai K, Georgopoulos K, Kee BL, Singh H, Clark MR. Ras orchestrates exit from the cell cycle and light-chain recombination during early B cell development. Nat Immunol. 2009;10(10):1110-7. Epub 2009/09/08. doi: ni.1785 [pii] 10.1038/ni.1785. PubMed PMID: 19734904; PMCID: 3057509.

369. Ferreiros Vidal I, Carroll T, Taylor B, Terry A, Liang Z, Bruno L, Dharmalingam G, Khadayate S, Cobb BS, Smale ST, Spivakov M, Srivastava P, Petretto E, Fisher AG, Merkenschlager M. Genome-wide identification of Ikaros targets elucidates its contribution to mouse B cell lineage specification and pre-B cell differentiation. Blood. 2013. doi: 10.1182/blood-2012-08-450114. PubMed PMID: 23303821.

370. Kathrein KL, Lorenz R, Innes AM, Griffiths E, Winandy S. Ikaros induces quiescence and T-cell differentiation in a leukemia cell line. Mol Cell Biol. 2005;25(5):1645-54. Epub 2005/02/17. doi: 10.1128/MCB.25.5.1645-1654.2005. PubMed PMID: 15713624; PMCID: 549358.

371. Yamashita I, Nagata T, Tada T, Nakayama T. CD69 cell surface expression identifies developing thymocytes which audition for T cell antigen receptor-mediated positive selection. Int Immunol. 1993;5(9):1139-50. PubMed PMID: 7902130.

372. Anderson G, Owen JJ, Moore NC, Jenkinson EJ. Characteristics of an in vitro system of thymocyte positive selection. J Immunol. 1994;153(5):1915-20. PubMed PMID: 7914216.

373. Swat W, Dessing M, von Boehmer H, Kisielow P. CD69 expression during selection and maturation of CD4+8+ thymocytes. Eur J Immunol. 1993;23(3):739-46. doi: 10.1002/eji.1830230326. PubMed PMID: 8095460.

374. Kearse KP, Takahama Y, Punt JA, Sharrow SO, Singer A. Early molecular events induced by T cell receptor (TCR) signaling in immature CD4+ CD8+ thymocytes: increased synthesis of TCR-alpha protein is an early response to TCR signaling that compensates for TCR-alpha instability, improves TCR assembly, and parallels other indicators of positive selection. J Exp Med. 1995;181(1):193-202. PubMed PMID: 7528767; PMCID: PMC2191831.

375. Tinsley KW, Hong C, Luckey MA, Park JY, Kim GY, Yoon HW, Keller HR, Sacks AJ, Feigenbaum L, Park JH. Ikaros is required to survive positive selection and to maintain clonal diversity during T cell development in the thymus. Blood. 2013. doi: 10.1182/blood-2012-12-472076. PubMed PMID: 23908463.

376. Mitchell JL, Seng A, Yankee TM. Ikaros, Helios, and Aiolos protein levels increase in human thymocytes after beta selection. Immunol Res. 2015. doi: 10.1007/s12026-015-8754-x. PubMed PMID: 26645971.

377. Hori T, Cupp J, Wrighton N, Lee F, Spits H. Identification of a novel human thymocyte subset with a phenotype of CD3- CD4+ CD8 alpha + beta-1. Possible progeny of the CD3- CD4- CD8- subset. J Immunol. 1991;146(12):4078-84. PubMed PMID: 1828260.

378. Res P, Blom B, Hori T, Weijer K, Spits H. Down-regulation of CD1 marks acquisition of functional maturation of human thymocytes and defines a control point in late stages of human T cell development. J Exp Med. 1997;185(1):141-51. PubMed PMID: 8996250; PMCID: PMC2196108.

379. Ross EM, Bourges D, Hogan TV, Gleeson PA, van Driel IR. Helios defines T cells being driven to tolerance in the periphery and thymus. Eur J Immunol. 2014;44(7):2048-58. doi: 10.1002/eji.201343999. PubMed PMID: 24740292.

380. Urban JA, Winandy S. Ikaros null mice display defects in T cell selection and CD4 versus CD8 lineage decisions. J Immunol. 2004;173(7):4470-8. Epub 2004/09/24. doi: 173/7/4470 [pii]. PubMed PMID: 15383578.

381. Tinsley KW, Hong C, Luckey MA, Park JY, Kim GY, Yoon HW, Keller HR, Sacks AJ, Feigenbaum L, Park JH. Ikaros is required to survive positive selection and to maintain clonal diversity during T-cell development in the thymus. Blood. 2013;122(14):2358-68. Epub 2013/08/03. doi: 10.1182/blood-2012-12-472076. PubMed PMID: 23908463; PMCID: 3790506.

382. Bellavia D, Mecarozzi M, Campese AF, Grazioli P, Talora C, Frati L, Gulino A, Screpanti I. Notch3 and the Notch3-up-regulated RNA-binding protein HuD regulate Ikaros alternative splicing. EMBO J. 2007;26(6):1670-80. doi: 10.1038/sj.emboj.7601626. PubMed PMID: 17332745; PMCID: PMC1829386.

383. Avitahl N, Winandy S, Friedrich C, Jones B, Ge Y, Georgopoulos K. Ikaros sets thresholds for T cell activation and regulates chromosome propagation. Immunity.

1999;10(3):333-43. Epub 1999/04/16. doi: S1074-7613(00)80033-3 [pii]. PubMed PMID: 10204489.

384. Rebollo A, Ayllon V, Fleischer A, Martinez CA, Zaballos A. The association of Aiolos transcription factor and Bcl-xL is involved in the control of apoptosis. J Immunol. 2001;167(11):6366-73. Epub 2001/11/21. PubMed PMID: 11714801.

385. Zhuang Y, Li D, Fu J, Shi Q, Lu Y, Ju X. Overexpression of AIOLOS inhibits cell proliferation and suppresses apoptosis in Nalm-6 cells. Oncology reports. 2014;31(3):1183-90. Epub 2014/01/09. doi: 10.3892/or.2013.2964. PubMed PMID: 24399134.

386. Vanhecke D, Verhasselt B, De Smedt M, Leclercq G, Plum J, Vandekerckhove B. Human thymocytes become lineage committed at an early postselection CD69+ stage, before the onset of functional maturation. J Immunol. 1997;159(12):5973-83. PubMed PMID: 9550395.

387. Chakraverty R, Flutter B, Fallah-Arani F, Eom HS, Means T, Andreola G, Schwarte S, Buchli J, Cotter P, Zhao G, Sykes M. The host environment regulates the function of CD8+ graft-versus-host-reactive effector cells. J Immunol. 2008;181(10):6820-8. Epub 2008/11/05. PubMed PMID: 18981100.

388. Awong G, Herer E, Surh CD, Dick JE, La Motte-Mohs RN, Zuniga-Pflucker JC. Characterization in vitro and engraftment potential in vivo of human progenitor T cells generated from hematopoietic stem cells. Blood. 2009;114(5):972-82. Epub 2009/06/06. doi: 10.1182/blood-2008-10-187013. PubMed PMID: 19491395.

389. Jung LK, Haynes BF, Nakamura S, Pahwa S, Fu SM. Expression of early activation antigen (CD69) during human thymic development. Clinical and experimental immunology. 1990;81(3):466-74. Epub 1990/09/01. PubMed PMID: 2204504; PMCID: 1534971.

390. Vanhecke D, Leclercq G, Plum J, Vandekerckhove B. Characterization of distinct stages during the differentiation of human CD69+CD3+ thymocytes and identification of thymic emigrants. J Immunol. 1995;155(4):1862-72. PubMed PMID: 7543535.

391. Janossy G, Bofill M, Rowe D, Muir J, Beverley PC. The tissue distribution of T lymphocytes expressing different CD45 polypeptides. Immunology. 1989;66(4):517-25. Epub 1989/04/01. PubMed PMID: 2523860; PMCID: 1385151.

392. Gillitzer R, Pilarski LM. In situ localization of CD45 isoforms in the human thymus indicates a medullary location for the thymic generative lineage. J Immunol. 1990;144(1):66-74. Epub 1990/01/01. PubMed PMID: 1688577.

393. Okumura M, Fujii Y, Inada K, Nakahara K, Matsuda H. CD45RA-R0+ subset is the major population of dividing thymocytes in the human. Eur J Immunol. 1992;22(11):3033-6. Epub 1992/11/01. doi: 10.1002/eji.1830221140. PubMed PMID: 1385159.

394. Sidhom I, Shaaban K, Soliman S, Ezzat S, El-Anwar W, Hamdy N, Yassin D, Salem S, Hassanein H, Mansour MT. Clinical significance of immunophenotypic markers in pediatric T-cell acute lymphoblastic leukemia. Journal of the Egyptian National Cancer Institute. 2008;20(2):111-20. Epub 2008/06/01. PubMed PMID: 20029466.

395. Kirstetter P, Thomas M, Dierich A, Kastner P, Chan S. Ikaros is critical for B cell differentiation and function. Eur J Immunol. 2002;32(3):720-30. Epub 2002/03/01. doi: 10.1002/1521-4141(200203)32:3<720::AID-IMMU720>3.0.CO;2-P [pii] 10.1002/1521-4141(200203)32:3<720::AID-IMMU720>3.0.CO;2-P. PubMed PMID: 11870616.

396. Palomero T, Lim WK, Odom DT, Sulis ML, Real PJ, Margolin A, Barnes KC, O'Neil J, Neuberg D, Weng AP, Aster JC, Sigaux F, Soulier J, Look AT, Young RA, Califano A, Ferrando AA. NOTCH1 directly regulates c-MYC and activates a feed-forward-loop transcriptional network promoting leukemic cell growth. Proc Natl Acad Sci U S A. 2006;103(48):18261-6. Epub 2006/11/23. doi: 10.1073/pnas.0606108103. PubMed PMID: 17114293; PMCID: 1838740.

397. Margolin AA, Palomero T, Sumazin P, Califano A, Ferrando AA, Stolovitzky G. ChIP-on-chip significance analysis reveals large-scale binding and regulation by human transcription factor oncogenes. Proc Natl Acad Sci U S A. 2009;106(1):244-9. Epub 2009/01/02. doi: 10.1073/pnas.0806445106. PubMed PMID: 19118200; PMCID: 2613038.

398. La Starza R, Borga C, Barba G, Pierini V, Schwab C, Matteucci C, Lema Fernandez AG, Leszl A, Cazzaniga G, Chiaretti S, Basso G, Harrison CJ, Te Kronnie G, Mecucci C. Genetic profile of T-cell acute lymphoblastic leukemias with MYC translocations. Blood. 2014;124(24):3577-82. doi: 10.1182/blood-2014-06-578856. PubMed PMID: 25270907.

399. Adamaki M, Lambrou GI, Athanasiadou A, Tzanoudaki M, Vlahopoulos S, Moschovi M. Implication of IRF4 aberrant gene expression in the acute leukemias of childhood. PLoS One.

2013;8(8):e72326. Epub 2013/08/27. doi: 10.1371/journal.pone.0072326. PubMed PMID: 23977280; PMCID: 3744475.

400. Grossmann V, Kern W, Harbich S, Alpermann T, Jeromin S, Schnittger S, Haferlach C, Haferlach T, Kohlmann A. Prognostic relevance of RUNX1 mutations in T-cell acute lymphoblastic leukemia. Haematologica. 2011;96(12):1874-7. Epub 2011/08/11. doi: 10.3324/haematol.2011.043919. PubMed PMID: 21828118; PMCID: 3232273.

401. Della Gatta G, Palomero T, Perez-Garcia A, Ambesi-Impiombato A, Bansal M, Carpenter ZW, De Keersmaecker K, Sole X, Xu L, Paietta E, Racevskis J, Wiernik PH, Rowe JM, Meijerink JP, Califano A, Ferrando AA. Reverse engineering of TLX oncogenic transcriptional networks identifies RUNX1 as tumor suppressor in T-ALL. Nat Med. 2012;18(3):436-40. Epub 2012/03/01. doi: 10.1038/nm.2610. PubMed PMID: 22366949; PMCID: 3298036.

402. Ferrando AA, Neuberg DS, Staunton J, Loh ML, Huard C, Raimondi SC, Behm FG, Pui CH, Downing JR, Gilliland DG, Lander ES, Golub TR, Look AT. Gene expression signatures define novel oncogenic pathways in T cell acute lymphoblastic leukemia. Cancer Cell. 2002;1(1):75-87. Epub 2002/06/28. PubMed PMID: 12086890.

403. Brown L, Cheng JT, Chen Q, Siciliano MJ, Crist W, Buchanan G, Baer R. Site-specific recombination of the tal-1 gene is a common occurrence in human T cell leukemia. EMBO J. 1990;9(10):3343-51. Epub 1990/10/01. PubMed PMID: 2209547; PMCID: 552072.

404. Beverly LJ, Capobianco AJ. Perturbation of Ikaros isoform selection by MLV integration is a cooperative event in Notch(IC)-induced T cell leukemogenesis. Cancer Cell. 2003;3(6):551-64. Epub 2003/07/05. doi: S1535610803001375 [pii]. PubMed PMID: 12842084.

405. Weng AP, Ferrando AA, Lee W, Morris JPt, Silverman LB, Sanchez-Irizarry C, Blacklow SC, Look AT, Aster JC. Activating mutations of NOTCH1 in human T cell acute lymphoblastic leukemia. Science. 2004;306(5694):269-71. Epub 2004/10/09. doi: 10.1126/science.1102160. PubMed PMID: 15472075.

406. Capone M, Hockett RD, Jr., Zlotnik A. Kinetics of T cell receptor beta, gamma, and delta rearrangements during adult thymic development: T cell receptor rearrangements are present in CD44(+)CD25(+) Pro-T thymocytes. Proc Natl Acad Sci U S A. 1998;95(21):12522-7. Epub 1998/10/15. PubMed PMID: 9770518; PMCID: 22863.

407. Tourigny MR, Mazel S, Burtrum DB, Petrie HT. T cell receptor (TCR)-beta gene recombination: dissociation from cell cycle regulation and developmental progression during T cell ontogeny. J Exp Med. 1997;185(9):1549-56. Epub 1997/05/05. PubMed PMID: 9151892; PMCID: 2196304.

408. Ciofani M, Schmitt TM, Ciofani A, Michie AM, Cuburu N, Aublin A, Maryanski JL, Zuniga-Pflucker JC. Obligatory role for cooperative signaling by pre-TCR and Notch during thymocyte differentiation. J Immunol. 2004;172(9):5230-9. Epub 2004/04/22. PubMed PMID: 15100261.

409. Taghon T, Yui MA, Pant R, Diamond RA, Rothenberg EV. Developmental and molecular characterization of emerging beta- and gammadelta-selected pre-T cells in the adult

mouse thymus. Immunity. 2006;24(1):53-64. Epub 2006/01/18. doi: 10.1016/j.immuni.2005.11.012. PubMed PMID: 16413923.

410. Daley SR, Hu DY, Goodnow CC. Helios marks strongly autoreactive CD4+ T cells in two major waves of thymic deletion distinguished by induction of PD-1 or NF-kappaB. J Exp Med. 2013;210(2):269-85. Epub 2013/01/23. doi: 10.1084/jem.20121458. PubMed PMID: 23337809; PMCID: 3570102.

411. Akimova T, Beier UH, Wang L, Levine MH, Hancock WW. Helios expression is a marker of T cell activation and proliferation. PLoS One. 2011;6(8):e24226. doi: 10.1371/journal.pone.0024226. PubMed PMID: 21918685; PMCID: PMC3168881.

412. Rajasagi M, Vitacolonna M, Benjak B, Marhaba R, Zoller M. CD44 promotes progenitor homing into the thymus and T cell maturation. J Leukoc Biol. 2009;85(2):251-61. Epub 2008/10/29. doi: 10.1189/jlb.0608389. PubMed PMID: 18955544.

413. Patel DD, Hale LP, Whichard LP, Radcliff G, Mackay CR, Haynes BF. Expression of CD44 molecules and CD44 ligands during human thymic fetal development: expression of CD44 isoforms is developmentally regulated. Int Immunol. 1995;7(2):277-86. Epub 1995/02/01. PubMed PMID: 7537537.

414. Aruffo A, Stamenkovic I, Melnick M, Underhill CB, Seed B. CD44 is the principal cell surface receptor for hyaluronate. Cell. 1990;61(7):1303-13. PubMed PMID: 1694723.

415. Marhaba R, Bourouba M, Zoller M. CD44v6 promotes proliferation by persisting activation of MAP kinases. Cellular signalling. 2005;17(8):961-73. Epub 2005/05/17. doi: 10.1016/j.cellsig.2004.11.017. PubMed PMID: 15894169.

416. Mielgo A, van Driel M, Bloem A, Landmann L, Gunthert U. A novel antiapoptotic mechanism based on interference of Fas signaling by CD44 variant isoforms. Cell death and differentiation. 2006;13(3):465-77. Epub 2005/09/17. doi: 10.1038/sj.cdd.4401763. PubMed PMID: 16167069.

417. Marhaba R, Bourouba M, Zoller M. CD44v7 interferes with activation-induced cell death by up-regulation of anti-apoptotic gene expression. J Leukoc Biol. 2003;74(1):135-48. Epub 2003/07/02. PubMed PMID: 12832452.

418. Zoller M, Schmidt A, Denzel A, Moll J. Constitutive expression of a CD44 variant isoform on T cells facilitates regaining of immunocompetence in allogeneic bone marrow transplantation. Blood. 1997;90(2):873-85. Epub 1997/07/15. PubMed PMID: 9226189.

419. Foger N, Marhaba R, Zoller M. CD44 supports T cell proliferation and apoptosis by apposition of protein kinases. Eur J Immunol. 2000;30(10):2888-99. Epub 2000/11/09. doi: 10.1002/1521-4141(200010)30:10<2888::AID-IMMU2888>3.0.CO;2-4. PubMed PMID: 11069071.

420. Rajasagi M, Marhaba R, Vitacolonna M, Zoller M. Thymocyte expansion and maturation: crosstalk of CD44v6 on thymocytes and panCD44 on stroma cells. Immunology and cell biology. 2010;88(2):136-47. Epub 2009/09/30. doi: 10.1038/icb.2009.70. PubMed PMID: 19786978.

421. Nakano K, Saito K, Mine S, Matsushita S, Tanaka Y. Engagement of CD44 up-regulates Fas ligand expression on T cells leading to activation-induced cell death. Apoptosis : an international journal on programmed cell death. 2007;12(1):45-54. Epub 2006/12/01. doi: 10.1007/s10495-006-0488-8. PubMed PMID: 17136494.

422. Huet S, Groux H, Caillou B, Valentin H, Prieur AM, Bernard A. CD44 contributes to T cell activation. J Immunol. 1989;143(3):798-801. Epub 1989/08/01. PubMed PMID: 2568380.

423. Petrie HT, Zuniga-Pflucker JC. Zoned out: functional mapping of stromal signaling microenvironments in the thymus. Annu Rev Immunol. 2007;25:649-79. Epub 2007/02/13. doi: 10.1146/annurev.immunol.23.021704.115715. PubMed PMID: 17291187.

424. Ilangumaran S, Briol A, Hoessli DC. CD44 selectively associates with active Src family protein tyrosine kinases Lck and Fyn in glycosphingolipid-rich plasma membrane domains of human peripheral blood lymphocytes. Blood. 1998;91(10):3901-8. PubMed PMID: 9573028.

425. Taher TE, Smit L, Griffioen AW, Schilder-Tol EJ, Borst J, Pals ST. Signaling through CD44 is mediated by tyrosine kinases. Association with p56lck in T lymphocytes. J Biol Chem. 1996;271(5):2863-7. PubMed PMID: 8576267.